UNIVERSITY OF CAMPINAS

SCHOOL OF FOOD ENGINEERING

PAMELA MAGALÍ BERMEJO

TOWARDS AN iSUCCELL *SACCHAROMYCES CEREVISIAE* PLATFORM FOR FUEL ETHANOL PRODUCTION

RUMO A UMA PLATAFORMA iSUCCELL DE *SACCHAROMYCES CEREVISIAE* PARA A PRODUÇÃO DE ETANOL COMBUSTÍVEL

CAMPINAS

2022

PAMELA MAGALÍ BERMEJO

TOWARDS AN iSUCCELL *SACCHAROMYCES CEREVISIAE* PLATFORM FOR FUEL ETHANOL PRODUCTION

RUMO A UMA PLATAFORMA iSUCCELL DE *SACCHAROMYCES CEREVISIAE* PARA A PRODUÇÃO DE ETANOL COMBUSTÍVEL

Thesis presented to the School of Food Engineering of the University of Campinas in partial fulfilment of the requirements for the degree of Doctor in Science.

Tese apresentada à Faculdade de Engenharia de Alimentos da Universidade Estadual de Campinas como parte dos requisitos exigidos para a obtenção do título de Doutora em Ciências.

Supervisor: Andreas Karoly Gombert

ESTE EXEMPLAR CORRESPONDE À VERSÃO FINAL DA TESE DEFENDIDA PELA ALUNA PAMELA MAGALÍ BERMEJO E ORIENTADA PELO PROF. DR. ANDREAS KAROLY GOMBERT

CAMPINAS

2022

Ficha catalográfica
Universidade Estadual de Campinas
Biblioteca da Faculdade de Engenharia de Alimentos
Gardênia Garcia Benossi - CRB 8/8644

B456

Bermejo, Pamela Magalí, 1983-
Towards an iSUCCELL *Saccharomyces cerevisiae* platform for fuel ethanol production / Pamela Magalí Bermejo. – Campinas, SP : [s.n.], 2022.

Orientador: Andreas Karoly Gombert.
Tese (doutorado) – Universidade Estadual de Campinas, Faculdade de Engenharia de Alimentos.

1. Biorrefinaria. 2. *Saccharomyces cerevisiae*. 3. Sacarose. 4. Celobiose. 5. Etanol. I. Gombert, Andreas Karoly, 1970-. II. Universidade Estadual de Campinas. Faculdade de Engenharia de Alimentos. III. Título.

Informações para Biblioteca Digital

Título em outro idioma: Rumo a uma plataforma iSUCCELL de *Saccharomyces cerevisiae* para a produção de etanol combustível
Palavras-chave em inglês:
Biorefinery
Saccharomyces cerevisiae
Sucrose
Cellobiose
Ethanol
Área de concentração: Bioenergia
Titulação: Doutora em Ciências
Banca examinadora:
Andreas Karoly Gombert [Orientador]
Boris Juan Carlos Ugarte Stambuk
Johana Rincones Pérez
Raúl Nicolás Comelli
Thiago Olitta Basso
Data de defesa: 18-04-2022
Programa de Pós-Graduação: Bioenergia

Identificação e informações acadêmicas do(a) aluno(a)
- ORCID do autor: https://orcid.org/0000-0002-1329-1631
- Currículo Lattes do autor: http://lattes.cnpq.br/1292351585009077

EXAMINATION COMMITTEE

Dr. Andreas Karoly Gombert

Universidade Estadual de Campinas

Dr. Boris Juan Carlos Ugarte Stambuk

Universidade Federal de Santa Catarina

Dra. Johana Rincones Pérez

Tradecorp do Brasil

Dr. Raúl Nicolás Comelli

Universidad Nacional del Litoral

Dr. Thiago Olitta Basso

Universidade de São Paulo

A Ata da Defesa com as respectivas assinaturas dos membros consta no SIGA/Sistema de Fluxo de Dissertação/Tese e na Secretaria do Programa da Unidade.

Dedicated to my love Pablo, for making me believe in myself.

ACKNOWLEDGEMENTS

My PhD journey has been longer than expected, and I have always believed that this section would be the most difficult part of the writing process. Now that I finally got here, I am convinced that I was right.

I have envisioned myself writing this section for so many times, and every time I ended up in a very emotional state. This moment is like watching a movie for the second time, you know what is going to happen, but you focus on the details and on the performance of the supporting actors and actresses that contribute to the story in different ways. No one achieves anything alone, and here I would like to thank all the people and Institutions that helped me make this accomplishment possible.

In the following lines, I will switch between English, Portuguese, and Spanish.

Andreas, meu chefe querido, como costumo te dizer. Minha gratidão por você é ENORME, e é difícil escrever estas linhas sem me emocionar. Jamais esquecerei aquela primeira conversa que tivemos na sua sala, em um absoluto espanhol porque meu português era inexistente na época. Mal sabia eu que aquela pessoa com aspecto um tanto sério e rígido, ia me demonstrar que as primeiras impressões podem estar muito enganadas. Obrigada por ter confiado em mim quando nem eu mesma conseguia, por ter me dado os espaços para eu expor meus sentimentos com total liberdade, pelo trato que sempre recebi de você, e por me dizer aquelas palavras de força em meus momentos de fraqueza. Por fim, e não menos importante, obrigada por tudo o que aprendi com você e por estar sempre disposto a me apresentar oportunidades profissionais.

Ronald, thank you so much for giving me the opportunity of experiencing one of the most unforgettable and wonderful times of my life – my stay in The Netherlands. Your kindness, sense of humour, and positivity made my experience at CBS even more special.

Adiphol, my sweet Adi, you have the ability to make everything around you colourful. Thank you so much for your endless patience, for your continuous support and sensitivity, and for being the sweetest mentor I could ever have. P.S.: Lunch time! 😊

Glei, você é certamente o responsável pela maior parcela do conhecimento que adquiri em biologia molecular. Você é O CARA de genética de leveduras, minha maior referência. Obrigada por tudo o que me ensinou!! Trabalhar com você durante o meu doutorado e o

projeto “CoronaYeast” foi espetacular. Aqui também quero agradecer ao Prof. **Gonçalo** por me permitir trabalhar no LGE durante parte do processo de doutoramento.

Rô e **Marquinhos**, obrigada pelos questionamentos e colocações nas reuniões de grupo que foram importantes para meu desenvolvimento profissional, assim como as experiências de PED que realizei com vocês como docentes. Sem tirar mérito ao aspecto profissional, o que mais levo comigo é a qualidade de pessoa que vocês são, e o trato carinhoso e respeitoso que sempre tiveram comigo. Obrigada, queridos!!

Chico e **Fifa**, o LEMeB nasceu com vocês. Obrigada por terem contribuído para o crescimento do lab, tanto em formação de recursos humanos quanto em conhecimento. Vocês são pessoas queridas para todos os Lemébios!

Pri, a rainha dos abraços!! Obrigada por esse dom que você tem, que com um simples olhar consegue enxergar quando eu preciso de um abraço. E nossa como é gostoso! Obrigada pelos cafés com desabafo, pela ajuda no HPLC, e por me fazer sentir uma pessoa especial. Te adoro, Pri!

Vijay, you are one of the best people I have ever met in my life, and I’m sure that you are not just a source of inspiration for me, but for everyone who knows you. Thank you so much for encouraging my research and for allowing me to grow as a professional with your insights and questioning. I appreciate your generosity, your sincere opinions, and your ready-to-help attitude in every step of the way.

Guti e **Su**, os amores que o LEMeB me deu! A amizade de vocês foi meu maior prêmio nesta passagem pelo doutorado. Vivemos muitíssimo juntas, rimos, choramos, xingamos, desabafamos (e a lista continua...). Sinto muito orgulho de vocês, de quem vocês são e das profissionais que se tornaram. Obrigada por tudo o que aprendo com vocês quase que diariamente, por celebrarem minhas conquistas e por fazerem com que as tristezas e frustrações do doutorado fossem mais leves quando eram compartilhadas com vocês.

Carlinha, compartilhar esta jornada com você fez toda diferença para mim. Aprendi muito com nossos bate-papos (*face-to-face* e virtuais) tentando entender o comportamento das nossas leveduras filhas. Suas palavras precisas e sua constante torcida foram muito importantes para mim, e tenho o privilégio de dizer que ganhei uma amiga que é o máximo e que admiro profundamente.

Jenni, minha filhinha cientista! Você foi a melhor IC que eu podia ter imaginado! Os dois anos que trabalhamos juntas foram de muito crescimento para mim, e isso em parte se deve a que você me desafiava constantemente para ser melhor. Obrigada pela disposição que você sempre teve, nunca uma reclamação, e pela compreensão no final do projeto quando as coisas não saíram como desejadas. Foi um grande aprendizado para as duas, não é? Não tenho dúvidas que você terá uma carreira de sucesso!

Brunito, **Wesley**, **Zé**, **Igor**, **Laurinha**, **Capone**, **Felipe F.**, **Bia**, **Felipe B.**, **Dani**, **Rosa**, **Aurélio**, **Lucas**, **Fer**, **Robson**, **Yara**, **Juliana**, **Carlinha V.**, **Susan**, **Dielle**, **Cris**, e **Allan**, os Lemébios das antigas e da nova era. Obrigada por fazerem do LEMeB um ambiente superlegal para trabalhar, por me ajudarem com minhas dúvidas do português, e pelos momentos divertidos que passamos fora do lab (*happy hours*, churras, nívers, praia, e qualquer outra desculpa para nós tomarmos umas brejas).

Vicky, **Sarita**, **Claire**, **Joanna**, **Tizi**, **Isabelle** (my officemate 😊), **Ad**, **Evy**, **April**, **Alexa**, **Ronald**, **Ronnie, Guillermo**, and **Blanca**, my labmates from the Fungal Physiology group at CBS-KNAW. I would also like to include **Sylvia** and **Frank** here. Thank you so much for your cosy welcome in the group, for being so friendly and helpful, for the funny lab outings and the Friday's borrels that keep a special place in my memories. I would also like to thank **Martin** for teaching me (without knowing) the first lesson I learned in NL: if you make a mistake and a Dutchman lets you know about it, it is not personal! Loved that and certainly adopted it in my life.

Fe, **Alê**, **Ju**, **Carlinha**, e **Monique**, os filhos do Glei! Obrigada por serem colegas tão legais e fazerem com que o LGE tenha um lugar especial no meu coração. Obrigada também pelo aprendizado juntos e pela boa disposição de vocês sempre!

Barby, **Emi**, **Matorra**, **Vir**, **Xime**, las hermanas que elegí. Ustedes fueron y serán siempre mi fuente de estabilidad emocional, con quienes quiero compartir todo siempre. Gracias por el aguante, por las palabras de aliento y por hacerme sentir que con esta hinchada todo lo consigo! Las amo!!!

Mami, **Papi**, **Matu** y **Abu Niní**, mis fans nº 1, ninguna conquista sería posible sin ustedes. Ese amor incondicional que hace que un día escuchen: "Flia, me voy a hacer el doctorado a Brasil", y de ustedes sólo reciba palabras de apoyo, cuando sé que no es fácil sobrellevar la distancia por momentos. Todo lo que soy es gracias a ustedes, a la vida que me proporcionaron y al amor más puro y genuino que me brindan a diario.

Pabli y **Boris**, los amores de mi vida. Imposible agradecerles sin llorar. Amor, esta tesis es para vos. Fuiste y sos mi sostén en todo. Mi mayor crítico también, y te agradezco por eso. No debe ser fácil lidiar con mis inseguridades y auto boicot constante, pero lo conseguimos! Esta conquista es nuestra. Y a vos bebé de mami, gracias por hacerme olvidar de los quilombos cada vez que abro la puerta de casa y venís corriendo a recibirme con saltos y millones de "*lambeijos*". Te voy a amar por siempre, hijo.

Talvez seja um tanto curioso o fato de agradecer à **música**, mas ela tem um protagonismo indiscutível na minha essência desde que sai da barriga da minha mãe. Cada etapa da minha vida esteve acompanhada de uma trilha sonora, um álbum, uma banda, um cantor, um estilo. E nesta jornada pelo doutorado, onde cores de todas as tonalidades estiveram presentes, a música sempre esteve para iluminar, acalmar e embelecer esses momentos.

O presente trabalho foi realizado com apoio da Coordenação de Aperfeiçoamento de Pessoal de Nível Superior – Brasil (CAPES) – Código de Financiamento 001. Agradeço ao Estado brasileiro através da **CAPES**, pela concessão da bolsa de doutoramento que permitiu o desenvolvimento desta tese e minha formação de nível superior. *Viva a educação pública, gratuita e laica!*

À **Fundação de Amparo à Pesquisa do Estado de São Paulo (FAPESP)**, pelo auxílio concedido na modalidade de Auxílio Regular e de Bolsa de Iniciação Científica, que permitiu o financiamento de parte dos trabalhos desenvolvidos nesta tese e a capacitação da Jennifer.

Ao **povo brasileiro** (nativo e por opção), por permitir minha formação de nível superior através do pagamento de impostos.

À **UNICAMP** e, especialmente, à **FEA** através do Programa Integrado de Pós-Graduação em Bioenergia, que me aceitou como aluna de Doutorado.

To the **CBS-KNAW Fungal Biodiversity Centre** (currently, Westerdijk Fungal Biodiversity Institute), for accepting me as a Visiting PhD student from August 2015 to February 2016.

“It’s not the strongest of the species that survive, nor the most intelligent, but the ones most responsive to change”.

Charles Darwin

ABSTRACT

Current second-generation (2G) fuel ethanol technologies are facing severe difficulties to become economically viable, having so far reached production volumes well below predictions made one or two decades ago. As an initiative to tackle some of the challenges inherent to these processes, here we propose an alternative concept that relies on the integration of first-generation (1G) and 2G sugarcane-based processes by mixing the sucrose-rich stream from the 1G process with a partially hydrolysed cellobiose-rich 2G stream in the fermentation step. The strategy also involves what we named a microbial "iSUCCELL" platform, responsible for carrying out fermentation of sucrose and cellobiose into ethanol, via active transport of the sugars and their subsequent intracellular hydrolyses. We first addressed the metabolism of each disaccharide in the yeast *Saccharomyces cerevisiae*, separately. The "iCELL" component was studied by engineering *S. cerevisiae* strains with the *Neurospora crassa* CDT-1 cellobiose transporter and six individual β-glucosidases from different filamentous fungi: one from *N. crassa* (GH1-1), one from *Aspergillus niger* (AN 8517), and four from *Podospora anserina* (PA 951, PA 3784, PA 6071, and PA 10293), the latter five being hitherto undescribed enzymes. Since none of the engineered strains initially sustained growth on cellobiose, a further laboratory evolution approach was applied to improve the kinetic performances of all strains. After completion of the evolution experiments, although the growth kinetics of all strains on cellobiose as a sole carbon source indeed improved, analysis of whole-genome sequencing data revealed that at least two of the evolution experiments had been contaminated with *Meyerozyma guilliermondii*, a yeast species that managed to settle in the cell population, probably because of its natural capacity to utilise cellobiose as carbon source. For the "iSUC" component of our strategy, we leveraged the properties of a *S. cerevisiae* iSUC strain obtained in a previous work (Basso *et al.* 2011), in terms of increased ethanol yields *vs*. a reference strain, and evaluated its performance in situations which are closer to the industrial scenario, i.e., in batch operation with excess sugar and in a miniaturised system mimicking the Brazilian 1G fuel ethanol process. The results from these studies showed that the iSUC strain was not able to display any increment in the ethanol yield on substrate, when compared to the reference strain that mainly hydrolysed sucrose extracellularly. Analysed together, the results presented in this thesis, although not leading to reach our initial goal, open the door for future studies aiming at demonstrating the

potential of the iSUCCELL approach in a robust industrial strain and in a real industrial environment.

RESUMO

As atuais tecnologias de produção de etanol combustível de segunda geração (2G), com base em matérias-primas lignocelulósicas, enfrentam sérias dificuldades para se tornarem economicamente viáveis, tendo até agora alcançado volumes de produção bem abaixo das previsões feitas há uma ou duas décadas. Como iniciativa para enfrentar alguns dos desafios inerentes a esses processos industriais, aqui propomos um conceito alternativo, baseado na integração de tecnologias de primeira geração (1G) e 2G, no contexto de biorrefinarias de cana-de-açúcar. O conceito envolve uma mistura da corrente rica em sacarose do processo 1G com uma corrente 2G parcialmente hidrolisada, rica em celobiose, na etapa de fermentação. A estratégia também envolve o que chamamos de plataforma microbiana "iSUCCELL", responsável por realizar a fermentação da sacarose e da celobiose em etanol, via transporte ativo dos açúcares e suas subsequentes hidrólises intracelulares. Primeiramente, abordamos separadamente o metabolismo de cada dissacarídeo na levedura *Saccharomyces cerevisiae*. O componente "iCELL" foi estudado através da engenharia de linhagens de *S. cerevisiae* com o transportador de celobiose CDT-1 de *Neurospora crassa* e seis β-glicosidases individuais de diferentes fungos filamentosos: uma de *N. crassa* (GH1-1), uma de *Aspergillus niger* (AN 8517) e quatro de *Podospora anserina* (PA 951, PA 3784, PA 6071 e PA 10293), sendo as cinco últimas enzimas ainda até então não descritas na literatura. Uma vez que nenhuma das linhagens engenheiradas inicialmente foi capaz de crescer em celobiose, uma posterior abordagem de evolução laboratorial foi conduzida para melhorar o desempenho cinético de todas as linhagens. Após a conclusão dos experimentos de evolução, embora a cinética de crescimento de todas as linhagens em celobiose como única fonte de carbono tenha melhorado, a análise dos dados de sequenciamento genômico revelou que pelo menos dois dos experimentos de evolução foram contaminados com *Meyerozyma guilliermondii*, uma espécie de levedura que conseguiu se estabelecer no sistema de cultivo, provavelmente devido à sua capacidade natural de utilizar a celobiose como fonte de carbono. Para o componente "iSUC" de nossa estratégia, lançamos mão das propriedades de uma linhagem iSUC de *S. cerevisiae* obtida em um trabalho anterior (Basso *et al.* 2011) e que apresenta maior rendimento em etanol, frente a uma linhagem referência. Avaliamos seu desempenho em situações mais condizentes com o cenário industrial, ou seja, em sistema de cultivo em batelada, com excesso de açúcar, e em um sistema miniaturizado que mimetiza o processo brasileiro de produção de etanol combustível 1G. Os resultados desses estudos mostraram que

a linhagem iSUC não foi capaz de apresentar incremento no rendimento em etanol, quando comparada à linhagem referência que hidrolisa a sacarose predominantemente no meio extracelular. Analisados em conjunto, os resultados apresentados nesta tese, embora não tenham conduzido ao nosso objetivo inicial, abrem as portas para estudos futuros que visem demonstrar o potencial da abordagem iSUCCELL em uma linhagem industrial robusta e em um ambiente industrial real.

LIST OF FIGURES

LIST OF TABLES

LIST OF ABBREVIATIONS AND ACRONYMS

1G	First-generation
2G	Second-generation
Agt1	α-glucoside-H^+ symporter
ATP	Adenosine triphosphate
ATPase	Adenosine triphosphatase
BGL	β-glucosidase
BLAST	Basic Local Alignment Search Tool
BLASTP	Protein Blast
BSA	Bovine Serum Albumin
CAPES	*Coordenação de Aperfeiçoamento de Pessoal de Nível Superior*
C12	Disaccharide sugars
C5	Pentose sugars
C6	Hexose sugars
CBH	Cellobiohydrolase
CBS-KNAW	CBS-KNAW Fungal Biodiversity Centre (currently Westerdijk Fungal Biodiversity Institute)
cDNA	Complementary DNA
CDT	Cellodextrin transporter
CDT-1/CDT-2	Cellodextrin transporters from *Neurospora crassa*
DNA	Deoxyribonucleic acid
DM	Dry mass
EDTA	Ethylenediamine tetraacetic acid
EG	Endoglucanase
EUROSCARF	European *Saccharomyces cerevisiae* archive for functional analysis
FAPESP	*Fundação de Amparo à Pesquisa do Estado de São Paulo*
FEA	School of Food Engineering
g	Gram
GH1-1	β-glucosidase from *Neurospora crassa*
GMO	Genetically Modified Organism
h	Hour
Hex Eq	Hexose Equivalent

Hxt	Hexose transporter from *Saccharomyces cerevisiae*
HXT2.4	Putative hexose transporter from *Scheffersomyces stipitis*
HO	Homothallic switching endonuclease gene
HPLC	High Performance Liquid Chromatography
IB	Institute of Biology
iCELL	Intracellular cellobiose hydrolysis
Imax	Isomaltase
iSUC	Intracellular sucrose hydrolysis
iSUCCELL	Intracellular sucrose and cellobiose hydrolyses
Kb	Kilobase
L	Litre
LEMeB	Bioprocess and Metabolic Engineering Laboratory
LGE	*Laboratório de Genômica e Expressão/Laboratório de Genômica e bioEnergia*
M	Molasses
MAL11	High-affinity maltose transporter gene
Malx1	Maltose-H^+ symporter
Malx2	Maltase
nm	Nanometre
PCR	Polymerase Chain Reaction
pH	Potential of Hydrogen
Pma1	Plasma membrane H^+-ATPase
p-NP	p-nitrophenol
p-NPG	p-nitrophenyl β-D-glucopyranoside
SdCBP	Cellobiose phosphorylase from *Saccharophagus degradans*
SDS	Sodium Dodecyl Sulfate
SJ	Sugarcane juice
SM	Synthetic Medium
Suc2	Invertase enzyme
TRIS	Tris(hydroxymethyl)aminomethane
TRS	Total Reducing Sugars
UNICAMP	University of Campinas

USP	University of São Paulo
YPD	Yeast extract-Peptone-Dextrose culture medium

LIST OF SYMBOLS

°C	Degree Celsius
Abs_{600}	Absorbance at 600 nm
N	Number of generations
μ_{max}	Maximum specific growth rate
$Y_{P/S}^{exp}$	Physiological product yield on substrate
$Y_{P/S}^{global}$	Global product yield on substrate
$Y_{x/S}^{exp}$	Physiological biomass yield on substrate
$Y_{x/S}^{global}$	Global biomass yield on substrate

TABLE OF CONTENTS

1 GENERAL INTRODUCTION

1.1 Background and motivation

The growth and the lifestyle of modern human societies have provoked a continuous increase in the energy demand and a rapid change in the Earth's climate. The main driver of global warming is the accumulation of greenhouse gases (GHGs) in the atmosphere (USGCRP 2017), primarily due to the extensive use and burning of fossil fuels (oil, coal, and gas), which by 2019 represented 80.9% of the world total energy supply (IEA 2019). To reduce GHG emissions and counteract climate change, multifaceted technological innovations have to be leveraged to provide the energy needed by human societies across the globe. Among the different possible energy forms, liquid fuels to power engines in the transportation sector need to move completely away from fossil-based sources to renewable ones. Ethanol-powered motors are such an option and have already proven to result in ~90% decrease in GHG emissions, when compared to conventional gasoline-fuelled engines (Jaiswal *et al.* 2017; UNICA 2020). While electric motors may be part of the solution in some parts of the world (Gramling 2021; Tabuchi and Plumer 2021), as long as the electricity is obtained from a renewable and carbon neutral source, it might not be the best alternative in all countries, e.g., in Brazil where the whole sugarcane chain has already been improved during decades. Ethanol is currently being used directly in car engines (as a standalone fuel or as a gasoline additive) but might also be employed as a source of hydrogen and further electricity to power electric engines in the near future (Henrique 2021; Silva 2021; Zaparolli 2021). Briefly, ethanol can be converted into hydrogen through a heterogeneous catalysis process. Then, this hydrogen can be used to feed the anode of a fuel cell, while the cathode is fed with oxygen (air), leading to the formation of water and electric energy, which is used to power the electric engine. Compared to conventional electric motors charged in specific charging stations, electric vehicles powered by ethanol could be very promising for Brazil (Zaparolli 2021). First, all the infrastructure needed to refuel cars with ethanol is already available in the country, and second, the main problem faced by conventional electric cars, i.e., the time needed to charge the battery, would be avoided.

Conventional (first-generation, 1G) ethanol produced primarily from corn and sugarcane in the United States and Brazil, respectively, account for 82% of the world’s total fuel ethanol production (RFA 2021). It should be noted that corn ethanol is increasing its share in Brazil

and already corresponds to ~10% of the total fuel ethanol volume produced in the country. In spite of the promises and beliefs that second-generation (2G) or cellulosic ethanol would currently respond for ~50% of the worldwide production (Soccol *et al.* 2010; Milanez *et al.* 2015; dos Santos *et al.* 2016), the reality shows that this figure is roughly about 1% (Jacobus *et al.* 2021). Strategies aimed at obtaining profitable 2G ethanol producing processes will imperatively depend on reducing the cost of conversion rather than the cost of the feedstock (Lynd *et al.* 2017). Integration of 2G processes to existing 1G facilities presents an attractive alternative to ease the implementation of 2G technologies, benefiting from: common unit operations, feedstock availability at the industrial site (or close to it), dilution of the inhibitors present in the 2G stream by mixing with the 1G stream, overall cost savings, and the possibility of diversifying the product portfolio of the biorefinery.

The research described in this thesis was motivated by this context. The yeast *Saccharomyces cerevisiae*, which is the main microorganism used to produce fuel ethanol via any of the technologies mentioned above (1G corn, 1G sugarcane or 2G), was also the microbial platform chosen in this work, which initially had the aim to evaluate a new paradigm that involved an engineered yeast strain capable of metabolising both sucrose and cellobiose intracellularly. This would enable, at least theoretically, a 2G process with a lower enzymatic load and with lower concentrations of inhibitors. It was not possible to fully engineer and evaluate such a strain, and thus this thesis reports our efforts towards this milestone.

1.2 Scope, objectives, and structure

This thesis aimed at developing a single *S. cerevisiae* strain capable of metabolising the disaccharides sucrose and cellobiose via intracellular routes in order to assess its potential as a yeast chassis for an integrated 1G+2G sugarcane-based fuel ethanol process. However, due to some experimental difficulties encountered along the way, we were forced to change our initial strategy and decided to tackle the metabolism of each disaccharide separately. The work presented in this thesis is divided into six chapters and a brief description of each is given below.

Chapter 2 puts forward the iSUCCELL concept introduced in this thesis - a new paradigm for a sugarcane-based biorefinery - in which a yeast chassis is used to convert sucrose and cellobiose into fuel ethanol via intracellular routes. This concept was published as a minireview article in the journal FEMS Yeast Research (Bermejo, Raghavendran and Gombert 2020), in a Thematic Issue on Yeast Synthetic Biology. In this chapter/article, we

describe and discuss the advantages of such an approach over the classical 1G and 2G standalone processes. Additionally, this work also reviews the attempts explored so far by the scientific community to engineer iSUC and iCELL pathways in yeast.

Chapters 3 and 4 address the iCELL component of our iSUCCELL strategy, corresponding to the analysis of intracellular cellobiose modules engineered in *S. cerevisiae*. The specific objectives of the work described in these chapters were:

- To screen and select a set of putative novel cellobiose transporters (CDTs) and intracellular β-glucosidases (BGLs) from fungal hosts via bioinformatics analysis;
- To construct plasmid vectors harbouring the above-mentioned candidate sequences as well as reference cellobiose-degrading genes from *Neurospora crassa* (CDT-1 and GH1-1);
- To assess the functionality of the BGL enzymes in *S. cerevisiae* by measuring the enzymatic activities in cell extracts;
- To engineer different *S. cerevisiae* iCELL strains with a genome-integrated CDT copy and an episomal version of an intracellular BGL;
- To evaluate the growth performance of engineered iCELL strains on different carbon sources;
- To investigate the kinetics of growth, substrate consumption, and ethanol formation of engineered iCELL strains during batch cultivations on cellobiose;
- To improve the kinetic performance of at least one engineered iCELL strain during growth on cellobiose via laboratory evolution;
- To characterise the physiology of the evolved iCELL strain/s during batch cultivations on cellobiose;
- To investigate the genetic changes selected in the evolved iCELL strain/s by whole-genome sequencing.

Chapter 5 addresses the iSUC component of our iSUCCELL strategy, corresponding to the analysis of an intracellular sucrose pathway engineered previously in *S. cerevisiae*. The specific objectives of the work described in this chapter were:

- To evaluate the fermentation performance of a previously engineered iSUC strain during batch cultivations on sucrose, and to compare it with a reference strain that mainly hydrolyses sucrose extracellularly;

- To calculate physiological parameters from shake-flask cultivations for the iSUC and reference strains on sucrose;

- To evaluate the physiology of the iSUC strain in industry-like conditions, i.e., in a miniaturised system mimicking the Brazilian 1G fuel ethanol process using industrial sugarcane molasses with sulphuric acid treatment and cell recycling.

Chapters 6 and 7 provide a general discussion and some conclusions and lessons learned throughout this work.

2 NEITHER 1G NOR 2G FUEL ETHANOL: SETTING THE GROUND FOR A SUGARCANE-BASED BIOREFINERY USING AN iSUCCELL YEAST PLATFORM

Article published in FEMS Yeast Research (2020), Vol. 20, No. 4.

Pamela Magalí Bermejo[1], Vijayendran Raghavendran[2], and Andreas Karoly Gombert[1,*]

[1]School of Food Engineering, University of Campinas, Campinas, SP, Brazil; [2]Department of Molecular Biology and Biotechnology, Firth Court, Western Bank, University of Sheffield, Sheffield, S10 2TN, UK.

***Corresponding author:** University of Campinas, School of Food Engineering, Rua Monteiro Lobato 80, Campinas, SP, 13083-862, Brazil. Tel: +55-19-35214031. E-mail: gombert@unicamp.br

2.1 Abstract

First-generation (1G) fuel ethanol production in sugarcane-based biorefineries is an established economic enterprise in Brazil. Second-generation (2G) fuel ethanol from lignocellulosic materials, though extensively investigated, is currently facing severe difficulties to become economically viable. Some of the challenges inherent to these processes could be resolved by efficiently separating, and partially hydrolysing the cellulosic fraction of the lignocellulosic materials into the disaccharide cellobiose. Here we propose an alternative biorefinery, where the sucrose-rich stream from the 1G process is mixed with a cellobiose-rich stream in the fermentation step. The advantages of mixing are threefold: 1) decreased concentrations of metabolic inhibitors that are typically produced during pretreatment and hydrolysis of lignocellulosic materials; 2) decreased cooling times after enzymatic hydrolysis prior to fermentation; 3) decreased availability of free glucose for contaminating microorganisms. The iSUCCELL platform will be built upon the robust *Saccharomyces cerevisiae* strains currently present in 1G biorefineries, which offer competitive advantage in non-aseptic environments, and into which intracellular hydrolyses of sucrose and cellobiose will be engineered. It is expected that high yields of ethanol can be achieved in a process with cell recycling, lower contamination levels and decreased antibiotic use, when compared to current 2G technologies.

Keywords: *Saccharomyces cerevisiae*, sucrose, cellobiose, biorefinery, fuel ethanol.

2.2 Introduction

Sugarcane is considered the most efficient crop for fuel ethanol production and a major player in energy diversification and sustainable development. Production of fuel ethanol from a mixture of sugarcane juice and molasses has been termed first-generation (1G) ethanol, fuel ethanol or bioethanol. In this non-aseptic and anaerobic process, the yeast *Saccharomyces cerevisiae* converts sugars into ethanol with typical yields around 90% of the theoretical maximum, which is equal to 0.511 g ethanol per g of hexose equivalent. The fermentation medium, known as 'must' in the industrial jargon, is prepared by mixing sugarcane juice - the liquid stream obtained from directly milling sugarcane - and diluted molasses, a dark brown viscous liquid generated as a by-product of edible sugar production. The fibrous residue left after sugarcane juice extraction, known as bagasse, is normally burnt in furnaces, which, depending on the efficiency of the boiler, not only provides the energy necessary to run the biorefinery (in the form of high-pressure steam and electricity), but also generates revenue by exporting excess electricity to the national grid. Thus, in a typical Brazilian sugarcane-based biorefinery, three major products are generated: sugar, ethanol, and electricity. Normally, the bioethanol plants have excess production capacity installed, to allow some flexibility in the sugar to ethanol production ratio, which can be finetuned depending on the prices of these commodities in the international market. The current sugarcane-based biorefinery has been comprehensively discussed, from different perspectives, in several review articles (Abreu-Cavalheiro and Monteiro 2013; Della-Bianca *et al.* 2013; Furlan *et al.* 2013; Gombert and van Maris 2015; Lopes *et al.* 2016; Vaz 2017; Ceccato-Antonini 2018; Paulino de Souza *et al.* 2018).

The sugarcane plant is composed of stem and straw (green tops and dry leaves). The stem – used for milling to obtain the sugarcane juice – represents 80 to 85% of the total plant biomass (Carvalho-Netto *et al.* 2014), and consists of 70% water, 16% sugars, and 14% fibre (or bagasse), whereas the remaining fractions of sugarcane (straw) are composed of lignocellulose. Since the cost of this raw material represents a major part of the final production costs of fuel ethanol, it would be very important to utilise the entire sugarcane plant in a more efficient way. One of the most popular strategies targets the use of the lignocellulosic fraction of sugarcane for the production of ethanol in a so-called second-generation (2G) process (Soccol *et al.* 2010; Canilha *et al.* 2012; dos Santos *et al.* 2016).

In the 2G process, part of the cellulose/hemicellulose-rich sugarcane bagasse is diverted to produce additional volumes of ethanol, which occurs without any expansion of the cultivation area. For this to happen, the recalcitrant lignocellulosic matrix must be broken down and hydrolysed, before yeast can ferment the sugars. Naturally, this will come at the expense of electricity generation (Dias *et al.* 2011; Furlan *et al.* 2013; Tapia Carpio and Simone de Souza 2019). On the other hand, since nearly 95% of sugarcane is presently harvested mechanically in the Central-South region of Brazil (Bordonal *et al.* 2018) encompassing 91% of the total planted area, additional lignocellulosic biomass such as sugarcane leaves, has been made available in the recent years. Furthermore, in many industrial units, the boilers currently employed to convert heat to electricity could be replaced with more efficient variants, thereby less bagasse would have to be burnt to generate the same amount of electricity (Dias *et al.* 2016). To give a more quantitative impression, ethanol production could be increased up to 50%, if all the sugarcane bagasse and straw were fermented to ethanol (Somerville *et al.* 2010; Pereira *et al.* 2015).

There are two 2G sugarcane-based biorefineries currently in operation in Brazil, but they are still struggling financially. GranBio, located in Alagoas state (Northeast region) uses energycane as a raw material. Energycane accumulates less soluble sugars and has more fibre per hectare than conventional sugarcane. Raízen, located in São Paulo state (Southeast region) uses lignocellulosic residues from sugarcane as their raw material and the 2G process site is integrated with the 1G fuel ethanol producing unit. Some recent works have discussed the main aspects of 2G sugarcane-based biorefineries (dos Santos *et al.* 2016; Sindhu *et al.* 2016; Valdivia *et al.* 2016; Jansen *et al.* 2017; Polizeli *et al.* 2017).

Some of the challenges involved in the 2G process are: 1) pretreatment and hydrolysis of lignocellulosic biomass releases compounds, such as acetic acid, furfural, and hydroxymethylfurfural, among others, which inhibit yeast in a concentration-dependent manner (Taherzadeh, Niklasson and Lidén 1997; Taherzadeh *et al.* 2000; Jönsson, Alriksson and Nilvebrant 2013; Jönsson and Martín 2016); 2) enzymatic hydrolysis preceding the fermentation step is typically carried out at a higher temperature (45 to 50 °C) (Canilha *et al.* 2012; Zabed *et al.* 2017) than the fermentation step (30 to 35 °C) (Abdel-Banat *et al.* 2010; dos Santos *et al.* 2016), necessitating the cooling of the hydrolysate before yeast can be inoculated, resulting in decreased productivities and/or increased equipment costs; 3) high cost of the enzymes required for the hydrolysis of pretreated biomass (Klein-Marcuschamer *et al.* 2012; Liu, Zhang and Bao 2016); 4) decreased productivities (or increased fermentation

times), due to the preferential use of glucose by yeast, to the detriment of the remaining carbon sources present in the medium (e.g. xylose), which is still the case even for engineered strains (Kim *et al.* 2012; Jansen *et al.* 2017); 5) contamination events during fermentation, and the inherent need to rely on antibiotics (or other antimicrobials) to minimise the bacterial load, which leads to higher costs and also environmental and public health issues. Infection is a persistent issue in current 1G biorefineries (Shaw *et al.* 2016; Ceccato-Antonini 2018), and the presence of the universal carbon and energy source glucose in the medium certainly aggravates this problem.

In this mini review article, we propose an alternative strategy to the stand-alone 2G fuel ethanol process, successfully addressing some of the challenges listed above. The raw material would still be sugarcane, but the principle is to combine the process streams from 1G and 2G biorefineries to yield a mixed stream. The 1G stream remains the same as that in current sugarcane-based biorefineries: a mixture containing sugarcane juice and molasses with sucrose as the predominant sugar constituent. However, for the 2G stream, our strategy is to have a few upstream steps that can separate the lignin and the hemicellulosic fraction in sugarcane bagasse to yield a cellulose rich fraction for hydrolysis. This could be achieved e.g. by pretreating the biomass with organosolvents that can delignify and solubilise the hemicellulose fraction present in the biomass to yield cellulose rich solids that have better enzymatic digestibility (Sun *et al.* 2016; Zhang, Pei and Wang 2016; Matsakas *et al.* 2019). The further use or conversion of the lignin and hemicellulose fractions is outside the scope of this mini-review, but there are different proposals in the literature (Canilha *et al.* 2013; Ragauskas *et al.* 2014; Vardon *et al.* 2015; Beckham *et al.* 2016; Arora, Sharma and Kumar 2018; Liao *et al.* 2020). The cellulose rich fraction, in turn, can be partially hydrolysed to cellobiose, instead of a complete hydrolysis to glucose as is normally performed in a 2G process, since the iSUCCELL yeast chassis we propose here is capable of hydrolysing cellobiose into glucose (intracellularly). The partial hydrolysis of cellulose into cellobiose eliminates the cost of supplementing the enzyme cocktail with β-glucosidase (BGL, production cost ~ 310 USD/kg of enzyme), the key enzyme component that breaks down cellobiose to glucose (Ferreira, Azzoni and Freitas 2018). By mixing the 1G and 2G streams, the time required for cooling the 2G stream (typically around 50 °C) before fermentation (~ 30 °C) can commence, will be reduced. Furthermore, the concentration of metabolic inhibitors will decrease according to the mixing proportion. Finally, by hydrolysing cellulose incompletely, the release of glucose is minimised, creating a less favourable environment for

the spread of contaminants, and avoiding the undesired effects of glucose repression over the consumption of other carbon sources by yeast.

We name our strategy iSUCCELL, for intracellular sucrose and cellobiose utilisation and it uses a mixture of 1G stream and partially hydrolysed 2G stream. This is achieved by metabolic engineering of industrial yeast strains that have better tolerance to metabolic inhibitors than wild or laboratory strains and have a favourable track record in non-aseptic processes with cell recycling including acid treatment. This is accomplished by introducing active transport systems for sucrose and cellobiose, followed by their hydrolysis in the cytosol via intracellular invertase and heterologously expressed BGL. The intracellular hydrolysis avoids/decreases the release of glucose in the extracellular environment and results in increased ethanol yield on sugars due to different energy conservation schemes (Basso *et al.* 2011). It should be noted, though, that a techno-economic assessment of this strategy is out of the scope of this article.

2.3 The concept of a sugarcane-based biorefinery using iSUCCELL yeast chassis

2.3.1 Process-related aspects

The emergence of lignocellulosic ethanol contributed enormously to our current vision of a biorefinery. Nowadays, research initiatives on sugarcane-based 2G ethanol are oriented towards a synergy with the 1G process, aiming at promoting the transition of Brazilian bioethanol plants into true biorefineries, with the ability to process all fractions of sugarcane and the potential to produce other, higher-value compounds. The integration of the sugarcane-based 2G process into the 1G sites already in place has shown advantages over stand-alone 2G technologies, improving the overall efficiency and energy balance of the plant (Dias *et al.* 2012; MacRelli, Mogensen and Zacchi 2012; Erdei *et al.* 2013; Lennartsson, Erlandsson and Taherzadeh 2014; Losordo *et al.* 2016). Process integration benefits from unit operations that are common to both 1G and 2G processes. Moreover, the availability of sugarcane bagasse on-site reduces cost and operational issues related to logistics, transportation, and storage of the lignocellulosic material (Soccol *et al.* 2010; Dias *et al.* 2012; Furlan *et al.* 2013; Losordo *et al.* 2016). Although there is a necessity to leave part of the straw in the field to augment soil carbon and to reduce soil erosion and water loss (Leal *et al.* 2013), a small portion of this straw could be transported to the plant and used in the boilers for cogeneration while the rest is diverted towards ethanol production (Dias *et al.* 2011; Furlan *et al.* 2013).

Different configurations have been evaluated for an integrated sugarcane-based 1G+2G fuel ethanol process, which include different combinations of the fermentation medium. A 1G+2G sugar stream can be generated by mixing sugarcane juice with either the hydrolysed C6 liquor (SJ+C6) (Dias *et al.* 2012; Furlan *et al.* 2013; Mariano *et al.* 2013), the hydrolysed C6 and C5 liquors (SJ+C6+C5) (Dias *et al.* 2013), or molasses and the C5 liquor (SJ+M+C5) (Losordo *et al.* 2016). Regardless of the configuration adopted, the 2G fraction requires prior pretreatment and hydrolysis to release the sugars before being mixed with the 1G sugar stream. The commercial enzyme preparations currently available for these applications contain a mixture of hydrolytic enzymes collectively known as cellulases and hemicellulases, although a set of other ancillary enzymes have also been identified as important accessory proteins (Sun *et al.* 2015). The cellulase complex, mostly produced from mutant strains of the fungus *Trichoderma reesei*, includes three types of enzymes working in a synergistic manner: endoglucanases (EGs), cellobiohydrolases (exoglucanases, CBHs), and BGLs. As a result of

the action of EGs and CBHs on cellulose, the disaccharide cellobiose is released as the main product, before being further hydrolysed into glucose by BGLs. Cellobiose is a strong inhibitor of both EGs and CBHs, and BGL alleviates this inhibition by cleaving cellobiose into two glucose molecules (Singhania *et al.* 2013). However, the BGL activity of *T. reesei* is also limited by its own product-inhibition from glucose (Chen, Hayn and Esterbauer 1992). Traditional commercial cellulase preparations, such as Spezyme® CP (Genencor) and Celluclast® 1.5L (Novozymes), contain low amounts of BGLs, causing the accumulation of cellobiose and subsequent product-inhibition of cellulases (Berlin *et al.* 2007; Pryor and Nahar 2010; Hu, Arantes and Saddler 2011; Qing and Wyman 2011; Agrawal *et al.* 2015, 2018; Rodrigues *et al.* 2015). Hence, to overcome this limitation and improve the rate and extent of saccharification, these commercial formulations are commonly blended with additional BGL, generally sourced from Aspergilli, such as the commercial BGL preparation Novozyme 188 (Berlin *et al.* 2007; Hu, Arantes and Saddler 2011; Zhai, Hu and Saddler 2016), which despite being less sensitive to feedback inhibition (Riou *et al.* 1998; Decker, Visser and Schreier 2001; Rajasree *et al.* 2013), represents additional costs to the process (Liu, Zhang and Bao 2016; Ferreira, Azzoni and Freitas 2018). Strategies to alleviate inhibition of cellulases by cellobiose or glucose via site-directed mutagenesis are being extensively investigated (Atreya, Strobel and Clark 2016; Guo, Amano and Nozaki 2016). The newest generations of cocktails, e.g Cellic CTec® series (Novozymes) and Accellerase® 1500 (Genencor), have improved significantly, containing many accessory enzymes leading to improved sugar conversions. Nevertheless, the cost of enzymes for manufacturing low value-added products such as ethanol is still significant and needs to be minimised.

In 2G processes, complete degradation of cellulose into glucose is a requirement since *S. cerevisiae* is not capable of utilising partially hydrolysed cellulose or cellodextrins (Lynd *et al.* 2002). However, in the last few years a paradigm involving partial hydrolysis of cellulose has begun to emerge (Galazka *et al.* 2010; Chen 2015; Parisutham *et al.* 2017), involving yeast platforms that can assimilate cellodextrins directly. Yet, intensive efforts in strain engineering and optimisation are mandatory to unravel ways to integrate the heterologous pathway into the endogenous metabolism, since process parameters such as high yield and productivity as well as strain robustness are vital for the success of this endeavour (Chen 2015).

The concept of an integrated 1G+2G fuel ethanol process and the approach of partial cellulose hydrolysis can be combined into a new type of sugarcane-based biorefinery, which can

deliver fuel ethanol from the 1G+cellobiose-rich sugar streams, as well as offer possibilities for product diversification from the C5 and lignin-rich fractions of sugarcane bagasse (Rabelo *et al.* 2011; Mariano *et al.* 2013; Ferreira Silva *et al.* 2014; Vardon *et al.* 2015; Beckham *et al.* 2016; Arora, Sharma and Kumar 2018; Unrean and Ketsub 2018) (Figure 2.1), opening the doors for new markets, spreading the risks, and increasing revenues (UNCTAD 2016).

The 1G stream, prepared by mixing sugarcane juice and molasses at various proportions, contains different concentrations of minerals, organic nutrients, and toxic compounds. While the juice is minerals-deficient (11-16% of total sugars on a wet-weight basis, with ~90% of sucrose and ~10% of glucose and/or fructose), molasses provides a minerals-rich syrup with up to 65% (w/w) of total sugars, with approximately 80% sucrose and ~20% glucose and fructose, in equal proportions (Wheals *et al.* 1999; Lino, Basso and Sommer 2018). On the other hand, it is expected that a typical 2G stream generated using commercial BGL-poor cellulase cocktails, e.g. Celluclast® 1.5L, on a mixture of pretreated sugarcane bagasse and straw, will release glucose with a ~30% yield (w/w) (Ávila, Forte and Goldbeck 2018). Thus, considering the numbers above, in the process proposed here, the 1G+cellobiose-rich stream would consist mainly of sucrose and cellobiose (C12 sugars), together with small amounts of monosaccharides (glucose and fructose, C6 sugars).

Since both sugar streams are processed at different temperatures (~30 °C for the 1G stream and ~50 °C for the cellobiose-rich stream), their mixture would decrease not only the cooling time necessary for subsequent fermentation to start, but also the energy and water usage. Furthermore, a mixed 1G+cellobiose-rich broth would decrease the stress imposed on yeast by inhibitors that are formed during lignocellulosic pretreatment, compared to a conventional 2G process, due to dilution of the cellobiose-rich (hydrolysate) stream with the 1G stream, vastly improving yeast performance (de Andrade *et al.* 2013; Erdei *et al.* 2013).

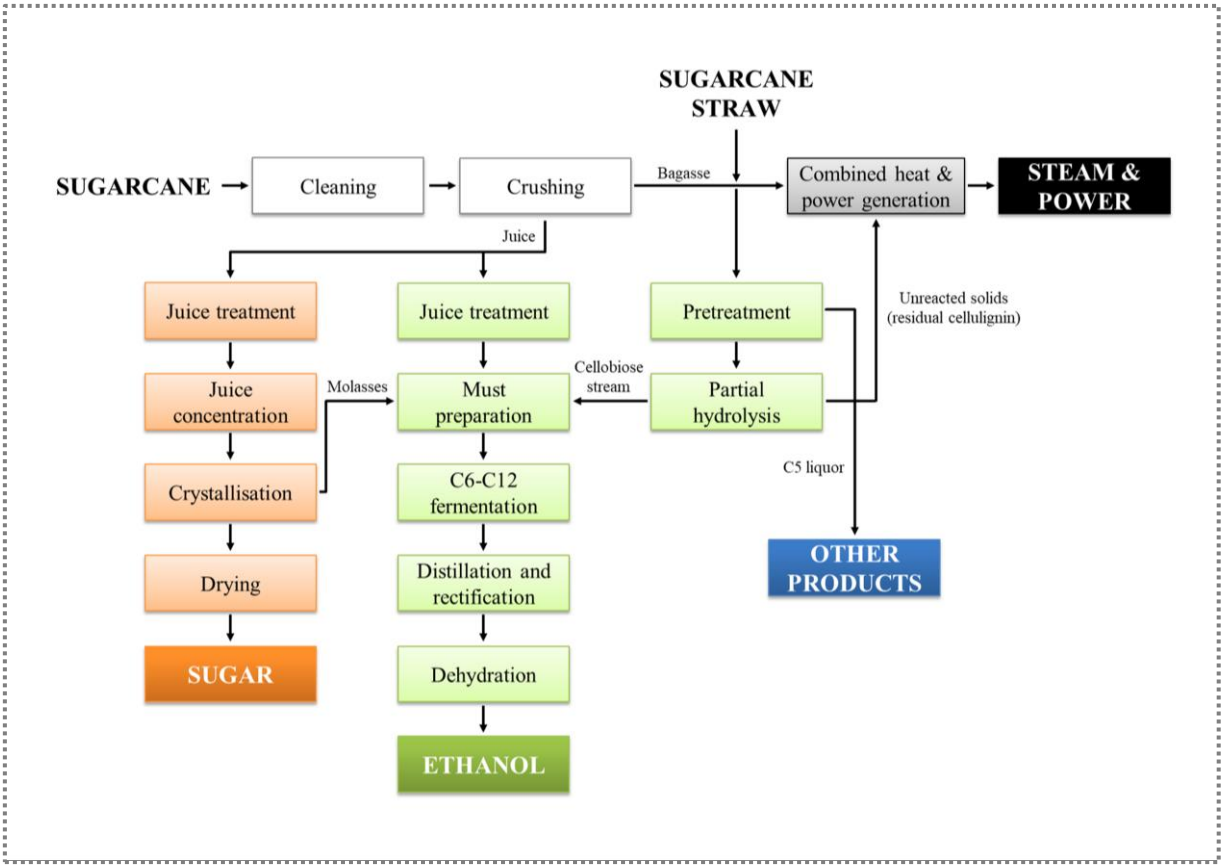

Figure 2.1. Schematic representation of a sugarcane-based biorefinery, in which the iSUCCELL yeast platform proposed here is applied (in the C6-C12 fermentation step). For this to occur, after cracking of lignocellulose, the cellulosic fraction is only partially hydrolysed to cellobiose, which is mixed with the 1G stream (Juice treatment). The end products of the biorefinery are highlighted (dark coloured rectangles). Adapted from Mariano *et al*. 2013.

2.3.2 Yeast-related aspects

The new sugarcane-based biorefinery proposed here requires new yeast platforms capable of both utilising the different sugars and tolerating the inhibitors present in the combined 1G+cellobiose-rich stream. Although this could be accomplished by different strategies, we propose the iSUCCELL platform, where sucrose and cellobiose are metabolised via active transport and intracellular hydrolysis using an engineered yeast (Figure 2.2). This approach involves the release of monomers inside the cell, and relies on the use of current industrial strain backgrounds commonly found in sugarcane-based biorefineries for metabolic engineering, due to their inherent robustness under industrial conditions (Basso *et al.* 2008; Della-Bianca and Gombert 2013; Della-Bianca *et al.* 2014). The advantages of this strategy in the context of yeast metabolism and process feasibility are summarised in Table 2.1.

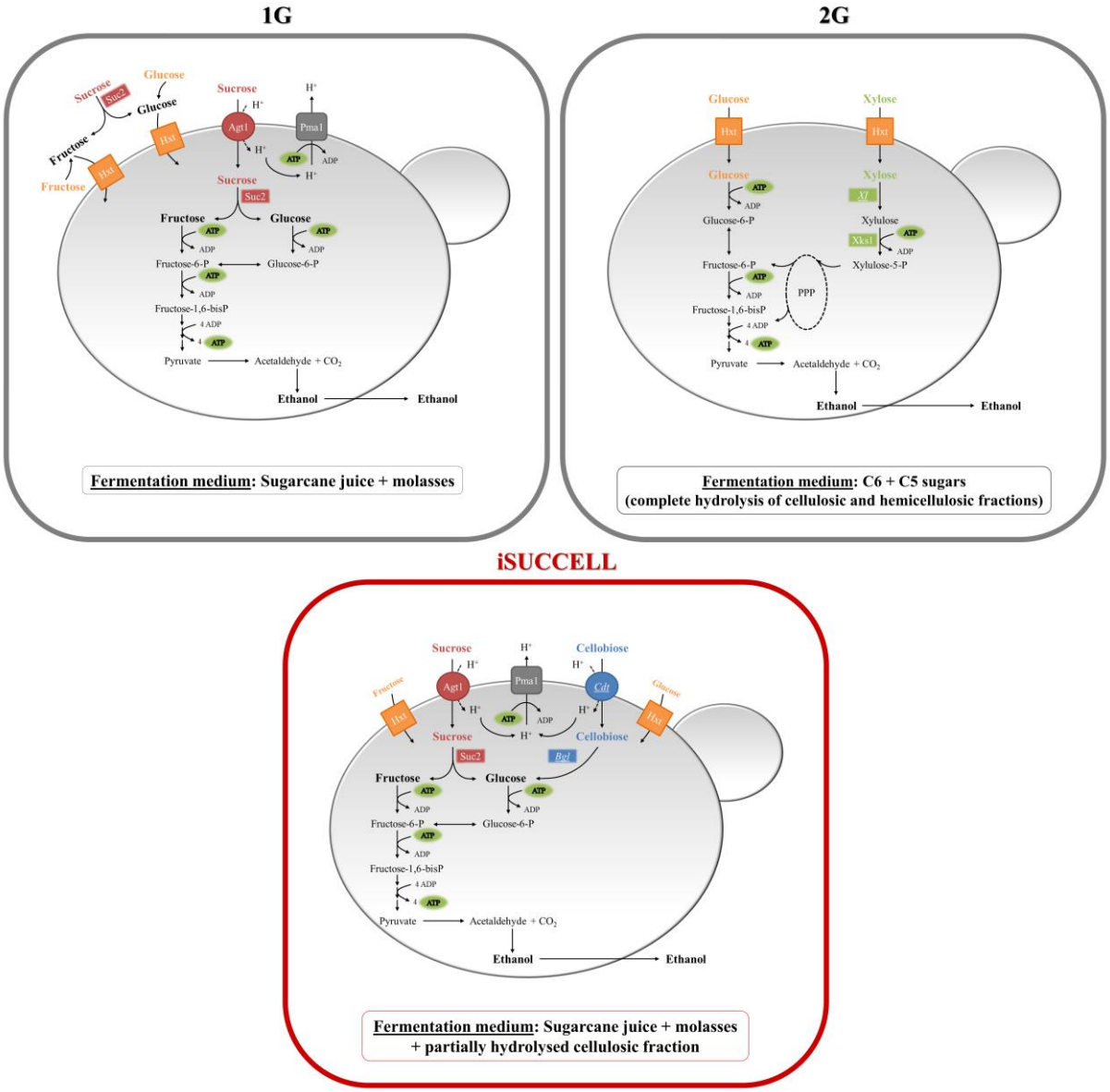

Figure 2.2. Comparison between yeast strains from 1G and 2G processes with the iSUCCELL yeast proposed as platform strain for an integrated sugarcane-based fuel ethanol process involving partial cellulose hydrolysis to cellobiose. The 1G fermentation medium contains C12 (sucrose) and some C6 (glucose and fructose) sugars. The 2G medium presented here consists of a typical stream containing C6 (glucose) and C5 (xylose) sugars as a result of a complete hydrolysis of the cellulosic and hemicellulosic fractions. The engineered 2G strain expresses a heterologous xylose isomerase (XI) to convert xylose into xylulose, which is subsequently phosphorylated into xylulose-5-phosphate by native xylulokinase (Xks1). The fermentation medium for the iSUCCELL yeast contains C12 (sucrose and cellobiose) and small amounts of C6 (glucose and fructose) sugars, as a result of a combined 1G+cellobiose-rich medium. Sucrose and cellobiose uptake are mediated by sucrose and cellobiose-H^+ symporters (Agt1 and Cdt, respectively) followed by hydrolysis of the disaccharides via intracellular hydrolases (Suc2 and Bgl, respectively) and H^+ extrusion by the plasma membrane ATPase Pma1. Uptake of glucose, fructose and xylose is mediated by native hexose transporters (Hxt). The iSUCCELL strain conserves 3 ATP for each disaccharide (sucrose or cellobiose) consumed, which results from glycolysis via the Embden-Meyerhof glycolytic pathway (+4 ATP/disaccharide) and H^+ extrusion via Pma1 (-1 ATP/disaccharide). Heterologous proteins are indicated by names in *italics* and underlined. PPP: non-oxidative pentose-phosphate pathway.

Table 2.1. Process and yeast-related advantages of an integrated sugarcane-based biorefinery using iSUCCELL yeast chassis.

Process or yeast-related challenges for fuel ethanol production	Advantage of the integrated sugarcane-based biorefinery using iSUCCELL yeast chassis
Different process temperature for ligno-cellulose hydrolysis (~50 °C) and fermentation (~30 °C)	A mixed 1G+cellobiose-rich stream reduces the cooling time between saccharification and fermentation, increasing productivity and/or saving equipment costs*
Operational costs owing to the use of enzymes	Supplementation with additional BGL in the cocktail is not required
High concentration of inhibitors in the 2G stream	A mixed 1G+cellobiose-rich stream dilutes the inhibitors' concentrations, minimising their harmful effects on yeast*
High incidence of bacterial contamination during fermentation	The intracellular hydrolysis of sucrose and cellobiose minimises the accumulation of extracellular glucose, reducing both the level and diversity of contaminants and subsequently the use of antibiotics and other antimicrobials
Ethanol yield on sugars	Active transport of sucrose and cellobiose present in the mixed stream, followed by intracellular hydrolysis to ethanol and CO_2, yields 3 net ATP/disaccharide, whereas their metabolism by extracellular hydrolysis leads to 4 ATP/disaccharide**. This decreased ATP yield leads to a higher fraction of the substrate being converted into ethanol (Basso *et al.* 2011)
Fructose accumulation leads to incomplete 1G fermentation because of low affinity of hexose transporters for fructose	When sucrose is hydrolysed intracellularly, the presence of unutilised extracellular fructose is minimised (Berthels *et al.* 2004)
Strain robustness	Use of robust industrial strains (commonly found in sugarcane-based 1G ethanol plants) as chassis for the iSUCCELL strategy eliminates the need to engineer alternative yeast strains (Della-Bianca and Gombert 2013; Pereira *et al.* 2014; Cola *et al.* 2020). Many of the strains currently employed in the Brazilian fuel ethanol industry are diploid (Della-Bianca *et al.* 2013) and should be amenable to engineering using e.g. CRISPR, capitalising on their innate robustness.

* These advantages do not rely exclusively on the iSUCCELL approach and could in principle be met by any other strategy involving an integrated 1G+2G process.

** Glucose and fructose fermentation into ethanol and CO_2 yields 2 ATP per mole of hexose. Thus, 4 ATP are formed when sucrose or cellobiose are metabolised via extracellular hydrolysis. When these disaccharides are metabolised via intracellular hydrolysis, 1 ATP per disaccharide is required to expel the H^+ that is taken up by the sucrose or cellobiose-H^+ symporters, reducing the total ATP yield to 3 ATP for each disaccharide.

2.4 Engineering the iSUCCELL yeast chassis for a new sugarcane-based biorefinery

2.4.1 Disaccharide utilisation by *S. cerevisiae*

Disaccharides such as sucrose (α-D-glucopyranosyl-(1→2)-β-D-fructofuranoside or β-D-fructofuranosyl-(2→1)-α-D-glucopyranoside), maltose (α-D-glucopyranosyl-(1→4)-α-D-glucopyranose), cellobiose (β-D-glucopyranosyl-(1→4)-β-D-glucopyranose) and lactose (β-D-galactopyranosyl-(1→4)-β-D-glucopyranose) are commonly encountered glucosides in yeast biotechnology. There is evidence that at least 151 yeast species are capable of fermenting sucrose, whereas 827 can grow on this sugar and 859 can grow on cellobiose, from a total of 1270 species tested for these phenotypes (Kurtzman, Fell and Boekhout 2011). In *S. cerevisiae*, the utilisation of sucrose is quite peculiar, since this sugar can be hydrolysed both extra- and intracellularly. In contrast, the utilisation of maltose (another α-glucoside) in *S. cerevisiae* is exclusively intracellular. Interestingly, β-glucosides such as cellobiose and lactose are not natural substrates for *S. cerevisiae* owing to the absence of assimilatory pathways.

2.4.2 The iSUC component

Due to the importance of sucrose as a substrate for industrial biotechnology, the metabolism of this sugar in yeast has interested the scientific community for decades. More recently, aspects involving sucrose and *S. cerevisiae* have been reviewed by (Marques *et al.* 2016). Sucrose catabolism in *S. cerevisiae* is initiated by either its hydrolysis outside the cells via invertase (encoded by the *SUC2* gene) - followed by assimilation of glucose and fructose via facilitated diffusion - or active transport of sucrose across the plasma membrane via sucrose-H^+ symporters, in which case it is followed by hydrolysis within the intracellular environment using the cytosolic form of invertase (Santos *et al.* 1982; Stambuk *et al.* 1999; Batista, Miletti and Stambuk 2004). Besides invertase, at least two additional sucrose-hydrolysing enzymes classified as α-glucosidases have been identified in *S. cerevisiae*, namely maltases (Malx2) (Khan, Zimmermann and Eaton 1973) and isomaltases (Imax) (Marques *et al.* 2017). Additionally, different permeases have been identified as sucrose-H^+ symporters in *S. cerevisiae*: a general α-glucoside-H^+ symporter encoded by the *AGT1* gene (which is different from the *MAL11* gene, in contrast to what is reported in the yeastgenome.org database

(Trichez *et al.* 2019)), and the maltose-H^+ symporters encoded by *MALx1* genes (where *x* represents the locus number) (Stambuk *et al.* 1999; Stambuk, Batista and de Araujo 2000).

These two modes of sucrose metabolism (extra- or intracellular) in *S. cerevisiae* have different energetics, a feature which has been explored by researchers to improve product yields on sucrose. When sucrose is fermented via the extracellular pathway, 4 mol ATP are formed per mol of sucrose, while only 3 mol ATP (25% lower) are produced when one mol of sucrose is metabolised intracellularly (Figure 2.2). This difference in ATP yield is due to the energy requirement of the proton-coupled symporter, which leads to the indirect expenditure of 1 ATP per proton taken up along with sucrose to maintain pH homeostasis in the cytoplasm and the proton motive force across the plasma membrane. Theoretically, a decrease in the ATP yield will divert a higher fraction of the carbon-source towards ethanol formation, thus increasing the ethanol yield on sucrose compared to its fermentation via the extracellular pathway. This fundamental concept was indeed demonstrated by Basso and collaborators (Basso *et al.* 2011) in a strategy that involved metabolic and evolutionary engineering approaches, resulting in a strain that displayed an 11% higher ethanol yield on sucrose, when compared to the parental strain, which mainly metabolised sucrose via the extracellular pathway. After molecular analysis of the improved phenotype, the authors revealed that up-regulation and duplication of the *AGT1* gene had occurred.

It can also be envisaged that intracellular sucrose hydrolysis (iSUC) might have additional advantages in the context of industrial sugarcane-based processes. Since fructose utilisation in *S. cerevisiae* is less favoured than glucose utilisation, unconsumed fructose is often found at the end of fermentation processes, which represents economic losses (Berthels *et al.* 2004). Furthermore, the presence of extracellular fructose may favour the proliferation of heterofermentative bacteria in the context of Brazilian sugarcane-based biorefineries. This type of contaminants showed preference for this sugar, over glucose, in cultures containing equal amounts of both monosaccharides (Basso *et al.* 2014). Thus, the intracellular sucrose assimilation route prevents the direct formation of fructose in the extracellular environment, potentially minimising this problem. Some fructose might still diffuse out into the medium if it is not rapidly metabolised. Thus, metabolic engineering of downstream steps in metabolism, such as overexpression of hexokinase, might be necessary to circumvent this potential issue.

2.4.3 The iCELL component

Cellobiose utilisation by *S. cerevisiae* can only be achieved by genetically modifying this organism. Analogously to sucrose metabolism, cellobiose utilisation can be accomplished by either extracellular hydrolysis and internalisation of the monosaccharides released or via import of the disaccharide and intracellular hydrolysis/phosphorolysis. The hydrolytic reaction (regardless of the location) is performed by BGLs. To achieve cellobiose utilisation, initial studies focused on expressing secretable or surface-displayed BGLs from diverse yeast and fungal origins (Machida *et al.* 1988; McBride *et al.* 2005; van Rooyen *et al.* 2005; Guo *et al.* 2011). However, these strategies generate extracellular glucose, which can have at least the following consequences: 1) higher risk of bacterial contamination (mainly in non-aseptic processes); 2) repression of the catabolism of other sugars present in the medium, and 3) end product inhibition of BGLs by glucose.

In 2010, Galazka *et al*. reported for the first time a *S. cerevisiae* strain expressing an intracellular cellobiose-metabolising pathway consisting of a cellodextrin transporter (CDT-1 or CDT-2) and a BGL (GH1-1) from the cellulolytic fungus *Neurospora crassa*. The engineered strains were able to grow on cellobiose and on longer cellodextrins, as well as to produce ethanol (Galazka *et al.* 2010). Despite the slow performance of the engineered strains, this breakthrough study paved the way for numerous publications aiming at developing efficient biocatalysts for cellobiose fermentation. One of the approaches aimed at exploring novel cellodextrin transporters and intracellular BGLs in order to confer *S. cerevisiae* cells the ability to ferment cellobiose more efficiently. In this regard, diverse cellobiose permeases from yeast or from other fungi different from *N. crassa* have been successfully expressed in *S. cerevisiae* (Sadie *et al.* 2011; Ha *et al.* 2013b; Li *et al.* 2013; Zhang *et al.* 2013; Bae *et al.* 2014; dos Reis *et al.* 2016; Casa-Villegas, Polaina and Marín-Navarro 2018; Nogueira *et al.* 2018), as well as alternative intracellular BGLs from yeast, bacteria and fungi (Bae *et al.* 2014; Fan *et al.* 2016; Casa-Villegas, Polaina and Marín-Navarro 2018) (Table 2.2).

Table 2.2. Cellobiose fermentation performances of different engineered *S. cerevisiae* strains.

Strain	Background	Genes	Gene origin	Genetic construction	Culture medium	Growth conditions	Improvements post-metabolic engineering?	Growth rate [1/h]	Cellobiose consumption rate [g/(L·h)]	Ethanol production rate [g/(L·h)]	Ethanol yield on cellobiose [g/g]	Reference
No name	YPH499 (Auxo, Lab)	*cdt-1*; *gh1-1*	*Neurospora crassa*; *Neurospora crassa*	*pPGK1-cdt-1-Myc-tag-tCYC1* (pRS426); *pPGK1-gh1-1-His-tag-tCYC1* (pRS425)	YNB + Drop-out mix + 2% cellobiose	30 °C, anaerobic, $OD_{initial} = 2.0$	No	NS	≈ 0.167[a]	≈ 0.075[a]	0.441 ± 0.001 g_{et}/g_{glu}	Galazka *et al.* (2010)
IBP1	CICIMY0086 (Polyploid, Ind)	*bglP*; *BGL1*	*Bacillus subtilis*; *Saccharomycopsis fibuligera*	*pPGK1-bglP-tPGK1* (pMGKR, integ); *pPGK1-BGL1-tPGK1* (pMGKR, integ)	YP + 1% cellobiose	30 °C, 150 rpm, aerobic, $OD_{initial} = 0.45$	No	0.11 ± 0.005	0.139[b]	NS	NS	Guo *et al.* (2011)
D801-130	D452-2 (Auxo, Lab)	*cdt-1*; *gh1-1*	*N. crassa*; *N. crassa*	*pPGK1-cdt-1-tCYC1* (pRS426); *pPGK1-gh1-1-tCYC1* (pRS425)	YP + 4% cellobiose	30 °C, oxygen-limited, $OD_{initial} = 1$	No	NS	1.667[b]	0.7	0.42	Ha *et al.* (2011a)
D452-2ET	D452-2 (Auxo, Lab)	*cdt-1*; *gh1-1*	*N. crassa*; *N. crassa*	*pPGK1-cdt-1-tCYC1* (pRS426); *pPGK1-gh1-1-tCYC1* (pRS425)	YP + 4% cellobiose	NS	No	NS	NS	0.37 ± 0.01	0.34 ± 0.01	Ha *et al.* (2011b)
CTY-C59	Classic Turbo Yeast (Ind)	*cdt-1*; *gh1-1*	*N. crassa*; *N. crassa*	*pENO2-cdt-1-tPGK1*; *pPDC1-gh1-1-tADH1* (pRS-kanMX, single-copy plasmid)	YP + 8% cellobiose	30 °C, 100 rpm, oxygen-limited, $OD_{initial} = 1$	Combinatorial transcriptional engineering	NS	2.18	0.74	0.39	Du *et al.* (2012)
R2	Classic Turbo Yeast (Ind)	Mutant *cdt-1*; Mutant *gh1-1*	*N. crassa*; *N. crassa*	*pTEF1-cdt-1-tPGK1*; *pPYK1-gh1-1-tADH1* (pRS-kanMX, single-copy plasmid)	YP + 8% cellobiose	30 °C, 100 rpm, oxygen-limited, $OD_{initial} = 0.2$	Directed Evolution	0.102 ± 0.002	2.65 ± 0.02	1.00 +/− 0.03	0.436 ± 0.004	Eriksen *et al.* (2013)
MT8-1/δCDTiBGL	MT8-1 (Auxo, Lab)	*cdt-1*; *BGL1*	*N. crassa*; *Aspergillus aculeatus*	*pPGK1-cdt-1-tPGK1* (pδU, integ); *pPGK1-gh1-1-tPGK1* (pδU, integ)	YP + 2% cellobiose	30 °C, mild agitation	No	NS	1.542[b]	0.533[b]	NS	Yamada *et al.* (2013)
#9-1-18	Classic Turbo Yeast (Ind)	*cdt-1*; *gh1-1*	*N. crassa*; *N. crassa*	*pENO2-cdt-1-tPGK1*; *pPDC1-gh1-1-tADH1* (pRS-KanMX, single-copy plasmid)	YP + 0.01% adenine hemisulfate + 8% cellobiose	30 °C, 100 rpm, oxygen-limited, $OD_{initial} = 1$	Directed Evolution + promoter engineering	NS	2.50 ± 0.21	0.89 ± 0.01	0.37 ± 0.01	Yuan et al., (2013)
No name	D452-2 (Auxo, Lab)	Mutant *cdt-1* (F213L); *SdCBP*	*N. crassa*; *Saccharophagus degradans*	*pRS426-cdt-1-GFP-tCYC1*; *pPGK1-SdCBP-tCYC1* (pRS425)	YP + 8% cellobiose	30 °C, oxygen-limited, $OD_{initial} = 1$	Evolutionary engineering	NS	1.72 ± 0.11	0.74 ± 0.05	0.44	Ha *et al.* (2013a)
HXT2.4(A291E)	D452-2 (Auxo, Lab)	Mutant *HXT2.4* (A291E); *gh1-1*	*Scheffersomyces stipitis*; *N. crassa*	*pPGK1-HXT2.4-tCYC1* (pRS426); *pPGK1-gh1-1-tCYC1* (pRS425)	YP + 8% cellobiose	30 °C, oxygen-limited, $OD_{initial} = 1$	Site-directed mutagenesis	NS	3.18	1.16	NS	Ha *et al.* (2013b)
JAY291-BTT	JAY291 (Auxo, haploid-derived Ind)	*cdt-1*; *gh1-1*	*N. crassa*; *N. crassa*	*pPGK1-gh1-1-tCYC1-pPGK1-cdt-1-tCYC1-pPGK1-cdt-1-tCYC1* (pRS425)	YP + 8% cellobiose	30 °C, oxygen-limited, $OD_{initial} = 1$	No	NS	2.30	0.87	NS	Ha *et al.* (2013c)

Table 2. Continued.

Strain	Background	Genes	Gene origin	Genetic construction	Culture medium	Growth conditions	Improvements post-metabolic engineering?	Growth rate [1/h]	Cellobiose consumption rate [g/(L·h)]	Ethanol production rate [g/(L·h)]	Ethanol yield on cellobiose [g/g]	Reference
Pc ST/Tt BG	D452-2 (Auxo, Lab)	Pc_ST; Tt_BG	*Penicillium chryso-genum*; *Thielavia terrestris*	*pGPD-Pc_ST* (p423); *pGPD-Tt_BG* (p425)	YP + 4% cellobiose	30 °C, 80 rpm	No	NS	1.02 ± 0.06	0.30 ± 0.01	0.38 ± 0.01	Bae *et al.* (2014)
D452-2	D452-2 (Auxo, Lab)	Mutant *cdt-1* (F213L); *SdCBP*	*N. crassa*; *S. degradans*	*pPGK1-cdt-1-GFP-tCYC1-pPGK1-SdCBP-tCYC1* (pRS426)	1.7 g/L YNB + Drop-Out mix + 10 g/L $(NH_4)_2SO_4$ + 1 g/L $MgSO_4 . 7H_2O$ + 6 g/L KH_2PO_4 + 100 mg/L adenine hemisulfate + 10 mg/L inositol + 100 mg/L glutamic acid + 20 mg/L lysine + 375 mg/L serine + 0.1 M 2-(N-morpholino) ethanesulfonic acid (MES) + 8% cellobiose (pH 6.0)	30 °C, 220 rpm, strict anaerobic, $OD_{initial} = 20$	Evolutionary engineering (in previous report)	NS	3.6 ± 0.05	1.5 ± 0.03	NS	Chomvong *et al.* (2014)
DCDT-1G	D452-2 (Auxo, Lab)	*cdt-1*; *gh1-1*	*N. crassa*; *N. crassa*	*pPGK1-cdt-1-tCYC1* (pRS426); *pPGK1-gh1-1-tCYC1* (pRS425)	YP + 8% cellobiose	30 °C, 100 rpm, oxygen-limited, $OD_{initial} = 1$	No	NS	≈ 2.21[b]	0.53 ± 0.01	0.39 ± 0.01	Kim *et al.* (2014a)
HHT	INVSc1 (Auxo, Lab)	Mutant *cdt-2* (Q207H/N311H/I505T); *gh1-1*	*N. crassa*; *N. crassa*	*pPYK1-gh1-1-tADH1-pTEF1-cdt-2-tPGK1* (pRS415)	YP + 420 mg/L Tween-80 + 10 mg/L ergosterol + 2% cellobiose	30 °C, anaerobic, $OD_{initial} = 10$	Directed evolution	NS	2.7 ± 0.02	1.1 ± 0.01	0.45 ± 0.01	Lian *et al.* (2014)
SyBE001603	SyBE001601 (Ind)	*cdt-1*; *gh1-1*	*N. crassa*; *N. crassa*	*pPGK1-cdt-1-tCYC1-pPGK1-gh1-1-tCYC1* (pRS426)	YP + 8% cellobiose (pH 5.5)	39 °C, 200 rpm, oxygen-limited, biorreator, $OD_{initial} = 1$	Evolutionary engineering	NS	3.04	1.50	0.49	Hu *et al.* (2016)
EJ2	D452-2 (Auxo, Lab)	*cdt-1*; *gh1-1*	*N. crassa*; *N. crassa*	*pPGK1-cdt-1-tCYC1* (pRS406, integ); *pPGK1-gh1-1-tCYC1* (pRS405, integ)	YP + 8% cellobiose	30 °C, 100 rpm, oxygen limited, $OD_{initial} = 1$	Evolutionary engineering	NS	2.73 ± 0.01	1.09 ± 0.00	0.40 ± 0.00	Oh *et al.* (2016)
DCT-2m	D452-2 (Auxo, Lab)	Mutant *cdt-2* (N309I); *SdCBP*	*N. crassa*; *S. degradans*	*pPGK1-cdt-2-tCYC1* (pRS426); *pPGK1-SdCBP-tCYC1* (pRS425)	YP + 8% cellobiose	30 °C, 100 rpm, oxygen limited, $OD_{initial} = 1$	Evolutionary engineering	NS	NS	0.70 ± 0.01	0.42 ± 0.01	Kim *et al.* (2018)
CEN-4B5BT	CEN.PK2-1D (Auxo, Lab)	*cdt-1*; *gh1-1*	*N. crassa*; *N. crassa*	*pPGK1-cdt-1-tCYC1* (pRS426); *pPGK1-gh1-1-tCYC1* (pRS424); *pPGK1-gh1-1-tCYC1* (pRS425)	YNB + Drop-out mix + 2% cellobiose (pH 5.5)	30 °C, 100 rpm, $OD_{initial} = 1$	No	NS	NS	0.36 ± 0.01	0.33 ± 0.01	Kim *et al.* (2019)

*only strains that hydrolyse cellobiose intracellularly are listed here; for each reference only the best performing strain is presented

NS: not specified.

[a]our calculation based on plotted data at 120 h.

[b]our calculation based on reported data.

Auxo: Auxotrophic; Ind: Industrial; Lab: Laboratory.

Besides cellobiose hydrolysis, BGLs may also catalyse a transglycosylation reaction (Bohlin *et al.* 2013), as transient accumulation of extracellular cellodextrins was observed during cellobiose-xylose co-fermentation (Ha *et al.* 2011a). Transglycosylation might be triggered when cells accumulate high levels of intracellular cellobiose (Kim *et al.* 2014a). Although the accumulated cellodextrins can be reutilised later on, the productivity of the overall process may be compromised due to the slower uptake of cellodextrins compared to cellobiose (Ha *et al.* 2011a). Hence, intracellular BGLs with reduced transglycosylation activities are crucial for better utilisation of cellobiose.

Much success has been achieved with the heterologous expression of the *N. crassa* pathway in *S. cerevisiae* (CDT-1 + GH1-1), followed by laboratory evolution (Wei *et al.* 2015; Hu *et al.* 2016; Oh *et al.* 2016) or combinatorial engineering approaches (Du *et al.* 2012; Eriksen *et al.* 2013; Yuan and Zhao 2013) (Table 2.2). Interestingly, the improved phenotypes reported by (Du *et al.* 2012; Yuan and Zhao 2013; Hu *et al.* 2016), regardless of the methodology employed, involved strains with higher mRNA levels of CDT-1 and GH1-1, compared to the parental strains, indicating a dose-dependent behaviour. Moreover, besides absolute values, an optimised GH1-1/CDT-1 gene expression ratio in the improved strains were also critical. This adjusted ratio probably led to a decreased intracellular accumulation of cellobiose, consequently decreasing the transglycosylation activity of GH1-1 and the cellodextrin accumulation in the medium (Hu *et al.* 2016; Oh *et al.* 2016). In accordance with this, two studies from the same lab reported that their evolved strains harboured higher copy numbers of CDT-1 and GH1-1 in their genomes, when compared to the unevolved strains (Wei *et al.* 2015; Oh *et al.* 2016). In addition, the evolved strain of Oh and co-workers (Oh *et al.* 2016) showed a GH1-1/CDT-1 copy number ratio similar to that of Yuan *et al*. (2013) (2:1 vs 2.5:1); it should be noted that Yuan and co-workers measured the mRNA levels. In contrast, the optimised strain obtained by Eriksen *et al*. (2013) had gene expression levels comparable to the wild-type strain, but involved overall higher CDT-1 and GH1-1 protein activities. Although no mutations were found in the coding regions of the CDT-1 and GH1-1genes in the previous reports (with the exception of Eriksen *et al.* 2013), single amino acid substitutions in cellobiose transporters were identified after evolutionary engineering in strains carrying other cellobiose-degrading pathways, such as CDT-1 + SdCBP (cellobiose phosphorylase from *Saccharophagus degradans*) (Ha *et al.* 2013a), HXT2.4 (putative hexose transporter from *Scheffersomyces stipitis*) + GH1-1 (Ha *et al.* 2013b), and CDT-2 + SdCBP

(Kim *et al.* 2018) (Table 2.2). These mutations were found to be responsible for enhanced transport activities.

Transcriptional and metabolite profiling have revealed that yeast cells fermenting cellobiose are subjected to severe physiological changes, compared to cells fermenting glucose, as reflected in the activation of mitochondrial function and a decrease in amino acid biosynthesis, and in a carbon starvation-like state of the plasma membrane ATPase (Pma1) (Lin *et al.* 2014; Chomvong *et al.* 2017). Furthermore, when cultivated in cellobiose medium, yeast cells accumulate high levels of trehalose and of intermediate metabolites in the γ-aminobutyrate (GABA) shunt pathway, improving the strain's tolerance to oxidative stress (Kim *et al.* 2014b; Yun *et al.* 2018).

Co-fermentation of cellobiose and xylose/galactose has been investigated to eliminate the challenges inherent to the presence of glucose in sugar mixtures (Kim *et al.* 2012). Glucose represses the transcriptional machinery responsible for the consumption of alternative sugars (Gancedo 1998; Kayikci and Nielsen 2015). However, when the disaccharides are hydrolysed intracellularly, glucose repression is minimised, enabling the co-consumption of cellobiose and xylose (Li *et al.* 2010; Ha *et al.* 2011a), leading to an increase in ethanol productivity. Moreover, when a mixture of cellobiose and xylose was supplemented with a small amount of glucose (< 10% of total sugars), the performance of the engineered strain was not affected (Li *et al.* 2010; Ha *et al.* 2011a), indicating that an intracellular cellobiose-hydrolysing (iCELL) strain would probably perform well under industrial conditions, as glucose will always be present in small amounts in the partially hydrolysed 2G stream. Alleviation of glucose repression was also observed in mixtures of cellobiose and galactose, yielding higher ethanol productivity in comparison to the sequential utilisation of sugars in a mixture of glucose and galactose (Ha *et al.* 2011b).

Although fuel ethanol has been the main product of interest in most of the studies discussed above, the formation of other biotechnological compounds has also been reported using the iCELL approach, e.g. 2,3-butanediol (Nan *et al.* 2014), lactic acid (Turner *et al.* 2016), and biosurfactants (Jayakody *et al.* 2018).

2.4.4 The iSUCCELL chassis

As detailed above, intracellular disaccharide utilisation in *S. cerevisiae* has been evaluated for a single disaccharide or for a disaccharide combined with the co-consumption of one or more monosaccharides. Our approach involves the intracellular utilisation of two disaccharides,

namely sucrose and cellobiose, in a single yeast chassis (Figure 2.2). When these two disaccharides are metabolised via symport and intracellular hydrolysis under anaerobic conditions, there is a 25% decrease in free-energy conservation, namely 4 to 3 mol ATP per mol of sugar, when compared to an extracellular route in which the released monosaccharides are transported via facilitated diffusion across the cell membrane (Basso *et al.* 2011). This platform could be used to ferment the sugars present in an industrial *must* obtained by mixing a sugarcane-based medium (juice and/or molasses), as currently used in Brazilian 1G biorefineries, and cellobiose-rich hydrolysates from the cellulosic fraction of sugarcane bagasse (or even from other lignocellulosic raw materials).

S. cerevisiae strains currently adopted by the Brazilian fuel ethanol industry have demonstrated high tolerance towards the stressors/inhibitors typically present both in a 1G and in a 2G context (Della-Bianca *et al.* 2013, 2014; Pereira *et al.* 2014; Cola *et al.* 2020). Two of the most widely employed strains in industry, namely *S. cerevisiae* PE-2 and CAT-1 (both are diploids), have already been engineered for xylose fermentation (Romaní *et al.* 2015), highlighting their potential for genetic manipulation, as well as for their use in a 2G process. Recently developed synthetic biology tools, such as the RNA-guided endonuclease mediated CRISPR/Cas method, should be leveraged to facilitate remodelling of native sucrose metabolism and the introduction of the heterologous cellobiose pathway. It should be noted that the CRISPR/Cas system has already been applied with great success both in laboratory and in industrial strains, enabling simultaneous introduction of multiple genetic modifications into the yeast genome without the need for multiple selectable markers (Stovicek, Holkenbrink and Borodina 2017; Lian, HamediRad and Zhao 2018).

Although the disaccharides sucrose and cellobiose could be cleaved intracellularly either via hydrolysis or via phosphorolysis, the iSUCCELL strategy proposed here involves hydrolysis, since this route benefits from decreased free-energy conservation, which in turn results in higher ethanol yields on sugar (Basso *et al.* 2011) (Figure 2.2). In order to achieve intracellular sucrose hydrolysis, the invertase-encoding *SUC2* gene could be either modified to constitutively and exclusively express the intracellular form of invertase (Basso *et al.* 2011), or be completely deleted, as this Δ*suc2 strain would still* hydrolyse sucrose via intracellular α-glucosidases (Dário 2012; Franken *et al.* 2013; Bahia *et al.* 2018). Since duplication of the *AGT1* gene proved crucial for improved sucrose fermentation in the evolved i*SUC2* strain developed by Basso *et al*. (2011), overexpression of native *AGT1* under

a stronger, constitutive promoter or introduction of extra *AGT1* copies might also be necessary.

To engineer *S. cerevisiae* for intracellular cellobiose hydrolysis, a heterologous cellobiose transporter and an intracellular BGL need to be expressed in the platform strain. It is noteworthy that most of the attempts for cellobiose fermentation in *S. cerevisiae* involve the use of episomal plasmids, hampering the applicability of these strains in large-scale industrial conditions. However, since the cellobiose pathway comprises only two genes, chromosomal integrations should not be a complex task with the efficient and well-developed CRISPR-based methodologies, offering precise control over gene stability and copy number (Da Silva and Srikrishnan 2012). Additional metabolic adjustments might be needed for the iSUCCELL yeast to achieve the productivities required for industrial applications. In this sense, adaptive laboratory evolution, systems biology, reverse engineering, and other combinatorial approaches could be useful. For instance, integration of CDT-1 and GH1-1 genes in multiple copies at a *ca.* 1:2 ratio could contribute to a faster fermentation of cellobiose (Oh *et al.* 2016). Integration of the mutated HXT2.4 (A291E) cellobiose transporter from *S. stipitis* could be implemented to harness the improved kinetic properties of this permease (Ha *et al.* 2013b). Additionally, modulation of two native transcription factors (overexpression of *SUT1* and deletion of *HAP4*) can be leveraged to speed cellobiose fermentation (Lin *et al.* 2014). Finally, if necessary, to avoid leakage of monosaccharides to the medium after intracellular hydrolysis, overexpression/finetuning of downstream steps, e.g., those catalysed by hexo- and/or glucokinases, might also be required.

2.5 Outlook/Conclusion

2G technologies are vital for producing additional amounts of fuel ethanol from existing feedstock, and for mitigating the deleterious effects of climate change. Despite extensive research and development, 2G fuel ethanol is yet to become a commercial success. The approach proposed here is unique in that it combines 1G and 2G process technologies with strain engineering for intracellular utilisation of sucrose and cellobiose, in robust *S. cerevisiae* strains currently used in the Brazilian fuel ethanol industries. The 'iSUCCELL' strategy utilises a mixture of 1G stream and a partially hydrolysed, cellobiose-rich 2G stream as a substrate and confers competitive advantages to both the microbe and the process, compared to currently existing strategies. The use of this strategy decreases the availability of free glucose that can be used by contaminating microbes, decreases the cooling time of the feed stream prior to fermentation (avoiding either decreased productivities or higher capital costs), decreases the process time through the co-consumption of sugars because of the absence of glucose repression, and finally, decreases the concentration of metabolic inhibitors that hinders the performance of yeasts. Modern CRISPR-based engineering technologies should be employed for initial strain engineering, after which other approaches, such as laboratory evolution combined with reverse engineering, should be exploited for metabolic fine-tuning. CRISPR-based metabolic engineering of industrial diploid strains has been successfully demonstrated for cellobiose (Ryan *et al.* 2014) and glycerol (Klein *et al.* 2016) utilisation, as well as for the production of 3-hydroxypropionic acid (Jessop-Fabre *et al.* 2016), S-adenosyl-L-methionine (Liu *et al.* 2019), and lactic acid from either glucose (Stovicek, Borodina and Forster 2015) or xylose (Lian *et al.* 2018). We hope the scientific community and eventually the fuel ethanol companies will embrace these proof of concepts to pursue scale-up, and possibly implement the iSUCCELL strategy in existing biorefineries.

2.6 Funding

We would like to acknowledge funding by *Coordenação de Aperfeiçoamento de Pessoal de Nível Superior* (CAPES, Brasília, Brazil) for a Ph.D. scholarship to PMB and for a post-doctoral PNPD scholarship to VR.

2.7 Conflict of interest

The authors declare they have no conflicts of interest involved in this work.

2.8 Rights and permissions

3 METABOLIC ENGINEERING OF *SACCHAROMYCES CEREVISIAE* FOR CELLOBIOSE UTILISATION

3.1 Abstract

Numerous metabolic engineering approaches for the production of fuel ethanol or value-added products have evidenced a strong interest in expanding the repertoire of sugar transporters or of key hydrolytic enzymes involved in the degradation of lignocellulosic biomass. To contribute to this matter, in the present study we used an *in-silico* approach to screen for novel cellodextrin transporters and intracellular β-glucosidases (BGLs) from fungal origin in order to allow cellobiose utilisation in yeast. Further functional analysis of five selected BGL candidates from *Aspergillus niger* and *Podospora anserina* exhibited extremely low enzymatic activities in cell extracts of *Saccharomyces cerevisiae*, compared to that of the characterised GH1-1 enzyme from the fungus *Neurospora crassa* (from 0.0034 to 0.015 *vs.* 1.9 U/mg protein). Despite these *in vitro* results, the BGL-expressing strains were subsequently co-transformed with the well-studied *N. crassa* CDT-1 transporter via CRISPR-Cas9-assisted genome editing. The resulting six engineered *S. cerevisiae* strains were evaluated for their ability to grow on cellobiose as the sole carbon and energy source, albeit with no satisfactory results. Since episomal expression of the GH1-1 enzyme has shown high activity in our enzymatic analyses, we hypothesised that chromosomal integration of CDT-1 gene might have limited the level of CDT-1 transcripts in the cell, resulting in insufficient amount of transporter molecules delivered in the plasma membrane of the strain harbouring CDT-1 and GH1-1 genes. Regarding the other engineered strains, the limitation might depend not only on the transport of the sugar, but also on its intracellular hydrolysis to glucose. In order to make these strains capable of growing on cellobiose, additional laboratory evolution will be pursued.

3.2 Introduction

Over the last two decades, intensive research and investment involving academia and industry have resulted in important progress towards the development of a feasible technology to produce fuel ethanol from plant biomass. Incentives for these joint efforts have been prompted by increasing concerns on energy security, sustainability, and global climate change (Solomon 2010). Compared to traditional production processes using starch or sugar-containing feedstocks, the utilisation of lignocellulosic plant biomass for fuel ethanol production involves at least two additional steps, namely chemical/physical pretreatment and enzyme-catalysed hydrolysis, in order to make the sugars accessible for subsequent microbial fermentation. This prerequisite is a consequence of the highly recalcitrant nature of the lignocellulose matrix found in the plant cell walls, responsible for providing structural support and resistance to pathogens in their natural environment (Miedes *et al.* 2014). Although different aspects of the whole production chain have been investigated for the implementation of 2G fuel ethanol, e.g., agricultural crops, biomass pretreatment, and enzyme hydrolysis, the field of metabolic engineering has not only made considerable advances in the improvement of engineered *Saccharomyces cerevisiae* strains, but also broadened the variety of products and microorganisms that can be used.

The concept of metabolic engineering emerged in the 1990s as the field related to the directed or rational improvement of cellular properties through the modification of specific biochemical reactions or the introduction of new ones using recombinant DNA technology (Ostergaard, Olsson and Nielsen 2000; Gombert and Basso 2020). The yeast *S. cerevisiae* has a long historical background on the production of 1G fuel ethanol due to its Generally Regarded As Safe (GRAS) status, its high efficiency in fermenting hexoses to ethanol (in terms of both rates and yields), and superior tolerance against harsh conditions, including ethanol concentrations above 10%, an extremely rate trait among living cells. Besides these intrinsic characteristics, *S. cerevisiae* possesses amenability for genetic engineering, which makes this yeast an excellent platform microorganism for metabolic engineering.

Some of the challenges that current 2G fuel ethanol processes face are related to the inhibitors released during biomass deconstruction, the inability of *S. cerevisiae* to utilise all sugars available in lignocellulose, and the incapacity of converting these other sugars into ethanol rapidly when glucose is present. Significant contributions to these issues have been addressed by different researchers worldwide (Jansen *et al.* 2017; Jin and Cate 2017; Cunha *et al.* 2019;

Oh and Jin 2020). While xylose metabolism in *S. cerevisiae* has challenged the scientific community for decades, other sugar substrates present in lignocellulosic biomass have also called the attention of metabolic engineers. Taking into account that the cost of biomass-derived fuels depends critically on the yield of sugar conversion to the final product (Maiorella *et al.* 2009), it is essential to drive research on the engineering of strains to ensure full consumption of all sugars. In this sense, the utilisation of cellobiose, a dimer of glucose released during the enzymatic hydrolysis of cellulose, has gained importance in the last decade as an alternative to circumvent the issues related to the presence of glucose in cellulosic hydrolysates, namely: 1) sequential utilisation of the sugars present in the medium due to so called glucose repression, 2) enzyme requirement for cellobiose hydrolysis to glucose, thereby increasing operational costs, and 3) dependence on antibiotics or other antimicrobial strategies due to potential contamination events during fermentation.

Direct utilisation of cellobiose by engineering a cellobiose utilisation system into *S. cerevisiae* has been deeply detailed in Chapter 2. Surprisingly, at present most studies into the application of this strategy in yeast are related to the use of the CDT-1 cellodextrin transporter from the cellulolytic fungus *Neurospora crassa*. Few published studies report the functional expression of cellodextrin transporters from other microorganisms. These few examples involved cellobiose uptake systems from other filamentous fungi (*Trichoderma reesei*, *Penicillium chrysogenum*, *Thielavia terrestris*, *Aspergillus niger*, *Penicillium oxalicum*, and *Aspergillus nidulans*) (Li *et al.* 2013; Zhang *et al.* 2013; Bae *et al.* 2014; dos Reis *et al.* 2016; Casa-Villegas, Polaina and Marín-Navarro 2018), and from yeast (*Scheffersomyces stipitis* and *Kluyveromyces lactis*) (Sadie *et al.* 2011; Varela *et al.* 2019). In nature, the fungal kingdom plays a central role in degrading plant biomass by secreting carbohydrate-active enzymes that act specifically on plant polysaccharides (Benoit *et al.* 2015). Cellulolytic enzymes release glucose and cellodextrins, which are subsequently transported into the fungal cell and metabolised intracellularly. Thus, fungal species are excellent candidates for the screening of new genes involved in cellobiose degradation.

Motivated by this context, the goal of this study was to extend the catalogue of available genes involved in cellobiose fermentation in *S. cerevisiae* by exploring novel cellobiose permeases and intracellular β-glucosidases (BGLs) from fungal origin. To this end, putative cellodextrin transporters and intracellular BGLs were identified by a bioinformatic survey, and selected candidates were heterologously expressed in *S. cerevisiae* by a combination of episomal and CRISPR/Cas-mediated expression. To assess the functionality of the individual

BGLs, the enzymatic activities in cell extracts of *S. cerevisiae* were determined. Intracellular cellobiose-utilising (iCELL) strains carrying the *N. crassa* CDT-1 transporter and different BGLs were constructed and evaluated for their ability to grow on different carbon sources, including cellobiose.

3.3 Material and Methods

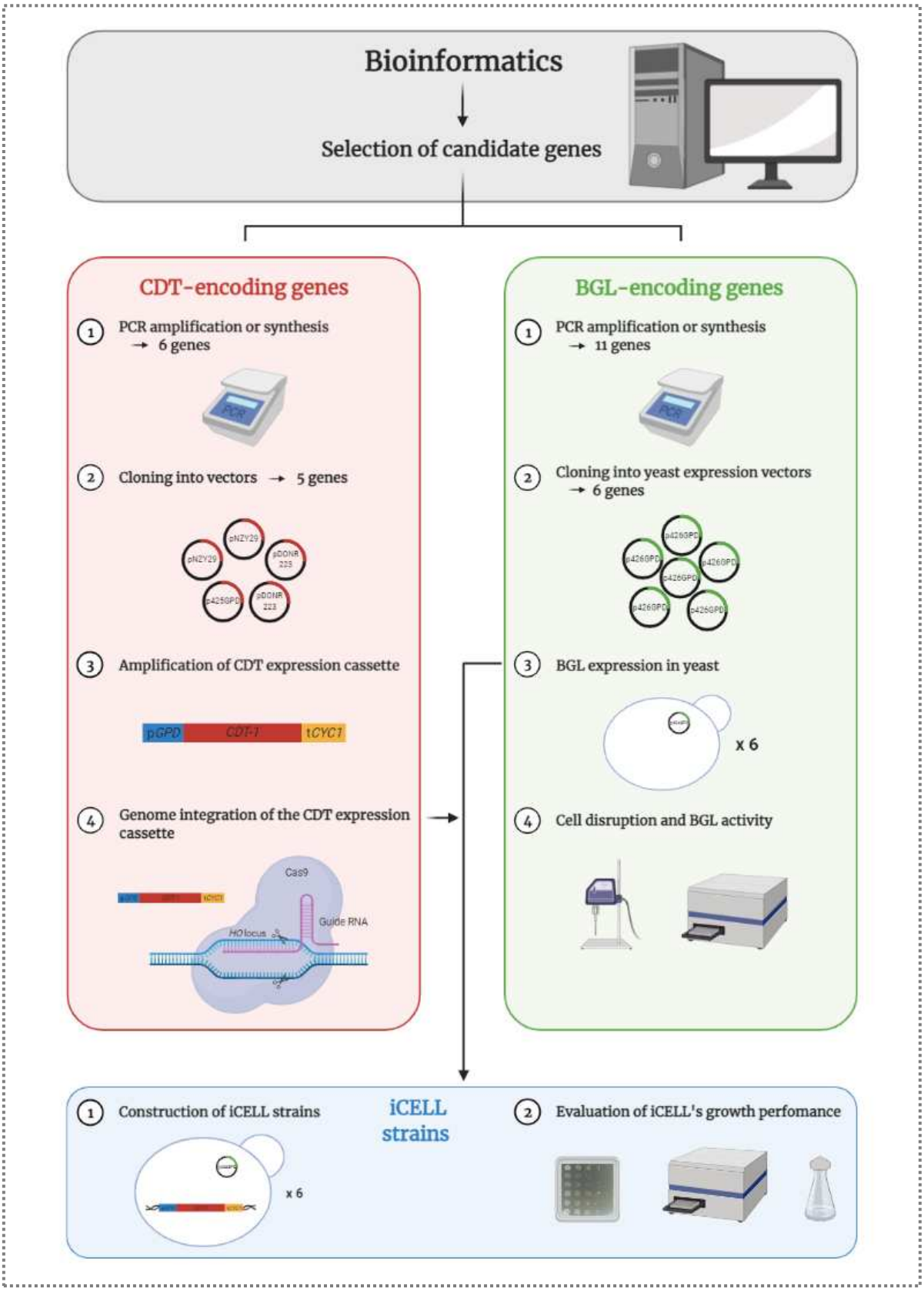

Figure 3.1. Schematic representation of the strategy adopted herein for metabolic engineering of *S. cerevisiae* for cellobiose utilisation.

3.3.1 Sequence and phylogenetic analysis

3.3.1.1 Cellodextrin transporters

The amino acid sequences of two characterised cellodextrin transporters (CDTs) from the cellulolytic fungus *N. crassa* (CDT-1 and CDT-2) (Galazka *et al.* 2010) were used as queries for a Basic Local Alignment Search Tool (BLAST) against the protein sequences (BLASTP) of seven selected fungal genomes obtained from the JGI Fungi Portal (https://genome.jgi.doe.gov/programs/fungi/index.jsf): *Agaricus bisporus, Aspergillus niger, Dichomitus squalens*, *Myceliophthora thermophila*, *Phanerochaete chrysosporium*, *Podospora anserina*, and *Trichoderma reesei*. These target genomes were selected according to their natural habitat and the expected ability to utilise cellobiose as carbon source (de Vries and Visser 2001; Patyshakuliyeva and de Vries 2011; van den Brink *et al.* 2013; Zhang *et al.* 2013; Rytioja *et al.* 2015; Couturier *et al.* 2016; Kameshwar and Qin 2017). In addition, these species were known to have good quality genomes at the time this analysis was performed (between 2015-2016), and some complementary DNAs (cDNAs) were available at the CBS-KNAW Fungal Biodiversity Centre (currently Westerdijk Fungal Biodiversity Institute), where this study was developed. The top ten hits from each BLASTP were collected and aligned using four different multiple sequence alignment programs: 1) MAFFT (https://www.ebi.ac.uk/Tools/msa/mafft/), 2) TM-Coffee (http://tcoffee.crg.cat/), 3) Clustal Omega (https://www.ebi.ac.uk/Tools/msa/clustalo/), and 4) MUSCLE (https://www.ebi.ac.uk/Tools/msa/muscle/). Different programs were assessed in order to analyse potential differences in each alignment and obtain reliable results. Then, a phylogenetic analysis was conducted with the Molecular Evolutionary Genetics Analysis (MEGA6) software, using the Neighbour-Joining method with 1000 bootstraps replicates. An ATP-binding cassette (ABC) transporter sequence from *N. crassa* was used as outgroup. Finally, selected sequences extracted from the phylogenetic tree were compared with TM-Coffee (http://tcoffee.crg.cat/) and submitted to the TMHMM (http://www.cbs.dtu.dk/services/TMHMM/) and InterPro (https://www.ebi.ac.uk/interpro/) servers for prediction of transmembrane domains as well as other putative domains and functions.

3.3.1.2 β-glucosidases

β-glucosidases (BGLs) are among the most widely studied and well characterised enzymes. Based on their amino acid sequences and structural similarities, these enzymes are mostly

placed in Glycoside Hydrolase families 1 and 3 (GH1, GH3) in the Carbohydrate-Active enZYmes Database (CAZy) (http://www.cazy.org/), a repository specialised in the enzymes that build and breakdown complex carbohydrates and glycoconjugates. For the screening of BGL candidates, sequences from four fungal strains were obtained from the CAZy database as well as from an internal database at CBS-KNAW: *A. niger* (representative for general Ascomycetes), *P. anserina* (representative for coprophilous Ascomycetes), *T. reesei* (representative for cellulolytic Ascomycetes), and *D. squalens* (representative for Basidiomycetes). Signal peptides were predicted using the SignalP server (http://www.cbs.dtu.dk/services/SignalP/). Since we aimed at selecting intracellular BGLs, only sequences without signal peptides were used for further analysis. The amino acid sequences of BGLs candidates without signal peptides were aligned with MUSCLE (https://www.ebi.ac.uk/Tools/msa/muscle/). Then, a phylogenetic tree was generated with MEGA6 software using the Neighbour-Joining method with a bootstrap of 500 replicates, which also included intracellular BGLs already characterised from other microorganisms, such as *N. crassa*, *T. reesei*, *Penicillium rubens*, *Thermothielavioides terrestris*, *Paenibacillus polymyxa*, and *Hanseniaspora guilliermondii* (Galazka *et al.* 2010; Bae *et al.* 2014; Guo *et al.* 2016; Casa-Villegas, Polaina and Marín-Navarro 2018). β-xylosidases (BXLs) from *A. niger* and *T. reesei* were used as outgroups.

3.3.2 Strains and maintenance

Escherichia coli DH5α (F^- *endA1 glnV44 thi-1 recA1 relA1 gyrA96 deoR nupG purB20* φ80d*lacZ*ΔM15 Δ(*lacZYA-argF*)U169, hsdR17($r_K^- m_K^+$), λ^-), DH10B (F^- *endA1 deoR*$^+$ *recA1 galE15 galK16 nupG rpsL* Δ*(lac)X74* φ80*lacZΔM15 araD139* Δ*(ara,leu)7697 mcrA* Δ*(mrr-hsdRMS-mcrBC)* Str^R λ^-), and DB3.1 (F- gyrA462 endA1 glnV44 Δ(sr1-recA) mcrB mrr hsdS20(r_B^-, m_B^-) ara14 galK2 lacY1 proA2 rpsL20(Sm^r) xyl5 Δleu mtl1) were used as host strains for gene cloning and manipulation. Bacterial strains were obtained from CBS-KNAW and from the *Laboratório de Genômica e Expressão* (LGE, currently *Laboratório de Genômica e bioEnergia*) at the Institute of Biology (IB)/UNICAMP. The *S. cerevisiae* strains used in this work (Table 3.1) belong to the congenic members of the CEN.PK family (van Dijken *et al.* 2000; Entian and Kötter 2007). The CEN.PK113-5D strain was kindly provided by Dr. Peter Kötter (EUROSCARF, Germany), whereas strain CEN.PK2-1D was obtained from LGE/IB/UNICAMP. To prepare stock cultures, yeast strains were grown in 50-mL polypropylene tubes containing 10 mL of either Yeast Extract-Peptone-Dextrose medium (YPD) or Synthetic Medium (SM) with 20 g/L initial glucose as carbon source, for strains

carrying plasmids with auxotrophic marker genes. YPD medium and SM were prepared as described in section 3.3.7. After 24-48 h growth at 30 °C and 200 rpm, 30% (v/v) glycerol was added, and 2-mL aliquots were stored at -80 °C. For bacterial stock cultures, cells were grown at 37 °C and 250 rpm in test tubes containing 4 mL of Luria-Bertani (LB) medium supplemented with 100 µg/mL of the appropriate antibiotic (ampicillin or spectinomycin). LB medium was prepared as described in section 3.3.7. After overnight growth, 20% (v/v) glycerol was added, and 2-mL aliquots were stored at -80 °C.

Table 3.1. Yeast strains used in this study.

STRAIN	FEATURE	ORIGIN
CEN.PK113-5D	*MATa MAL2-8^{C} SUC2 ura3-52*	Dr. P. Kötter, (EUROSCARF, Germany)
CEN.PK2-1D	*MATα MAL2-8^{c} SUC2 ura3-52 his3D1 leu2-3_112 trp1-289*	Dr. G. A. G. Pereira (UNICAMP, Brazil)
PBY_01	CEN.PK113-5D/p426GPD-AN 8517	This study
PBY_02	CEN.PK113-5D/p426GPD-PA 951	This study
PBY_03	CEN.PK113-5D/p426GPD-PA 3784	This study
PBY_04	CEN.PK113-5D/p426GPD-PA 6071	This study
PBY_05	CEN.PK113-5D/p426GPD-PA 10293	This study
PBY_06	CEN.PK113-5D/p426GPD-GH1-1	This study
PBY_07	CEN.PK113-5D/p426GPD empty	This study
PBY_08	CEN.PK113-5D/*HO-GPD*-CDT-1-*CYC1-HO*	This study
PBY_09	CEN.PK113-5D/*HO-GPD*-CDT-1-*CYC1-HO*/p426GPD-AN 8517	This study
PBY_10	CEN.PK113-5D/*HO-GPD*-CDT-1-*CYC1-HO*/p426GPD-PA 951	This study
PBY_11	CEN.PK113-5D/*HO-GPD*-CDT-1-*CYC1-HO*/p426GPD-PA 3784	This study
PBY_12	CEN.PK113-5D/*HO-GPD*-CDT-1-*CYC1-HO*/p426GPD-PA 6071	This study
PBY_13	CEN.PK113-5D/*HO-GPD*-CDT-1-*CYC1-HO*/p426GPD-PA 10293	This study
PBY_14	CEN.PK113-5D/*HO-GPD*-CDT-1-*CYC1-HO*/p426GPD-GH1-1	This study
PBY_15	CEN.PK113-5D/*HO-GPD*-CDT-1-*CYC1-HO*/p426GPD empty	This study

3.3.3 Molecular biology techniques

PCR amplification for cloning purposes was performed with Phusion High-Fidelity DNA Polymerase (New England Biolabs, Ipswich, USA and Thermo Scientific, Waltham, USA). Diagnostic PCR was performed using GoTaq DNA Polymerase (Promega, Madison, USA). Both enzymes were used according to the manufacturers' instructions. Oligonucleotides were purchased from Integrated DNA Technologies (IDT, Coralville, USA) and Exxtend (Campinas, Brazil). Deoxyribonucleotide triphosphate (dNTP) mix for use in PCR and cDNA synthesis was purchased from Thermo Scientific (Waltham, USA). Separation of DNA fragments was performed in 1% (w/v) agarose gel in TAE buffer (40 mM Tris-acetate pH 8.0 and 1 mM EDTA). DNA visualisation from agarose gel was performed with GelRed

(Biotium, Fremont, California, USA) or ethidium bromide (0.5 μg/mL final concentration) (Invitrogen, Carlsbad, USA). DNA fragments were purified from gels or directly from PCR reactions using the Wizard SV Gel and PCR Clean-Up Start-Up Kits (Promega, Madison, USA). Restriction endonucleases and T4 DNA ligase (Promega, Madison, USA) were used according to manufacturer's instructions. Plasmids were isolated from *E. coli* according to a standard procedure (Green and Sambrook 2012). Yeast genomic DNA (gDNA) was extracted according to Lõoke, Kristjuhan and Kristjuhan (2011). Briefly, the methodology involves lysis of yeast colonies or cells from liquid culture in a lithium acetate–SDS solution and subsequent precipitation of DNA with ethanol. DNA concentration was estimated with NanoDrop 2000 at 260 nm (Thermo Scientific, Waltham, USA).

3.3.4 RNA isolation and cDNA synthesis

The mycelial samples for RNA extraction were collected by filtration after overnight, 24 h or 48 h growth of *T. reesei* QM6a and RC 30-38 strains, and immediately frozen in liquid nitrogen. Frozen mycelia were subsequently ground in a TissueLyser II (Qiagen, Germantown, USA), and total RNA was isolated using the TRIzol reagent (Invitrogen, Carlsbad, USA), according to the manufacturer's instructions. Total RNA samples were purified with the NucleoSpin RNA Clean-up Kit (Macherey-Nagel, Düren, Germany). Contaminating gDNA was removed by an rDNase solution directly on the silica membrane. RNA integrity was verified by 1% (w/v) agarose gel electrophoresis and RNA quantity estimated by NanoDrop 2000 spectrophotometer (260 nm) (Thermo Scientific, Waltham, USA). Total RNA was subsequently converted into cDNA with the ThermoScript™ RT-PCR System (Invitrogen, Carlsbad, USA), according to the manufacturer's instructions.

3.3.5 Plasmid constructions

Plasmids containing CDT or BGL-encoding genes (Table 3.2). were constructed as described below. A list with all primers used can be found in Table 3.3.

cDNA and gDNA sequences from *A. niger*, *D. squalens* and *T. reesei* were obtained from CBS-KNAW or synthesised, as described above (section 3.3.4). Each open reading frame (ORF) from *A. niger* and *D. squalens* (AN 3028, AN 6623, AN 6436, AN 3736, AN 8517, DS 104403, DS 101924, and DS 179877) was amplified from the corresponding cDNA or gDNA using primers CBS PBO_008/CBS PBO_010 (AN 3028), CBS PBO_033/CBS PBO_036 (AN 6623), CBS PBO_037/CBS PBO_040 (AN 6436), CBS PBO_041/CBS PBO_043 (AN 3736),

CBS PBO_044/CBS PBO_046 (AN 8517), CBS PBO_012/CBS PBO_014 (DS 104403), CBS PBO_056/CBS PBO_057/CBS PBO_039 (DS 101924); CBS PBO_060/CBS PBO_061/CBS PBO_062 (DS 179877) (Table 3.3). PCR amplicons AN 3028 and DS 104403 were purified and cloned into the commercial pDONR™223 via the Gateway® Technology (Invitrogen, Carlsbad, California, USA), according to the manufacturer's instructions. Recombinant plasmids were transformed into DH5α cells and selected in LB medium supplemented with 100 µg/mL spectinomycin. Resulting transformants were confirmed by colony-PCR and DNA sequencing (Macrogen Inc., Amsterdam, The Netherlands). BGL amplicon AN 3736 was purified and cloned into the pGEM®-T vector system (Promega, Madison, Wisconsin, USA), according to the manufacturer's instructions, whereas AN 8517 was directly cloned into the p426GPD expression vector via *Spe*I and *Hin*dIII digestion and ligation. This episomal plasmid containing the constitutive *GPD* promoter, the *CYC1* terminator and *URA3* auxotrophic marker gene was kindly provided by Prof. Dr. Jean-Marc Daran from the Industrial Microbiology section at the Delft University of Technology (TU Delft, The Netherlands). Recombinant plasmids were transformed into DH5α cells and selected in LB medium supplemented with 100 µg/mL ampicillin. Resulting transformants were confirmed by colony-PCR and DNA sequencing (Macrogen Inc., Amsterdam, The Netherlands).

Selected CDT and BGL sequences belonging to *P. anserina* (PA 558, PA 601, PA 951, PA 3784, PA 6071, and PA 10293) were synthesised by NZYTech (Lisbon, Portugal) and delivered within the pNZY29 vector (Table 3.2). All the sequences were codon-optimised for expression in *S. cerevisiae,* according to the manufacturer's algorithm. In order to express the BGL genes in *S. cerevisiae*, each ORF was digested from the corresponding source of material and subsequently cloned into p426GPD via *Spe*I and *Hin*dIII digestion and ligation. Recombinant plasmids were transformed into DH5α cells and selected in LB medium supplemented with 100 µg/mL ampicillin. Resulting transformants were confirmed via restriction analysis.

Coding genes from *N. crassa*, CDT-1 and GH1-1, were amplified by PCR with primer pairs LGE PBO_020/LGE PBO_021 and LGE PBO_007/LGE PBO_008 (Table 3.3), respectively, from a plasmid kindly provided by Prof. Dr. Gonçalo Amarante Guimarães Pereira from LGE/IB/UNICAMP (pCDT-1-GH1-1). The CDT-1 amplicon yielded a fragment flanked by 30 and 26 bp overlaps at 5' and 3', respectively, with a plasmid backbone (p425GPD). Assembly of p425GPD-CDT-1 (Table 3.2) was made by *in vivo* homologous recombination

of 350 ng purified CDT-1 and 500 ng linearized p425GPD. The latter was obtained by removal of the *XYL* sequence from plasmid p425GPD-XYL using *Bam*H1 restriction sites (this plasmid was also provided by Prof. Dr. G. A G. Pereira). After isolation of p425GPD-CDT-1 from CEN.PK2-1D (Leu^-) cells and propagation in *E. coli* DH10B, correct assembly of the CDT-1 expression cassette was verified by diagnostic PCR and enzymatic digestion with *Bam*H1.

Table 3.2. Plasmids used in this study.

PLASMID	RELEVANT CHARACTERISTICS	ORIGIN
pDONR223	Cloning vector, Gateway system	CBS-KNAW (The Netherlands)
pDONR223-AN 3028	Vector carrying the AN 3028 gene from *A. niger*	This work
pDONR223-DS 104403	Vector carrying the DS 104403 gene from *D. squalens*	This work
pNZY29-PA 558	Vector carrying the PA 558 gene from *P. anserina*	This work
pNZY29-PA 601	Vector carrying the PA 601 gene from *P. anserina*	This work
pNZY29-PA 951	Vector carrying the PA 951 gene from *P. anserina*	This work
pNZY29-PA 3784	Vector carrying the PA 3784 gene from *P. anserina*	This work
pNZY29-PA 6071	Vector carrying the PA 6071 gene from *P. anserina*	This work
pNZY29-PA 10293	Vector carrying the PA 10293 gene from *P. anserina*	This work
pCDT-1-GH1-1	Vector carrying the CDT-1 and GH1-1 genes from *N. crassa*	Dr. G. A. G. Pereira (UNICAMP, Brazil)
p425GPD-XYL	Backbone vector use for cloning CDT-1 gene under p_{GPD} and t_{CYC1}	Dr. G. A. G. Pereira (UNICAMP, Brazil)
p425GPD-CDT-1	*2µm LEU2* p_{GPD}-CDT-1-t_{CYC1}	This work
pGS_004.30	*2µm KanMX* p_{TEF1}-Cas9-t_{CYC1} p_{SNR52}-sgRNA-t_{SUP4}	Dr. G. A. G. Pereira (UNICAMP, Brazil)
p426GPD	*2µm URA3* p_{GPD}-t_{CYC1}	Dr. J. M. Daran (TU Delft, The Netherlands)
p426GPD-AN 8517	*2µm URA3* p_{GPD}-AN 8517-t_{CYC1}	This work
p426GPD-PA 951	*2µm URA3* p_{GPD}-PA 951-t_{CYC1}	This work
p426GPD-PA 3784	*2µm URA3* p_{GPD}-PA 3784-t_{CYC1}	This work
p426GPD-PA 6071	*2µm URA3* p_{GPD}-PA 6071-t_{CYC1}	This work
p426GPD-PA 10293	*2µm URA3* p_{GPD}-PA 10293-t_{CYC1}	This work
p426GPD-GH1-1	*2µm URA3* p_{GPD}-GH1-1-t_{CYC1}	This work

Table 3.3. Primers used in this study.

OLIGO NAME	SEQUENCE	FEATURES

CBS PBO_008	GGGGACAAGTTTGTACAAAAAAGCAGGCTTCATGGCT GAGAAAACCGCCAC	attB1 site; AN 3028f
CBS PBO_010	GGGGACCACTTTGTACAAGAAAGCTGGGTTTTACTTCA TCTCCTCGATCTCCGTAAG	attB2 site; AN 3028r
CBS PBO_012	GGGGACAAGTTTGTACAAAAAAGCAGGCTTCATGTCG ATCATCCATCGAGAAGATAG	attB1 site; DS 104403f
CBS PBO_014	GGGGACCACTTTGTACAAGAAAGCTGGGTTCTAAGCG CTCTTCTCGTCGAGG	attB2 site; DS 104403f
LGE PBO_020	GTTTCGACGGATTCTAGAACTAGT**GGATCC**ATGTCGT CTCACGGCTCCCA	p425GPD homology*;* ***Bam*H1** site; CDT-1f
LGE PBO_021	TCGAATTCCTGCAGCCCGGG**GGATCC**CTAAGCAACGA TAGCTTCGGAC	p425GPD homology; ***Bam*H1** site; CDT-1r
LGE PBO_009	GCTATTTTATAAGATTCAGG	-
LGE PBO_011	GCTTACTTCCTCTTCAAC	-
FMO_010	GTGACCTTGTAACTCCTGCTGTAAAAAGTATGGCTTGG ATGCAAATTAAAGCCTTCGAGC	-
FMO_019	TCTCTACCTTACGGTTTGTGACGATCACGTTCCGCTG**T CATTATCAATACTCGCCATTTC**	*HO* homology; **p425GPD homology**
FMO_020	CTGGACCATCTCCATAATGAAGCCTTACATGTTTGGCA CG**GCAAATTAAAGCCTTCGAGC**	*HO* homology; **p425GPD homology**
CBS PBO_033	CGGAATTCCGTCGACATGGCCCCCAAAGAGGACATG	*Sal*I site; AN 6623f
CBS PBO_036	CGGAATTCCTCGAG**TCA**AGCGTAATCTGGAACATCGT ATGGGTAAGGTCCAGGCACCATAGTCCATG	*Xho*I site, **stop**; HA tag; AN 6623r
CBS PBO_037	CGGAATTCCGGATCCATGGCACGTCTGGACGTGGAAA AAAC	*Spe*I site; AN 6436f
CBS PBO_040	CGGAATTCCAAGCTT**CTA**AGCGTAATCTGGAACATCG TATGGGTACAACCCAACCCAATACCTCGTCCTCTC	*Hin*dIII site, **stop**; HA tag; AN 6436r
CBS PBO_041	CGGAATTCCGGATCCATGCCGCTTCCCTTTCGGGAC	*Spe*I site; AN 3736f
CBS PBO_043	CGGAATTCCAAGCTT**CTA**AGCGTAATCTGGAACATCG TATGGGTAGTAGTATCCCCGCAACGGGAGATCTC	*Hin*dIII site, **stop**; HA tag; AN 3736r
CBS PBO_044	CGGAATTCCACTAGTATGGGTTCAGCAACAGCTTCAAC CTTG	*Spe*I site; AN 8517f
CBS PBO_046	CGGAATTCCAAGCTT**TTA**AGCGTAATCTGGAACATCGT ATGGGTATTTCTTCTCGATATACTGGCTGAAAATCTGG C	*Hin*dIII site, **stop**; HA tag; AN 8517r
CBS PBO_056	CGGAATTCCACTAGTATGTCAACGAAGTTGCCAAGC	*Spe*I site; DS 101924f
CBS PBO_057	**TGA**AGCGTAATCTGGAACATCGTATGGGTAAGACGAA ATATGCTCGTTGAACC	**stop**; HA tag; DS 101924m
CBS PBO_039	CGGAATTCCAAGCTT**CTA**AGCGTAATCTGGAACATCG TATGGGTA	*Hin*dIII site, **stop**; HA tag; stop

CBS PBO_060	CGGAATTCCACTAGTATGTCGCACTCATTCCTGAACG	*Spe*I site; DS 179877f
CBS PBO_061	**TAG**AGCGTAATCTGGAACATCGTATGGGTATAGCCCA ACCCAAGTGAAACC	**stop**; HA tag; DS 179877m
CBS PBO_062	CGAATAACCGAATTC**TAG**AGCGTAATCTGGAACATCG TATGGGTA	*Eco*RI site, **stop**; HA tag; stop
LGE PBO_007	TCCACTAGTATGTCTCTTCCTAAGGATT	*Spe*I; GH1-1f
LGE PBO_008	TCCAAGCTT**TTA**AGCGTAATCTGGAACATCGTATGGGT AGTCCTTCTTGATCAAAGA	*Hin*dIII site, **stop**; HA tag; GH1-1r

3.3.6 Strain constructions

S. cerevisiae transformations were carried out using a lithium acetate-based protocol, according to Gietz and Woods (2002). Integration of the CDT-1 expression cassette into CEN.PK113-5D's genome (strain PBY_08; Table 3.1) was performed via the CRISPR-Cas9 system targeting the *HO* locus. For this purpose, we used a single-DNA plasmid (pGS_004.30, Table 3.2), carrying a dominant selection marker (*kanMX*) and both Cas9 and guide RNA (gRNA) expression cassettes, kindly provided by Prof. Dr. G. A. G. Pereira. The CDT-1 expression fragment was PCR-amplified from p425GPD-CDT-1 plasmid using primers FMO_019 and FMO_020 (Table 3.3), generating a cassette with 40 bp homology to the *HO* locus in CEN.PK strains. Co-transformation of these cells was made with 1 μg of pGS_004.30 and 10 or 20 μL of non-purified donor DNA (CDT-1 expression cassette). Confirmation of targeted integration was verified by diagnostic PCR, after isolation of gDNA from yeast colonies.

To construct BGL-expressing strains, 500 ng of each BGL-harbouring plasmid (Table 3.2) was transformed into CEN.PK113-5D cells yielding strains PBY_01 to PBY_06 (Table 3.1).

Strains expressing the CDT-1 cassette and every individual BGL sequence were constructed by transformation of 500 ng of each BGL-harbouring plasmid into PBY_08, resulting in strains PBY_09 to PBY_14 (Table 3.1).

3.3.7 Culture media

E. coli was grown in LB medium; 100 μg/mL of the appropriate antibiotic was added to the medium when required. LB medium contained 10 g/L tryptone, 10 g/L NaCl, and 5 g/L yeast extract. For solid LB medium, 15 g/L agar was added. Sterilisation was carried out by autoclaving at 121 °C for 20 min. *S. cerevisiae* strains were routinely cultivated at 30 °C and

200 rpm in YPD medium, composed of 10 g/L yeast extract, 20 g/L peptone, and 20 g/L dextrose. Sterilisation was carried out by separately autoclaving glucose from peptone and yeast extract, to avoid caramelisation (Maillard reaction). When required, 20 g/L agar was added to the peptone/yeast extract solution prior to heat sterilisation (121 °C for 20 min). To select transformants using an amino acid auxotrophic marker, a synthetic complete medium (SCM) was used, which contained 1.7 g/L yeast nitrogen base (without amino acids and without ammonium sulphate) (BD Difco™, Franklin Lakes, USA), 5 g/L $(NH_4)_2SO_4$, 20 g/L glucose, 20 g/L agar, and 0.44 g/L appropriate Drop-Out mixture (Ura^- or Leu^-), prepared according to Clontech Laboratories (2009). To select transformants resistant to geneticin, 200 mg/L G418 was added to the medium.

For RNA extraction from *T. reesei*, QM6a and RC 30-38 strains were grown in 250-mL shake-flasks in complete medium (CM) with 8 g/L cellobiose during overnight, 24 or 48 h growth. The CM contained a minimal medium (MM) with salts and trace elements supplemented with 2 g/L tryptone, 1 g/L casamino acids, 1 g/L yeast extract, 0.5 g/L yeast ribonucleic acids, and adjusted to pH 6 with NaOH. The MM contained 6 g/L $NaNO_3$, 1.5 g/L KH_2PO_4, 0.5 g/L KCl, 0.5 g/L $MgSO_4.7H_2O$, and 0.2 mL/L Vishniac trace element solution, which was filter-sterilised and added to the medium after autoclaving (121 °C for 20 min). The trace element solution was prepared according to Vishniac and Santer (1957).

Yeast growth assays in liquid SM were performed according to Verduyn *et al.* (1992), with the substitution of ammonium for urea as the sole nitrogen source, in order to prevent excessive acidification during cultivation. To supplement the missing sulphate in the medium, K_2SO_4 was added as in (Luttik *et al.* 2000; van Leeuwen *et al.* 2009). SM contained vitamins, trace metals, salts, a nitrogen source, and a carbon and energy source, including 6.6 g/L K_2SO_4, 3.0 g/L KH_2PO_4, 0.5 g/L $MgSO_4.7H_2O$, 2.3 g/L urea, and 20 g/L cellobiose, glucose or lactose with an initial pH adjusted to 6.0 using KOH 2 M. Urea, cellobiose, glucose and lactose solutions were filter-sterilised through 0.22 μm pore membranes and added to the medium after autoclaving (121 °C for 20 min). Vitamins and trace elements solutions (Verduyn *et al.* 1992) were prepared as 1000x stocks and sterilised by filtration or autoclaving, respectively, before addition to the medium. For solid media, the original medium prepared according to Verduyn *et al.* (1992) was employed, with the addition of 20 g/L agar prior to heat sterilisation.

3.3.8 Cultivation conditions

3.3.8.1 Microplate cultivations

Growth profiles of the recombinant yeast strains in cellobiose- or glucose-containing media were evaluated using sterile 96-microwell plates (CELLSTAR® flat bottom, No. 655161 - Greiner Bio-One, Kremsmünster, Austria) and the automated plate reader Tecan Infinite M200 Pro, according to Beato *et al.* (2016) with some modifications. Briefly, pre-cultures were prepared by transferring cells from one fresh colony on solid SM with 20 g/L glucose to 50-mL polypropylene tubes containing 3 mL of SM with 20 g/L initial glucose. After 48 h incubation at 30 °C and 200 rpm (Innova 4430 shaker incubator, New Brunswick Scientific, Edison, USA), an aliquot was collected to make 1 mL of cell suspension with an absorbance at 600 nm (Abs_{600}) equal to 0.5. Following three washing procedures with sterile distilled water, 10 µL of this suspension was used to inoculate a single well containing 90 µL of SM with either 20 g/L cellobiose or glucose, dropping the initial sugar concentration to 18 g/L. For the blank wells, 10 µL of sterile distilled water was added to the wells filled with 90 µL of the corresponding medium (three wells per blank). The plate was then sealed with PCR polyester sealing film (Axygen® UC-500, Corning Life Sciences, Tewksbury, USA) and incubated at 30 °C and 198.4 rpm (3.5 mm of amplitude) in the automated plate reader. Cultivations were run in triplicates (three wells on the same plate) and cell growth was monitored by measuring the Abs_{600} approximately every 50 min. Maximum specific growth rates (μ_{max}) were calculated from at least five data points obtained from the slope of a semi-logarithmic (using the natural logarithm) plot of absorbance versus time generated using data within the exponential growth phase. These values together with averages and standard deviations were calculated using Microsoft Excel.

3.3.8.2 Shake-flask cultivations

Shake-flask cultivations were performed in duplicates in 250-mL cotton-capped unbaffled Erlenmeyer flasks with silicone tubing connected to an outside needle, which allowed sampling using a syringe, without the need to open the flask during sampling (Appendix I). To avoid contamination, the tubing was kept closed by a Mohr clamp during cultivation and opened during sampling. Flasks containing 50 mL of SM with 20 g/L initial cellobiose were incubated at 30 °C and 200 rpm in a rotary shaker (Innova 4430, New Brunswick Scientific, Edison, USA) under an air atmosphere. Pre-cultures were prepared by transferring cells from one colony on solid SM with 20 g/L glucose to 50-mL polypropylene tubes containing 3 mL

of SM with 20 g/L initial glucose, except for strain PBY_07, whose inoculum was prepared as described below. After 24 h growth at 30 °C and 200 rpm, the pre-inoculum was transferred to 125-mL unbaffled Erlenmeyer flasks containing 22 mL of SM with 20 g/L initial cellobiose. After 3-4 days of growth, cultures were centrifuged at 3000 rpm for 5 min (NT810 centrifuge, Novatecnica, Piracicaba, Brazil) and the supernatant discarded; cells were washed twice with sterile distilled water and resuspended in 1 mL of SM before inoculating 250-mL Erlenmeyer flasks with an initial Abs_{600} of approximately 0.1. Inoculum of PBY_07 was prepared by growing cells from a single colony in a 125-mL Erlenmeyer flask filled with 25 mL of SM with 20 g/L initial glucose for 48 h at 30 °C and 200 rpm. No incubation on cellobiose was performed with this strain for the inoculum preparation. Shake-flasks were incubated for days, and samples taken at different time points to measure cell concentration (indirectly via Abs_{600}) and pH.

3.3.9 Enzymatic assay of β-glucosidase activity

For preparation of cell extracts, yeast cells were harvested during the exponential growth phase of shake-flask cultures containing 100 mL of SM with 10 g/L initial glucose (Abs_{600} = 1 to 1.5). Samples were harvested, washed, and prepared for sonication according to Postma *et al.* (1989). Briefly, samples were centrifuged at 4 °C and 5000 rpm for 10 min (SORVALL® RC-26 PLUS centrifuge - DuPont, Wilmington, USA), washed twice with ice-cold freeze buffer (10 mM potassium phosphate, pH 7.5, and 2 mM EDTA), washed once with sonication buffer (100 mM potassium phosphate, pH 7.5, and 2 mM $MgCl_2$) and resuspended in 4 mL of ice-cold sonication buffer + 40 µL of 0.1 M 1,4-Dithiothreitol (DTT). Cell extracts were prepared by sonication with 3 g glass beads of 425-600 µm (Sigma-Aldrich, Missouri, USA) at 0 °C in 4 bursts of 30 seconds with 90 second intervals in an ultrasonic probe sonicator/cell disruptor mixer (DES500, UNIQUE, Indaiatuba, Brazil) operated at maximum power (99%). Unbroken cells and debris were removed by centrifugation (4 °C, 20 min, 20000 rpm) and the supernatant was used as the cell extract for enzyme activity assays. BGL activity was measured by incubating 80 µL of cell extracts with 0.5 or 1 mM p-nitrophenyl β-D-glucopyranoside (p-NPG) in 50 mM potassium phosphate buffer (pH 6) or 100 mM potassium phosphate buffer (pH 7), respectively. The release of p-nitrophenol (p-NP) from p-NPG was monitored by colorimetric change at 405 nm in the automated plate reader Tecan Infinite M200 Pro. The mixture was allowed to react for 0, 5, 10, 15, 20, 30 and 40 min at 30 °C or 37 °C. The reaction was stopped by addition of 100 µL of Na_2CO_3 1 M. The linear range of the reaction was determined. The amount of p-NP released was quantified by p-NP

standard curves in 50 mM potassium phosphate buffer (pH 6) or 100 mM potassium phosphate buffer (pH 7). The experiments were carried out in triplicate, with average and standard deviation values calculated using Microsoft Excel. Protein levels in cell extracts were determined using the Lowry assay (Lowry *et al.* 1951). One unit (U) of β-glucosidase activity was defined as the amount of enzyme required to release 1 μmol of p-NP per minute from p-NPG in the reaction conditions. The specific activity of the sample solution was determined by dividing the enzyme activity (U/mL) by the protein concentration (mg/mL). For a detailed explanation of the calculations performed to determine the specific BGL activities, please refer to Appendix II.

3.3.10 Serial dilution spot assay

The dilution spot assay was performed according to the protocol reported by Madeira-Jr and Gombert (Madeira-Jr and Gombert 2018), with the following modifications. For each strain, cells from a single colony were transferred to a 50-mL polypropylene tube, containing 10 mL of SM with 20 g/L initial galactose (pre-inoculum). After 24 h growth at 30 °C and 200 rpm (Innova 4430 shaker incubator, New Brunswick Scientific, Edison, USA), a defined volume of this culture was transferred to a second tube containing 10 mL of the same fresh medium, making the cell suspension with an initial Abs_{600} of 0.1 (inoculum). The tubes were incubated at 30 °C and 200 rpm for further 8 h (until exponential growth phase). Thereafter, cells were harvested, washed 3x with sterile distilled water, resuspended in sterile water to obtain an Abs_{600} of 0.05 (0.05×10^{0}) in 1 mL of cell suspension, and four successive dilutions (0.05×10^{-1}, 0.05×10^{-2}, 0.05×10^{-3}, and 0.05×10^{-4}) were prepared. 5 μL of each dilution were carefully spotted with a pipette onto the surface of Petri dishes containing solid SM with 20 g/L of either glucose, cellobiose or lactose as sole carbon sources. The plates were incubated at 30 °C (502 incubator, FANEM, São Paulo, Brazil) for different time periods and photographs were taken at appropriate time points.

3.3.11 Analytical methods

Cell growth from shake-flask samples was monitored by Abs_{600} measurements using a spectrophotometer (Genesys 20, Thermo Scientific, Waltham, USA). The pH of each sample was read using a pHmeter (Digimed DM21, São Paulo, Brazil).

3.4 Results and Discussion

Most of the results from this chapter were achieved at CBS-KNAW Fungal Biodiversity Centre (currently Westerdijk Fungal Biodiversity Institute) in Utrecht, The Netherlands, and at LGE/IB/UNICAMP, as a result of a six-month research internship under the supervision of Prof. Dr. Ronald de Vries and a collaboration with Dr. Gleidson Silva Teixeira, respectively. A schematic representation of the work carried out is presented in Figure 3.1. The bioinformatic work as well as the construction of the cloning vectors were performed at CBS-KNAW. The expression plasmids and construction of the iCELL strains were developed at LGE/IB/UNICAMP, whereas the enzymatic and cultivation assays were performed at LEMeB/FEA/UNICAMP.

3.4.1 *In silico* identification of putative fungal genes involved in cellobiose degradation

3.4.1.1 Cellodextrin transporters

We initiated this study by applying a bioinformatics approach to identify novel cellodextrin transporters in a group of selected fungal strains (see section 3.3.1.1) that participate in decomposition of plant matter. To this end, the well characterised cellodextrin transporters from *N. crassa*, CDT-1 and CDT-2, were submitted to a BLASTP search *versus* the selected fungal genomes. This analysis resulted in 83 putative transporters, whose evolutionary relationships were further evaluated (Figure 3.2). The CDT phylogenetic tree revealed a well-supported clade (bootstrap value of 90) that clustered nine sequences closely related to CDT-1: Podan2|558, Spoth2|43941, Aspni NRRL3 1|03028, Trire2|3405, Trire2|67752, Agabi_varbisH97_2|195794, Agabi_varbisH97_2|195761, Dicsq1|104403, and Podan2|601. These nine orthologs are 35 to 74% identical in amino acid sequence to CDT-1 (Table 3.4) and classified as sugar transporters of the Major Facilitator Superfamily (MFS) in the functional analysis predicted by the InterPro server (Figure 3.3). This range of identity (~ > 30% and < 80%) allows for the selection of novel candidates who are different from the query (not a close homologue), but do have conserved sequences similar to the reference (Kamble, Srinivasan and Singh 2019). Sequence analysis using TM-Coffee also showed high similarity between CDT-1 and the nine closely related candidates in all functional domains, predicting a total of 12 transmembrane domains (Figure 3.4). This analysis was in agreement with the results from the TMHMM software (Appendix III). These data obtained through a combination of bioinformatics tools strongly support the role of these proteins as potential CDTs in their natural hosts.

At this point, it should be noted that only candidate sequences similar to CDT-1 were considered in our analysis. One of the reasons for this was that, when expressed in yeast, CDT-1 provides faster cellobiose fermentation performances than CDT-2-expressing strains (Galazka *et al.* 2010; Kim *et al.* 2014a). Moreover, there is evidence that CDT-2 works as a simple facilitator (Kim *et al.* 2014a), different from CDT-1 that functions as a proton symporter. Since transport mediated by active transporters benefits from decreased free-energy conservation, which in this case results in higher ethanol yields on sugar (Basso *et al.* 2011), we excluded from the analysis those sequences more related to CDT-2. On the other hand, we focused on those candidates in close relationship with CDT-1 to maximise the chances of obtaining successful results when expressed in yeast, since functional expression of CDT-1 in *S. cerevisiae* has already been demonstrated in several reports, as detailed in Table 2.2 (Chapter 2).

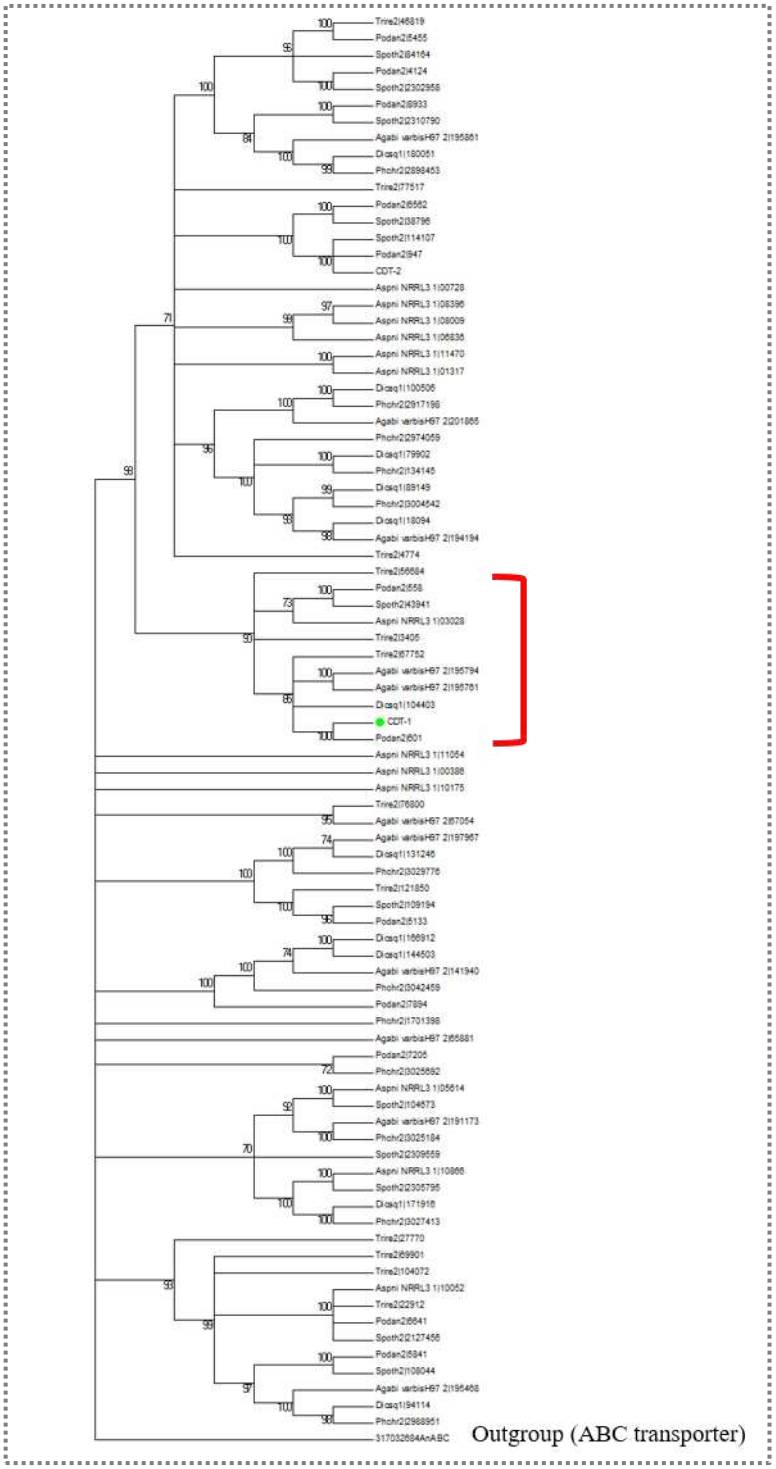

Figure 3.2. Phylogenetic analysis of predicted and identified fungal CDT sequences. The Neighbour-Joining tree (1000 bootstraps) shows a clade with nine sequences that cluster close to CDT-1 (highlighted in a red square bracket). Species used for the analysis can be found in section 3.3.1.1. Sequence alignment was performed with the MAFFT program, although the analysis from different alignment methods showed essentially similar results. An ABC transporter from *N. crassa* was included as outgroup. Only the bootstraps above 70 are shown on the branches.

Table 3.4. Sequence similarity between CDT-1 and the nine closely related sequences obtained from the phylogenetic analysis.

NAME	NOTATION	ORGANISM	EVALUE	% IDENT
Podan2|601	PA 601	*P. anserina S mat+*	0.00 E000	74.4
Agabi_varbisH97_2|195794	AB 195794	*A. bisporus var bisporus (H97) v2.0*	4.52 E-128	46.7
Agabi_varbisH97_2|195761	AB 195761	*A. bisporus var bisporus (H97) v2.0*	2.23 E-127	46.3
Dicsq1|104403	DS 104403	*D. squalens v1.0*	5.97 E-117	43.8
Spoth2|43941	MT 43941	*M. thermophila (Sporotrichum thermophile) v2.0*	3.27 E-105	41.6
Podan2|558	PA 558	*P. anserina S mat+*	4.19 E-101	40.1
Trire2|3405	TR 3405	*T. reesei v2.0*	4.64 E-089	39.1
Aspni_NRRL3_1|03028	AN 3028	*A. niger NRRL3*	7.07 E-083	37.9
Trire2|67752	TR 67752	*T. reesei v2.0*	1.52 E-086	35.3

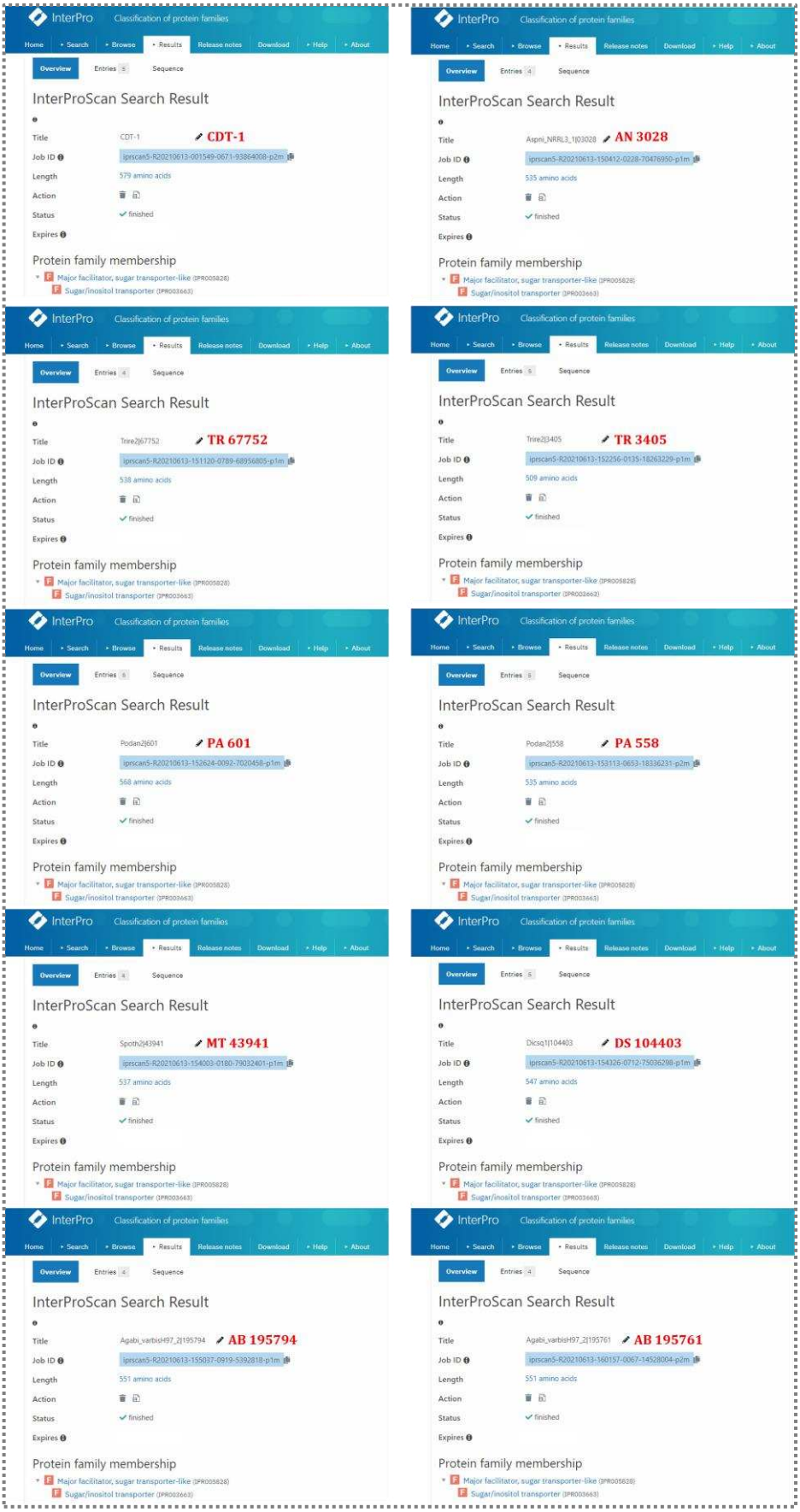

Figure 3.3. Functional analysis of the nine closely related sequences to CDT-1. According to the predictive models of the InterPro server, all proteins are classified as sugar transporters of the MFS family.

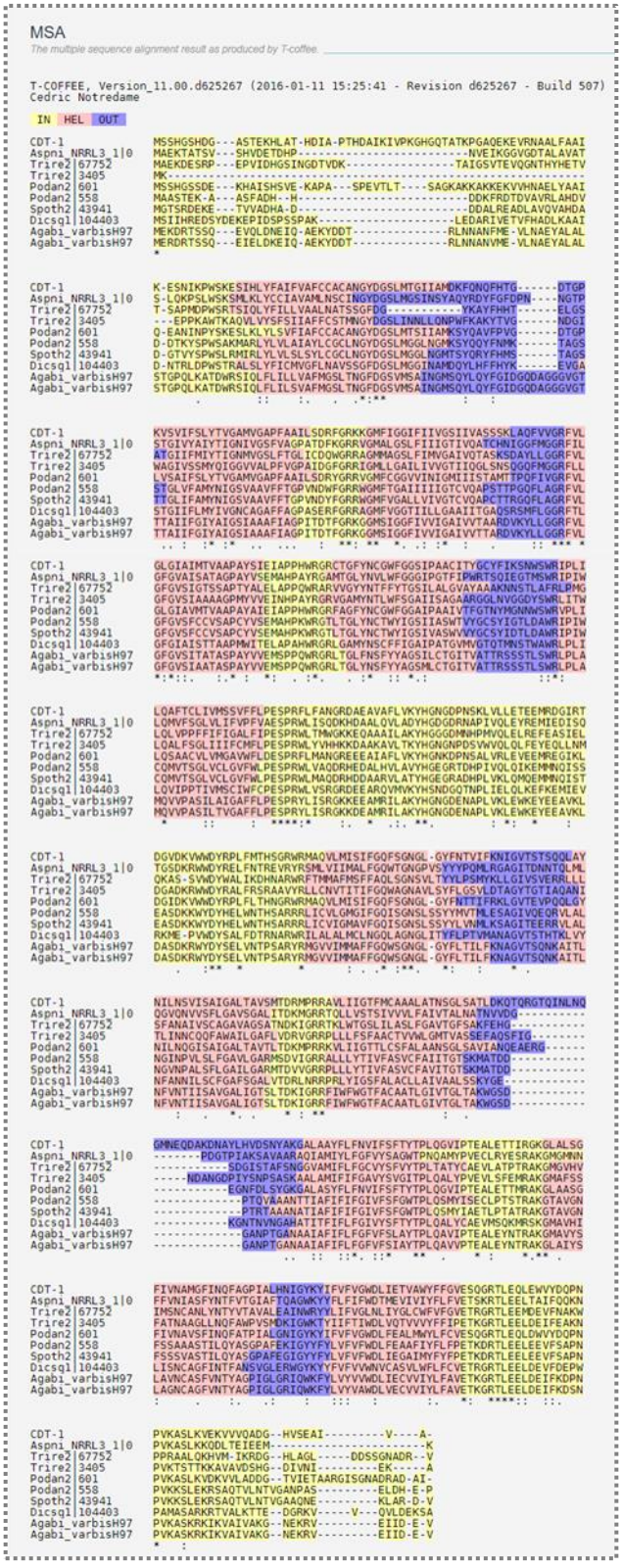

Figure 3.4. TM-Coffee alignment between CDT-1 and the nine closely related sequences resulting from the phylogenetic analysis. Different protein domains are highlighted in yellow (internal), pink (transmembrane) and blue (external). Twelve transmembrane domains are predicted in all sequences.

Among the nine closest sequences to CDT-1, five of them were selected for further expression studies in *S. cerevisiae*, which also included the *N. crassa* CDT-1 sequence as positive control to compare transporter performances. This set of selected candidates included members of both Asco- and Basidiomycetes that were actively studied within de Vries' group at CBS-KNAW, where this part of the work was developed (Table 3.5). By the time this analysis was performed, very few published studies had involved expression of sugar transporters from basidiomycetes in yeast (López *et al.* 2008; Wahl *et al.* 2010; Gonçalves *et al.* 2016). Basidiomycete fungi might have more disaccharide transporters than Ascomycetes (personal communication with Dr. de Vries), but the correct expression of these genes in *S. cerevisiae* is more challenging than their ascomycete counterparts (Harvey *et al.* 2018), probably due to the inability of the host to process the rich intron content found in basidiomycete genes (Kupfer *et al.* 2004), in case they are not removed prior to heterologous expression. Another possibility is that the closer phylogenetic proximity between ascomycete fungi and *S. cerevisia*e (which also belongs to the Ascomycota phylum) increases the chances of these genes being functional in yeast.

Table 3.5. CDT candidate sequences selected for heterologous expression in *S cerevisiae*.

PHYLUM	ORGANISM	NOTATION
Ascomycota	*A. niger*	AN 3028
	P. anserina	PA 558 and PA 601
	T. reesei	TR 67752
	N. crassa	CDT-1
Basidiomycota	*D. squalens*	DS 104403

3.4.1.2 Intracellular β-glucosidases

For the intracellular BGLs, we screened for sequences without signal peptides from predicted BGL candidates within families GH1 and GH3, obtained from the CAZy database as well as from an internal database at CBS-KNAW. For this analysis, we assumed that sequences with signal peptides will be secreted by fungi, while sequences without signal peptides will function inside the cells. The absence of signal peptides in the sequences was an important criterion, since an extracellular BGL in the original source microorganism could experience improper folding in the cytoplasm of *S. cerevisiae* if expressed without its native secretion signal sequence (Njokweni, Rose and van Zyl 2012).

Next, the phylogeny of these sequences as well as of already characterised BGLs from other microorganisms was evaluated. As presented in Figure 3.5, the phylogenetic tree showed a clear separation between BXLs and BGLs, as well as a division among BGLs into two subgroups of enzymes, those belonging to GH families 1 or 3, each of which gathers proteins with similar sequences and conserved sequence motifs. According to this analysis, we selected four representatives from the GH1 family and seven from the GH3 for further heterologous expression in yeast, comprising a total of ten predicted BGLs and one characterised enzyme as positive control (GH1-1 from *N. crassa*) (Galazka *et al.* 2010) (Table 3.6).

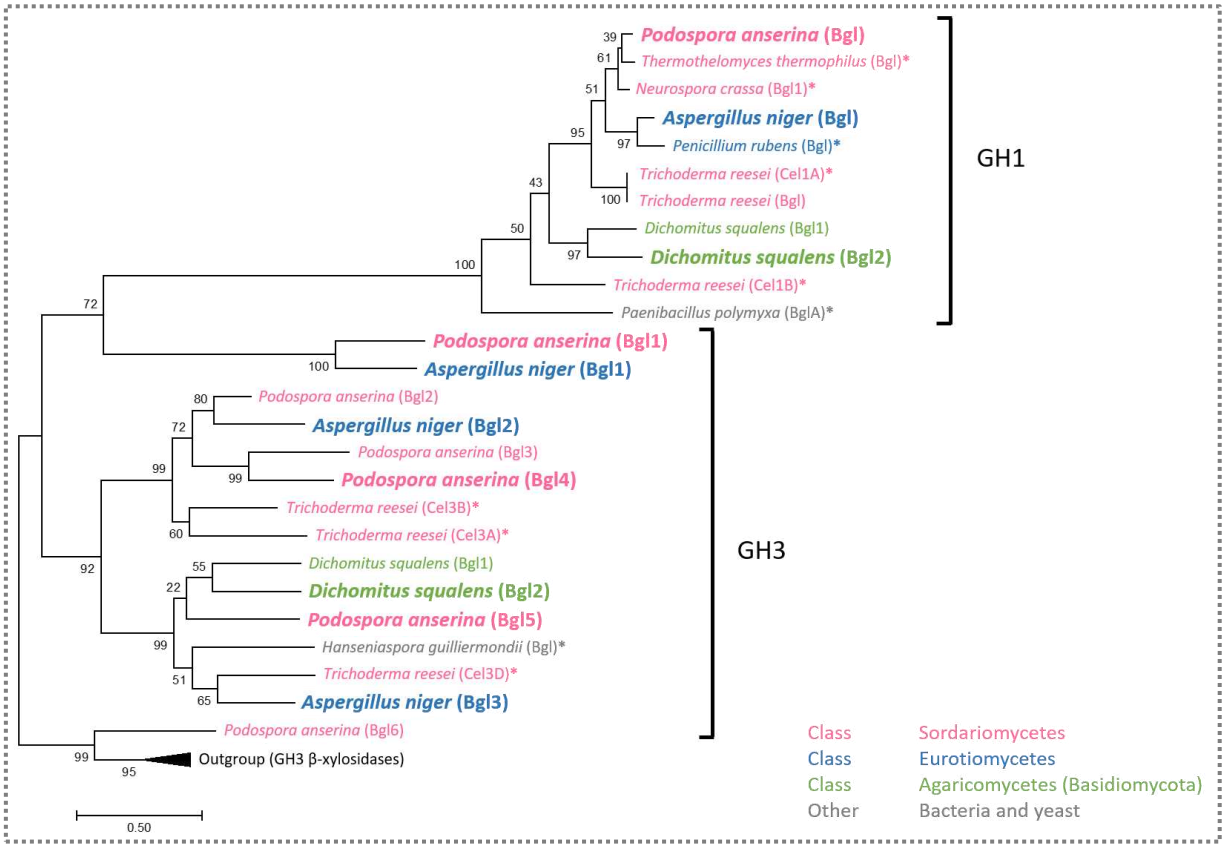

Figure 3.5. Phylogenetic analysis of predicted and characterised BGLs from different microorganisms. Six BXLs from *A. niger* and *T. reesei* were included as outgroup. Enzymes with an asterisk have been already characterised elsewhere (see section 3.3.1.2 for references). BGLs selected for this study are highlighted in **bold** font.

Table 3.6. BGL candidate sequences selected for heterologous expression in *S cerevisiae*.

GH FAMILY	ORGANISM	NAME	NOTATION
1	*P. anserina*	Bgl	PA 10293
1	*N. crassa*	Bgl1	GH1-1*

1	*A. niger*	Bgl	AN 8517
1	*D. squalens*	Bgl2	DS 101924
3	*P. anserina*	Bgl1	PA 6071
3	*A. niger*	Bgl1	AN 6623
3	*A. niger*	Bgl2	AN 3736
3	*P. anserina*	Bgl4	PA 3784
3	*D. squalens*	Bgl2	DS 179877
3	*P. anserina*	Bgl5	PA 951
3	*A. niger*	Bgl3	AN 6436

GH: Glycoside Hydrolase.

* The *N. crassa* GH1-1 sequence was included as positive control (well-described enzyme).

3.4.2 Heterologous expression of fungal intracellular BGLs in *S. cerevisiae*

To assess the functionality of the BGL candidates in *S. cerevisiae*, we decided to express each individual coding sequence via episomal expression, driven from the constitutive GPD promoter. The cloning process demanded a significant effort and due to time limitations we moved forward with only six out of the eleven BGL originally selected sequences.

Different sources of genetic material were used to amplify and clone the selected coding genes into p426GPD. The AN 8517 sequence from *A. niger* was amplified from cDNA available at CBS-KNAW; the *N. crassa* GH1-1 coding sequence was amplified from a GH1-1-harbouring plasmid obtained from LGE/IB/UNICAMP; and all sequences belonging to *P. anserina* (PA 951, PA 3784, PA 6071, and PA 10293) were synthesised and codon-optimised. All six expression plasmids were successfully constructed by traditional digestion/ligation procedures (Figure 3.6), and subsequently transformed into *S. cerevisiae* CENPK113-5D strain (Ura^-), yielding strains PBY_01 to PBY_06 (Table 3.1). Transformation of the empty plasmid was also performed (PBY_07). Transformants with the Ura^+ phenotype were isolated.

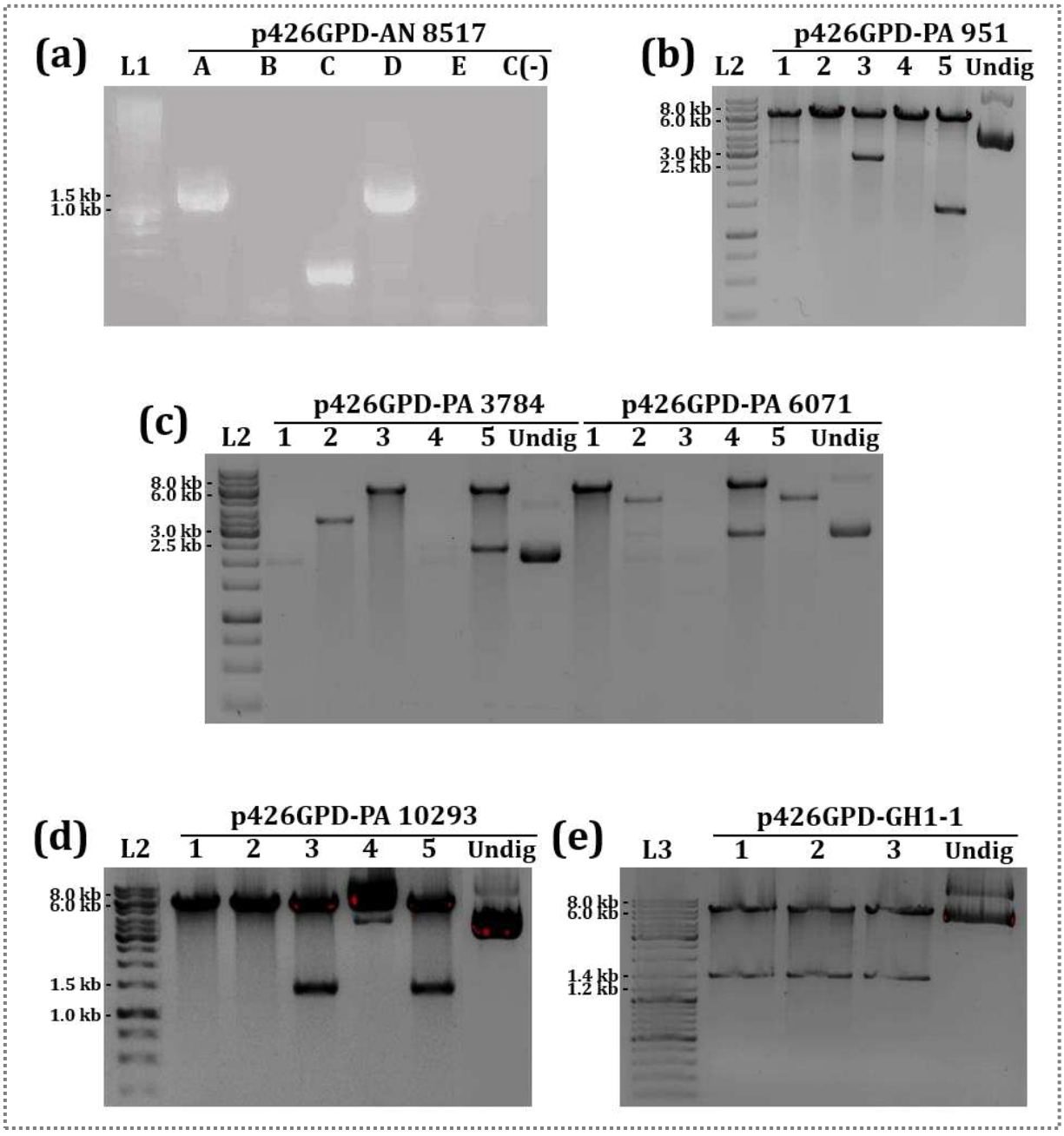

Figure 3.6. Confirmation of BGL cloning into p426GPD. (a) The first lane (L1) corresponds to the Hyperladder 1kb (Bioline). Lanes A-E show the PCR results of five randomly picked colonies with primers CBS PBO_044 and CBS PBO_046 that amplify the AN 8517 ORF. Expected size of the PCR product is 1491 bp. A negative control without a DNA template is also included. Clones A and D resulted positive for the reaction and were finally confirmed by DNA sequencing. **(b)**, **(c)** and **(d)** Plasmids from five randomly picked clones were prepared and analysed by restriction with *Spe*I and *Hin*dIII, which remove each insert from the vectors. Successful cloning results in digestion fragments of 2778 and 6570 bp (for p426GPD-PA 951, lane 3); 2346 and 6570 bp (for p426GPD-PA 3784, lane 5); 2730 and 6570 bp (for p426GPD-PA 6071, lane 4) and 1464 and 6570 bp (for p426GPD-PA 10293, lanes 3 and 5). Undigested plasmids are also included as controls. Lane L2 refers to the GeneRuler 1kb DNA Ladder (Thermo Scientific). **(e)** Plasmids from three randomly picked clones were prepared and analysed by restriction with *Spe*I and *Hin*dIII, which remove the GH1-1 insert from the vector resulting in digestion fragments of 1464 and 6570 bp (lanes 1, 2 and 3). Undigested plasmid is also included as control. Lane L3 refers to the GeneRuler DNA Ladder Mix (Thermo Scientific).

After transformation of each BGL-encoding plasmid into *S. cerevisiae*, intracellular BGL activities were measured at 30 °C and pH 6 or 7 in cell extracts supplemented with p-NPG. For this analysis, we chose pH and temperature values according to their proximity to the physiological conditions, because the enzymes were supposed to function inside the cells. Among all six BGLs tested, GH1-1 showed the highest specific activity at both pHs assayed, corresponding to roughly 130-550 times higher than the other novel BGLs (Figure 3.7). Experimental parameters, such as pH and temperature, are well-known to exert a great influence on the activity of enzymes. For instance, as with many ordinary chemical reactions, raising the temperature generally speeds up the rate of an enzyme-catalysed reaction (of course, this increase is only up to a certain point). Thus, we further increased the reaction temperature from 30 to 37 °C in order to investigate whether this condition would have a positive effect on the enzymatic performances. However, no relevant differences were observed in the resulting hydrolytic activities towards p-NPG (data not shown). An important consideration here is that we did not measure the potential extracellular BGL activities in the culture media, which would have allowed us to eliminate (or not) the possibility of protein secretion via nonconventional pathways (Nombela, Gil and Chaffin 2006; Giuliani, Grieve and Rabouille 2011). Most importantly, a more accurate analysis should have included the activity of the control strain harbouring the empty plasmid, in order to measure the basal activity of the cell towards p-NPG.

GH1-1 is a well-described enzyme in the literature, and it is noticeable how big are the differences in the values reported for its activity, even when very similar methodologies were employed. For instance, Eriksen *et al*. reported a GH1-1 activity of 0.193 U/mg protein assayed with 1 mM p-NPG in 100 mM potassium phosphate buffer at pH 7 and 30 °C (Eriksen *et al.* 2013), whereas Bae *et al*. measured an activity ~14 times lower at the same temperature, but using 0.5 mM p-NPG in 50 mM potassium phosphate buffer at pH 6 (Bae *et al.* 2014). It is unlikely that a variation of one pH unit together with the concentration of the substrate would cause such a difference, as was observed with our results, so probably the strain background, the promoter strength, the plasmid copy number, and the conditions used for strain cultivation could explain part of these differences. Moreover, for the determination of a reaction velocity (i.e., enzyme activity) it is important to ensure that only the linear part of the curve “product concentration” (or “converted substrate concentration”) *vs*. “time” is considered (referred to as initial velocity), as aberrant and incorrect results are obtained when the velocity is calculated outside this linear range (Bisswanger 2014). Since BGL activities

are frequently determined in non-continuous assays (only one single point is used for the calculation), this could also contribute to the differences observed in the activity values reported in the scientific literature. In our study, the initial velocity of the BGL reactions was derived from at least four time points in the linear part of the curves (Appendix II). The GH1-1 activities we determined were considerably higher than the ones reported above (2.0 and 1.9 U/mg protein at pH 6 and 7, respectively), under the same assay conditions. Thus, it becomes clear that activity values should be interpreted with caution when using comparative analyses. Despite this remark, all the activities calculated in this work were obtained under the same experimental conditions and submitted to the same data treatment, thus a proper comparison could be made within our dataset.

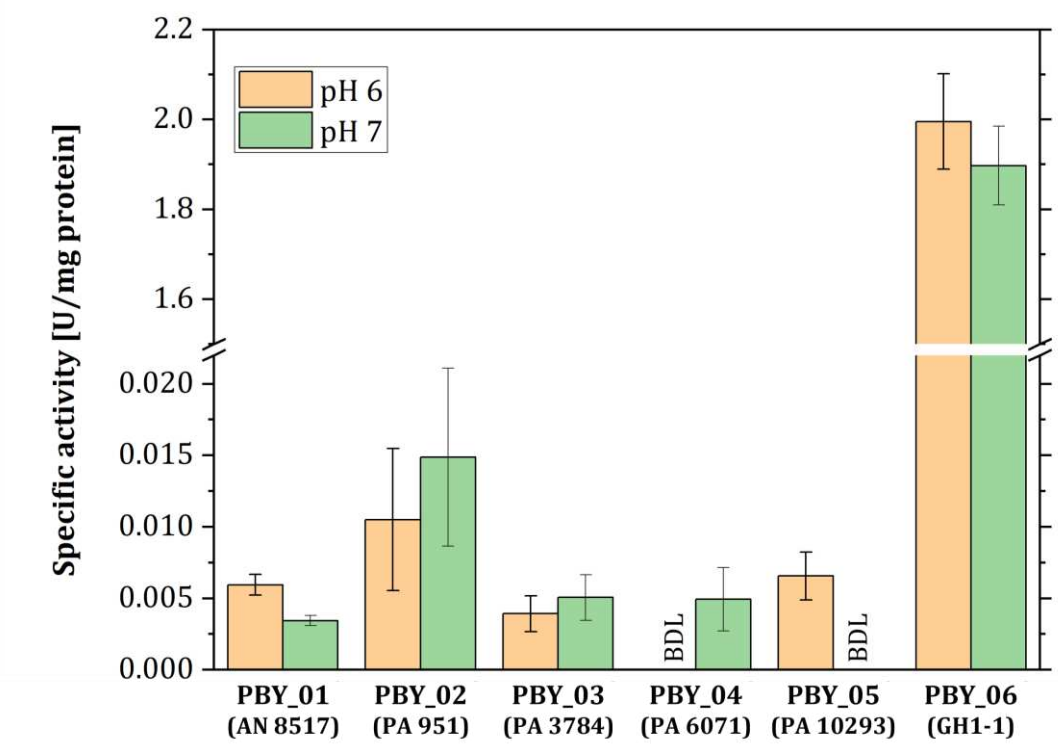

Figure 3.7. Specific enzyme activities of BGLs from fungal origin. The catalytic activities were measured in cell extracts of *S. cerevisiae* strains transformed with AN 8517 (PBY_01), PA 951 (PBY_02), PA 3784 (PBY_03), PA 6071 (PBY_04), PA 10293 (PBY_05), and GH1-1(PBY_06) (Table 3.1) in potassium phosphate buffer at pH 6 or 7 and 30 °C. One unit of BGL activity was defined as the amount of enzyme required to release 1 µmol of p-NP per minute from p-NPG in the reaction conditions. Values are the mean of three replicates. Error bars represent standard deviations among triplicates. BDL: below detection limit.

3.4.3 Engineering of intracellular cellobiose-utilising (iCELL) yeast strains

Prior to the intracellular hydrolysis of cellobiose, this disaccharide needs to be transported from the extracellular to the intracellular environment of the yeast cell. To introduce a

cellobiose transporter in *S. cerevisiae*, we designed a strategy based on genome integration, different from the plasmid-mediated expression of the intracellular hydrolases. The reason for this was to achieve a more precise expression, avoiding the potential cytotoxicity of overexpressing proteins associated with membranes (Wagner *et al.* 2006). While being a much faster strategy, plasmid-based cloning suffers from high copy number variation in the cell population, whereas by chromosomal integration we usually control the number of insertions (Ryan *et al.* 2014).

From previous phylogenetic analysis (section 3.4.1), five predicted CDT sequences from *A. niger*, *D. squalens*, *P. anserina*, and *T. reesei* as well as the characterised CDT-1 transporter from *N. crassa* were selected for subsequent cloning into *S. cerevisiae*. Candidate ORFs AN 3028 and DS 104403 from *A. niger* and *D. squalens*, respectively, were amplified from the corresponding cDNA and cloned via the Gateway system for further manipulation (plasmids pDONR223-AN 3028 and pDONR223-DS 104403, Table 3.2). Each construct was confirmed by colony-PCR and DNA sequencing (data not shown). Selected sequences from *P. anserina* (PA 558 and PA 601) were synthesised and delivered within plasmids pNZY29-PA 558 and pNZY29-PA 601, respectively (Table 3.2). Regarding sequence TR 67752, due to unavailability of genetic material from *T. reesei*, we synthesised the cDNA from total RNA isolated from two *T. reesei* strains, after cellobiose induction in complete medium along different hours of cultivation. Even though the resulting RNA integrity (determined by gel electrophoresis) and cDNA concentration were good for further PCR (data not shown), it was not possible to amplify the TR 67752 ORF from this cDNA. Apparently, for some reason, the gene was not expressed under the conditions used to induce its expression (8 g/L cellobiose in complete medium for overnight, 24 h or 48 h growth). Due to time limitations, we decided not to continue with this approach and discarded the TR 67752 sequence from our set of candidates.

Since we were provided with a plasmid-encoded CDT-1 gene, to construct a linear CDT-1 expression cassette for genome integration, we leveraged the yeast homologous recombination machinery to assemble the CDT-1 amplicon into a yeast vector where expression was driven from the constitutive *GPD* promoter and the *CYC* terminator. Correct assembly of this cassette was confirmed by diagnostic PCR and *Bam*H1 digestion (Figure 3.8). Although we successfully managed to construct this cassette, other cloning strategies such as double-joint PCR (Yu *et al.* 2004) and Gibson assembly (Gibson *et al.* 2009) were also extensively tried, without success.

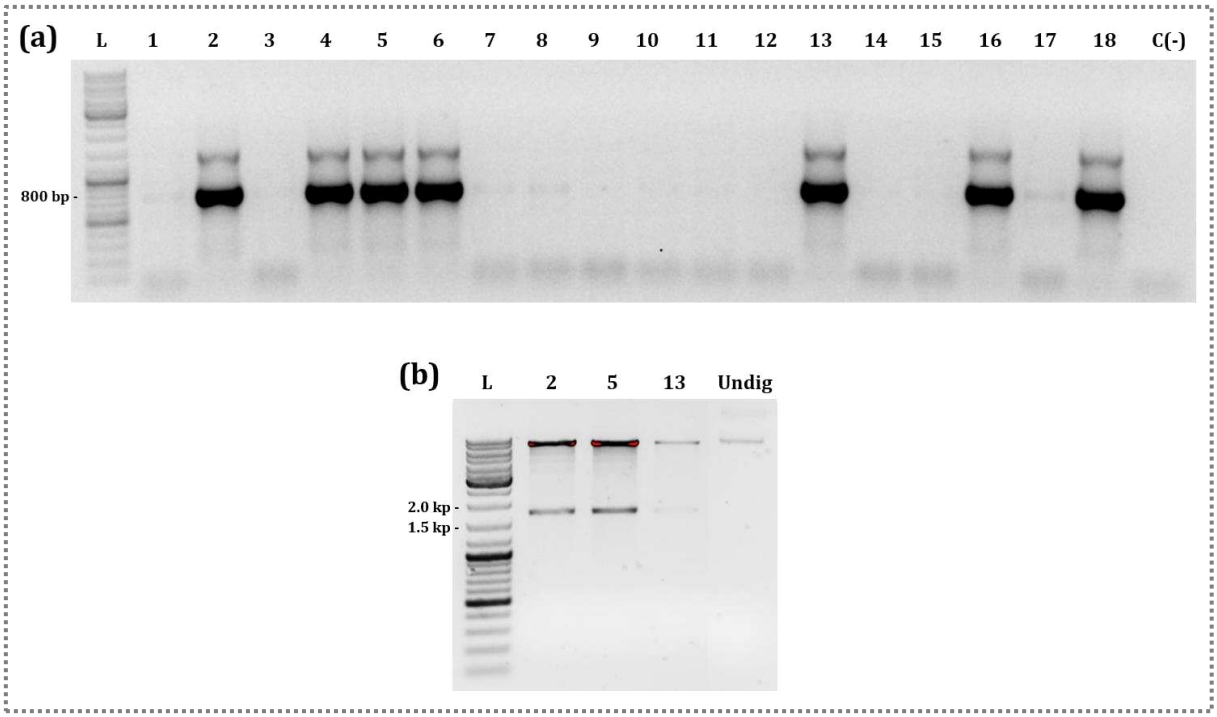

Figure 3.8. Confirmation of CDT-1 assembly into the backbone vector. (a) Diagnostic PCR of eighteen randomly picked colonies using primers LGE PBO_011 and FMO_010, pairing part of the ORF and part of the vector. Successful PCR results in a fragment with a length of 725 bp (lanes 2, 4, 5, 6, 13, 16 and 18). The first lane (L) contains the GeneRuler DNA Ladder Mix (Thermo Scientific) and the last one contains a negative control. **(b)** Digestion with *Bam*H1 removes the entire CDT-1 ORF from p425GPD-CDT-1 generating two DNA fragments of 1746 and 7728 bp (lanes 2, 5 and 13). Clones 2, 5 and 13 correspond to the same three clones indicated in **(a)**. L refers to the GeneRuler DNA Ladder Mix (Thermo Scientific). Undigested plasmid was also used as control.

The CDT-1 expression cassette was subsequently amplified from its harbouring vector yielding a construct flanked by ~40 bp homology arms to the *HO* locus in CEN.PK strains, which allowed its integration via CRISPR-Cas mediated homologous recombination. The *HO* gene encodes for an endonuclease that initiates interconversion of the mating-type locus and promotes diploidization of haploid strains. Almost all laboratory strains have a mutation at this locus, being considered as a neutral site for integration.

To integrate the CDT-1 expression cassette into the *S. cerevisiae* CEN.PK113-5D strain, we co-transformed this cassette (donor DNA or repair fragment) together with a single plasmid carrying both components required to edit the DNA, i.e., the Cas9 endonuclease and the gRNA, that guides the nuclease to the *HO* locus (pGS_004.30). For appropriate controls, we also performed a simple transformation with the plasmid pGS_004.30 and without it (negative control). An efficient gRNA should cause a double-strand break in the yeast genome and, therefore lead to no-growth or a very low growth pattern on the G418 plate of cells transformed with pGS_004.30, meaning the RNA-guided Cas9 has successfully cut the DNA

that was not repaired by Non-Homologous End Joining (NHEJ) mechanisms. In contrast, an efficient gRNA should lead to considerable growth in the condition with pGS_004.30 plus the donor DNA, meaning the RNA-guided Cas9 has successfully cut the DNA, that was then successfully repaired by Homologous Recombination (HR). These growth patterns were indeed observed in our transformations (Figure 3.9). Curiously, the number of colonies yielded when the "CRISPR-Cas9 plasmid" and the repair fragment were co-transformed into CEN.PK113-5D was independent of the amount of donor DNA used (10 or 20 µL, approximately 60 colonies per plate). Although not shown here, transformation with a control plasmid carrying a G418 resistance marker but without the CRISPR elements was also performed (positive control), yielding a plate full of colonies.

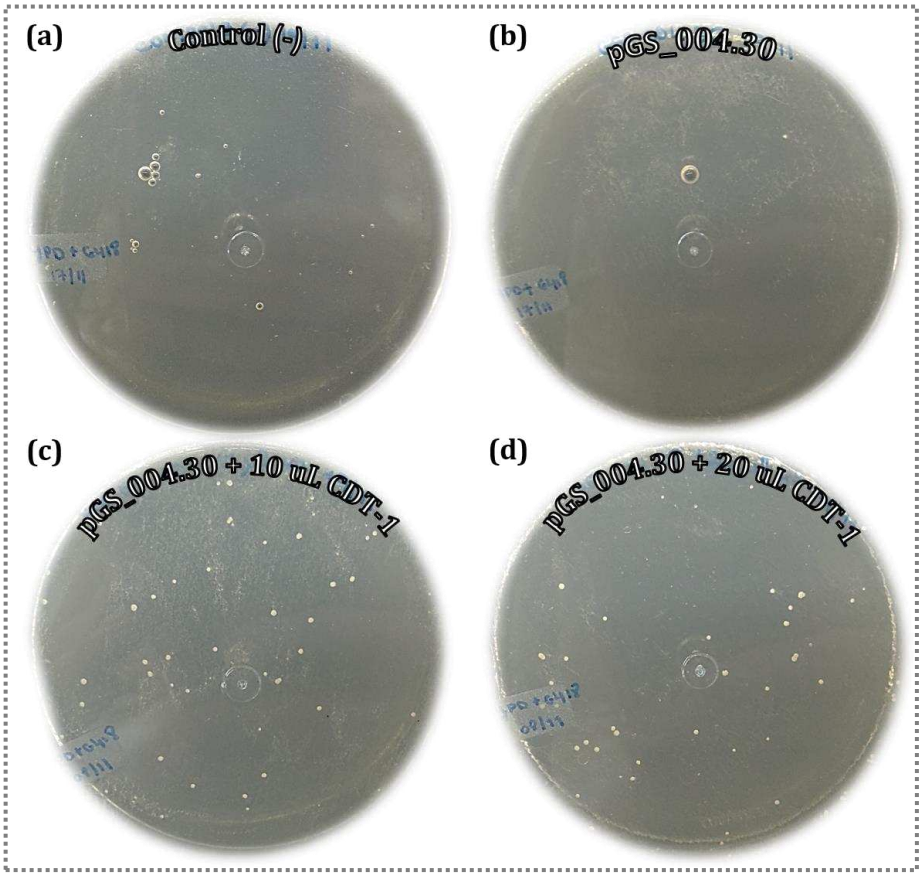

Figure 3.9. Integration of CDT-1 into the yeast genome by the CRISPR-Cas9 strategy. *S. cerevisiae* CEN.PK113-5D cells were transformed with no DNA **(a)**, with the "CRISPR-Cas9 plasmid" (pGS_004.30) **(b)**, co-transformed with pGS_004.30 and 10 µL of the CDT-1 expression cassette **(c)** or 20 µL of the CDT-1 expression cassette **(d)**. All transformants were selected on YPD medium supplemented with 200 mg/L G418. Plates (c) and (d) yielded approximately 60 colonies per plate, whereas no colonies were visible on plates **(a)** and **(b)**.

To confirm the correct integration of the CDT-1 expression cassette into the *HO* locus, genomic DNA of eighteen randomly picked colonies was extracted and verified by PCR using two different sets of primers (Figure 3.10). As a result, six out of the eighteen tested colonies contained the desired genotype, confirming the correct integration of CDT-1 into the yeast genome. The absence of amplicons in the other remaining colonies might indicate inefficient DNA edition, either because the DNA was not cut by the Cas9 or because it was cut and repaired by NHEJ mechanisms. Additionally, the quick protocol used for gDNA extraction from yeasts (Lõoke, Kristjuhan and Kristjuhan 2011) is very useful because it simplifies the screening, but does not generate as pure DNA as the traditional methods based on enzymatic degradation or glass beads beating, followed by cell lysis with detergent and extraction of gDNA with phenol-chloroform, leading to potential false negatives. We did not explore this issue further since the confirmed colonies were sufficient to allow for the continuation of this work.

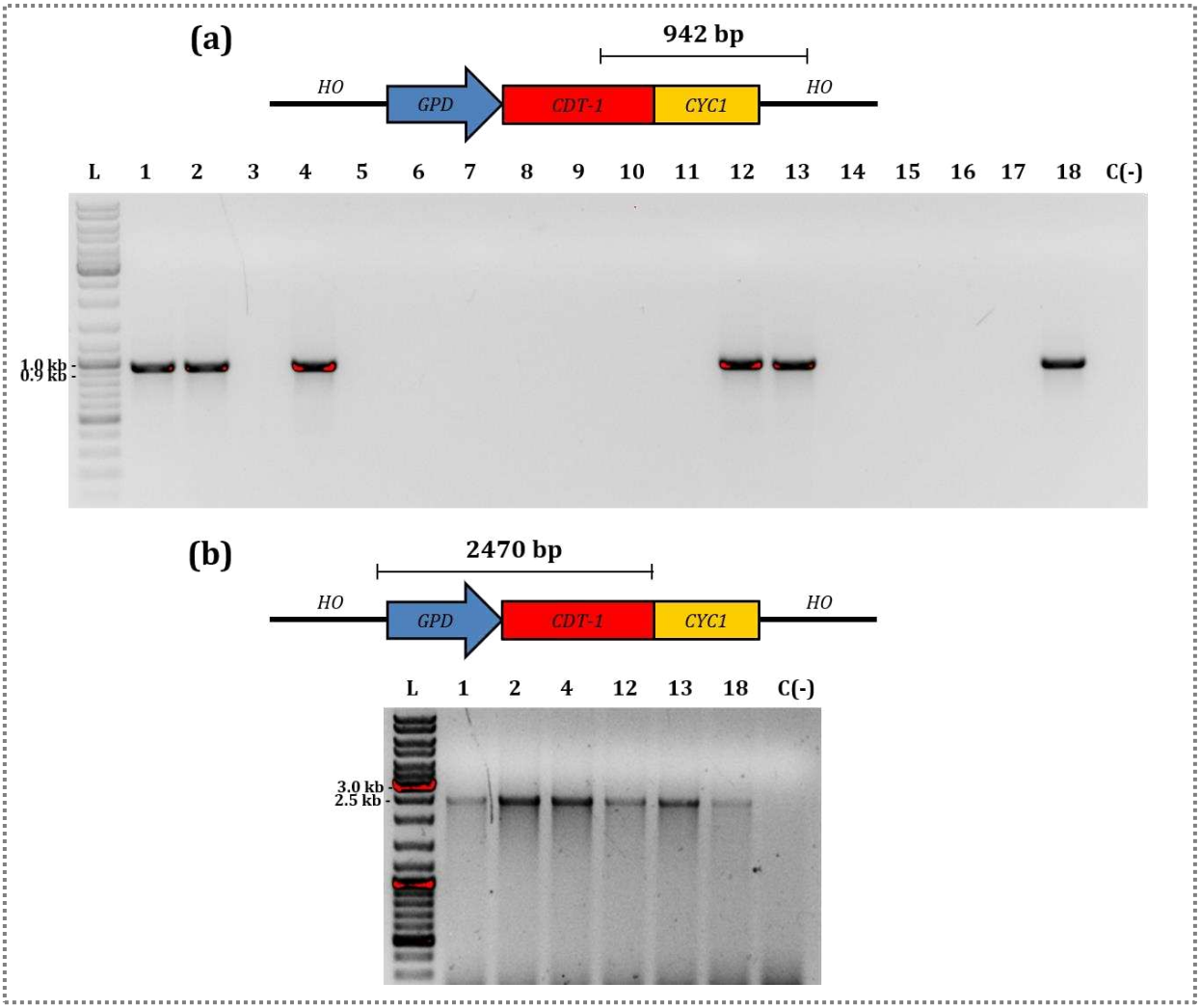

Figure 3.10. Molecular confirmation of CDT-1 integration into the HO locus. (a) Diagnostic PCR of eighteen randomly picked colonies using primers LGE PBO_011 and LGE PBO_009. Successful PCR results in a fragment with a length of 942 bp (lanes 1, 2, 4, 12, 13, and 18). The first lane (L) contains the GeneRuler DNA Ladder Mix (Thermo Scientific) and the last one contains a negative control. **(b)** Diagnostic PCR of previous six positive clones using primers FMO_019 and LGE PBO_021. All tested colonies contained a fragment with the expected size (2470 bp). The first lane (L) contains the GeneRuler DNA Ladder Mix (Thermo Scientific) and the last one contains a negative control.

Although we successfully managed to integrate the CDT-1 transporter into *S. cerevisiae*'s genome, this task took us much effort and around one year of work (negative results not reported here). Thus, due to time limitations, the work with the other selected fungal transporters could not be continued, and the development of this study proceeded with the strains harbouring only the transporter already described.

In order to engineer the CDT-1-expressing strain (PBY_08) to catabolise cellobiose, PBY_08 cells were transformed with the recombinant plasmids carrying each specific BGL coding sequence, yielding strains PBY_09 to PBY_14 (Table 3.1). Transformation with the empty

plasmid was also performed (PBY_15 strain). Transformants with the Ura$^+$ phenotype were isolated.

3.4.4 Evaluation of iCELL's growth performance on different carbon sources

To assess the ability of the engineered iCELL strains to grow on cellobiose and on other carbon sources, different growth assays on solid and liquid media were performed.

We first grew the strains by serial dilution on plates containing SM supplemented with either cellobiose, glucose or lactose. Glucose is the preferred carbon source for most microorganisms and was used as a positive control. Lactose, on the contrary, is not a natural substrate for *S. cerevisiae*, but it has been suggested that the *N. crassa* CDT-1 transporter can transport lactose and that the GH-1 enzyme has additional activity as β-galactosidase (Liu *et al.* 2016). Additionally, it was recently shown that lactose and cellobiose utilisation are intrinsically related in yeast that can naturally metabolise both sugars (Varela *et al.* 2019). For these reasons, and to investigate whether the other novel BGLs presented in this work would be able to hydrolyse lactose, we evaluated growth on lactose as well. An important consideration here is that the *S. cerevisiae* PBY_07 strain, harbouring no transporter and an empty version of the plasmid, was spotted on every plate as a control strain.

As can be observed from the results in Figure 3.11, all strains were able to grow on glucose after 36 h of incubation reaching similar biomass yields, as indicated by their comparable colony sizes in the last dilution. When the different carbon sources are compared, the plate with glucose yielded noticeable bigger colonies than those with cellobiose or lactose, for all strains. This phenotype is probably due to two reasons: 1) hexose transport in *S. cerevisiae* is carried out by a suite of almost 20 transporters, which guarantee higher specific rates of transport (Bisson *et al.* 1993; Kruckeberg 1996), as opposed to the transport of cellobiose, which is mediated by the sole heterologously expressed CDT-1 gene; 2) hexose transport occurs via facilitated diffusion (Lagunas 1993), whereas the mechanism for cellobiose transport is energy-dependent (symport), meaning that cells need to spend part of the energy they obtain for sugar transport, decreasing the amount of energy available for other cellular functions, such as anabolism and growth.

When comparing the cellobiose- and lactose-containing plates, there seems to be some correlation between both conditions, i.e., strains that grew more on cellobiose, such as PBY_09 and PBY_14, also grew more on lactose. This observation is reflected on the increased colony sizes of strains PBY_09 and PBY_14 (especially on cellobiose), when

compared to the other strains on the same plate. However, the behaviour of the control strain (PBY_07) on cellobiose and on lactose did not allow us to obtain clear-cut results from this experiment, since this strain should not grow on either of these sugars and displayed substantial amount of residual growth on both plates. The reason for this might be ascribed to the utilisation of internal carbohydrate reserves accumulated during the pre-cultivations on galactose, prior to spotting onto the plates (François and Parrou 2001). Galactose is known to exert a less intense catabolite repression effect in yeast than its stereoisomer glucose (Gonçalves *et al.* 1997; Rodríguez and Flores 2000), so we speculated that this carbon source would be preferable over glucose during inocula preparation, especially considering that cellobiose and lactose are unusual substrates for *S. cerevisiae*.

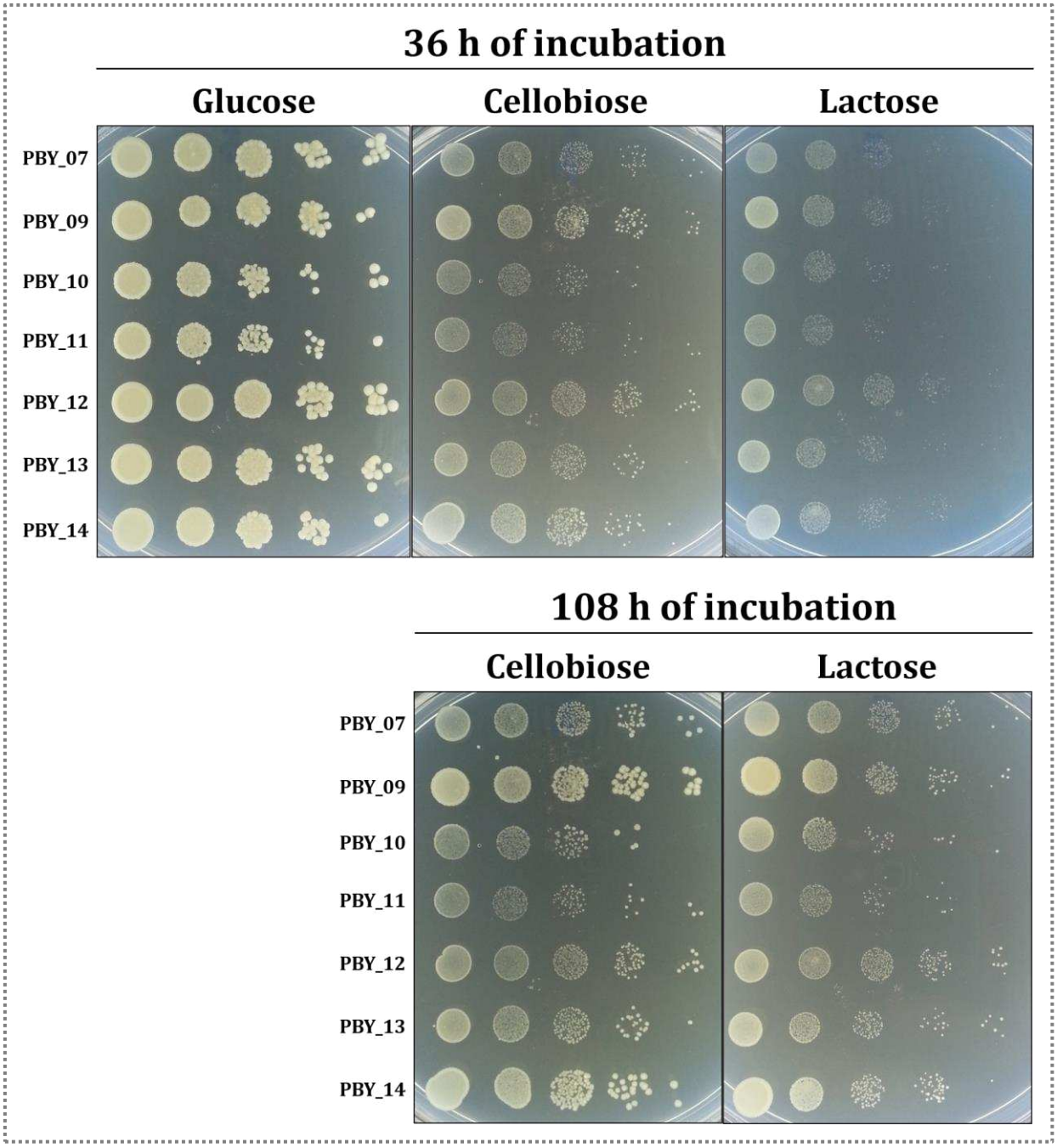

Figure 3.11. Growth of the engineered iCELL *S. cerevisiae* strains on solid SM supplemented with different carbon sources. Cells were pre-grown in liquid SM with 20 g/L initial galactose and serial dilutions were spotted onto plates (dilution increases from left to right), as described in section 3.3.10, and incubated at 30 °C. Pictures were taken after 36 and 108 h, as indicated above. *S. cerevisiae* PBY_07 expressing no cellobiose-degrading genes was used as control strain.

Due to the qualitative nature of these cultivations on solid media, we decided to further analyse the strains in liquid media, which was performed using microplate cultivations in SM with either 18 g/L initial cellobiose or glucose. As expected, all engineered strains grew on glucose as the sole carbon source (Figure 3.12), with μ_{max} between 0.14 to 0.19 h^{-1} (Figure 3.13), and good reproducibility among the replicates (Appendix IV). However, the low μ_{max}

exhibited by these strains (< 0.2 h^{-1}) deserves some attention, since the typical μ_{max} value of the prototrophic *S. cerevisiae* CEN.PK113-7D strain is around 0.37 h^{-1} in SM under growth conditions very similar to the ones performed in this study (Beato *et al.* 2016). μ_{max} values calculated on the basis of absorbance measurements depend on several factors, such as the equipment used to measure light scattering, the distance between the light source and the light detector, and the width of the light beam, among others (Stevenson *et al.* 2016). Particularly in microtiter plates, small variations in the methodology, such as agitation, inoculum preparation and standardisation, can also impose a great influence on these values, not to mention the calculation procedure. Recently, these and other important considerations regarding μ_{max} calculations and interpretations have been addressed by our research group (Rodrigues, Della-Bianca and Gombert 2021), highlighting the importance of avoiding μ_{max} comparisons between different works when these data are obtained from absorbance measurements.

The strain background (CEN.PK113-5D) used in this study is auxotrophic for uracil. This auxotrophy serves as a selection marker and is complemented by the introduction of the *URA3* gene via a multi-copy plasmid. There is evidence that the use of plasmids for genetic engineering applications can entail metabolic (or protein) burden in the cells, which is exhibited by decreased growth rates compared with cells without plasmids, particularly when auxotrophic markers are employed (as in this case) (Karim, Curran and Alper 2013). This metabolic burden is commonly associated with the energy and metabolic costs related to maintaining and replicating the plasmid in the cell, as well as overexpressing the cloned gene of interest. Another example of physiological alterations of auxotrophic strains is provided by Çakar *et al*. (1999). In this study, auxotrophs for leucine complemented with a plasmid-based *LEU2* selection marker exhibited lower final cell densities than the isogenic prototrophic strain (Çakar, Sauer and Bailey 1999). These facts related to the use of auxotrophic yeast strains with complementing vectors may explain the low μ_{max} values observed with the engineered strains, compared to the CEN.PK113-7D prototrophic strain.

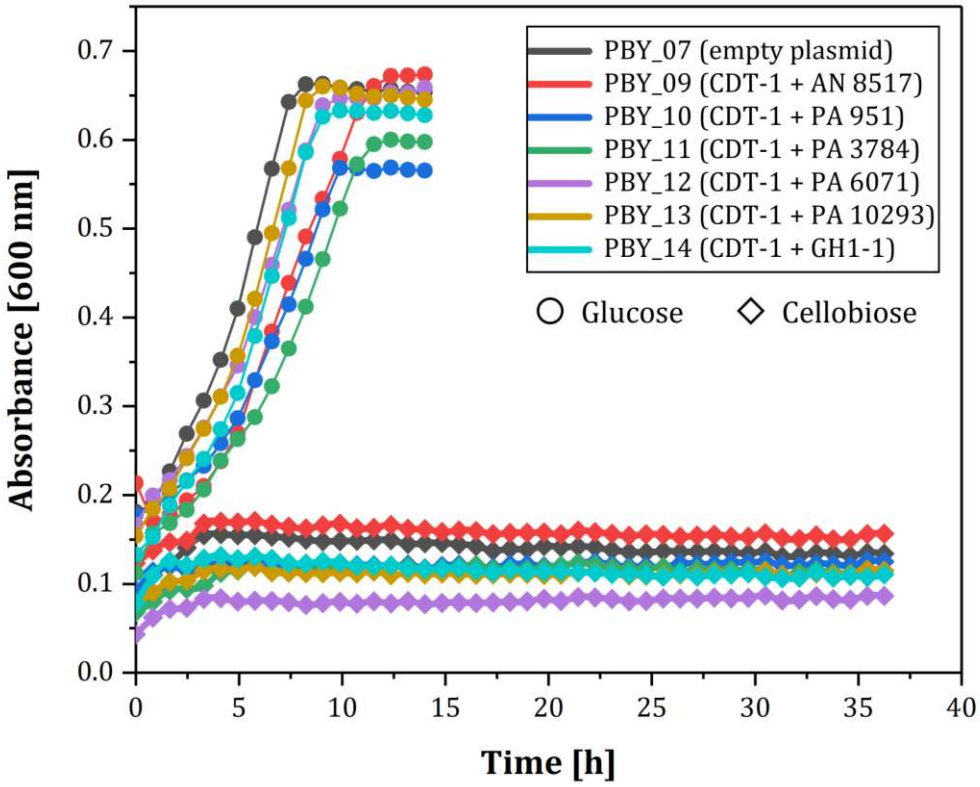

Figure 3.12. Growth profiles of the iCELL S. cerevisiae strains on glucose and on cellobiose in microplates. Cells PBY_09 to PBY_14 were cultured in SM with either 18 g/L initial cellobiose or glucose as the sole carbon and energy sources. *S. cerevisiae* PBY_07 expressing no cellobiose-degrading genes was used as control strain. One representative culture of each triplicate cultivation is shown in the figure.

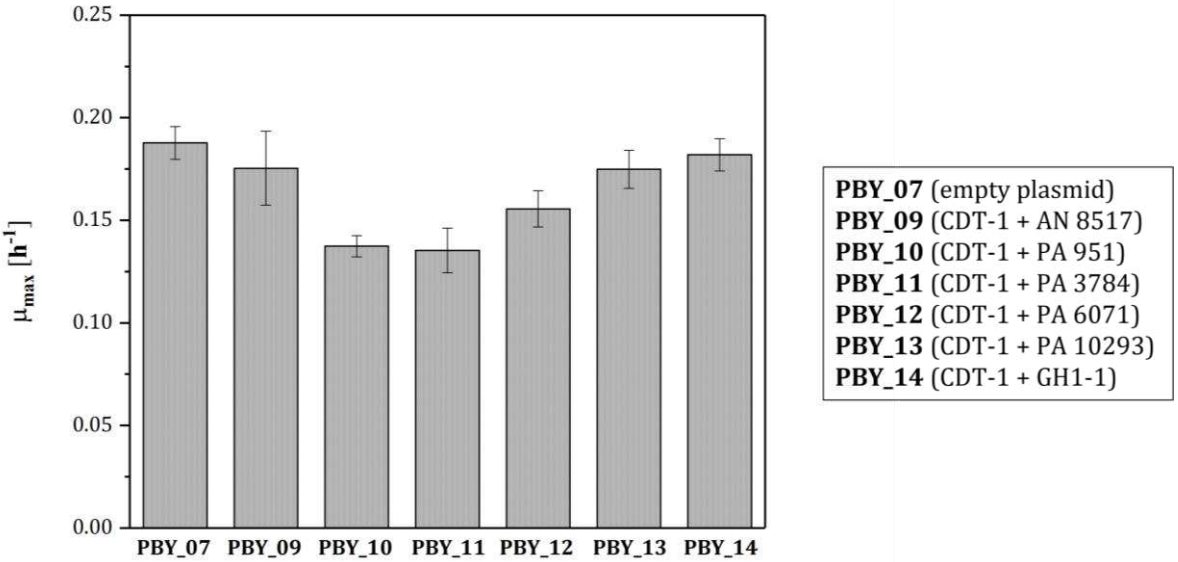

Figure 3.13. μ_{max} of iCELL strains grown on glucose. Cells PBY_07 to PBY_14 were cultivated in microplates containing SM with 18 g/L initial glucose, as described in section 3.3.8.1. Values are the mean of three replicates. Error bars represent standard deviations among triplicates.

On the other hand, when the cultivations were performed with cellobiose as the sole carbon source, no growth was observed for any of the strains during 60 h of cultivation (Figure 3.12, only the first 36 h are depicted). The behaviour of strain PBY_14 expressing the *N. crassa* cellobiose transport and consumption system (CDT-1 + GH1-1) was quite surprising, since *S. cerevisiae* strains harbouring these two genes are capable of growing on this sugar, albeit at low rates, without laboratory evolution (Galazka *et al.* 2010; Ha *et al.* 2011a, 2013c; Bae *et al.* 2014; Kim *et al.* 2019). Furthermore, our enzymatic assays have demonstrated functional expression of GH1-1 enzyme (Figure 3.7). These results propelled us to consider whether the conditions imposed under microplate cultivation were hampering growth of this strain on cellobiose. The availability of oxygen in this micro scale setup is uncertain, as it depends on the culture volume (or headspace), the efficiency of agitation, and the permeability of the sealing film to oxygen. Oxygen limitation on a strain with potential low disaccharide transport capacity could be drastic, as exhibited by certain yeasts whose growth on particular disaccharides exclusively rely on respiration (Kluyver-positive strains) (Fukuhara 2003). Thus, to verify whether growth on cellobiose was for some reason not observable due to some peculiarity of the microplate system employed (for instance, oxygen limitation), Erlenmeyer-type shake-flask cultivations were subsequently performed in SM with 20 g/L initial cellobiose under an air atmosphere (Figure 3.14).

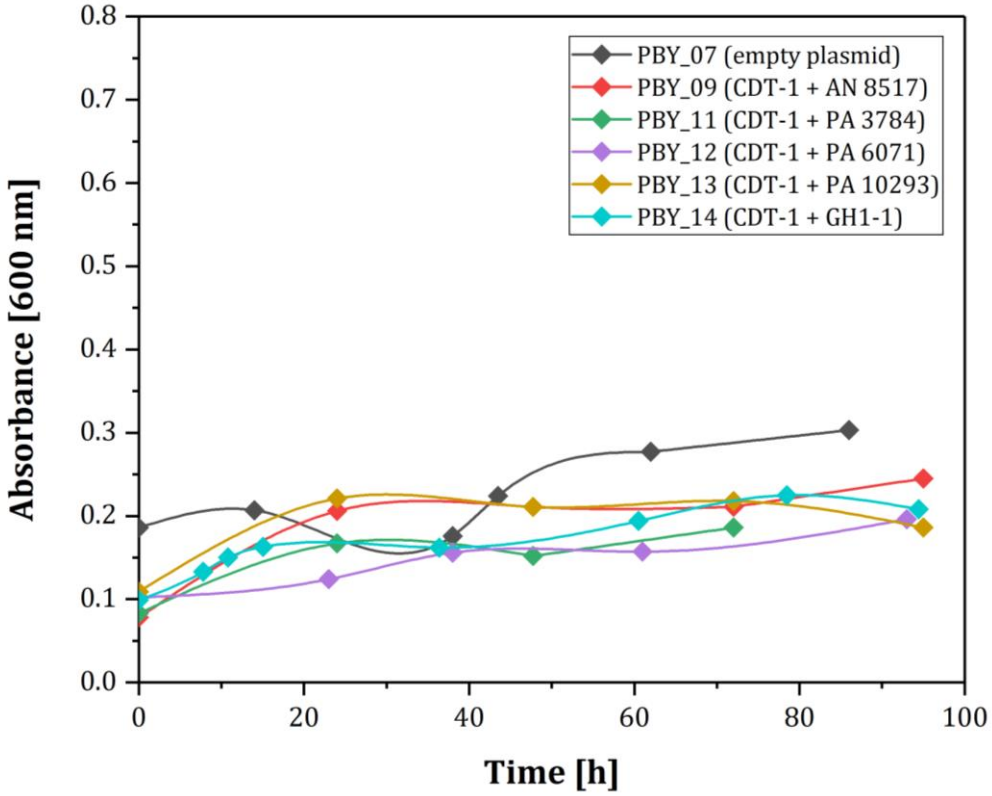

Figure 3.14. Growth profiles of iCELL *S. cerevisiae* strains on cellobiose in cotton-plugged shake-flasks. Cells PBY_09 to PBY_14 were cultured in SM with 20 g/L initial cellobiose as the sole carbon source. One representative culture of each triplicate cultivation is shown in the figure.

However, even under aerated shake-flask cultivation conditions, neither PBY_14 (CDT-1 + GH1-1) nor the other iCELL strains showed growth on cellobiose during almost 100 h of cultivation (Figure 3.14). It should be noticed that strain PBY_10 (CDT-1 + PA 951) was not depicted in Figure 3.14 because it had serious limitations to grow even on glucose during the pre-inoculum step. This growth defect was carried since the preparation of the stocks on glycerol, and even at present, we do not have a proper explanation for this behaviour.

Results obtained from our growth assays on cellobiose confirm that there was no extracellular hydrolysis of cellobiose, either spontaneous or mediated by the BGLs, which would have allowed the strains to grow in the different cultivation systems. Additionally, they suggest that sugar transport might be limiting growth on cellobiose, especially of PBY_14, which has a highly active intracellular BGL (Figure 3.7). Regarding the other engineered strains, the limitation appears to be double, owed not only to the transport step, but also to the low activity of the fungal BGLs (Figure 3.7). Although we cannot exclude non-functional expression of the transporter (neither the transport activity nor the cellular localisation was evaluated), the chromosomal copy of *CDT-1* probably led to insufficient expression levels of

the transporter, resulting in a limited amount of CDT-1 molecules delivered to the plasma membrane. A similar limitation was observed with an engineered *S. cerevisiae* strain carrying a xylodextrin-specific transporter from *Trichoderma virens* in a chromosomally integrated copy, which grew on xylodextrin almost as slow as the control without the transporter (Zhang *et al.* 2017). When this transporter was expressed from a plasmid, there was a dramatic increase in growth (Zhang *et al.* 2017). A similar phenomenon was also observed in a previous work from our group, where a sucrose-negative *S. cerevisiae* strain expressing a functional sucrose-phosphorylase and chromosomally-integrated sucrose facilitators from plant origin did not sustain growth on sucrose (personal communication with Dr. Wesley Marques), and to enable the yeast to grow on this sugar the transporters had to be introduced via multi-copy plasmids (Marques *et al.* 2018a).

Besides gene copy number, the heterologous expression of integrated genes can be affected by their localisation within the genome. In this study, we targeted CDT-1 insertion at the *HO* locus, whose sole cellular role involves mating type switching, showing no consequences on yeast growth when inactivated (Baganz *et al.* 1997). Thus, it should be unlikely that this was the cause for the poor growth of the iCELL strains on cellobiose. In addition, the expression of CDT-1 was driven by the strong *GPD* promoter and *CYC1* terminator, regulatory elements commonly used in yeast metabolic engineering strategies.

Independent of being chromosomally integrated or plasmid-mediated, functional expression of heterologous membrane proteins has proven to be challenging (dos Reis *et al.* 2016; Marques *et al.* 2018a). Although there are many examples of successful approaches in *S. cerevisiae* (Wahl *et al.* 2010; Kim *et al.* 2014a; Hara *et al.* 2017; Nogueira *et al.* 2018), improper folding and translocation into the membrane is a common outcome in the scientific literature of heterologous transporters (Froissard *et al.* 2006; Zhang *et al.* 2017; Podolsky *et al.* 2021), which leads to protein accumulation in subcellular compartments thereby reducing the amount of protein available at the cell membrane. Since we did not employ any reporter gene to track cellular localization of CDT-1, we were not able to test this possibility. Another possibility that could be limiting the number of CDT-1 proteins residing in the plasma membrane is rapid endocytic removal. CDT-1 endocytosis in *S. cerevisiae* is mediated by four primary endogenous α-arrestins and promoted by the presence of cellobiose (Sen *et al.* 2016), meaning that CDT-1 possesses a sequence and/or structural feature that recruits the ubiquitination machinery when cultivated on cellobiose. When cells deficient in these α-

arrestins are engineered, the increased content of CDT-1 molecules in the plasma membrane allow for better growth on cellobiose compared to wild-type cells (Sen *et al.* 2016).

Although our results comprising the *N. crassa* cellobiose pathway differ from those reported elsewhere (Galazka *et al.* 2010; Ha *et al.* 2011a, 2013c; Bae *et al.* 2014; Kim *et al.* 2019), there is a consensus in the scientific literature that the CDT-1 + GH1-1 module in *S. cerevisiae* must be improved in terms of rate in order to attain efficient cellobiose utilisation. Efforts to optimize cellobiose performance in CDT-1 + GH1-1-expressing strains have included not only experimental evolution (Eriksen *et al.* 2013; Hu *et al.* 2016; Oh *et al.* 2016), but also transcriptional engineering (Du *et al.* 2012), and systems biology approaches (Lin *et al.* 2014; Chomvong *et al.* 2017), resulting in insufficient improvements in cellobiose metabolism for industrial applications, evidencing the challenges faced by yeast when altering central carbon metabolism.

3.5 Conclusions and Perspectives

In this study we aimed at addressing the utilisation of the disaccharide cellobiose by engineered *S. cerevisiae*, exploring novel CDTs and intracellular BGLs from fungal origin. A total of fifteen genes potentially involved in cellobiose transport and hydrolysis were identified by a bioinformatics survey and selected for further expression in yeast. The cloning process demanded a significant effort and due to time limitations, further exploration of putative CDTs and of some BGLs had to be interrupted. Despite this, the study allowed for the identification of five new intracellular BGL-encoding genes from the Ascomycetes *A. niger* and *P. anserina*. However, taking the extremely low enzyme activity values measured in cell extracts of *S. cerevisiae*, we cannot affirm whether these genes were functionally expressed in this yeast. In contrast, the expression of the *N. crassa* control enzyme GH1-1 was satisfactory, yielding the highest BGL activities tested in this study. In spite of these results, additional CRISPR-Cas9-mediated integration of the widely studied *N. crassa* CDT-1 transporter in the GH1-1-expressing strain (PBY_14) did not confer the capability to grow on cellobiose as the sole carbon source. Thus, we hypothesised that the main limitation in this strain is the transport of the sugar, as the chromosomal copy of *CDT-1* might not ensure a sufficient amount of transporter molecules in the cell membrane. In order to make this strain capable of growing on cellobiose, we could in principle take two different approaches at this point: 1) increase the expression of the CDT-1 gene via e.g., increasing its copy number in the yeast genome or expressing the gene from a multi-copy plasmid, or 2) use laboratory evolution to allow the strain to increase its growth rate on cellobiose. Since we could not be sure that a limitation in transport capacity alone was the cause for the absence of growth on cellobiose, we decided to pursue the second approach (Chapter 4).

Lastly, the CDT-1 transporter was also integrated in other BGL-expressing strains (PBY_09 to PBY_13), but as expected from the presented data with PBY_14, the strains did not display growth on cellobiose. These strains were also taken to the next step of this work, which was laboratory evolution on cellobiose for increased growth rates on this sugar (Chapter 4).

3.6 Acknowledgements

The authors would like to thank Prof. Dr Ronald de Vries and Dr. Adiphol Dilokpimol for the reception and support at CBS-KNAW Fungal Biodiversity Centre, as well as the fruitful contributions regarding the screening and cloning of the CDTs and BGLs. Additionally, a special thanks to Dr. Gleidson Silva Teixeira for all the support, knowledge, and discussions on the construction of the iCELL platforms. Finally, thank you to LGE/IB/UNICAMP for the infrastructure provided during the development of the strains.

4 LABORATORY EVOLUTION AND PHYSIOLOGICAL CHARACTERISATION OF YEAST STRAINS EVOLVED FOR GROWTH ON CELLOBIOSE

4.1 Abstract

Previous work resulting from Chapter 3 demonstrated that co-expression of a cellodextrin transporter and six individual intracellular β-glucosidases from fungal origin did not enable *Saccharomyces cerevisiae* strains to grow on cellobiose. In the present study, we subjected five of these strains to several generations of selective growth on cellobiose media, monitored by microscopic and kinetic analyses. Throughout the course of the evolution lines, single colonies were isolated and selected for their high maximum specific growth rates (μ_{max}) on cellobiose in microplate cultivations. Further testing during shake-flask cultivation in the presence of oxygen revealed that all selected isolates exhibited fully respiratory growth on cellobiose, with μ_{max} between 0.24 to 0.34 h^{-1}, and high biomass yields on sugar (0.49-0.61 $g_{DM}/g_{cellobiose}$). To force cellobiose fermentation, two of these clones were subsequently cultivated under low oxygen availability with different sugar levels and initial cell densities. However, even after ~one week of cultivation, no growth or cellobiose consumption was observed. To investigate the genetic determinants underlying the metabolic characteristics acquired by the strains, we sequenced a group of six clones isolated from two independent evolution experiments. Analysis of the genomic data revealed that another yeast species, *Meyerozyma guilliermondii*, managed to settle and compete with *S. cerevisiae* in the successive rounds of cultivation, because of its natural capacity to utilise cellobiose as carbon source. Given the lack of knowledge on the mechanism of cellobiose utilisation, the genes involved, and the way that cellobiose is catabolised by this yeast, we believe that our physiological and sequencing data could provide information for future work on these open questions to broaden our understanding of the potential of *M. guilliermondii* for biotechnological applications.

4.2 Introduction

As introduced in Chapters 2 and 3, *Saccharomyces cerevisiae* is the most attractive cell factory in industrial biotechnology, whose spectrum of utilisation exceeds by far the traditional processes involving bread making and production of ethanol for beverages or fuels. The development of genetic engineering tools has made possible the production of heterologous proteins (including vaccines and other pharmaceuticals) (Ro *et al.* 2006; Galao *et al.* 2007; Nandy and Srivastava 2018), bulk and fine chemicals (Chemler, Yan and Koffas 2006; Borodina and Nielsen 2014; Nandy and Srivastava 2018), and advanced biofuels (Nandy and Srivastava 2018), as well as broadened the palette of substrates that *S. cerevisiae* can utilise (Turner *et al.* 2018). Additionally, engineered yeast can be designed to improve intrinsic cellular properties such as tolerance to harsh conditions, or enhance products yields by finetuning endogenous metabolism (Basso *et al.* 2011; Cunha *et al.* 2019; Zahoor *et al.* 2020; van Aalst *et al.* 2022). In all these applications, strain optimisation is vital, since high product titre, yield, and productivity are critical for industrial applications (Stephanopoulos 2007). On the other hand, from a scientific perspective, the optimisation of microbial platforms has an important value in fundamental research, as it allows for the identification of genes responsible for certain traits of interest and the understanding of biological processes (Marques *et al.* 2017).

Evolutionary engineering, a term first introduced by Butler and collaborators (1996), and later also referred to as laboratory evolution, adaptive laboratory evolution, directed evolution or experimental evolution, has been employed as a complementary tool in metabolic engineering approaches to generate optimised microbial systems (Mans, Daran and Pronk 2018). Rational design of metabolic pathways is not a simple task, since it demands a good understanding of the microbial system and the ability to predict how the pathways will indeed work in the cell. Laboratory evolution has an important advantage in this sense, as it allows for the selection of high-performing strains without having prior knowledge of the mechanisms behind the process. The principle relies on the generation of genetic diversity within a population of cells and the selection of superior variants. When subjecting cells to defined growth conditions (a.k.a. selective pressure) for prolonged periods of time, natural mutations will occur throughout the course of cultivation, generating a heterogeneous population of cells. Those cells endowed with a competitive advantage under the particular conditions used, will be enriched in the population, allowing for the selection of mutants with higher specific growth rates, lower death rates, and/or increased biomass sedimentation (Mans, Daran and Pronk

2018). This methodology exploits intrinsic characteristics of microbial cells, such as fast growth and simple nutrient requirements, allowing cultivation of cells for several hundred generations within several weeks or months. Some studies have also used artificial mutagenesis to increase the genetic variability of the initial population (Teunissen *et al.* 2002; Çakar *et al.* 2005; Liu and Hu 2010).

The strategies for yeast laboratory evolution commonly involve batch and/or continuous cultivation setups, whose criteria of choice depend on technical, practical, and scientific considerations (Dunham 2010). Serial transfers in shake-flasks, tubes or even in 96-well microplates (bath cultivation) is recognized as an efficient, easy to establish, and inexpensive methodology, selecting for mutants with a higher maximum specific growth rate (μ_{max}) (Mans, Daran and Pronk 2018). Different endeavours aiming at improving the capacity to utilise non-favoured carbon sources in yeast, such as cellobiose (Eriksen *et al.* 2013; Hu *et al.* 2016; Oh *et al.* 2016), xylose (Sonderegger and Sauer 2003; Liu and Hu 2010; Lee, Jellison and Alper 2014), glycerol (Ho *et al.* 2017), lactose (Guimarães *et al.* 2008b, 2008a), and arabinose (Wisselink *et al.* 2007), as well as of mixed carbon sources (Kuyper *et al.* 2005; Wisselink *et al.* 2009; Sanchez *et al.* 2010; Farwick *et al.* 2014), have been particularly successful using this approach. Other examples of special interest include strategies for increasing ethanol yields, such as engineering free energy conservation (Basso *et al.* 2011), decreasing glycerol formation (Guadalupe-Medina *et al.* 2014), and improving yeast robustness (Çakar *et al.* 2005; Tomás-Pejó *et al.* 2010). In some other works, the subject of study has been the mechanisms of evolution, providing valuable information on the resistance of living microorganisms to toxic compounds or tolerance to high temperatures (Kildegaard *et al.* 2014; Caspeta and Nielsen 2015; González-Ramos *et al.* 2016).

From a scientific perspective, identifying the genetic basis underlying the improved phenotype is vital to comprehensively understand the mechanisms involved and subsequently use this information for rational engineering of cell factories. However, determining which genetic modifications are responsible for the improvement is not a simple task. Genome sequencing and gene expression data can bring valuable insights into the elucidation of the mutations that contribute to the observed phenotype (Guimarães *et al.* 2008a; Wenger *et al.* 2011). Additionally, reimplementation of these mutations into an unevolved strain background (commonly known as reverse engineering) can be carried out to investigate the relationship between the mutations and the resulting improved phenotype (Marques *et al.* 2018b; Perli *et al.* 2020).

The goal of the study described in this chapter was to investigate whether laboratory evolution can improve the growth rates of previously engineered intracellular cellobiose-utilising (iCELL) *S. cerevisiae* strains on cellobiose and to characterise the evolved phenotypes by physiological and molecular analyses. To this end, the iCELL strains were individually subjected to serial transfer for several generations of selective growth on cellobiose, until we obtained single colony isolates with $\mu_{max} > 0.1\ h^{-1}$, representing ~1/3 of the value commonly observed on glucose for wild-type strains of this species. Further physiological characterisations of the best-performing evolved candidates of each strain were made by shake-flask cultivations in the presence of oxygen and high levels of sugar. Finally, cultivations under low oxygen availability were also attempted with some evolved strains, in order to verify whether fermentation of cellobiose was also possible.

4.3 Material and Methods

4.3.1 Strains and maintenance

The *S. cerevisiae* strains used in this work (Table 4.1) belong to the congenic members of the CEN.PK family (van Dijken *et al.* 2000; Entian and Kötter 2007) and were constructed as described in Chapter 3. Two different stock cultures were prepared from each laboratory evolution experiment: stocks of the cell population and stocks of single-cell isolates. Stocks of cell population were made from yeast cultures collected at the end of each evolution cycle in Synthetic Medium (SM) with 20 g/L initial cellobiose (see section 4.3.2 for more details), whereas stocks of single colonies were prepared from colonies isolated on solid SM with 20 g/L cellobiose and subsequently grown on liquid SM with 20 g/L initial glucose for 24 h at 30 °C and 200 rpm. SM was prepared as described in section 4.3.3. For both stocks, 30% (v/v) glycerol was added and 2-mL aliquots were stored at -80 °C.

Table 4.1. Yeast strains used in this study.

STRAIN	FEATURE	ORIGIN
PBY_09	CEN.PK113-5D/*HO-GPD*-CDT-1-*CYC1-HO*/p426GPD-AN 8517	This study
PBY_10	CEN.PK113-5D/*HO-GPD*-CDT-1-*CYC1-HO*/p426GPD-PA 951	This study
PBY_11	CEN.PK113-5D/*HO-GPD*-CDT-1-*CYC1-HO*/p426GPD-PA 3784	This study
PBY_12	CEN.PK113-5D/*HO-GPD*-CDT-1-*CYC1-HO*/p426GPD-PA 6071	This study
PBY_13	CEN.PK113-5D/*HO-GPD*-CDT-1-*CYC1-HO*/p426GPD-PA 10293	This study
PBY_14	CEN.PK113-5D/*HO-GPD*-CDT-1-*CYC1-HO*/p426GPD-GH1-1	This study
PBY_09ev A2	CEN.PK113-5D/*HO-GPD*-CDT-1-*CYC1-HO*/p426GPD-AN 8517 (single colony isolate from evolution of PBY_09, replicate A2)	This study
PBY_09ev A3	CEN.PK113-5D/*HO-GPD*-CDT-1-*CYC1-HO*/p426GPD-AN 8517 (single colony isolate from evolution of PBY_09, replicate A3)	This study
PBY_09ev A5	CEN.PK113-5D/*HO-GPD*-CDT-1-*CYC1-HO*/p426GPD-AN 8517 (single colony isolate from evolution of PBY_09, replicate A5)	This study
PBY_11ev A2	CEN.PK113-5D/*HO-GPD*-CDT-1-*CYC1-HO*/p426GPD-PA 3784 (single colony isolate from evolution of PBY_11, replicate A2)	This study
PBY_11ev A3	CEN.PK113-5D/*HO-GPD*-CDT-1-*CYC1-HO*/p426GPD-PA 3784 (single colony isolate from evolution of PBY_11, replicate A3)	This study
PBY_11ev A5	CEN.PK113-5D/*HO-GPD*-CDT-1-*CYC1-HO*/p426GPD-PA 3784 (single colony isolated from evolution of PBY_11, replicate A5)	This study
PBY_12ev B2	CEN.PK113-5D/*HO-GPD*-CDT-1-*CYC1-HO*/p426GPD-PA 6071 (single colony isolate from evolution of PBY_12, replicate B2)	This study
PBY_12ev B5	CEN.PK113-5D/*HO-GPD*-CDT-1-*CYC1-HO*/p426GPD-PA 6071 (single colony isolate from evolution of PBY_12, replicate B5)	This study
PBY_12ev B6	CEN.PK113-5D/*HO-GPD*-CDT-1-*CYC1-HO*/p426GPD-PA 6071 (single colony isolated from evolution of PBY_12, replicate B6)	This study
PBY_13ev C2	CEN.PK113-5D/*HO-GPD*-CDT-1-*CYC1-HO*/p426GPD-PA 10293 (single colony isolate from evolution of PBY_13, replicate C2)	This study
PBY_13ev C3	CEN.PK113-5D/*HO-GPD*-CDT-1-*CYC1-HO*/p426GPD-PA 10293 (single colony isolate from evolution of PBY_13, replicate C3)	This study
PBY_13ev C5	CEN.PK113-5D/*HO-GPD*-CDT-1-*CYC1-HO*/p426GPD-PA 10293 (single colony isolate from evolution of PBY_13, replicate C5)	This study
PBY_14ev A2	CEN.PK113-5D/*HO-GPD*-CDT-1-*CYC1-HO*/p426GPD-GH1-1	This study

	(single colony isolate from evolution of PBY_14, replicate A2)	
PBY_14ev A3	CEN.PK113-5D/*HO-GPD*-CDT-1-*CYC1-HO*/p426GPD-GH1-1 (single colony isolate from evolution of PBY_14, replicate A3)	This study
PBY_14ev A5	CEN.PK113-5D/*HO-GPD*-CDT-1-*CYC1-HO*/p426GPD-GH1-1 (single colony isolate from evolution of PBY_14, replicate A5)	This study

4.3.2 Laboratory evolution

Laboratory evolution experiments were performed by serial transfers using 50-mL polypropylene tubes containing 10 mL of SM with 20 g/L initial cellobiose in an incubator shaker (OrbiCult™ IBS-R-19-1, ESCO, Singapore) set at 30 °C and 200 rpm. For each of the strains (PBY_09 to PBY_14) (Table 4.1), three evolution lines were carried out in parallel (A, B, and C) from cells pre-grown on 20 g/L initial glucose (inoculum). After 48 h growth at 30 °C and 200 rpm (OrbiCult™ IBS-R-19-1, ESCO, Singapore), an aliquot of each inoculum was transferred to 50-mL polypropylene tubes containing 10 mL of SM with 20 g/L initial cellobiose to start a cycle with an initial absorbance at 600 nm (Abs_{600}) of 0.1. At the end of each cycle (determined by visual inspection of enough turbidity), an aliquot of the culture was transferred to a new tube with fresh medium to start a next cycle with an initial Abs_{600} of 0.1. Initial transfers (cycles) for strains PBY_09 and PBY_14 were made after 3-4 days, while for strains PBY_11, PBY_12, and PBY_13 the time interval was 4-5 days. Later, each new cultivation cycle was established after 2-3 days of incubation for all strains, corresponding to ~5 generations/cycle. After a given number of transfers, the subcultures were streaked onto plates containing solid SM with 20 g/L cellobiose and some larger colonies were selected for evaluation of the kinetic profiles, as detailed in section 4.3.3.1. Serial transfers were repeated until we obtained single colony isolates with μ_{max} > 0.1 h^{-1} on cellobiose. In case any contamination event arose, the subculture was discarded, and the evolution was re-initiated from previous stocks at -80 °C (cell population stock). The number of generations (*n*, cell divisions) that occurred during each cycle was estimated from the following formula: $n = \log_2 Abs_{final} - \log_2 Abs_{initial}$.

4.3.3 Culture media and cultivation conditions

Yeast strains were cultivated in SM according to Verduyn *et al.* (1992), with the substitution of ammonium for urea as the sole nitrogen source, to prevent excessive acidification during cultivation. To supplement the missing sulphate in the medium, K_2SO_4 was added as in (Luttik *et al.* 2000; van Leeuwen *et al.* 2009). SM contained vitamins, trace metals, salts, a nitrogen source, and a carbon and energy source, including 6.6 g/L K_2SO_4, 3.0 g/L KH_2PO_4,

0.5 g/L $MgSO_4.7H_2O$, 2.3 g/L urea, and 20 g/L cellobiose or glucose with an initial pH adjusted to 6.0 using KOH 2 M. Urea, cellobiose, and glucose solutions were filter-sterilised through 0.22 μm pore membranes and added to the medium after autoclaving the remaining components (121 °C for 20 min). Vitamins and trace elements solutions (Verduyn *et al.* 1992) were prepared as 1000x concentrated stocks and sterilised by filtration or autoclaving, respectively, before addition to the medium. For solid media, the original medium prepared according to Verduyn *et al.* (1992) was employed, with the addition of 20 g/L agar prior to heat sterilisation.

4.3.3.1 Microplate cultivations

Cell growth of single-cell isolates obtained throughout the course of the evolution experiments was evaluated using sterile 96-microwell plates (CELLSTAR® flat bottom, No. 655161 - Greiner Bio-One, Kremsmünster, Austria) and the automated plate reader Tecan Infinite M200 Pro, according to Beato *et al.* (2016) with some modifications. Briefly, pre-cultures were prepared by transferring cells from one fresh colony on solid SM with 20 g/L glucose to 50-mL polypropylene tubes containing 3 mL of SM with 20 g/L initial glucose (pre-inoculum). These colonies were selected based on their larger size on previous plates containing SM with 20 g/L cellobiose. After 24 h growth at 30 °C and 200 rpm (OrbiCult™ IBS-R-19-1, ESCO, Singapore), 300 μL of the pre-inoculum was transferred to a new polypropylene tube containing 2.7 mL of SM with 20 g/L initial cellobiose (inoculum). After 48 h incubation at 30 °C and 200 rpm, an aliquot was collected to make 1 mL of cell suspension with an Abs_{600} of 0.5. Following three washing procedures with sterile distilled water, 10 μL of this suspension was used to inoculate a single well containing 90 μL of SM with 20 g/L cellobiose, resulting in an initial sugar concentration of 18 g/L. For the blank wells, 10 μL of sterile distilled water was added to the wells filled with 90 μL of the corresponding medium (three wells per blank). The plate was then sealed with PCR polyester sealing film (Axygen® UC-500, Corning Life Sciences, Tewksbury, USA) and incubated at 30 °C and 198.4 rpm (3.5 mm of amplitude) in the automated plate reader. Cultivations were run in triplicates (three wells on the same plate) and cell growth was monitored automatically by measuring the Abs_{600} approximately every 50 min in each well. μ_{max} values were calculated from at least five data points in the linear region of a semi-logarithmic (using the natural logarithm) plot of absorbance versus time, as the slope of a linear regression using these points. These values together with averages and standard deviations were calculated using Microsoft Excel.

4.3.3.2 Shake-flask cultivations under high oxygen availability

Shake-flask cultivations were performed in duplicates in 500-mL cotton-capped unbaffled Erlenmeyer flasks with silicone tubing connected to an outside needle, which allowed sampling using a syringe, without the need to open the flask during sampling (Appendix I). To avoid contamination, the tubing was kept blocked by a Mohr clamp during the entire cultivation and only opened during sampling. Flasks containing 100 mL of SM with 20 g/L initial cellobiose were incubated at 30 °C and 200 rpm in a rotary shaker (Innova 4430, New Brunswick Scientific, Edison, USA) under an air atmosphere. Pre-cultures were prepared by transferring cells from one colony on solid SM with 20 g/L glucose to 50-mL polypropylene tubes containing 3 mL of SM with 20 g/L initial glucose. After 24 h growth at 30 °C and 200 rpm, the pre-inoculum was transferred to 125-mL unbaffled Erlenmeyer flasks containing 22 mL of SM with 20 g/L initial cellobiose. After another 24 h growth at 30 °C and 200 rpm, cultures were centrifuged at 3000 rpm for 5 min (NT810 centrifuge, Novatecnica, Piracicaba, Brazil) and the supernatant discarded; cells were washed twice with sterile distilled water and resuspended in 1 mL of SM with 20 g/L initial cellobiose before inoculating 500-mL Erlenmeyer flasks with an initial Abs_{600} of approximately 0.1. Shake-flasks were incubated until the cells reached the stationary phase of growth. Samples were taken at different time points to measure cell concentration (indirectly via Abs_{600}), pH, and concentrations of substrate and extracellular metabolites, according to section 4.3.4. Prior to sampling, care was taken to dispense the dead volume that remains in the silicone tubing.

4.3.3.3 Shake-flask cultivations under low oxygen availability

Cultivations minimising oxygen transfer were performed without replicates in 500-mL unbaffled Erlenmeyer flasks capped with silicone stoppers and equipped with two norprene tubings: one connected to an internal silicone tubing and an outside needle for inoculating, sampling, and nitrogen purging, and the other one (coupled to a gas filter) used for CO_2 release (Appendix I). To avoid contamination, sampling connections were kept blocked by a Mohr clamp during the entire cultivation and only opened during sampling. Flasks containing 300 mL of SM with 20 or 40 g/L initial cellobiose were purged with nitrogen gas (99.996% purity) for 30 min prior to inoculation, to reduce the availability of oxygen in the system. Pre-cultures were prepared by transferring cells from one colony on solid SM with 20 g/L glucose to 50-mL polypropylene tubes containing 10 mL of SM with 20 g/L initial glucose. After 48 h growth at 30 °C and 200 rpm (Innova 4430, New Brunswick Scientific, Edison, USA), the pre-inoculum was transferred to 500-mL unbaffled Erlenmeyer flasks containing 90 mL of

SM with 20 g/L initial cellobiose. After another 48 h growth at 30 °C and 200 rpm, cultures were centrifuged at 3000 rpm for 5 min (NT810 centrifuge, Novatecnica, Piracicaba, Brazil) and the supernatant discarded; cells were washed twice with sterile distilled water and resuspended in 1 mL of SM with 20 or 40 g/L initial cellobiose before inoculating 500-mL Erlenmeyer flasks with an initial Abs_{600} of ~0.1 or 1. Cultures were incubated at 30 °C and 100 rpm for days. Samples were taken at different time intervals to measure cell concentration (indirectly via Abs_{600}) and concentrations of substrate and extracellular metabolites, according to section 4.3.4. After every sampling event, cultures were sparged with nitrogen for 3 min to reduce oxygen transfer.

4.3.4 Analytical methods

Cell or biomass concentration from shake-flask cultivations was indirectly monitored by Abs_{600} measurements using a spectrophotometer (Genesys 20, Thermo Scientific, Waltham, USA), and directly determined by gravimetry in terms of dry cell mass (the latter only for cultivations in the presence of oxygen), according to Olsson and Nielsen (1997). Dry cell mass measurements were performed in duplicates (two determinations for each flask) only at the end of each cultivation. Briefly, 5 mL of culture broth were filtered through pre-weighed nitrocellulose membranes with a pore diameter of 0.45 μm, using a vacuum system. The membranes were then washed with distilled water, dried in a microwave oven at 255 W for 10 min, and cooled down for 15 min in a desiccator, before being weighed again. This procedure was repeated until the filter achieved constant dry mass. The dry cell mass concentration (X_{DM}) was calculated by dividing the difference between the filter's dry mass after and before filtration by the sample volume.

The pH of shake-flask samples was read using a pHmeter (Digimed DM21, São Paulo, Brazil).

Substrate and extracellular metabolites (cellobiose, glucose, glycerol, acetic acid, and ethanol) from shake-flask cultivations had their concentrations determined by High Performance Liquid Chromatography (HPLC) after filtration of the samples (using positive pressure) through 0.22 μm-pore membranes using a syringe. HPLC analysis was performed using an Accela equipment (Thermo Scientific, Waltham, USA) coupled with a refractive index detector (Waters 2410, Milford, USA) and an Aminex HPX-87H column (Bio-Rad, Hercules, USA). The HPLC separation was conducted at 30 °C with 0.05 mM (pH 4.41) H_2SO_4 as a mobile phase at a flow rate of 0.6 mL/min.

4.3.5 Calculation of physiological parameters

Data obtained from cultivations under high oxygen availability were used to calculate physiological parameters, such as μ_{max}, global biomass yields on substrate ($Y_{X/S}$), and specific substrate consumption rates (q_S), as follows.

μ_{max} values were calculated as the slope of the straight line of an Ln (Abs_{600}) *vs.* time plot generated using at least five data points within the exponential growth phase.

$Y_{X/S}$ were obtained by dividing the total amount of biomass produced by the total amount of substrate consumed; $Y_{x/s}\ (g_{DM}/g_{substrate}) = \frac{(X_{DM,final} - X_{DM,initial})}{(S_{initial} - S_{final})}$.

q_S were obtained taking the ratio between the μ_{max} and the $Y_{X/S}$; $q_S\ (g_{substrate}/g_{DM} * h) = -\frac{\mu_{max}}{Y_{x/s}}$.

All these values together with averages and mean deviations were calculated using Microsoft Excel.

4.3.6 Whole-genome sequencing

The three evolved isolates derived from *S. cerevisiae* PBY_12 (CDT-1 + PA 6071) and PBY_13 (CDT-1 + PA 10293) were sequenced at the Life Sciences Core Facility (LaCTAD) from UNICAMP. DNA extraction was performed using DNeasy UltraClean Microbial Kit following the manufacturer's guidelines (Qiagen, Germantown, USA). Sequencing was carried out on an Illumina MiSeq machine, producing 300 bp reads (paired-end). Coverage (relative to a 12 Mbp haploid genome) was 54, 72, and 52× for the PBY_12-derived isolates (B2, B5, and B6, respectively) and 62, 63, and 54x for the isolates derived from PBY_13 (C2, C3, and C5, respectively).

The fastq files containing the sequencing results were analysed using a pipeline recommended by the Research Computing Faculty of Applied Sciences (RCFAS), Harvard University, which included: (1) trimming with NGmerge (Gaspar 2018), (2) alignment against the *S. cerevisiae* S288c reference genome (yeastgenome.org, release R642-1-2) with Bwa (http://bio-bwa.sourceforge.net), (3) conversion of .sam to .bam files and validation of the final .bam file with Picard (http://broadinstitute.github.io/picard). Sequencing analysis was performed by Prof. Dr. Andreas K. Gombert.

4.4 Results

The work carried out in this chapter was entirely performed at the Bioprocess and Metabolic Engineering Laboratory (LEMeB), at the School of Food Engineering (FEA)/UNICAMP, with the collaboration of Jennifer Alves Lanza, as a result of a scientific initiation project sponsored by the *Fundação de Amparo à Pesquisa do Estado de São Paulo* (FAPESP), grant number 2018/23977-3. A schematic representation of the approach carried out is presented in Figure 4.1.

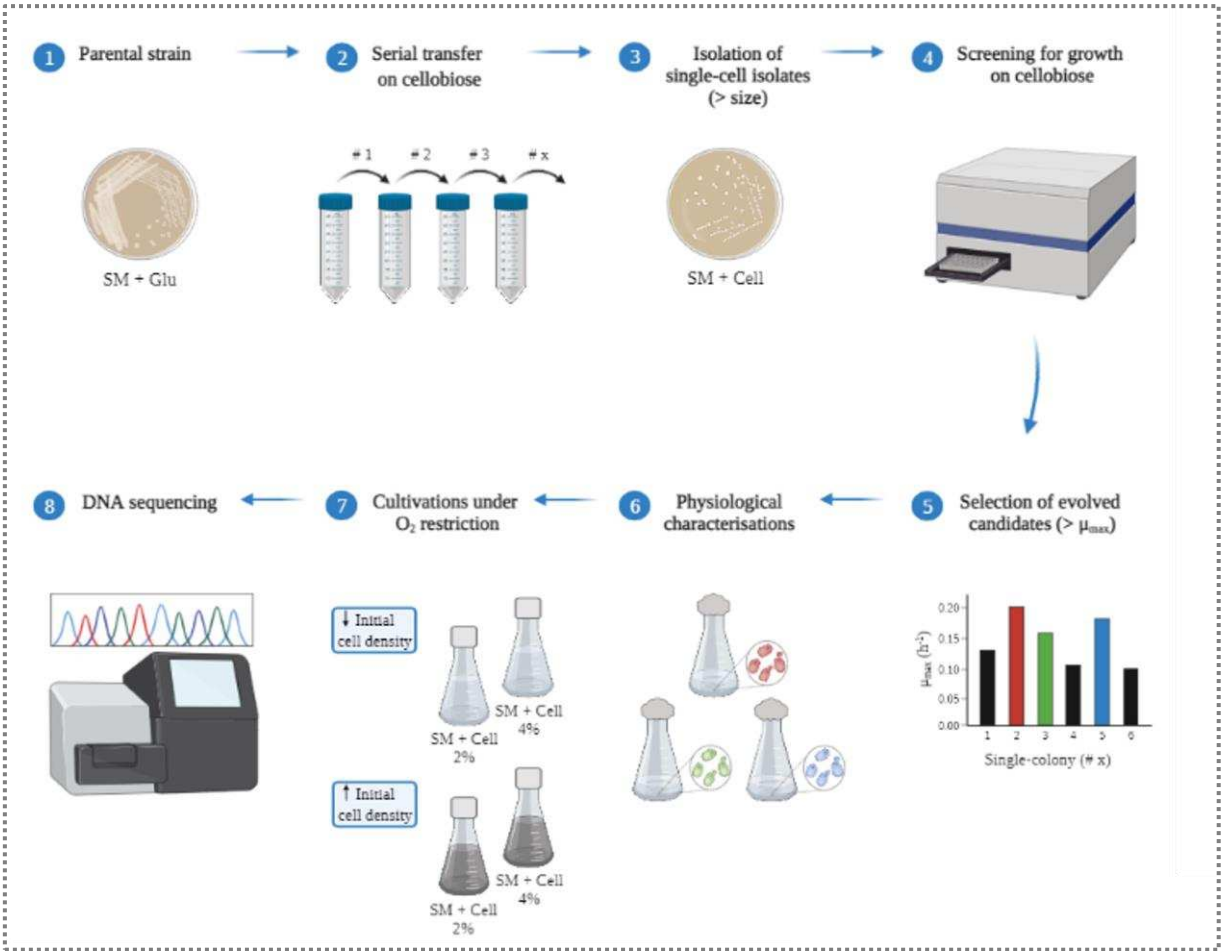

Figure 4.1. Schematic representation of the strategy adopted herein for laboratory evolution of the iCELL *S. cerevisiae* strains and subsequent evaluation in the presence and absence of oxygen. Glu = Glucose; Cell = cellobiose.

4.4.1 Laboratory evolution of engineered iCELL *S. cerevisiae* strains for rapid growth on cellobiose

Engineered iCELL *S. cerevisiae* strains were constructed by introducing the *Neurospora crassa* CDT-1 cellodextrin transporter and six intracellular β-glucosidases (BGLs) from *N. crassa* (GH1-1), *Aspergillus niger* (AN 8517), and *Podospora anserina* (PA 951, PA 3784, PA 6071, and PA 10293), as described in Chapter 3 of this thesis. Due to the initial absence of growth displayed by these strains on cellobiose as the sole carbon and energy source (Chapter 3), we decided to implement a laboratory evolution strategy to improve (or accelerate) their growth on this sugar. The strategy consisted of serial transfers on SM with 20 g/L cellobiose. Three independent lines of evolution (A, B, and C) were established for each strain, to ensure that at least one of these lines evolved successfully, as contamination events are frequent when this methodology is employed (Dunham 2010; LaCroix *et al.* 2015; Huang *et al.* 2018). Although the experiment was individually initiated with all six iCELL strains (PBY_09 to PBY_14, Table 4.1), strain PBY_10 (CDT-1 + PA 951) showed enormous difficulties to grow both in solid and liquid media with either cellobiose or glucose. Thus, after numerous attempts at cultivating this strain with frequent episodes of bacterial contamination (4-5 months of work), we decided to exclude this strain from our schedule. The problems related to the growth of PBY_10 had already been mentioned in Chapter 3.

Laboratory evolution of strains PBY_09 (CDT-1 + AN 8517), PBY_11 (CDT-1 + PA 3784), PBY_12 (CDT-1 + PA 6071), PBY_13 (CDT-1 + PA 10293), and PBY_14 (CDT-1 + GH1-1) was monitored via: 1) microscopic analysis of each subculture before transfer; 2) macroscopic analysis of colonies' appearance on agar plates; and 3) qualitative and quantitative analyses of the growth profiles and μ_{max} changes of single-cell isolates obtained at different stages of the evolution experiments (Figure 4.1). Microbiological analyses after each evolution cycle (transfer) were carried out to monitor the morphology of the cells and to guarantee the quality of the culture for the next transfer, excluding eventual contamination episodes. This procedure allowed us to observe morphological changes in all iCELL strains over the course of the evolution experiments, though these changes were different among the strains. PBY_09 and PBY_14-derived cells underwent major changes, from cells with the ovoid shape characteristic of *S. cerevisiae* cells in the beginning of the evolution lines (Figure 4.2 A) to more elongated and clustered cells (Figures 4.2 B and 4.2 C), finally reaching a morphology similar to pseudohyphae in more advanced stages of the evolution (Figure 4.2 D).

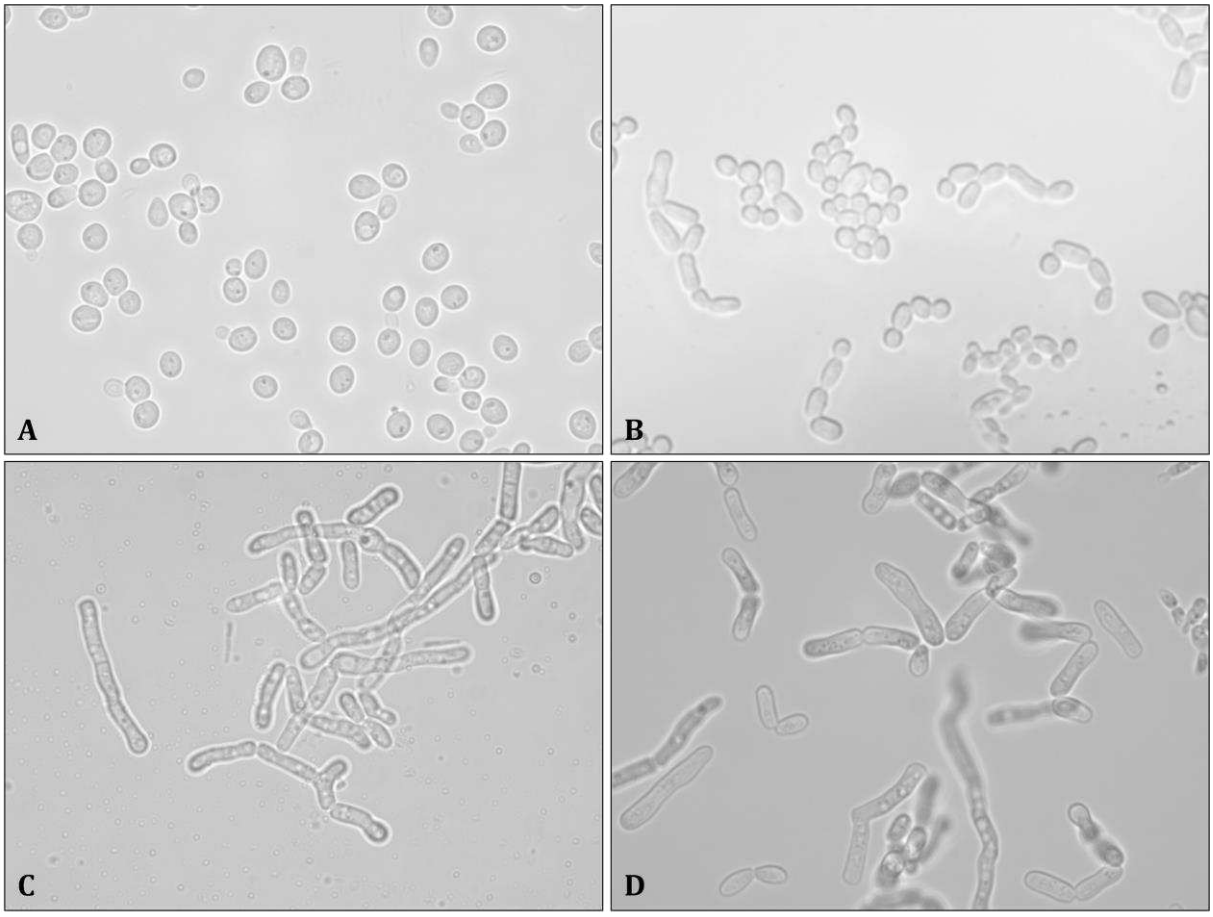

Figure 4.2. Micrograph of PBY_14 cells along the course of the evolution on cellobiose. (A) Morphology of the cells from the parental strain; **(B)** PBY_14-derived cells after ~20 generations of evolution; **(C)** PBY_14-derived cells after ~56 generations of evolution; and **(D)** PBY_14-derived cells after ~134 generations of evolution. Cells were examined using the 100X objective lens of an optical microscope. The same behaviour was observed with PBY_09 cells, although this strain was evolved for only a few generations.

Along with changes in morphology, the aspect of colonies derived from PBY_09 and PBY_14 changed from the smooth colony morphotype in the early stages of the evolution to rough colonies in more advanced stages (data not shown). Pseudohyphal morphology and rough colonies are common phenomena associated with flocculent or fast-sedimenting yeast (Reis *et al.* 2013). Regarding cells of PBY_11, PBY_12, and PBY_13, the changes in morphology over the evolution were much less pronounced than those observed with PBY_09 and PBY_14, exhibiting formats similar to the ones shown in Figure 4.2 B.

In parallel to the microbiological analyses, single colonies were isolated throughout the course of the evolution lines to evaluate their growth profiles and μ_{max} values on cellobiose during microplate cultivations. As shown in Figure 4.3, a considerable increase in the specific growth rate was observed in all iCELL strains submitted to laboratory evolution, as none of the parental strains exhibited growth on cellobiose, and after several transfers in medium with a

constant selective pressure, μ_{max} reached values higher than 0.1 h^{-1}. The results presented here belong to one of the three evolution lines established for each iCELL strain: PBY_09 line A, PBY_11 line A, PBY_12 line B, PBY_13 line C, and PBY_14 line A.

The isolates originated from the iCELL strains with higher μ_{max} on cellobiose, as inferred using microplate cultivations, represented good candidates to be further characterised using shake-flask cultivations, since these values were close to or even slightly higher than the values determined for the parental strains on glucose (between 0.14 to 0.19 h^{-1}). It is noteworthy, though, that in almost all strains more generations of selective growth did not result in clones with higher μ_{max} (Figure 4.3), which can be explained by at least two factors: 1) the number of clones evaluated at each stage was not sufficient to represent the behaviour of the heterogeneous population of cells; or 2) the evolution reached a *plateau*. Despite this, the μ_{max} values obtained after laboratory evolution of the iCELL strains were satisfactory for the continuation of this work (μ_{max} > 0.1 h^{-1}), so the evolution experiments were interrupted at this point.

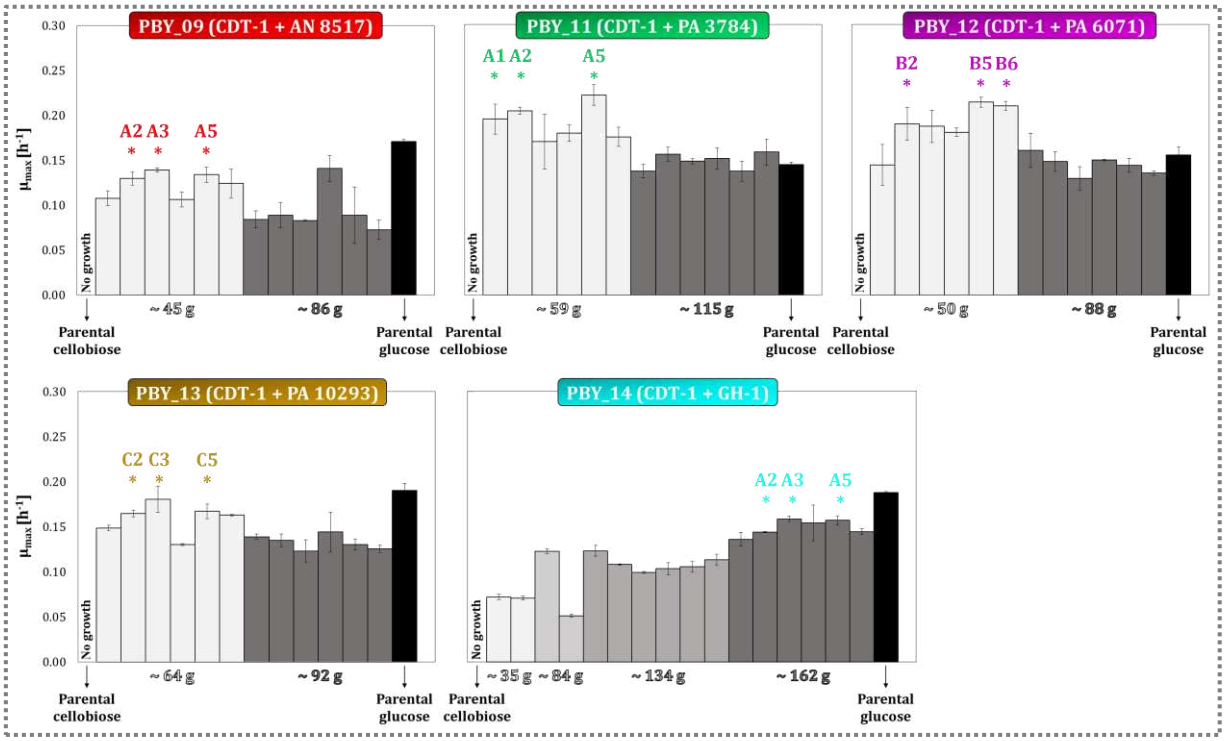

Figure 4.3. μ_{max} variation of single colonies isolated along the evolution lines of the iCELL strains on cellobiose. The bars with the same colour of each strain correspond to independent clones isolated from the same evolution cycle. The μ_{max} values correspond to the average values obtained from triplicate cultivations on microtiter plates. The error bars correspond to standard deviations. The letter "g" under the bars refers to the total number of generations estimated at each evolution cycle. The clones highlighted with asterisks were selected for further characterisation in shake-flasks.

4.4.2 Physiological characterisation of evolved iCELL strains in the presence of oxygen

To investigate the physiology of the evolved iCELL strains on cellobiose in a more quantitative manner, the best three candidates of each strain (clones with higher μ_{max} during microplate cultivations, section 4.4.1) were selected for cultivation in shake-flasks in the presence of oxygen. Single-cell isolates selected for this characterisation on 20 g/L initial cellobiose are highlighted with asterisks in Figure 4.3. Since iCELL strains had been subjected to several generations of growth on cellobiose during laboratory evolution, we decided to grow them on glucose (a non-selective sugar), in order to reset their metabolism and to guarantee that any improved phenotype would be due to mutations and evolution, and not to simple physiological adaptation. For this purpose, cells were grown for four consecutive rounds on glucose (twice on solid medium and twice on liquid medium), prior to the cultivation on cellobiose in shake-flasks. According to the growth profiles depicted in Figure 4.4, all evolved clones followed the same behaviour previously observed in microplates (data not shown), even after four cultivations on glucose-based media, which suggests that stable mutations are indeed responsible for these phenotypes after laboratory evolution. The μ_{max} values reached by these evolved isolates were between 0.24 and 0.34 h^{-1} (Table 4.2), showing that growth kinetics clearly improved in comparison to the parental strains (Figure 3.14 – Chapter 3). It should be noted that clone A5 derived from PBY_09 (CDT-1 + AN 8517), originally selected for cultivation in shake-flasks (Figure 4.3), is not depicted in Figure 4.4 because the cultures presented fast-sedimenting or flocculation phenotypes, which made it difficult to monitor cell density by absorbance (Figure 4.5). This complex phenomenon, evidenced by cells that sink to the bottom of the flasks, has been observed in experimental evolution both in batch and continuous cultivation regimes, resulting in undesired consequences for the experiment and for further application in many industrial processes (Oud *et al.* 2013; Rebnegger *et al.* 2016; Hope *et al.* 2017). Since this feature was out of the scope of this study, after two attempts exhibiting the same behaviour, we decided not to continue with this clone.

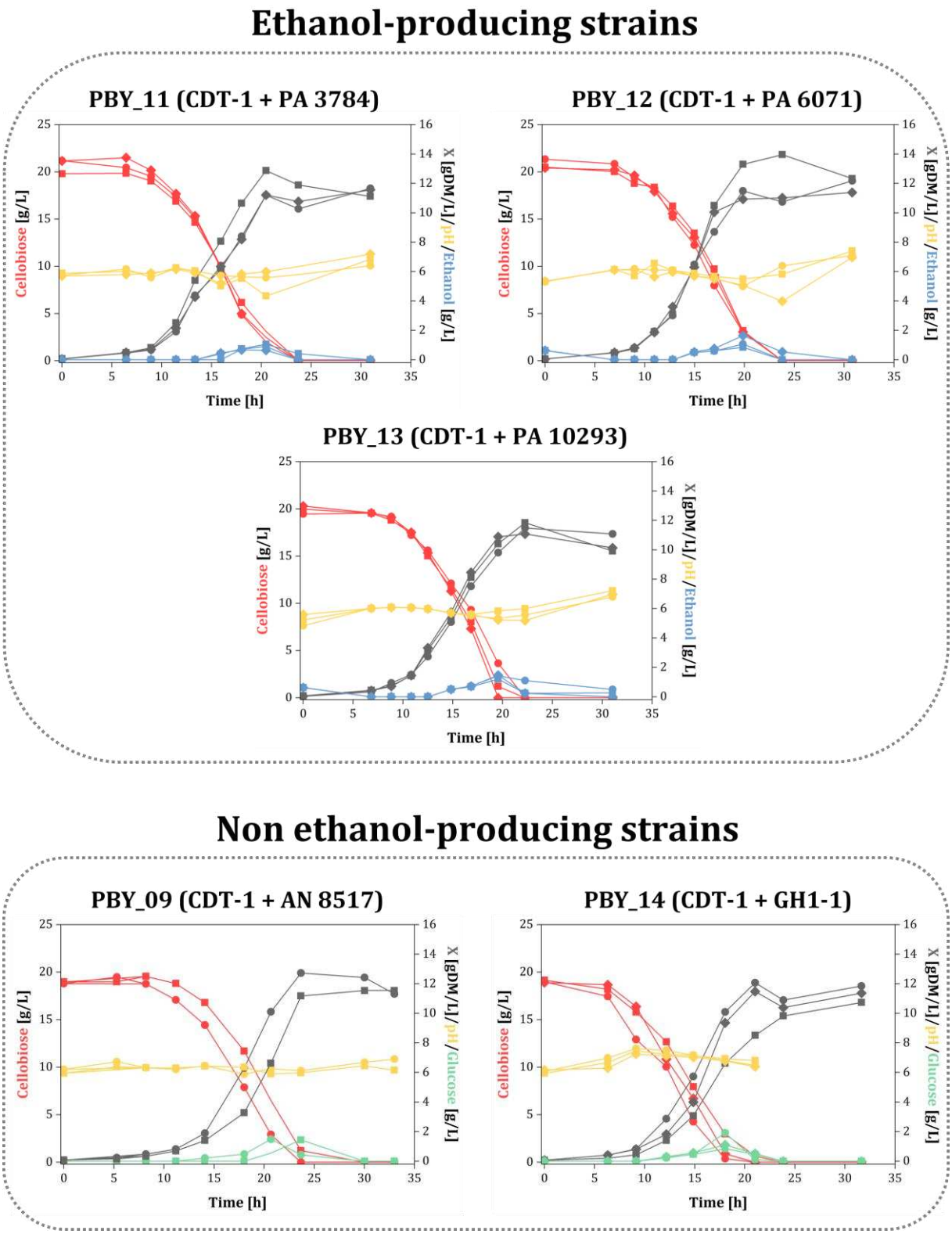

Figure 4.4. Physiological characterisation of evolved isolates derived from the iCELL strains in shake-flasks with SM and 20 g/L initial cellobiose. Profiles of cell growth, pH and extracellular metabolites (cellobiose, glucose, and ethanol) correspond to one representative of duplicate cultivations. Symbols denote as follows: (■) PBY_09ev A2, PBY_11ev A1, PBY_12ev B2, PBY_13ev C2, and PBY_14ev A2; (●) PBY_09ev A3, PBY_11ev A2, PBY_12ev B5, PBY_13ev C3, and PBY_14ev A3; (♦) PBY_11ev A5, PBY_12ev B6, PBY_13ev C5, and PBY_14ev A5.

Figure 4.5. Fast-sedimenting phenotype displayed by A5 cells derived from PBY_09 after ~45 generations of evolution on cellobiose medium. The image from the bottom of an Erlenmeyer-type shake flask shows early stages of the kinetic experiment.

Two groups of strains are evidenced in Figure 4.4: cells that produced some ethanol under the conditions employed (isolates from PBY_11, PBY_12, and PBY_13) and cells that did not produce any ethanol (isolates from PBY_09 and PBY_14). Cellobiose and glucose profiles in Figure 4.4 confirm that the growth displayed by all evolved isolates was due to the complete uptake of cellobiose and its subsequent consumption, since no glucose was generated outside the cells in the first hours of the cultivations. This excludes the possibility of extracellular hydrolysis of cellobiose, either spontaneous or mediated by the BGLs via non-conventional secretion pathways in *S. cerevisiae* (Nombela, Gil and Chaffin 2006; Giuliani, Grieve and Rabouille 2011), or even due to cell lysis and exposure of the intracellular BGLs to the extracellular space. The presence of a small accumulation of glucose (< 2 g/L, subsequently consumed) in cultures of PBY_09 and PBY_14 at 18-20 h of cultivation, is probably due to leakage of accumulated intracellular glucose (via passive transport), resulting from an imbalance between BGL and glycolytic activities. Potentially, it could also be caused by some cell disruption. In turn, no glucose, or negligible amounts (below the lower limit employed in the calibration curve - 0.1 g/L), were observed in cultures derived from PBY_11, PBY_12, and PBY_13. Since these were precisely the strains that formed some ethanol during cultivation on cellobiose, it seems that overall, they possess a higher glycolytic capacity than the strains evolved from PBY_09 and PBY_014, which did not produce any ethanol. This higher glycolytic capacity, besides resulting in ethanol formation, prevented the leakage of glucose to the extracellular medium.

By analysing the pH profiles along the cultivations, we noticed that they followed a similar trend in all evolved strains: during the first hours of cultivation the extracellular pH increased; then it dropped, and by the end it increased again reaching a pH around 7.0. *S. cerevisiae* is known for its acidification capacity when cultivated on glucose, mainly due to the excretion of organic acids to the medium, a phenomenon even more pronounced during fermentative growth (Lapathitis and Kotyk 1998; Kotyk, Lapathitis and Křenková 1999). We speculate that a similar behaviour might occur during cellobiose consumption, especially considering that the pH decrease in cultures of the non-fermenting strains (PBY_09 and PBY_14) was accompanied by the appearance of extracellular glucose (Figure 4.4). The pH increase observed in the initial part of the cultivations is probably due to the symport activity of CDT-1 involved in cellobiose consumption, which removes one mol of protons from the extracellular medium, per mol of cellobiose consumed by the cell population. When *S. cerevisiae* grown on glucose exhausts this sugar and finally respires the ethanol produced by fermentation, a switch in the pH trend, from decreasing to increasing, is typically observed (Coppella and Dhurjati 1989), which is related to the utilisation of the organic acids excreted during glucose metabolism (Locher *et al.* 1993). Since media alkalinisation with the evolved strains occurred when cellobiose (and ethanol) were depleted, we hypothesise that consumption of organic acids might partially explain the increase in pH. However, a slow H^+ extrusion by the Pma1 pump might also play an important role, as this ATPase displays a limited activity in cellobiose media due to the absence of extracellular glucose sensing (Chomvong *et al.* 2017).

Fermentative growth in *S. cerevisiae* under aerobic conditions occurs at high rates of sugar metabolism (i.e., at high sugar consumption rates or in the presence of high sugar levels). Indeed, when we analyse the sugar consumption rates in the two groups of strains, we notice that cellobiose is consumed slightly more slowly in the non-fermenting PBY_09 and PBY_14 strains (0.42 to 0.44 $g_{cellobiose}/g_{DM}$*h) compared to the fermenting PBY_11, PBY_12, and PBY_13 counterparts (0.54 to 0.64 $g_{cellobiose}/g_{DM}$*h) (Table 4.2). However, the behaviour of clone A2 derived from PBY_14 does not fit this pattern and we do not have a proper explanation for this.

As evidenced from the high cell densities (~11 g/L) and overall biomass yields (0.55-0.61 $g_{DM}/g_{cellobiose}$) attained on cellobiose (Figure 4.4 and Table 4.2), it can be concluded that the metabolism of this sugar in the non-fermenting PBY_09 and PBY_14 strains is fully respiratory. Apart from the absence of ethanol, no other common by-product was detected in

these cultures, at least not using refractive index detection coupled to the HPLC separation employed here. These results suggest that all evolved isolates of PBY_09 and PBY_14 are Crabtree negative for cellobiose, as even at high external concentrations of sugar (20 g/L), these strains only produced biomass and CO_2 (the latter not measured), in contrast to the typical fermentative metabolism exhibited by *S. cerevisiae* on glucose. On the other hand, although all clones derived from PBY_11, PBY_12, and PBY_13 were able to catabolise part of the sugar through fermentation, the amount of ethanol produced was very small, reaching up to 1.5 g/L, which was mostly consumed by the strains at the end of the cultivations. This behaviour indicates that the evolution experienced by the strains did not affect their capacity to utilise ethanol as a carbon and energy source, one of the hallmarks of *S. cerevisiae*, according to the make-accumulate-consume hypothesis (Hagman *et al.* 2013). Thus, in all these strains, the metabolism of cellobiose is also predominantly respiratory, leveraging high biomass concentrations (10-12 g/L) and high overall biomass yields (between 0.49 and 0.58 $g_{DM}/g_{cellobiose}$) (Figure 4.4 and Table 4.2).

Table 4.2. Physiological parameters of evolved isolates derived from the iCELL strains grown on cellobiose during microplate or shake-flask cultivations in the presence of oxygen. Averages, mean deviations, and standard deviations were, respectively, obtained from duplicates (shake-flask cultivations) or triplicate (microplate cultivations) experiments.

				Microplates	**Shake-flasks**		
Strain	**BGL-encoding gene**	**Nº of gen.**	**Single-cell isolate**	**μ_{max} (h^{-1})**	**μ_{max} (h^{-1})**	**$Y_{X/S}$ (g_{DM}/g_{cellob})**	**q_s (g_{cellob}/g_{DM}*h)**
PBY_09ev	AN 8517 *A. niger*	~45	A2	0.13 ± 0.01	0.24 ± 0.00	0.57 ± 0.03	0.42 ± 0.02
		~45	A3	0.14 ± 0.00	0.24 ± 0.00	0.57 ± 0.00	0.43 ± 0.00
		~45	A5	0.13 ± 0.01	ND	ND	ND
PBY_11ev	PA 3784 *P. anserina*	~59	A1	0.20 ± 0.02	0.33 ± 0.00	0.54 ± 0.02	0.60 ± 0.02
		~59	A2	0.20 ± 0.00	0.34 ± 0.01	0.55 ± 0.00	0.61 ± 0.01
		~59	A5	0.22 ± 0.01	0.34 ± 0.00	0.54 ± 0.00	0.64 ± 0.01
PBY_12ev	PA 6071 *P. anserina*	~50	B2	0.19 ± 0.02	0.31 ± 0.00	0.58 ± 0.02	0.54 ± 0.02
		~50	B5	0.21 ± 0.01	0.32 ± 0.00	0.56 ± 0.01	0.58 ± 0.00
		~50	B6	0.21 ± 0.00	0.33 ± 0.00	0.58 ± 0.02	0.57 ± 0.02
PBY_13ev	PA 10293 *P. anserina*	~64	C2	0.16 ± 0.00	0.32 ± 0.02	0.49 ± 0.00	0.64 ± 0.03
		~64	C3	0.18 ± 0.01	0.34 ± 0.01	0.57 ± 0.00	0.61 ± 0.01
		~64	C5	0.17 ± 0.01	0.34 ± 0.01	0.53 ± 0.03	0.64 ± 0.05
PBY_14ev	GH1-1 *N. crassa*	~162	A2	0.14 ± 0.00	0.32 ± 0.01	0.55 ± 0.00	0.57 ± 0.03
		~162	A3	0.16 ± 0.00	0.26 ± 0.02	0.61 ± 0.02	0.43 ± 0.03
		~162	A5	0.16 ± 0.01	0.27 ± 0.00	0.61 ± 0.01	0.44 ± 0.02

$Y_{X/S}$ = Global biomass yield on cellobiose ($g_{DM}/g_{cellobiose}$).
q_S = Specific cellobiose consumption rate ($g_{cellobiose}/g_{DM}$*h).
ND = not determined.

4.4.3 Performance of evolved iCELL strains under oxygen limitation

Based on the physiological responses of the evolved iCELL strains on cellobiose, we wondered whether we could force the fermentation of cellobiose by growing the yeast cells under a more restrictive oxygen environment. Different concentrations of sugar (20 or 40 g/L) and initial cell concentrations (Abs_{600} ~0.1 or 1) were chosen to maximise the chances of obtaining successful results, due to the influence of these variables in the mode by which sugars are metabolised in *S. cerevisiae* (Brown and Johnson 1970). Since this was a preliminary evaluation, the cultivations were made without replicates and only two evolved isolates that did not display any ethanol formation during shake-flask cultivations in the presence of oxygen were tested (PBY_09 clone A3 and PBY_14 clone A2) (Figure 4.6). However, even after ~one week of cultivation using the shake-flask system that minimises oxygen transfer, almost no growth or cellobiose consumption was observed in the conditions assayed, and only cultivations made at high initial cell density (Abs_{600} ~1) showed some formation of ethanol and other by-products (< 0.5 g/L, data not shown). These results suggest that the improvement observed in the metabolism of cellobiose in the presence of oxygen was not sufficient to ensure growth of these strains under oxygen limitation, a phenomenon that has been termed the Kluyver effect (Fukuhara 2003). In other words, to achieve fermentative growth, the strains will require higher specific cellobiose consumption rates.

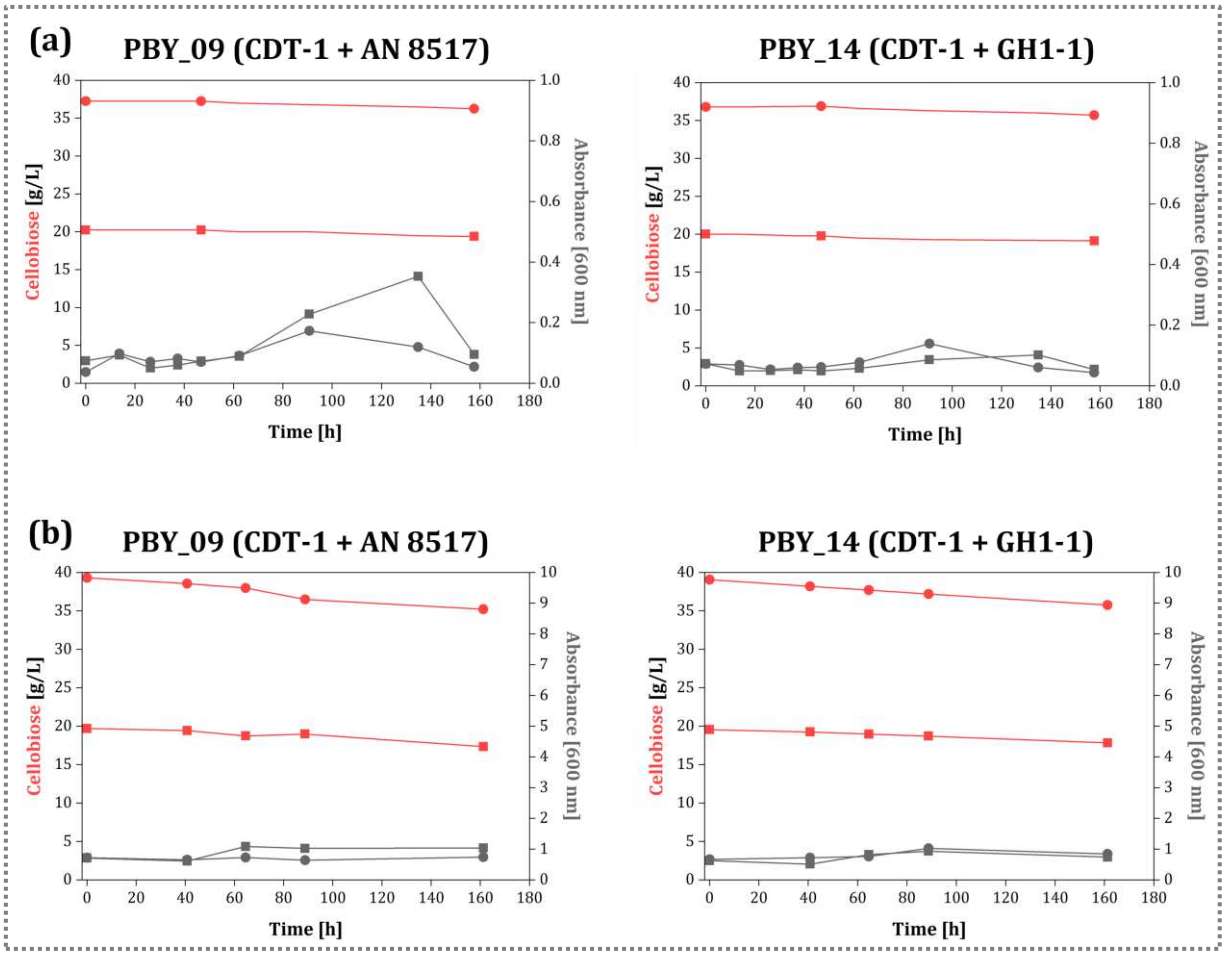

Figure 4.6. Kinetic profiles of evolved iCELL isolates derived from PBY_09 and PBY_14 during shake-flask cultivations on cellobiose under oxygen limitation. Cultivations were performed in SM without replicates and initiated with **(a)** an Abs_{600} ~0.1 and 20 g/L (■) or 40 g/L (●) cellobiose, and **(b)** an Abs_{600} ~1 and 20 g/L (■) or 40 g/L (●) cellobiose.

Based on previous analyses, it seems that the evolved isolates originated from PBY_09 and PBY_14 resulted in Kluyver-positive for cellobiose, as the growth displayed on this disaccharide occurred exclusively under respiratory conditions. Thus, the cellobiose uptake step might be playing an important role in this limitation, even after several generations of selective growth, since insufficient activity of the CDT-1 transporter might not be able to sustain the high cellobiose uptake rates necessary for fermentative growth. However, we also noticed that pH may have contributed to this limitation. By lowering the initial pH in the evolution experiments from 6 to a more acidic value (4-5), we should have enabled faster consumption of cellobiose, because the proton gradient for symport would be higher. In addition, yeast prefer pH between 3 and 5, so probably we should have taken this into consideration by the time these experiments were performed. Finally, we cannot ignore that low BGL activities in the evolved strains might also be limiting growth under these conditions. Additional experiments would be necessary to confirm these hypotheses.

Compared to the setup employed for aerobic cultivations (Appendix I), the system we developed to force fermentative growth attempted to reduce the amount of oxygen that diffuses into the system in four ways: 1) by changing the cotton stopper for a silicone stopper; 2) by using norprene tubing instead of silicone tubing, which has a 40-times lower permeability to oxygen (da Costa *et al.* 2018); 3) by flushing the culture medium with a high-purity inert gas (N_2) to remove oxygen from the system; 4) by increasing the culture volume (from 100 to 300 mL) and reducing the stirring speed (from 200 to 100 rpm), which lowers oxygen transfer. Although this system did not create a strict anaerobic environment, the results obtained here evidence that oxygen availability must have dropped substantially. Additionally, these results highlight the high dependence of oxygen for cellobiose metabolism in the evolved strains.

Evolved *S. cerevisiae* cells for faster growth on xylose showed a similar lack of capacity to grow on xylose under strict anaerobic conditions after 30 cycles of evolution under aerobiosis (Kuyper *et al.* 2004). To further select for anaerobic growth on xylose, the authors submitted the culture to a partial limitation of oxygen for 10 cycles and then switched to a fully anaerobic environment for another 10 more cycles, after which they could isolate a mutant capable of growing under these strict conditions (Kuyper *et al.* 2004).

4.4.4 Investigation of the genetic changes selected in evolved iCELL strains

To further investigate the mechanisms involved in the respiration-dependent growth phenotype displayed by the evolved iCELL strains, we sequenced the six isolates derived from *S. cerevisiae* PBY_12 (CDT-1 + PA 6071) and PBY_13 (CDT-1 + PA 10293). To our surprise, analysis of the genomic data revealed that all DNA samples did not belong to *S. cerevisiae*, but rather to another yeast, *Meyerozyma guilliermondii* (formerly known as *Pichia guilliermondii* or *Candida guilliermondii*). This means that the evolution experiments conducted with at least PBY_12 and PBY_13 were contaminated with a cellobiose-utilising yeast species that managed to settle and compete in the cell population.

Identification of yeast species is commonly made by PCR amplification and sequencing of the Internal Transcribed Spacer (ITS) regions and the D1/D2 region of the 26S rDNA gene (Kurtzman and Robnett 1998; Petti 2007). Resulting sequences are then aligned against reference libraries and identified. Here, the contaminant was identified by sequencing of the reads generated during the process of whole-genome sequencing. Randomly selected reads derived from every clone were aligned against the NCBI (National Center for Biotechnology

Information) database by using a BLASTn search. All of them were 100% identical with *M. guilliermondii* strains (data not shown). In addition, the percentage of reads aligned against the reference genome (*S. cerevisiae* CEN.PK113-7D strain) was about 7%, while the expected value should be > 90% (Table 4.3). Future work will be needed to evaluate whether the evolution experiments established for PBY_09, PBY_11, and PBY_14 suffered from the same contamination phenomena.

Table 4.3. Sequencing data from the clones derived from strains PBY_12 and PBY_13. Coverage was expressed with respect to a 12 MB haploid genome. Reference genome: *S. cerevisiae* CEN.PK113-7D.

Strain	**Nº of reads**	**Nº of bases**	**Coverage**	**% alignment *vs*. ref genome**
PBY_12ev B2	1086662	651997200	54.3 x	7.2
PBY_12ev B5	1435089	861053400	71.8 x	6.5
PBY_12ev B6	1032483	619489800	51.6 x	7.2
PBY_13ev C2	1241435	744861000	62.1 x	7.3
PBY_13ev C3	1265940	759564000	63.3 x	7.2
PBY_13ev C5	1070014	642008400	53.5 x	6.2

4.5 Discussion

In Chapter 3 we described the application of metabolic engineering to construct yeast chassis for cellobiose utilisation via intracellular hydrolysis (referred to as iCELL strains). Nevertheless, co-expression of a cellodextrin transporter and individual BGLs did not confer them the ability to grow on this sugar as the sole carbon and energy source. To achieve cellobiose utilisation without making any additional rational genetic modification, which could be extremely risky and time-consuming, we opted to submit the strains to laboratory evolution, based on the power of this methodology for improving kinetic performances in a relatively short period of time. After several generations of selective growth on cellobiose-based media, we selected promising candidates in all five evolution experiments, and assessed their physiology during shake-flask cultivations on cellobiose under different oxygen availability. As a result, we obtained strains that grew efficiently on cellobiose in the presence of oxygen, reaching μ_{max} between 0.24 and 0.34 h^{-1}. However, cellobiose metabolism in these strains resulted in poor or no ethanol production. All sugar was metabolised for biomass (and accompanying CO_2) formation, achieving biomass yields between 0.49 to 0.61 $g_{DM}/g_{cellobiose}$. While these μ_{max} values approach the ones observed for *S. cerevisiae* during growth on glucose (Verduyn *et al.* 1990), the biomass yield values are somewhat higher than the typical values of ~0.50 $g_{DM}/g_{glucose}$ observed for this yeast species during purely respiratory growth (da Costa *et al.* 2018).

At this point of the work, we believed that laboratory evolution had clearly improved cellobiose uptake in the five iCELL strains, allowing for full consumption of the sugar, but with a rate of uptake not high enough for fermentative growth. Indeed, the inability of some of the strains to grow under oxygen limitation was consistent with the respiratory response observed under aerobic conditions. However, sequencing data revealed that at least two of the evolution experiments had been contaminated and (potentially) dominated with *M. guilliermondii*, a yeast species that, as far as we are aware, was not available in our laboratory by the time these experiments were made. Based on these unexpected findings, here we would like to make some considerations and discuss lessons learned from this episode.

Throughout the course of the evolution lines that led to the isolation of *M. guilliermondii*, we were aware of some gradual changes in cell morphology, similar to the ones shown in Figure 4.2 B. Although these observations caused some concerns in the beginning, we shared the micrographs with expert colleagues and got to know that this phenomenon was indeed very

frequent in evolution experiments with *S. cerevisiae* (Brown and Hough 1965; Adams *et al.* 1985; Weusthuis *et al.* 1993; Jansen *et al.* 2005; Dário 2012; Nijland *et al.* 2019). Many of the examples available in the scientific literature are related to yeast evolved for increased sugar uptake, and the altered morphology (more elongated cells) is commonly ascribed to the possibility of allowing the cells to insert additional permeases in the cell membrane, as a result of an increased cells' surface area to volume ratio (Adams *et al.* 1985; Groeneveld, Stouthamer and Westerhoff 2009). If cellular growth in our strains was controlled by cellobiose transport, this hypothesis would be reasonable.

Although it is widely known that contamination events are very frequent in evolution experiments, we also know that this type of result rarely ends up being published. One exception to this is a paper from a work that applied laboratory evolution to improve the xylose-fermenting capacity of an industrial *S. cerevisiae* strain. In this work, the authors found that a contaminant – lately identified as *Candida intermedia* – had managed to compete with *S. cerevisiae* and cope with the inhibiting environment of the xylose-rich lignocellulosic hydrolysate (Geijer *et al.* 2020). This discovery led to the origin of a new research line within the group that focuses on non-conventional yeast species with potential biotechnological traits (Moreno *et al.* 2017, 2019, 2020).

The detection of *M. guilliermondii* after 18 months of work taught us about the importance of using molecular means from time to time to certify the identity of the microbial species present in the cell population, i.e., those based on DNA barcode markers (D1/D2 or ITS regions). This strategy would allow the researcher to detect the presence of a potential contaminant, but its elimination would require corrective action. In this regard, creating frozen fossil records (stock of cell population) every certain amount of time can enable the experiment to be restarted from the previous stock if needed. Additional strategies can be taken to eliminate potential external contamination; for instance, by introducing an antibiotic marker gene in the strain that will be evolved, submitting the population to the specific antibiotic from time to time, and removing the marker at the end of the evolution process (personal communication with Dr. Leandro Vieira dos Santos from the Brazilian Biorenewable National Laboratory). When conducting multiple evolution lines in parallel, as in this work, one could use different antibiotic markers for each line in order to reduce the possibility of cross contamination.

M. guilliermondii is an ascomycetous yeast found in diverse environments, including soil, water, air, insects, plants, food products, tree bark, decaying wood, human skin, and mucosal

microflora. The ubiquitous presence of *M. guilliermondii* in nature makes it difficult to speculate about the origin of the contamination, especially considering that there are no records of this yeast in our laboratory. *M. guilliermondii* is a typical aerobic yeast, with a standard growth temperature of 30 °C, that cannot grow under strict anaerobic conditions. Its ability to utilise cellobiose as carbon source is well-described (Freer 1991; Rodríguez *et al.* 2004; Kurtzman 2011; Khattab and Kodaki 2016; da Silveira *et al.* 2020; Mo *et al.* 2021), but reports differ regarding its capacity to catabolise cellobiose via fermentation, suggesting that this property is strain-dependent (Freer 1991; Khattab and Kodaki 2016; Lopes *et al.* 2018). Despite its natural capacity to ferment both glucose and xylose, *M. guilliermondii* has been poorly investigated for lignocellulosic ethanol, probably due to its low ethanol tolerance compared to *S. cerevisiae* (Sidana, Kaur and Yadav 2022). The two most explored features of *M. guilliermondii* for biotechnological applications are its ability to overproduce riboflavin under iron limitation and to convert xylose to xylitol (Meyrial *et al.* 1991; Papon *et al.* 2013).

Our in-house isolated *M. guilliermondii* strain showed a respiratory metabolism during growth on cellobiose, making this strain not suitable for the purpose of this work. However, the potential of this non-conventional yeast for processes that require dissimilation of the carbon source via respiration cannot be ignored. One of these possibilities targets *M. guilliermondii* as a cell factory for the production of BGLs with attractive characteristics for cellulosic ethanol and winemaking (as aroma enhancer) (Rodríguez *et al.* 2004; da Silva *et al.* 2019). For this purpose, it would be necessary to purify and characterise the BGL produced by our isolated strain. In this sense, *M. guilliermondii* is already known as a promising producer of industrially relevant enzymes, such as inulinase, α-amylase, α-rhamnosidase, lipase, nitrilase, and phytase (Papon *et al.* 2013; Yan *et al.* 2021). Another possibility is the application of *M. guilliermondii* in the field of biosensors, to detect the presence of cellobiose in samples by measuring oxygen consumption (Shkil *et al.* 2009; Toussaint *et al.* 2016). Cellobiose determination is of special interest in the wood industry, as a way to assay wood decomposition by fungi in earlier stages (Toussaint *et al.* 2016). When cultured in cellobiose-containing samples, our *M. guilliermondii* isolate will respire the sugar and the oxygen consumed (measured electrochemically) can be correlated to the concentration of cellobiose in the samples.

Lastly, the mechanism underlying *M. guilliermondii*'s cellobiose metabolism has not been investigated yet. Leveraging the genomic sequence of our in-house isolate would be valuable to identify genes responsible for cellobiose assimilation, to provide insight into the strain-

dependent catabolism of cellobiose in this yeast, and to make the sequencing data available for other scientific purposes. Recently, *M. guilliermondii* GXDK6 strain has been genome sequenced and it could serve for comparative purposes (Mo *et al.* 2021). Genetic engineering tools for *M. guilliermondii* have been made available in the last decade and should contribute to this identification (Papon *et al.* 2015). Non-conventional yeasts are now gaining special attention in biotechnology and our physiological and genomic data of *M. guilliermondii* could broaden our understanding of the potential of this yeast as a cell factory (Geijer, Ledesma-Amaro and Tomás-Pejó 2022).

4.6 Acknowledgements

The authors would like to thank Jennifer Alves Lanza for the active work dedicated to the development of this chapter. JAL was responsible for conducting the evolution experiments, and the shake-flask cultivations, in collaboration with the doctoral candidate PMB.

5 PHYSIOLOGY OF A *SACCHAROMYCES CEREVISIAE* STRAIN THAT METABOLISES SUCROSE INTRACELLULARLY

5.1 Abstract

In this study, we assessed the iSUC component of our iSUCCELL strategy as a follow up of the study conducted by Basso *et al*. (2011), who obtained a *Saccharomyces cerevisiae* i*SUC2*e strain that displayed an 11% higher ethanol yield on sucrose in chemostat cultivation, when compared to a reference strain that utilises sucrose mainly via extracellular hydrolysis. Industrial reality is dramatically different from such a condition in at least the following aspects: 1) fermentations are not carried out in continuous mode (with some exceptions), but rather in fed-batch mode with cell recycling and a high inoculum concentration; 2) the medium is extremely complex and nitrogen-poor, prepared from sugarcane juice and molasses; 3) cultivations are not monoseptic, but rather run in the presence of microbial contaminants; 4) temperature and pH are not kept constant, but rather fluctuate; 5) sugar and ethanol concentrations reach much higher values than those utilised in Basso *et al*. (2011)'s experiments. To move one step closer to industrial conditions, we first cultivated the i*SUC2*e and reference (CEN.PK113-7D) strains in shake-flasks with sucrose as the sole carbon source. The performance of i*SUC2*e in this study showed four important discrepancies compared to sucrose-limited chemostats: it accumulated a higher level of hexoses than CEN.PK113-7D, it did not exhibit any improvement in the ethanol yield, it attained similar biomass yields than CEN.PK113-7D, and it produced 3 times more glycerol than the reference strain. When the i*SUC2*e and CEN.PK113-7D strains were subsequently cultivated in a miniaturised system developed to recapitulate the industrial features described above, both strains showed similar CO_2 production, cell viability, and more importantly, similar ethanol yields at the end of five rounds of fermentation on sugarcane molasses with acid treatment and cell recycling. Furthermore, compared to CEN.PK113-7D, the i*SUC2*e strain again presented increased production of glycerol in all fermentation cycles. We conclude with caution that the improvements in fermentation performance observed in sucrose-limited chemostats could not be extrapolated to the conditions applied in this work. We also speculate that the increased levels of glycerol in the i*SUC2*e cultures may be a consequence of the prolonged adaptation to a nutrient-poor medium, which caused an osmotic response when switching to excess nutrients.

5.2 Introduction

Chapters 3 and 4 of this thesis focus on the intracellular hydrolysis of cellobiose by engineered *Saccharomyces cerevisiae* (iCELL) strains. As comprehensively discussed in Chapter 2, the iSUCCELL yeast platform envisaged in this thesis requires, in addition to cellobiose transport and its subsequent intracellular hydrolysis, the metabolism of sucrose via an intracellular hydrolytic (iSUC) pathway. One of the benefits of relocating sucrose hydrolysis from the extracellular to the intracellular environment, in the context of fuel ethanol production, is that such a strain displays a higher ethanol yield on sucrose than its parental background (Basso *et al.* 2011). The reason for this is due to the energy costs of sucrose-H^+ symport, which reduce free-energy (ATP) conservation in iSUC cells from 4 to 3 mol ATP per mole of sucrose fermented. To compensate for this lower ATP yield, the iSUC cells are forced to deviate a larger fraction of the carbon and energy source towards energy production, which under anaerobic conditions translates into higher ethanol production. Basso *et al*. (2011) already confirmed this prediction in an elegant study that led to an evolved i*SUC*2 (i*SUC*2e) strain in which sucrose is taken up by sucrose-H^+ symport mediated by the native Agt1 permease and hydrolysed by the intracellular form of invertase (*SUC2* gene). To drive predominant and constitutive expression of the intracellular invertase, the native *SUC2* promoter was replaced by the *ADH* promoter, in such a way that its integration interrupted the *SUC2* signal peptide for extracellular targeting. As a result, the i*SUC2*e strain was capable of improving the ethanol yield on sucrose by 11%, with a concomitant 30% and 20% decrease in the biomass and glycerol yields, respectively, when compared to reference cells that mainly hydrolyse sucrose extracellularly. The findings from this promising proof-of-concept study - carried out using quantitative chemostat cultivations with a defined medium - still need to be evaluated under conditions resembling the industrial process used to produce fuel ethanol from sucrose-based feedstocks, such as sugarcane (Marques *et al.* 2016).

In the Brazilian sugarcane-based first-generation (1G) fuel ethanol industry, fermentation is carried out mainly using fed-batch operation and non-defined media, typically a combination of unsterile sugarcane juice and diluted molasses. While sugarcane juice has some nutritional deficiencies for yeast cells, molasses carries substances that are known to interfere with the fermentation process, such as high levels of aluminium and potassium (Basso, Basso and Rocha 2011). The Brazilian 1G process in sugarcane biorefineries is characterised by four remarkable peculiarities: non-aseptic conditions, high cell density fermentation, acid treatment between fermentations, and cell recycling. These unique characteristics ensure short

fermentation times, less substrate loss for biomass production, and lower bacterial contamination (Basso, Basso and Rocha 2011).

Due to the importance of studying yeast physiology in industry-like conditions, in our research group a bench-scale cultivation setup was recently developed and benchmarked to mimic the industrial process used in sugarcane biorefineries (Raghavendran *et al.* 2017). To verify whether the benefits accrued with the i*SUC2*e strain in the previous laboratory setup (Basso *et al.* 2011), in terms of increased ethanol yields, have the potential to hold in industry, the goal of the study described in this chapter was to assess how the i*SUC2*e strain would perform in situations which are closer to the industrial scenario, i.e., in batch operation with excess sugar and in a miniaturised system mimicking the Brazilian 1G fuel ethanol process using industrial media with sulphuric acid treatment and cell recycling.

5.3 Material and Methods

5.3.1 Strains and maintenance

The *S. cerevisiae* strains used in this work (Table 5.1) belong to the congenic members of the CEN.PK family (van Dijken *et al.* 2000; Entian and Kötter 2007), except for the industrial PE-2 strain. The CEN.PK113-7D strain was kindly provided by Dr. Peter Kötter (EUROSCARF, Germany). The i*SUC2*e strain (named IMM007 in the original work) was kindly provided by Prof. Dr. Thiago Olitta Basso from the University of São Paulo (USP, Brazil). The Brazilian fuel ethanol strain PE-2 was obtained from Dr. Luiz Carlos Basso from USP, Brazil. To prepare stock cultures, yeast strains from single colonies on plates were grown in 50-mL polypropylene tubes containing 10 mL of Yeast Extract-Peptone-Dextrose medium (YPD). The YPD medium was prepared as described in section 5.3.2. After 24 h growth at 30 °C and 200 rpm, 30% (v/v) glycerol was added, and 2-mL aliquots were stored at -80 °C.

Table 5.1. Yeast strains used in this study.

STRAIN	RELEVANT GENOTYPE	ORIGIN	REFERENCE
CEN.PK113-7D	MATa *mal13 AGT1 MAL12 MAL2-8c TRP1 SUC2*	Dr. P. Kötter, (EUROSCARF, Germany)	van Dijken *et al.* 2000
i*SUC2*e	MATa *mal13 AGT1 MAL12 MAL2-8c trp1-289 TRP1*-P_{ADH1}::i*SUC2* evolved	Dr. T. O. Basso (USP, Brazil)	Basso *et al.* 2011
PE-2	Diploid strain	Dr. L. C. Basso (USP, Brazil)	Basso *et al.* 2008

5.3.2 Culture media and cultivation conditions

S. cerevisiae strains were routinely cultivated at 30 °C and 200 rpm either in YPD medium or Synthetic Medium (SM) with 20 g/L initial sucrose as carbon source. The YPD medium, composed of 10 g/L yeast extract, 20 g/L peptone, and 20 g/L dextrose, was sterilised by separately autoclaving (121 °C for 20 min) glucose from peptone and yeast extract, to avoid caramelisation (Maillard reaction). When required, 20 g/L agar was added to the peptone/yeast extract solution prior to heat sterilisation (121 °C for 20 min). In the case of the 1G scaled down experiment (section 5.3.4), the concentration of dextrose in the YPD medium was 40 g/L.

The SM was prepared according to Verduyn *et al.* (1992), with the substitution of ammonium for urea as the sole nitrogen source, to prevent excessive acidification during cultivation. To supplement the missing sulphate in the medium, K_2SO_4 was added as in (Luttik *et al.* 2000; van Leeuwen *et al.* 2009). SM contained vitamins, trace metals, salts, a nitrogen source, and a carbon and energy source, including 6.6 g/L K_2SO_4, 3.0 g/L KH_2PO_4, 0.5 g/L $MgSO_4.7H_2O$, 2.3 g/L urea, and 20 g/L sucrose with an initial pH adjusted to 6.0 using KOH 2 M. Sucrose and urea solutions were filter-sterilised through 0.22 μm pore membranes and added to the medium after autoclaving (121 °C for 20 min). Vitamins and trace elements solutions (Verduyn *et al.* 1992) were prepared as 1000x stocks and sterilised by filtration or autoclaving, respectively, before addition to the medium.

Sugarcane molasses was obtained from Usina Iracema mill (Iracemápolis, São Paulo, Brazil) containing approximately 50% (mass/volume) total reducing sugars (TRS). Two molasses solutions were prepared for the spot assay (section 5.3.3) and the 1G scaled down system (section 5.3.4), according to Raghavendran *et al.* (2017): molasses with ~19.4% and 10% TRS. For solid molasses with 19.4% TRS, 20 g/L agar was added prior to heat sterilisation (121 °C for 20 min).

5.3.2.1 Shake-flask cultivations under high oxygen availability

Shake-flask cultivations were performed in duplicates in 500-mL cotton-capped unbaffled Erlenmeyer flasks with silicone tubing connected to an outside needle, which allowed sampling using a syringe, without the need to open the flask during sampling (Appendix I). To avoid contamination, the tubing was kept closed by a Mohr clamp during cultivation and opened during sampling. Flasks containing 100 mL of SM with 20 g/L initial sucrose were incubated at 30 °C and 200 rpm in a rotary shaker (Innova 4430, New Brunswick Scientific, Edison, USA) under an air atmosphere. Inocula were prepared by transferring cells from one colony on a YPD plate to 250-mL unbaffled Erlenmeyer flasks containing 50 mL of SM with 20 g/L initial sucrose. After ~24 h growth at 30 °C and 200 rpm, cultures were centrifuged at 3000 rpm for 5 min (NT810 centrifuge, Novatecnica, Piracicaba, Brazil) and the supernatant discarded; cells were washed twice with sterile distilled water and resuspended in 1 mL of SM with 20 g/L initial sucrose before inoculating 500-mL Erlenmeyer flasks with an initial absorbance at 600 nm (Abs_{600}) of approximately 0.2. Shake-flasks were incubated until the cells reached the stationary phase of growth. Samples were taken at different time points to measure cell concentration (indirectly via Abs_{600}), pH, and concentrations of substrate and

extracellular metabolites, according to section 5.3.5. Prior to sampling, care was taken to dispense the dead volume that remains in the silicone tubing.

5.3.2.2 Shake-flask cultivations under low oxygen availability

Cultivations minimising oxygen transfer were performed without replicates in 500-mL unbaffled Erlenmeyer flasks capped with silicone stoppers and equipped with two norprene tubing: one connected to an internal silicone tubing and an outside needle for inoculating, sampling, and nitrogen purging, and the other one (coupled to a gas filter) used for CO_2 outlet (Appendix I). To avoid contamination, sampling connections were kept closed by a Mohr clamp during cultivation and opened during sampling. Flasks containing 300 mL of SM with 20 g/L initial sucrose were purged with nitrogen gas (99.996% purity) for 30 min prior to inoculation, to reduce the availability of oxygen in the system. Inocula were prepared in the same manner as described for the shake-flask cultivations under oxygen excess. Shake-flasks were incubated at 30 °C and 100 rpm until the cells reached the stationary phase of growth. Samples were taken hourly to measure cell concentration (indirectly via Abs_{600}), pH, and concentrations of substrate and extracellular metabolites, according to section 5.3.5. After every sampling event, cultures were sparged with nitrogen for 3 min to reduce oxygen content.

5.3.3 Serial dilution spot assay

The dilution spot assay was performed according to the protocol reported by Della-Bianca and Gombert (Della-Bianca and Gombert 2013), with the following modifications. For each strain, cells from a single colony on YPD plates were resuspended in sterile distilled water to make 1 mL of the cell suspension with an initial Abs_{600} of 1 (10^0). Thereafter, five successive dilutions (10^{-1}, 10^{-2}, 10^{-3}, 10^{-4}, and 10^{-5}) were prepared. Spots of 3 µL of each dilution were carefully placed with a pipette onto the surface of Petri dishes containing solid molasses with 19.4% TRS. The plates were incubated for at least 48 h at 30 °C (502 incubator, FANEM, São Paulo, Brazil) and photographed.

5.3.4 Laboratory scale system mimicking the 1G fuel ethanol industry

This experiment was carried out as described by Raghavendran *et al*. (2017). Briefly, each experiment was initiated from one colony of the desired yeast strain inoculated in 500-mL baffled flasks containing 100 mL of YPD medium (with 4% glucose) and incubated at 30 °C and 200 rpm (Innova 4430, New Brunswick Scientific, Edison, USA). After 12 h growth,

cultures were transferred to 2-L flasks containing 1 L of sterile diluted molasses (10% TRS) for biomass propagation under static conditions at 30 °C (PsycroTherm, New Brunswick Co., Edison, USA). After total sugar consumption (about 36 h), the cells were centrifuged (3000 rpm for 15 min) and approximately 3.6 g of wet biomass was added to 50-mL polypropylene tubes, previously weighed. The wet biomass was suspended in 2 mL of supernatant from a previous cultivation (free of yeast) plus 6 mL of water, representing the "vat foot" used in the Brazilian 1G ethanol production process in sugarcane biorefineries. At times 0, 2, and 4 h, 9.33 mL of molasses (19.4% TRS) were added to the conical tubes, emulating the fed-batch process. Every 2 h, the tubes were gently shaken to remove the trapped CO_2 and weighed. This was performed during 10 h and the experiment was carried out at 34 °C (PsycroTherm, New Brunswick Co., Edison, USA). After each fermentation cycle, the tubes were left on the bench overnight. In the following day, the tubes were weighed, homogenised, and 1 mL of sample was taken for microbiological analysis (viability and contamination). After that, the tubes were centrifuged (3000 rpm for 15 min) and the supernatant (wine) was stored for HPLC analysis. The pelleted yeast biomass was weighed and treated with 0.5 M H_2SO_4 (to reach pH 2.5) during 1 h. Finally, the tubes were centrifuged (3000 rpm for 15 min) and the acid solution was withdrawn for "vat foot" preparation and starting of the next fermentation cycle. Experiments were performed in duplicate.

5.3.5 Analytical methods

Cell or biomass concentration from shake-flask cultivations was indirectly monitored by Abs_{600} measurements using a spectrophotometer (Genesys 20, Thermo Scientific, Waltham, USA), and directly determined by gravimetry in terms of cell dry mass, according to Olsson and Nielsen (1997). Cell dry mass measurements were performed in triplicates (three determinations for each flask) only at the end of each cultivation. Briefly, 10 mL of culture broth was filtered onto dry, pre-weighted nitrocellulose membranes of 0.45 μm, using a vacuum system. The membranes were then washed with distilled water, dried in a microwave oven at 255 W for 10 min, and cooled down for 15 min in a desiccator, before being weighed again. If more than 30 mg dry mass was present on the filter, the drying and cooling steps were repeated until constant mass. The dry cell mass concentration (X_{DM}) was calculated by dividing the difference between the filter's dry mass after and before filtration by the sample volume.

The pH of shake-flask samples was read using a pHmeter (Digimed DM21, São Paulo, Brazil).

Substrate and extracellular metabolites (sucrose, glucose, fructose, glycerol, and ethanol) had their concentrations determined by High Performance Liquid Chromatography (HPLC) after filtration of the samples through 0.22 μm-pore membranes using a syringe. HPLC analysis was performed using an Accela equipment (Thermo Scientific, Waltham, USA) coupled with a refractive index detector (Waters 2410, Milford, USA) and an Aminex HPX-87H column (Bio-Rad, Hercules, USA). The HPLC separation was conducted at 30 °C with 5 mM (pH 2.42) H_2SO_4 as a mobile phase at a flow rate of 0.6 mL/min. Under such conditions of operation, sucrose and KH_2PO_4 (both components of the SM) leave the column at the same retention time (Appendix V). The determination of sucrose in these samples was thus possible because all inorganic nutrients and vitamins present in the SM are in excess, i.e., the carbon source being the limiting component. This consideration allowed for the quantification of sucrose by subtracting the concentration of the "KH_2PO_4" component from the concentration of the "sucrose + KH_2PO_4" component. The concentration of KH_2PO_4 was easily determined considering that, in the last 4 samples of all cultivations, the area of the "sucrose + KH_2PO_4" peaks remained virtually constant.

5.3.6 Calculation of physiological parameters

Data obtained from shake-flask cultivations were used to calculate physiological parameters, such as μ_{max}, biomass ($Y_{X/S}$) and product ($Y_{P/S}$) yields on substrate, maximum specific substrate consumption rates ($q_{S,\,max}$), and maximum specific product formation rates ($q_{P,\,max}$), as follows.

μ_{max} values were calculated as the slope of the straight line of an Ln (Abs_{600}) *vs.* time plot generated using at least six data points within the exponential growth phase.

$Y_{X/S}$ and $Y_{P/S}$ were determined using data from the exponential growth phase ($Y_{X/S}^{exp}$ and $Y_{P/S}^{exp}$; referred to as physiological yields) or data from the initial and final time points ($Y_{X/S}^{global}$ and $Y_{P/S}^{global}$; referred to as process or global yields). Physiological yields were calculated as the absolute value of the slope of the straight line from a X_{DM} *vs.* substrate concentration (S) plot, and a product concentration (P) *vs.* S plot, respectively. For this purpose, S, P, and X_{DM} were plotted against time and the experimental data fitted to a polynomial equation; the fitted concentration values within the exponential growth phase were considered for physiological yield determinations (Appendix VI). Global yields were

obtained by dividing the total amount of biomass ($X_{DM,\ final} - X_{DM,\ initial}$) or product ($P_{final} - P_{initial}$) formed by the total amount of substrate consumed ($S_{initial} - S_{final}$), again using X_{DM}, P, and S fitted values. For the determination of S, we considered all three carbohydrates present in the cultures (sucrose, glucose, and fructose) as hexose-equivalents (Hex Eq). To add sucrose to glucose and fructose, in $g_{Hex\ Eq}$/L, sucrose concentrations were multiplied by 1.052631, because each 342.3 g of sucrose corresponds to 360.3 g of glucose + fructose.

$q_{S,\ max}$ and $q_{P,\ max}$ were calculated as follows: $q_{S,max}\ (g_{substrate}/g_{DM} * h) = -\frac{\mu_{max}}{Y_{x/s}exp}$ and $q_{P,max}\ (g_{product}/g_{DM} * h) = \frac{\mu_{max}}{Y_{x/s}exp} * Y_{P/S}$.

All these values together with averages and mean deviations were calculated using Microsoft Excel.

Data obtained from the mimicked 1G experiment were used to calculate ethanol yields on substrate employing a correction factor for high cell density cultivations, as described by Raghavendran *et al.* (2017). A detailed description of the calculations made can be found in Appendix VII.

5.4 Results and Discussion

The work carried out in this chapter was entirely performed at the Bioprocess and Metabolic Engineering Laboratory (LEMeB), at the School of Food Engineering (FEA)/UNICAMP.

5.4.1 Physiology of *S. cerevisiae* i*SUC2*e in shake-flasks under conditions favouring oxygen transfer

To initiate our studies with the i*SUC2*e strain, we first assessed its physiology under batch growth and compared it with that of a *SUC2* reference strain (CEN.PK113-7D), known for its predominant extracellular sucrose hydrolysis (Basso 2011). For this purpose, we employed shake-flask cultivations using SM supplemented with sucrose, the composition of which was very similar to the one used in the chemostat cultivations performed by Basso *et al.* (2011). Whereas in the latter work a rather anaerobic atmosphere was obtained in the chemostat setup, the experimental system employed here promoted oxygen transfer from the surrounding environment (air) to the cultures (Appendix I), as already discussed in Chapter 4 (section 4.4.3).

The growth profiles displayed by the i*SUC2*e and CEN.PK113-7D strains on sucrose under these conditions (Figure 5.1) resulted in μ_{max} values of 0.30 ± 0.00 h^{-1} and 0.33 ± 0.00 h^{-1}, respectively. A clear longer deceleration phase was observed for i*SUC2*e (4 h *vs*. 2 h for CEN.PK113-7D) (Figure 5.1), presumably due to the lower affinity ($K_{m,\ sucrose}$ ~6 mM ~ 2.1 g/L) of the Agt1p transporter as compared to that of the high-affinity hexose transporters ($K_{m,\ glucose}$, 1 to 2 mM = 0.2 to 0.4 g/L) (Özcan and Johnston 1999), since at this stage sucrose concentrations in the i*SUC2*e cultures were near the K_m value of Agt1p (data not shown). In terms of rates, the i*SUC2*e strain was capable of using the substrate less efficiently, as it displayed a 21% lower specific substrate consumption rate (2.60 ± 0.01 $g_{Hex\ Eq}/g_{DM}$*h) than the CEN.PK113-7D strain (3.28 ± 0.08 $g_{Hex\ Eq}/g_{DM}$*h) (Table 5.2), similar to the reduction encountered in anaerobic batch bioreactors ($q_{s,\ iSUC2e}$ = 2.90 ± 0.13 $g_{Hex\ Eq}/g_{DM}$*h *vs*. $q_{s,\ CEN.PK113\text{-}7D}$ = 3.50 ± 0.04 $g_{Hex\ Eq}/g_{DM}$*h) (Table 5.3).

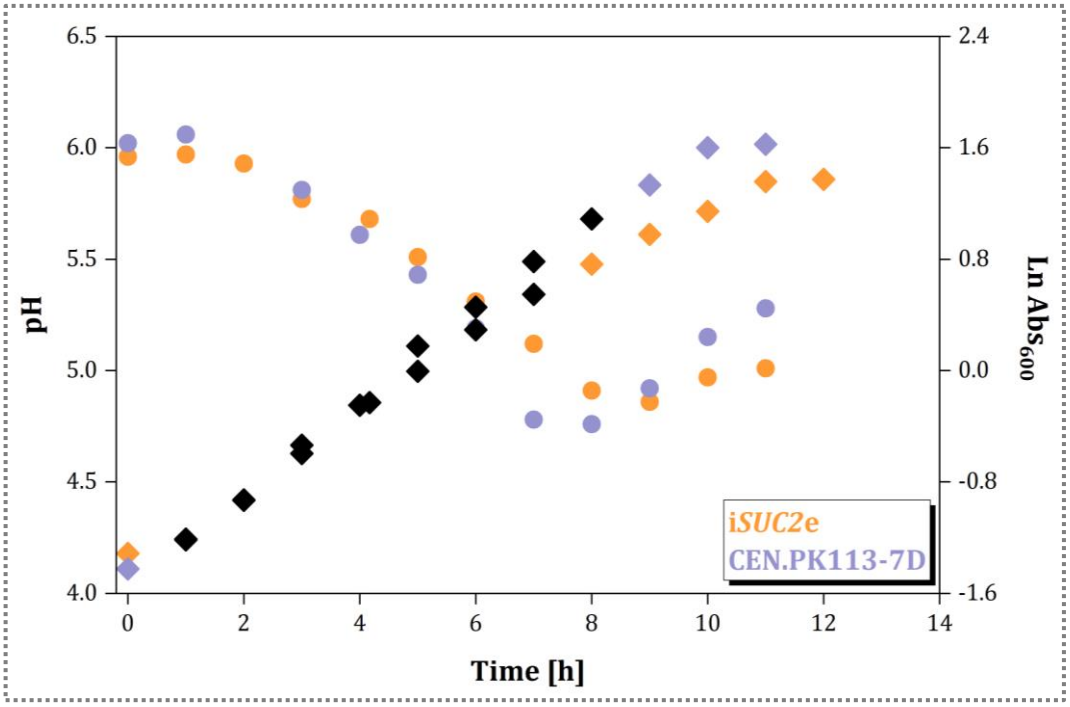

Figure 5.1. Growth and pH profiles of *S. cerevisiae* i*SUC2*e and CEN.PK113-7D during batch cultivations on sucrose under conditions favouring oxygen transfer. Cell concentration was indirectly assessed by measurements of Abs_{600} and expressed as Ln Abs_{600}. Symbols denote as follows: (♦) Ln Abs_{600} (●) pH. The black diamonds correspond to values from the exponential growth phases. Cultivations were carried out in shake-flasks with SM and 20 g/L initial sucrose. One representative dataset of duplicate cultivations is shown.

According to the data reported by Basso *et al*. from anaerobic batch and chemostat cultures of i*SUC2*e performed in bioreactors (Table 5.3), we were expecting a lower accumulation of released hexoses in the broth, a higher ethanol yield on substrate, and a concomitant lower biomass yield than the reference strain, as a result of the relocation of sucrose metabolism. However, this was not what we observed in shake-flask cultivations under conditions favouring oxygen transfer. Monosaccharide levels in the i*SUC2*e cultures (3.3 g/L glucose and 4.6 g/L fructose) were higher than in CEN.PK113-7D's (2.4 g/L glucose and 2.7 g/L fructose), although they appeared at later time points (7-8 h for i*SUC2*e and 2-5 h for CEN.PK113-7D). (Figure 5.2 and Table 5.2). Since sucrose hydrolysis in the i*SUC2*e strain mainly occurs within the intracellular space (Basso *et al.* 2011), we speculate that hexose accumulation at the end of the exponential growth phase of i*SUC2*e is caused by leakage of hexoses from the cytosol to the extracellular space, due to rapid sucrose hydrolysis by intracellular invertase. This, in turn, could be caused by the higher specific sucrose consumption rate inherent to batch cultivations, when cells grow at μ_{max}, in contrast to growth at a dilution rate of 0.10 h^{-1} employed in the chemostat cultivations. Despite this consideration, the i*SUC2*e strain still shows a lower production of released monomers during

anaerobic batch cultivation in bioreactors, when compared to our work (Table 5.3). It is worth pointing out that Basso's data from anaerobic bioreactors were obtained during the third repetitive batch cycle, when the when the kinetic profiles reached some stabilisation, while our data resulted from a sole batch round.

Another intriguing fact regarding the released monosaccharides is the high levels of extracellular glucose (1.9 g/L) present at the beginning of both i*SUC2*e and CEN.PK113-7D cultivations (Figure 5.2). This observation raised a few hypotheses and considerations that are discussed next. 1) Considering that the cells of the inocula were washed twice before inoculation, it would be unlikely that the origin of these levels of glucose comes from these sources; 2) spontaneous (non-biological) sucrose hydrolysis does not occur at pH 6 (Marques *et al.* 2017), which was the initial pH established in our cultivations (Figure 5.1); 3) the sampling procedure used in this work does not eliminate the possibility of small sucrose consumption by the cells between sampling and freezing, due to the action of extracellular invertase. Although care was taken to minimise this issue, the action of extracellular invertase during sampling could potentially explain the initial glucose levels produced in CEN.PK113-7D cultures, but not those observed in cultures of i*SUC2*e; 4) the existence of a low extracellular sucrose hydrolytic activity of unknown identity has been predicted in i*SUC2*e (Basso *et al.* 2011); however, this sole activity should not be responsible for the high levels of glucose observed at t = 0 h.

Concerning the ethanol yield on substrate - the most important parameter related to the iSUC strategy - it remained similar for both strains, either in terms of the physiological (exponential growth phase) or the process (global) yield. Thus, the $Y_{Et/S}^{exp}$ displayed by the i*SUC2*e and reference strains were 0.308 ± 0.003 $g_{Et}/g_{Hex\ Eq}$ and 0.322 ± 0.000 $g_{Et}/g_{Hex\ Eq}$, respectively, whereas the $Y_{Et/S}^{global}$ was 0.329 ± 0.004 $g_{Et}/g_{Hex\ Eq}$ for i*SUC2*e and 0.314 ± 0.002 $g_{Et}/g_{Hex\ Eq}$ for CEN.PK113-7D. As a result, the different ways employed to calculate this parameter led to a difference of only 5% between the strains (Table 5.2). In terms of biomass production, i*SUC2*e also achieved similar $Y_{X/S}^{exp}$ and $Y_{X/S}^{global}$ (0.114 ± 0.000 $g_{DM}/g_{Hex\ Eq}$ and 0.145 ± 0.003 $g_{DM}/g_{Hex\ Eq}$, respectively) to those attained by the reference strain (0.101 ± 0.004 $g_{DM}/g_{Hex\ Eq}$ and 0.141 ± 0.005 $g_{DM}/g_{Hex\ Eq}$, respectively). With the aim of capturing the effects of the i*SUC2*e strategy on a single parameter, and also highlighting any fine difference between the strains, we calculated the ethanol yields on biomass ($Y_{Et/X}$), by dividing $Y_{Et/S}$ by $Y_{X/S}$. (Table 5.2). While the $Y_{Et/X}^{global}$ did not evidence any difference in the fermentation performance of i*SUC2*e and CEN.PK113-7D strains (2.27 ± 0.08 g_{Et}/g_{DM} and 2.22 ± 0.09

g_{Et}/g_{DM}, respectively), the $Y_{Et/X}^{exp}$ suggested some better performance of CEN.PK113-7D (3.20 ± 0.12 g_{Et}/g_{DM}) over the i*SUC2*e strain (2.70 ± 0.02 g_{Et}/g_{DM}). Lastly, we also noticed that the levels of glycerol at the end of the cultivations of i*SUC2*e were substantially higher (0.3 g/L), when compared to that of the reference strain (< 0.1 g/L) (Table 5.2). This hyperproduction of glycerol by i*SUC2*e was not coupled to a higher biomass yield on substrate, which could suggest that part of this glycerol was generated for reasons other than acting as an electron sink for reoxidising NADH produced in biosynthesis.

Another essential role of glycerol is to act as an osmoregulator when *S. cerevisiae* is exposed to a hyperosmotic environment, preventing the outflow of water molecules from the cells (Nevoigt and Stahl 1997). Although osmotically stressed cells accumulate glycerol within the cytosol, there is evidence that substantial amounts of this compound are lost from the cells by facilitated diffusion (Edgley and Brown 1983; Duskova *et al.* 2015). Furthermore, *S. cerevisiae* cells subjected to a hyperosmotic shock exhibit extracellular overproduction of glycerol (Modig *et al.* 2007). Considering that the i*SUC2*e strain was obtained after prolonged adaptation to carbon limitation (Basso *et al.* 2011), once exposed to excess nutrients, the cells might accumulate some glycerol to counterbalance the external osmotic pressure, part of which would eventually diffuse from the cells to the extracellular medium, especially at high growth rates (Olz *et al.* 1993), as is the case during batch growth. However, this hyperproduction of glycerol was not observed in anaerobic batch bioreactors (Basso 2011). Indeed, it has been reported that cells grown anaerobically present an attenuated response to osmotic shock because their higher intrinsic capacity to produce glycerol under such conditions enable them to adapt and recover faster than aerobic-grown cells (Krantz *et al.* 2004). Additional studies would be necessary to investigate whether this trait was indeed acquired by the i*SUC2*e strain during the evolution it was subject to.

The above-mentioned results indicate that during the respiratory-fermentative conditions encountered in these batch cultivations in shake-flasks, in which oxygen transfer is favoured, the i*SUC2*e strain was not able to display its potential to improve ethanol yields on sucrose relative to the reference strain. Since the i*SUC2*e strain was obtained after long-term evolution in anaerobic sucrose-limited chemostats, the presence of oxygen in our experiments might indeed compromise the strain's desired performance.

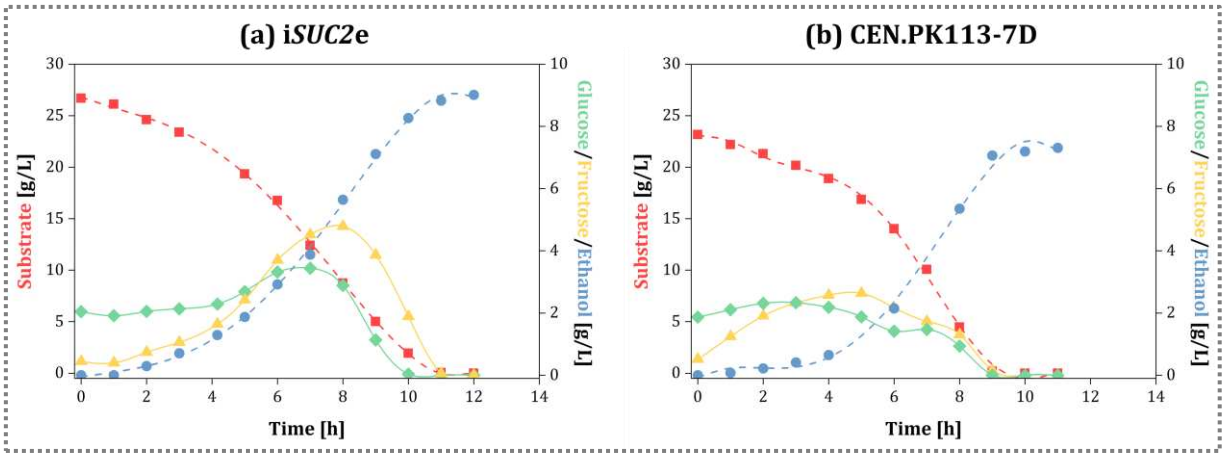

Figure 5.2. Substrate and metabolite profiles of *S. cerevisiae* (a) i*SUC2*e and (b) CEN.PK113-7D during batch cultivations on sucrose under conditions favouring oxygen transfer. Substrate represent the sum of sucrose, glucose, and fructose concentrations in $g_{Hex\ Eq}$/L. Symbols denote as follows: (■) substrate concentration, (♦) glucose concentration, (▲) fructose concentration, (●) ethanol concentration. Dashed lines represent trend lines obtained via polynomial fitting. Cultivations were carried out in shake-flasks with SM and 20 g/L initial sucrose. One representative of duplicate cultivations is shown.

Table 5.2. Physiological data of *S. cerevisiae* i*SUC2*e and CEN.PK113-7D strains grown on sucrose during shake-flask cultivations under different conditions of oxygen availability. Data represent the mean of two experiments and the average deviation.

	High oxygen availability		**Oxygen limitation**
	CEN.PK113-7D	**i*SUC2*e**	**i*SUC2*e**
μ_{max} [h^{-1}]	0.33 ± 0.00	0.30 ± 0.00	0.24 ± 0.01
X_f [g_{DM}/L]	3.4 ± 0.1	4.2 ± 0.1	1.0 ± 0.1
Glu_{max} [$g_{Hex\ Eq}$/L]	2.4 ± 0.0	3.3 ± 0.1	3.2 ± 0.4
Fru_{max} [$g_{Hex\ Eq}$/L]	2.7 ± 0.0	4.6 ± 0.2	4.0 ± 0.1
Gly_f [g_{Gly}/L]	< 0.1	0.3 ± 0.0	0.9 ± 0.0
$Y_{X/S}^{global}$ [$g_{DM}/g_{Hex\ Eq}$]	0.141 ± 0.005	0.145 ± 0.003	0.041 ± 0.003
$Y_{X/S}^{exp}$ [$g_{DM}/g_{Hex\ Eq}$]	0.101 ± 0.004	0.114 ± 0.000	0.078 ± 0.011
$Y_{Et/S}^{global}$ [$g_{Et}/g_{Hex\ Eq}$]	0.314 ± 0.002	0.329 ± 0.004	0.361 ± 0.017
$Y_{Et/S}^{exp}$ [$g_{Et}/g_{Hex\ Eq}$]	0.322 ± 0.000	0.308 ± 0.003	0.295 ± 0.004
$Y_{Et/X}^{global}$ [g_{Et}/g_{DM}]	2.22 ± 0.09	2.27 ± 0.08	8.85 ± 1.07
$Y_{Et/X}^{exp}$ [g_{Et}/g_{DM}]	3.20 ± 0.12	2.70 ± 0.02	3.76 ± 0.59
$q_{S,\ max}$ [$g_{Hex\ Eq}/g_{DM}$*h]	3.28 ± 0.08	2.60 ± 0.01	3.08 ± 0.36
$q_{Et,\ max}$ [g_{Et}/g_{DM}*h]	1.06 ± 0.02	0.80 ± 0.01	0.91 ± 0.12

Y^{global} = Yields calculated based on the initial and final data points.

Y^{exp} = Yields calculated based on data from the exponential growth phase.

Table 5.3. Physiological data of *S. cerevisiae* i*SUC2*e and CEN.PK113-7D strains during anaerobic sucrose-limited chemostat cultivations and batch cultivations on 20 g/L initial sucrose, carried out in bioreactors. The data represent the mean of two experiments and the average deviation. Data extracted from Basso (2011).

	Chemostat cultivation		**Batch cultivation**	
	CEN.PK113-7D	**i*SUC2*e**	**CEN.PK113-7D**	**i*SUC2*e**
μ_{max} [h^{-1}]	0.1	0.1	0.35 ± 0	0.23[a]
Glu_{max} [$g_{Hex\ Eq}$/L]	0.05 ± 0	0.01 ± 0	5	1.5
Fru_{max} [$g_{Hex\ Eq}$/L]	0.11 ± 0.03	0.03 ± 0	8	3
$Y_{X/S}$ [$g_{DM}/g_{Hex\ Eq}$]	0.092 ± 0.001	0.067 ± 0.001	0.100 ± 0.001	0.081 ± 0.004
$Y_{Et/S}$ [$g_{Et}/g_{Hex\ Eq}$]	0.384 ± 0.005	0.427 ± 0.009	0.350 ± 0.004[b]	0.413 ± 0.009[b]
$Y_{Et/X}$ [g_{Et}/g_{DM}]	4.17 ± 0.10[c]	6.37 ± 0.23 [c]	3.50 ± 0.08 [c]	5.10 ± 0.36 [c]
$q_{S,\ max}$ [$g_{Hex\ Eq}/g_{DM}$*h]	1.12 ± 0.01	1.53 ± 0.02	3.50 ± 0.04	2.90 ± 0.13

$q_{Et,\ max}$ [g_{Et}/g_{DM}*h]	0.43 ± 0.01	0.65 ± 0.02	1.23 ± 0.01	1.22 ± 0.06

Cultivations were performed in SM with ammonium sulphate (instead of urea) as the nitrogen source, supplemented with the growth factors ergosterol (10 mg/L) and Tween 80 (420 mg/L). The data from chemostat cultures were obtained during the steady-state at a dilution rate of 0.10 h^{-1}, while those from anaerobic batch cultures were obtained during the third repetitive batch cycle.

[a] Calculated by the author of this thesis based on values from $Y_{X/S}$ and $q_{S,\ max}$.
[b] Yields calculated based on data of the initial and final points (Y^{global}).
[c] Calculated by the author of this thesis based on values from $Y_{Et/S}$ and $Y_{X/S}$.

5.4.2 Physiology of *S. cerevisiae* i*SUC2*e in shake-flasks under conditions minimising oxygen transfer

In view of the results presented above, we wondered whether the availability of oxygen was interfering with i*SUC2e*'s performance during batch growth on sucrose. To verify this possibility, we further submitted the strain to a more anaerobic environment by employing the experimental setup that decreases oxygen transfer from the surroundings to the culture medium (Appendix I).

The effect of a lower oxygen availability on the growth of i*SUC2*e on sucrose resulted in a decrease in μ_{max} from 0.30 ± 0.00 h^{-1} to 0.24 ± 0.01 h^{-1} (Table 5.2), a value that is close to the 0.23 h^{-1} determined by Basso (2011) in anaerobic bioreactors (Table 5.3). Moreover, oxygen limitation also affected the duration of the deceleration phase (5 h *vs*. 4 h under excess oxygen) and led to the presence of residual substrate at the end of the experiment (1.8 g/L fructose) (Figures 5.2 and 5.3). Since all conditions in the two shake-flask setups used here were the same, except for the oxygen availability, these results clearly demonstrate the influence of oxygen availability on the growth of *S. cerevisiae*. Furthermore, they validate the utilisation of our experimental design for anaerobic purposes in shake-flasks.

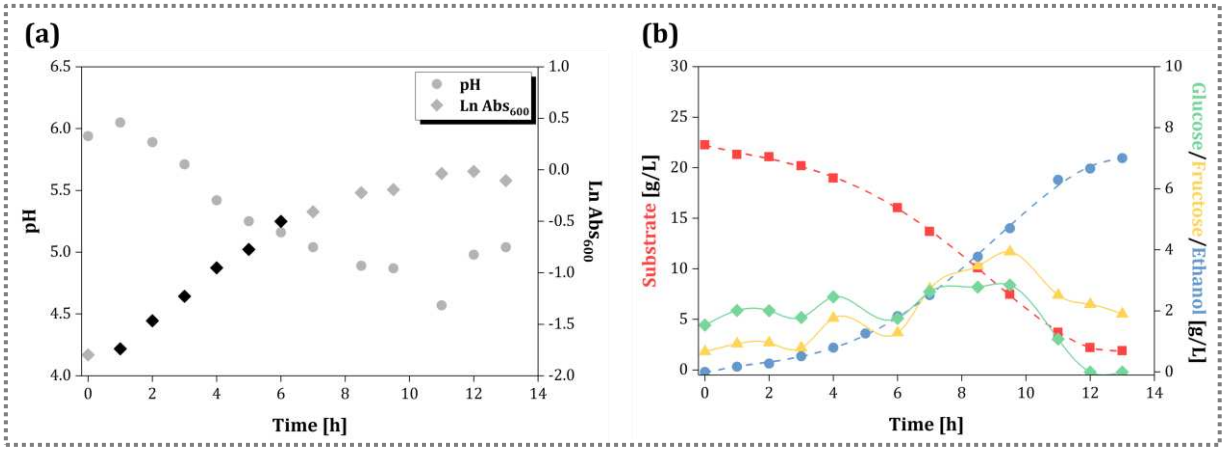

Figure 5.3. Profiles of cell growth and pH (a) and substrate and metabolites (b) of *S. cerevisiae* i*SUC2*e during batch cultivation on sucrose under conditions minimising oxygen transfer. Cell concentration was indirectly assessed by measurements of Abs_{600} and expressed as Ln Abs_{600}. The black diamonds in **(a)** correspond to values from the exponential growth phases. Substrate represent the sum of sucrose, glucose, and fructose concentrations in $g_{Hex\ Eq}$/L. Symbols in **(b)** denote as follows: (■) substrate concentration, (♦) glucose concentration, (▲) fructose concentration, (●) ethanol concentration. Dashed lines represent trend lines obtained via polynomial fitting. Cultivations were carried out in shake-flasks with SM and 20 g/L initial sucrose. One representative of duplicate cultivations is shown.

Although hexose accumulation levels were equivalent under high and low oxygen availability (Table 5.2), the i*SUC2*e strain in the "anaerobic" system achieved a 4 times lower final biomass (1.0 ± 0.1 g_{DM}/L) than in the "aerobic" one (4.2 ± 0.1 g_{DM}/L). This led to a decrease in the biomass yield on substrate under oxygen limitation, when compared to the cultivations with excess oxygen, that was evidenced in the $Y_{X/S}^{exp}$ (0.114 ± 0.000 $g_{DM}/g_{Hex\ Eq}$ *vs.* 0.078 ± 0.011 $g_{DM}/g_{Hex\ Eq}$), but more notably in the $Y_{X/S}^{global}$ (0.145 ± 0.003 $g_{DM}/g_{Hex\ Eq}$ *vs.* 0.041 ± 0.003 $g_{DM}/g_{Hex\ Eq}$) (Table 5.2). Curiously, this reduction in biomass yield was not accompanied by a clear increase in the ethanol yield on substrate, since the physiological parameter remained comparable under high and low oxygen availability (0.308 ± 0.003 $g_{Et}/g_{Hex\ Eq}$ and 0.295 ± 0.004 $g_{Et}/g_{Hex\ Eq}$, respectively), but the global yield in the "anaerobic" condition was 10% higher (0.361 ± 0.017 $g_{Et}/g_{Hex\ Eq}$ *vs.* 0.329 ± 0.004 $g_{Et}/g_{Hex\ Eq}$) (Table 5.2). The differences observed in the global and physiological yields might be ascribed to the shorter exponential growth phase (and longer deceleration phase) encountered when the i*SUC2*e strain was cultivated under oxygen limitation, which means that this phase is not as predominant as in the "aerobic" condition. At this point it would have been important to evaluate the reference strain under this same growth condition, in order to have a better understanding of the influence of oxygen on the performance of i*SUC2*e.

It is widely assumed that strict anaerobic growth of *S. cerevisiae* imposes supplementation of media with anaerobic growth factors (ergosterol and/or Tween 80), since yeast depends on

oxygen for the synthesis of sterols and fatty acids. Our “anaerobic” cultivations were not provided with these components, and we believe that this could have impaired i*SUC2*e’s growth. This possibility relies on the 2-fold decrease in the global biomass yield achieved in our “anaerobic” experiment (0.041 ± 0.003 $g_{DM}/g_{Hex\ Eq}$), when compared to the one determined by Basso in bioreactors (0.081 ± 0.004 $g_{DM}/g_{Hex\ Eq}$). Recently, it has been demonstrated that even in the absence of these anaerobic factors, *S. cerevisiae* is capable of growing under an extremely low oxygen availability, albeit at very low biomass yields on substrate (da Costa *et al.* 2019).

Allied to previous results, a 3-fold increase in glycerol levels was observed in the “anaerobic” setup (0.9 ± 0.00 g/L), as compared to the system favouring oxygen transfer (0.3 ± 0.00 g/L) (Table 5.2). The primary role of glycerol formation during alcoholic fermentation is to maintain the redox balance of the cell, by reoxidising the excess NADH produced during synthesis of biomass and organic acids, to regenerate NAD^+ for glycolysis (van Dijken and Scheffers 1986). Due to the Crabtree effect, formation of glycerol as a by-product in ethanol production is not exclusive to anaerobic conditions, although under aerobiosis it is formed at much lower levels, as our results with i*SUC2*e in the “aerobic” system show. This is because during mixed respiro-fermentative growth the cells allow for partial regeneration of NAD^+ by respiration (Bakker *et al.* 2001). During fermentation of *S. cerevisiae* under anaerobic conditions, it is expected that 4-5% of the carbon source is converted into glycerol (Nissen *et al.* 2000), which in this case would result in the production of ~1 g/L of glycerol, close to the 0.9 g/L produced by i*SUC2*e in our “anaerobic” setup (Table 5.2).

5.4.3 Performance of *S. cerevisiae* i*SUC2*e in a mimicked industrial process with sugarcane molasses

After assessing the i*SUC2*e strain during batch cultivations, we sought to evaluate its performance under conditions resembling the industrial fuel ethanol scenario encountered in sugarcane biorefineries, i.e., fed-batch cultivations in industrial media (sugarcane molasses), high ethanol concentrations, lack of asepsis, and cell recycling with sulfuric acid treatment.

We first evaluated whether i*SUC2*e would grow on a molasses-based medium, by spotting it on a molasses-agar plate in parallel with the *S. cerevisiae* CEN.PK113-7D and PE-2 strains, the latter being one the most widely used industrial strain in the Brazilian fuel ethanol sector. As can be seen in Figure 5.4, i*SUC2*e grew less than the PE-2 strain, and also less than CEN.PK113-7D, which corresponds to i*SUC2*e's parental background. Nevertheless, it did

grow and thus we decided to cultivate i*SUC2*e and its parental strain in the five-cycle fermentation system that emulates the Brazilian 1G fuel ethanol production from sugarcane (Raghavendran *et al.* 2017).

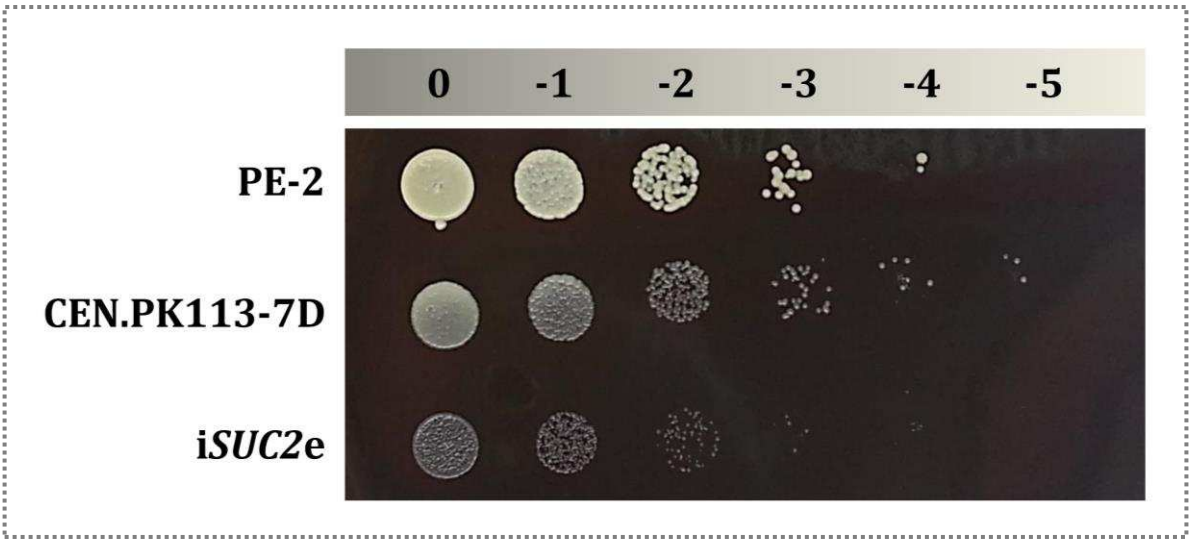

Figure 5.4. Growth of *S. cerevisiae* strains on sugarcane molasses. Cells were pre-grown in solid YPD media and serial dilutions from single colonies were spotted on the plate (dilution increases from left to right), as described in section 5.3.3.

As depicted in Figure 5.5, the CO_2 profiles of the i*SUC2*e and CEN.PK113-7D strains yielded similar results over the cycles, with a slightly (and consistently) higher CO_2 production by the i*SUC2*e strain starting in the 2nd cycle. During the five-cycle process, we also determined the increase or decrease in yeast biomass from one cycle to another and the viability of the cells (Figure 5.6). The fed-batch process was initiated with the same biomass (3.61 ± 0.00 g) and cell viability (98%) for both strains, and ended up with the same biomass level (3.60 ± 0.09 g) and a 7%-point decrease in cell viability (91%) for i*SUC2*e, whereas for strain CEN.PK113-7D we observed a 15% increase in biomass (4.15 ± 0.09 g) and a 4%-point decrease in cell viability (93%).

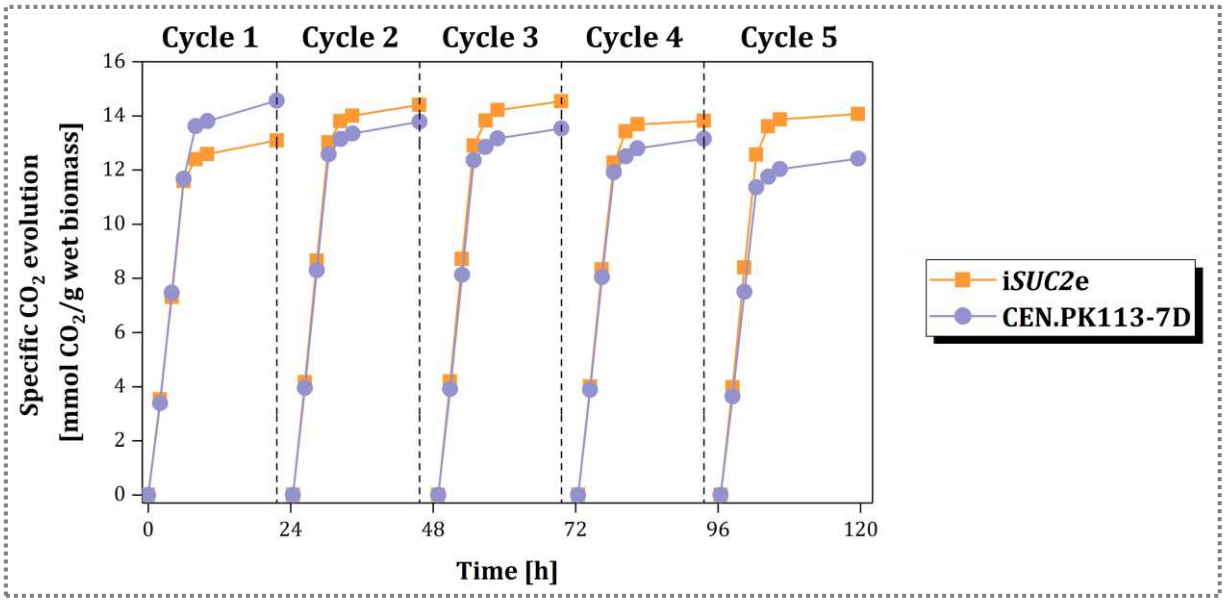

Figure 5.5. CO_2 profiles of *S. cerevisiae* i*SUC2*e and CEN.PK113-7D strains over the five fermentation cycles in the mimicked 1G system on sugarcane molasses. Data represent the kinetics of a typical experiment followed by the mass loss of CO_2 (normalised) over time. One representative dataset of duplicate cultivations is shown.

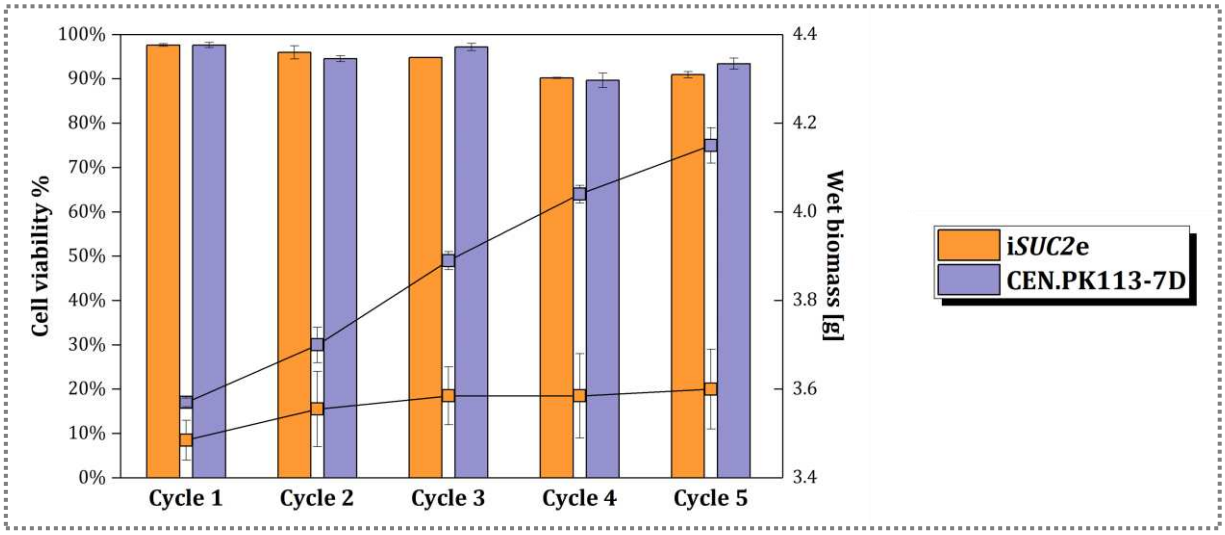

Figure 5.6. Cell viability (columns) and biomass change (lines) of *S. cerevisiae* i*SUC2*e and CEN.PK113-7D strains over the five fermentation cycles in the mimicked 1G system on sugarcane molasses. Data represent the mean of two experiments and the average deviation.

When we analyse the ethanol yields along the cycles (Figure 5.7) – the parameter we were mostly interested at – we noticed high variability between the yields presented by CEN.PK113-7D, while a rather constant value of ~86% of the theoretical maximum was accrued for i*SUC2*e. Moreover, ~2% of the sucrose present in molasses (initially 125 g/L) were left unconsumed by the reference strain at the end of the cycles (data not shown), whereas no residual sucrose was observed in the i*SUC2*e cultures. Despite these differences,

the ethanol produced for both strains at the end of the whole process was virtually the same (Figure 5.7). As had been noticed during the batch cultivations in SM (Table 5.2), the glycerol levels at the end of all fermentation cycles on molasses were between 2 to 11% higher for i*SUC2*e than the reference strain (Figure 5.8). In this case, this difference could be owed to the residual substrate present at the end of every cycle conducted with CEN.PK113-7D. Taken together, the results from this section show minor differences between the i*SUC2*e and CEN.PK113-7D strains during the five fermentation cycles on molasses with cell recycling and acid treatment.

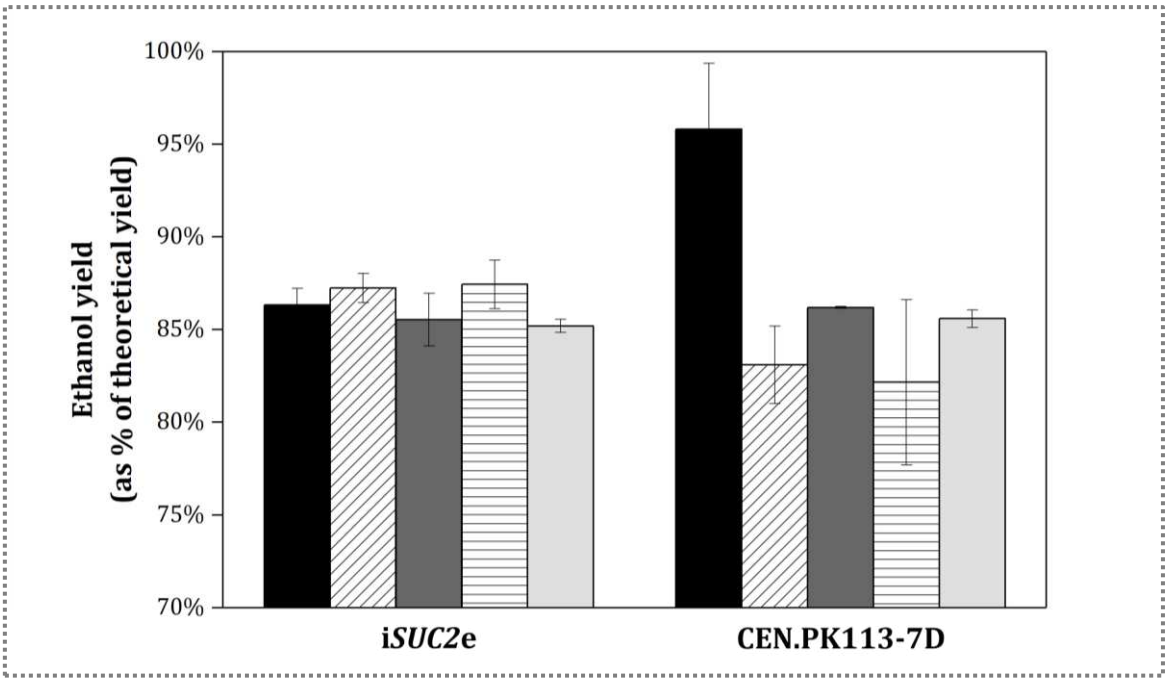

Figure 5.7. Ethanol yield (as a % of the theoretical maximum - 0.511 $g_{Et}/g_{Hex\ Eq}$) for *S. cerevisiae* i*SUC2*e and CEN.PK113-7D strains over the five fermentation cycles in the mimicked 1G system on sugarcane molasses. *Black fill:* cycle 1; *diagonal lines:* cycle 2; *dark grey fill:* cycle 3; *horizontal lines:* cycle 4; *light grey fill:* cycle 5. Data represent the mean of two experiments and the average deviation.

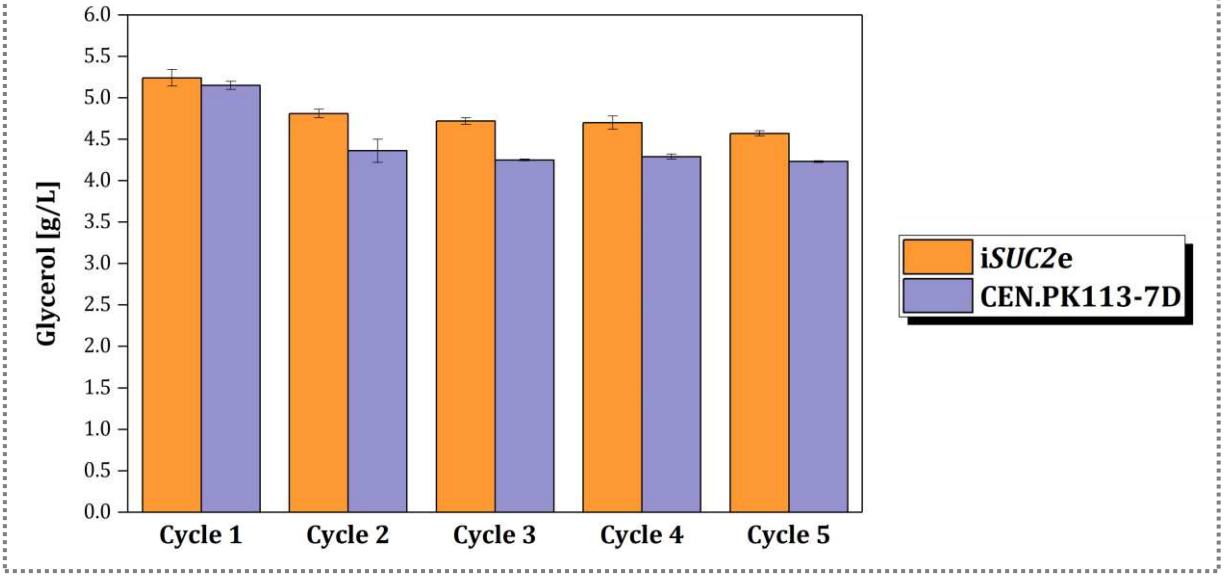

Figure 5.8. Glycerol levels for *S. cerevisiae* i*SUC2*e and CEN.PK113-7D strains at the end of the five fermentation cycles in the mimicked system on sugarcane molasses. Data represent the mean of two experiments and the average deviation.

5.5 Conclusions

In this study, our aim was to take a step forward in the investigation of the i*SUC2*e strain developed by Basso *et al*. (2011), using cultivation conditions closer to the ones employed in industry; firstly, in batch operation with non-limiting resources and, lastly, in a scaled down system mimicking the Brazilian 1G fuel ethanol process in industrial media with sulphuric acid treatment and cell recycling.

During batch cultivation in SM under conditions favouring oxygen transfer, the i*SUC2*e strain was not capable of displaying the benefits acquired during sucrose-limited anaerobic chemostats, as compared to the reference strain. This was accompanied by substantial increase in glycerol levels in the i*SUC2*e cultures relative to CEN.PK113-7D, while the biomass yield remained similar for both strains. The reason behind this hyperproduction of glycerol is still an open question. One of the possibilities we raised was related to the role of glycerol as an osmoprotective molecule in yeast, considering that the i*SUC2*e strain was isolated from a sucrose-limited environment and subsequently cultivated under excess nutrients. The i*SUC2*e strain has now been sequenced and we are in the process of analysing the data. Based on the findings related to the production of glycerol, it would be interesting to see if the strain harbours any mutated gene involved in the regulation of osmotic balance. On the other hand, besides assessing the question at the DNA level, we could also approach it at the RNA, protein, or metabolite level by, for instance: 1) determining the intracellular levels of glycerol over time in i*SUC2*e and CEN.PK113-7D batch cultures on sucrose; 2) by measuring the mRNA levels or the activity of the cytosolic glycerol-3-phosphate dehydrogenase, key enzyme in glycerol synthesis, since its expression is enhanced when cells are osmotically stressed (Nevoigt and Stahl 1997).

We speculated that the presence of oxygen might have affected the strain's fermentation performance, so we further cultivated the i*SUC2*e strain under conditions that minimised oxygen transfer. Oxygen limitation negatively influenced the growth of i*SUC2*e, but overall, it improved the capacity of the strain to produce ethanol, as expected, when compared to the situation of excess oxygen. Since we did not cultivate the reference strain under this same growth condition, we were not able to analyse how the presence of oxygen affected the success of the iSUC strategy.

When the i*SUC2*e and CEN.PK113-7D strains were submitted to five-cycle fed-batch cultivations in molasses with cell recycling and acid treatment, the strains showed minor

differences in terms of fermentation performance and cell viability. These results, in addition to those obtained from shake-flasks cultivations in the presence of oxygen, indicate that the benefits acquired by i*SUC2*e are context-dependent. In other words, the success of metabolic engineering strategies not only requires the correct integration of the pathway/s in the cell, but also the appropriate context to evaluate the desired effect.

We conclude that a successful metabolic engineering strategy established in a proof-of-principle type of work requires some tweaking before it can be implemented in the real industrial process. This is especially challenging in the case of sugarcane-based biorefineries in Brazil, where process conditions vary daily and each of the ~350 units in operation are different from the remaining ones.

5.6 Acknowledgements

We would like to thank Prof. Dr. Thiago Olitta Basso from USP (Brazil) for the fruitful discussions related to this work. We would also like to thank Thaís Granço from Usina Iracema sugarcane mill for kindly providing us sugarcane molasses.

6 GENERAL DISCUSSION

The work explored in this thesis arose as an idea of developing a single yeast strain suitable for an integrated sugarcane-based 1G+2G fuel ethanol process, where the sugar stream is rich in the disaccharides sucrose and cellobiose, a composition that can, in principle, be targeted using proper conditions in upstream operations in a biorefinery. To pursue this concept, there was an initial need to perform extensive work on strain engineering, and due to the difficulties encountered along the way, some decisions were made. The most important one consisted in first addressing sucrose and cellobiose metabolism separately.

In Chapter 2, we extensively discussed the motivations and advantages behind what we named the iSUCCELL yeast, an engineered strain capable of metabolising sucrose and cellobiose via parallel active transport and intracellular hydrolysis of the two sugars. The iSUCCELL strategy arises as an alternative to tackle some of the challenges inherent to 1G and 2G sugarcane-based fuel ethanol production, which encompass aspects related to the process and the yeast chassis.

Since 2016, the use of Genetically Modified Organisms (GMOs) is a reality in Brazilian 2G fuel ethanol plants. One important aspect we did not approach when we envisioned the iSUCCELL concept is related to necessary process modifications when dealing with GMOs. Cell recycling and non-aseptic conditions, for instance, are trademarks in Brazilian 1G ethanol - a process that relies on selected non genetically engineered yeast strains. In a 1G+2G fermentation process conducted by GMOs, these aspects would need to be reconsidered, because the engineered strain could be replaced by wild-type yeasts or other microbial contaminants (dos Santos *et al.* 2016). Furthermore, due to the concerns regarding the potential health risks associated with GMOs, yeast waste would become not suitable for commercialization as dried yeast for animal feeding (a by-product of the 1G ethanol industry), compromising the costs of the process (Basso, Basso and Rocha 2011). Despite these considerations, the market of microbial GMOs in Brazil is in expansion, not only for 2G ethanol – which depends exclusively on these strains – but also for corn ethanol (Jacobus *et al.* 2021), which currently represents ~9% of total Brazilian production (USDA 2021).

In Chapter 3, we experimentally addressed the iCELL component of our iSUCCELL strategy, i.e., the intracellular cellobiose hydrolytic pathway. For this purpose, we employed a well-described cellobiose module from the fungus *Neurospora crassa* (comprising the CDT-1

transporter and the GH1-1 β-glucosidase), but also explored the vast source of unknown biomass-degrading genes in other fungi to screen for new candidates with promising characteristics. Nevertheless, this approach did not bring the results we had expected. First, due to the efforts invested in the cloning process, we were not able to evaluate the functionality of potential cellobiose transporters we had shortlisted in the bioinformatics survey. Instead, for cellobiose uptake we worked with an integrated version of the *N. crassa* CDT-1 gene, widely reported in the scientific literature. Second, although we successfully managed to clone five new putative intracellular β-glucosidases in yeast, the extremely low enzyme activity values measured in cell extracts of *Saccharomyces cerevisiae* questioned us whether these genes were functionally expressed in yeast or whether the proteins were indeed intracellular β-glucosidases, as we had predicted. These questions may have been answered by using a negative control in our enzymatic determinations (empty plasmid) and by also measuring the enzyme activity in the culture supernatant, procedures that we failed to do. In contrast, when we used the *N. crassa* GH1-1 enzyme to handle the intracellular hydrolysis of cellobiose, the enzyme was functional in yeast and achieved high activity values. Third, co-expression of the CDT-1 transporter and the six intracellular β-glucosidases individually did not enable *S. cerevisiae* strains to grow on cellobiose as the sole carbon and energy source. Once gene expression varies according to the way the gene/s of interest is/are delivered in the host (plasmid vector or chromosomal integration) (Ryan *et al.* 2014), the performance of the strain expressing CDT-1 and the active GH-1 enzyme seemed to be affected by limited *CDT-1* copy number, due to expression via genome integration. This, in turn, would not ensure enough transporter molecules in the cell membrane to sustain growth.

To tackle the absence of growth displayed by the engineered iCELL strains on cellobiose, in Chapter 4 we opted to leverage the properties of laboratory evolution for improving kinetic performances in a relatively short period of time. Instead of making additional rational engineering to increase *CDT-1* copy number, we followed this path bearing in mind that improving cellobiose transport capacity alone would be insufficient to enable growth of the strains carrying the enzymes different from GH1-1. After several months of evolution, selection of promising candidates, and characterisation during batch cultivations on cellobiose medium, we ended up with single-cell isolates that grew efficiently on cellobiose, albeit without the capacity to drive ethanol production, an observation that could be attributed to the so-called Kluyver effect (Fukuhara 2003). Further genome sequencing led to the unfortunate discovery of a yeast contaminant - *Meyerozyma guilliermondii* - in at least two of our

evolution experiments, a species that managed to settle in the cellobiose-rich medium due to its intrinsic capacity to utilise cellobiose as carbon source. This finding could not be predicted clearly by visual inspection of the cultures under the microscope or of colonies. Contamination is always a threat in evolution experiments, and despite being the worst outcome we could have ever expected at this stage of the work, it worked as a lesson learned for future evolution attempts in our group. Equally important is the possibility of our physiological and genomic data to contribute to the extremely scarce knowledge on the physiology and metabolism of cellobiose in *M. guilliermondii*, and thus opening new opportunities for non-conventional yeasts in biotechnology.

In Chapter 5, we experimentally addressed the iSUC component of our iSUCCELL strategy, i.e., the intracellular sucrose hydrolytic pathway. As a follow up of the notable benefits presented by an engineered intracellular sucrose-hydrolysing *S. cerevisiae* strain (i*SUC2*e) in sucrose-limited chemostats (Basso *et al.* 2011), we sought to investigate the performance of i*SUC2*e under conditions closer to the ones employed in industry. These conditions comprised a preliminary evaluation of the strain during batch operation on sucrose (carried out in shake-flasks), and then during a fermentation process mimicking the Brazilian sugarcane biorefinery. We conclude with caution that the improvements in fermentation performance observed in sucrose-limited chemostats could not be extrapolated to the conditions applied in this work. The ethanol yield on sugar is the key parameter into the iSUC strategy and the different methodologies we employed for its determination (also discussed by Bermejo *et al.* 2021) did not result in important differences between the i*SUC2*e and reference strains. Furthermore, the glycerol levels produced in both contexts assayed were higher for i*SUC2e* than for CEN.PK113-7D, especially those observed during “aerobic” shake-flask cultivations, an observation that we could not fully explain.

Demonstrating improvements in ethanol production is indeed a difficult task to achieve. Bro *et al*. (2006) already evidenced this limitation when they pursued a metabolic engineering strategy predicted to increase the ethanol yield by 10%, but experimentally this parameter did not change significantly. In a similar fashion, Shiroma *et al*. (2014) achieved less than 3% increase in ethanol yield by blocking mitochondrial degradation in sake yeast, an approach that could not be extended to fuel ethanol strains of the same species (Eliodório *et al.* 2022). In addition to the strategy itself, the resulting ethanol yield can also be influenced by experimental conditions, as noticed in the different yield improvements obtained from anaerobic chemostat cultures of i*SUC2*e (11% increase) and those from anaerobic batch

cultures (18% increase, which exceeded theoretical predictions) (Basso 2011). This difference highlighted the dependence of the context in the assessment of this yield.

7 GENERAL CONCLUSIONS AND FUTURE WORK

The results presented and the lessons learned while this doctoral work was carried out led to the following conclusions:

- The iSUCCELL concept introduced in this work corresponds to an attractive initiative to tackle some of the challenges inherent to 1G and 2G sugarcane-based fuel ethanol processes. Experimental validation in a robust industrial strain and in a real industrial environment is still necessary to consolidate the concept;

- *In silico* prediction, though efficient and time effective to search for novel enzymes with desired characteristics, does not guarantee enzyme functionality when expressed in heterologous hosts;

- Laboratory evolution experiments are continuously threatened by contamination. To prevent this from happening, in addition to good handling practices, visual monitoring of cultures and colonies, and regular storing of frozen stocks, researchers should always check at intervals either the identity of the strains in the cell population using molecular methods or use drug markers to track the presence of the strain of interest;

- The in-house isolated *Meyerozyma guilliermondii* strain grows efficiently on cellobiose in the presence of oxygen and its catabolism occurs using respiratory metabolism;

- The *Saccharomyces cerevisiae* i*SUC2*e strain was not able to display any improvement in fermentation performance either during batch cultivations on sucrose under conditions favouring oxygen transfer or during a mimicked industrial sugarcane-based fermentation process, as compared to the reference strain, which somehow contrasts with the previous results reported by Basso *et al.* (2011), obtained in chemostat cultures.

Along this thesis some paths and questions were opened that can be explored in future studies, as summarised below:

- The four predicted cellobiose transporters from *Aspergillus niger* (AN 3028), *Dichomitus squalens* (DS 104403), and *Podospora anserina* (PA 558 and PA 601),

already assembled in cloning vectors, could be individually expressed in yeast together with the *Neurospora crassa* GH1-1 enzyme, and their transport capacities be assessed by providing the strains with cellobiose. To avoid potential growth limitations, transporter expression should be mediated via multi-copy plasmids;

- Genome assembly of our *M. guilliermondii* strain could be performed by using the genome of strain GXDK6 as reference (Mo *et al.* 2021). These data can be subsequently employed for screening of genes responsible for cellobiose metabolism in this yeast, using a homology-based approach with known cellobiose transporters and β-glucosidases (both intra and extracellular) as queries. To experimentally identify the role of these genes in *M. guilliermondii*, it would be necessary to delete each gene individually and overexpress it via plasmids;

- We were not able to determine if the availability of oxygen negatively affected the performance of i*SUC2*e during batch growth. To address this question, the reference strain (CEN.PK113-7D) could be cultivated in our "anaerobic" shake-flask device and the results compared with the ones obtained with i*SUC2*e. These data, together with the results from the "aerobic" system could provide some insight into this hypothesis. Alternatively, aerobic batch bioreactor cultivations of i*SUC2*e and CENPK113-7D strains could be carried out and compared with the anaerobic batch bioreactor cultivations already performed (Basso 2011);

- The discrepancy observed between our results from "aerobic" shake-flask cultures with i*SUC2*e and those from anaerobic batch bioreactors (Basso 2011), regarding glycerol overproduction in the former situation, could be further investigated focusing on the influence of oxygen in cells exposed to an hyperosmotic medium (Krantz *et al.* 2004). To this end, it would be interesting to evaluate the physiology of i*SUC2*e and the reference strain during aerobic and anaerobic batch and chemostat cultivations, measuring both intracellular and extracellular glycerol contents, and key enzymes, transcripts or metabolites involved in glycerol metabolism. Whole-genome sequencing of i*SUC2*e, already in progress, could also shed some light at the gene level.

REFERENCES

Abdel-Banat BMA, Hoshida H, Ano A *et al.* High-temperature fermentation: how can processes for ethanol production at high temperatures become superior to the traditional process using mesophilic yeast? *Appl Microbiol Biotechnol* 2010;**85**:861–7.

Abreu-Cavalheiro A, Monteiro G. Solving ethanol production problems with genetically modified yeast strains. *Brazilian J Microbiol* 2013;**44**:665–71.

Adams J, Paquin C, Oeller PW *et al.* Physiological characterization of adaptive clones in evolving populations of the yeast, *Saccharomyces cerevisiae*. *Genetics* 1985;**110**:173–85.

Agrawal R, Gaur R, Mathur A *et al.* Improved saccharification of pilot-scale acid pretreated wheat straw by exploiting the synergistic behavior of lignocellulose degrading enzymes. *RSC Adv* 2015;**5**:71462–71.

Agrawal R, Semwal S, Kumar R *et al.* Synergistic enzyme cocktail to enhance hydrolysis of steam exploded wheat straw at pilot scale. *Front Energy Res* 2018;**6**:122.

Arora R, Sharma NK, Kumar S. Valorization of by-products following the biorefinery concept: commercial aspects of by-products of lignocellulosic biomass. *Advances in Sugarcane Biorefinery*. Elsevier Inc., 2018, 163–78.

Atreya ME, Strobel KL, Clark DS. Alleviating product inhibition in cellulase enzyme Cel7A. *Biotechnol Bioeng* 2016;**113**:330–8.

Ávila PF, Forte MBS, Goldbeck R. Evaluation of the chemical composition of a mixture of sugarcane bagasse and straw after different pretreatments and their effects on commercial enzyme combinations for the production of fermentable sugars. *Biomass and Bioenergy* 2018;**116**:180–8.

Bae Y-H, Kang K-H, Jin Y-S *et al.* Molecular cloning and expression of fungal cellobiose transporters and β-glucosidases conferring efficient cellobiose fermentation in *Saccharomyces cerevisiae*. *J Biotechnol* 2014;**169**:34–41.

Baganz F, Hayes A, Marren D *et al.* Suitability of replacement markers for functional analysis studies in *Saccharomyces cerevisiae*. *Yeast* 1997;**13**:1563–73.

Bahia FM, de Almeida GC, de Andrade LP *et al.* Rhamnolipids production from sucrose by engineered *Saccharomyces cerevisiae*. *Sci Rep* 2018;**8**:2905.

Bakker BM, Overkamp KM, van Maris AJA *et al.* Stoichiometry and compartmentation of NADH metabolism in *Saccharomyces cerevisiae*. *FEMS Microbiol Rev* 2001;**25**:15–37.

Basso LC, de Amorim H V, de Oliveira AJ *et al.* Yeast selection for fuel ethanol production in Brazil. *FEMS Yeast Res* 2008;**8**:1155–63.

Basso LC, Basso TO, Rocha SN. Ethanol production in Brazil: the industrial process and its impact on yeast fermentation. In: Bernardes, MAS (ed.). *Biofuel Production-Recent Developments and Prospects*. IntechOpen, 2011, 85–100.

Basso TO. Melhoramento da fermentação alcoólica em *Saccharomyces cerevisiae* por engenharia evolutiva. *Tese (Univ São Paulo, São Paulo)*, 2011. https://www.teses.usp.br/teses/disponiveis/87/87131/tde-14092011-153623/pt-br.php.

Basso TO, Gomes FS, Lopes ML *et al.* Homo- and heterofermentative lactobacilli differently affect sugarcane-based fuel ethanol fermentation. *Antonie van Leeuwenhoek* 2014;**105**:169–77.

Basso TO, de Kok S, Dario M *et al.* Engineering topology and kinetics of sucrose metabolism in *Saccharomyces cerevisiae* for improved ethanol yield. *Metab Eng* 2011;**13**:694–703.

Batista AS, Miletti LC, Stambuk BU. Sucrose fermentation by *Saccharomyces cerevisiae* lacking hexose transport. *J Mol Microbiol Biotechnol* 2004;**8**:26–33.

Beato FB, Bergdahl B, Rosa CA *et al.* Physiology of *Saccharomyces cerevisiae* strains isolated from Brazilian biomes: new insights into biodiversity and industrial applications. *FEMS Yeast Res* 2016;**16**:1–14.

Beckham GT, Johnson CW, Karp EM *et al.* Opportunities and challenges in biological lignin valorization. *Curr Opin Biotechnol* 2016;**42**:40–53.

Benoit I, Culleton H, Zhou M *et al.* Closely related fungi employ diverse enzymatic strategies to degrade plant biomass. *Biotechnol Biofuels* 2015;**8**:1–14.

Berlin A, Maximenko V, Gilkes N *et al.* Optimization of enzyme complexes for lignocellulose hydrolysis. *Biotechnol Bioeng* 2007;**97**:287–96.

Bermejo PM, Badino A, Zamberlan L *et al.* Ethanol yield calculations in biorefineries. *FEMS*

Yeast Res 2021;**21**:1–6.

Bermejo PM, Raghavendran V, Gombert AK. Neither 1G nor 2G fuel ethanol: setting the ground for a sugarcane-based biorefinery using an iSUCCELL yeast platform. *FEMS Yeast Res* 2020;**20**, doi: 10.1093/femsyr/foaa027.

Berthels NJ, Cordero Otero RR, Bauer FF *et al.* Discrepancy in glucose and fructose utilisation during fermentation by *Saccharomyces cerevisiae* wine yeast strains. *FEMS Yeast Res* 2004;**4**:683–9.

Bisson LF, Coons DM, Kruckeberg AL *et al.* Yeast sugar transporters. *Crit Rev Biochem Mol Biol* 1993;**28**:259–308.

Bisswanger H. Enzyme assays. *Perspect Sci* 2014;**1**:41–55.

Bohlin C, Praestgaard E, Baumann MJ *et al.* A comparative study of hydrolysis and transglycosylation activities of fungal β-glucosidases. *Appl Microbiol Biotechnol* 2013;**97**:159–69.

Bordonal R de O, Carvalho JLN, Lal R *et al.* Sustainability of sugarcane production in Brazil. A review. *Agron Sustain Dev* 2018;**38**:13.

Borodina I, Nielsen J. Advances in metabolic engineering of yeast *Saccharomyces cerevisiae* for production of chemicals. *Biotechnol J* 2014;**9**:609–20.

Bro C, Regenberg B, Förster J *et al.* In silico aided metabolic engineering of *Saccharomyces cerevisiae* for improved bioethanol production. *Metab Eng* 2006;**8**:102–11.

Brown CM, Hough JS. Elongation of yeast cells in continuous culture. *Nature* 1965;**206**:676–8.

Brown CM, Johnson B. Influence of the concentration of glucose and galactose on the physiology of *Saccharomyces cerevisiae* in continuous culture. *J Gen Microbiol* 1970;**64**:279–87.

Butler PR, Brown M, Oliver SG. Improvement of antibiotic titers from *Streptomyces* bacteria by interactive continuous selection. *Biotechnol Bioeng* 1996;**49**:185–96.

Çakar PZ, Sauer U, Bailey JE. Metabolic engineering of yeast: the perils of auxotrophic hosts. *Biotechnol Lett* 1999;**21**:611–6.

Çakar ZP, Seker UOS, Tamerler C *et al.* Evolutionary engineering of multiple-stress resistant

Saccharomyces cerevisiae. *FEMS Yeast Res* 2005;**5**:569–78.

Canilha L, Chandel AK, Suzane T *et al.* Bioconversion of sugarcane biomass into ethanol: an overview about composition, pretreatment methods, detoxification of hydrolysates, enzymatic saccharification, and ethanol fermentation. *J Biomed Biotechnol* 2012;**2012**:1–15.

Canilha L, Rodrigues R de CLB, Antunes FAF *et al.* Bioconversion of hemicellulose from sugarcane biomass into sustainable products. In: Chandel AK, da Silva SS (eds.). *Sustainable Degradation of Lignocellulosic Biomass - Techniques, Applications and Commercialization*. IntechOpen, 2013, 15–45.

Carvalho-Netto O V, Bressiani JA, Soriano HL *et al.* The potential of the energy cane as the main biomass crop for the cellulosic industry. *Chem Biol Technol Agric* 2014;**1**.

Casa-Villegas M, Polaina J, Marín-Navarro J. Cellobiose fermentation by *Saccharomyces cerevisiae*: comparative analysis of intra versus extracellular sugar hydrolysis. *Process Biochem* 2018;**75**:59–67.

Caspeta L, Nielsen J. Thermotolerant yeast strains adapted by laboratory evolution show trade-off at ancestral temperatures and preadaptation to other stresses. *mBio* 2015;**6**.

Ceccato-Antonini SR. Conventional and nonconventional strategies for controlling bacterial contamination in fuel ethanol fermentations. *World J Microbiol Biotechnol* 2018;**34**:80.

Chemler JA, Yan Y, Koffas MAG. Biosynthesis of isoprenoids, polyunsaturated fatty acids and flavonoids in *Saccharomyces cerevisiae*. *Microb Cell Fact* 2006;**5**:1–9.

Chen H, Hayn M, Esterbauer H. Purification and characterization of two extracellular β-glucosidases from *Trichoderma reesei*. *Biochim Biophys Acta (BBA)/Protein Struct Mol* 1992;**1121**:54–60.

Chen R. A paradigm shift in biomass technology from complete to partial cellulose hydrolysis: lessons learned from nature. *Bioengineered* 2015;**6**:69–72.

Chomvong K, Kordić V, Li X, Bauer S, Gillespie AE, Ha SJ, Oh EJ, Galazka JM, Jin YS, Cate JH. Overcoming inefficient cellobiose fermentation by cellobiose phosphorylase in the presence of xylose. *Biotechnol Biofuels* 2014;**7**:85.

Chomvong K, Benjamin DI, Nomura DK *et al.* Cellobiose consumption uncouples

extracellular glucose sensing and glucose metabolism in *Saccharomyces cerevisiae*. *mBio* 2017;**8**:e00855-17.

Clontech Laboratories I. *Yeast protocols handbook*, 2009.

Cola P, Procópio DP, Alves AT de C *et al.* Differential effects of major inhibitory compounds from sugarcane-based lignocellulosic hydrolysates on the physiology of yeast strains and lactic acid bacteria. *Biotechnol Lett* 2020;**42**:571–82.

Coppella SJ, Dhurjati P. A detailed analysis of *Saccharomyces cerevisiae* growth kinetics in batch, fed-batch, and hollow-fiber bioreactors. *Chem Eng J* 1989;**41**:27–35.

Couturier M, Tangthirasunun N, Ning X *et al.* Plant biomass degrading ability of the coprophilic ascomycete fungus *Podospora anserina*. *Biotechnol Adv* 2016;**34**:976–83.

Cunha JT, Romaní A, Costa CE *et al.* Molecular and physiological basis of *Saccharomyces cerevisiae* tolerance to adverse lignocellulose-based process conditions. *Appl Microbiol Biotechnol* 2019;**103**:159–75.

da Costa BLV, Basso TO, Raghavendran V *et al.* Anaerobiosis revisited: growth of Saccharomyces cerevisiae under extremely low oxygen availability. *Appl Microbiol Biotechnol* 2018;**102**:2101–16.

da Costa BLV, Raghavendran V, Franco LFM *et al.* Forever panting and forever growing: physiology of *Saccharomyces cerevisiae* at extremely low oxygen availability in the absence of ergosterol and unsaturated fatty acids. *FEMS Yeast Res* 2019;**19**, doi: 10.1093/femsyr/foz054.

Dário MG. Efeito da alteração na captação de sacarose ao metabolismo de *Saccharomyces cerevisiae*. *Tese (Univ São Paulo, São Paulo)*, 2012. https://www.teses.usp.br/teses/disponiveis/87/87131/tde-04062012-114632/pt-br.php.

da Silva NA, Srikrishnan S. Introduction and expression of genes for metabolic engineering applications in *Saccharomyces cerevisiae*. *FEMS Yeast Res* 2012;**12**:197–214.

da Silva RR, da Conceição PJP, de Menezes CLA *et al.* Biochemical characteristics and potential application of a novel ethanol and glucose-tolerant β-glucosidase secreted by *Pichia guilliermondii* G1.2. *J Biotechnol* 2019;**294**:73–80.

da Silveira FA, Fernandes TAR, Bragança CRS *et al.* Isolation of xylose-assimilating yeasts

and optimization of xylitol production by a new *Meyerozyma guilliermondii* strain. *Int Microbiol* 2020;**23**:325–34.

de Andrade RR, Rabelo SC, Maugeri Filho F *et al.* Evaluation of the alcoholic fermentation kinetics of enzymatic hydrolysates from sugarcane bagasse (*Saccharum officinarum* L.). *J Chem Technol Biotechnol* 2013;**88**:1049–57.

Decker CH, Visser J, Schreier P. β-Glucosidase multiplicity from *Aspergillus tubingensis* CBS 643.92: purification and characterization of four β-glucosidases and their differentiation with respect to substrate specificity, glucose inhibition and acid tolerance. *Appl Microbiol Biotechnol* 2001;**55**:157–63.

Della-Bianca B., Gombert AK. Stress tolerance and growth physiology of yeast strains from the Brazilian fuel ethanol industry. *Antonie van Leeuwenhoek* 2013;**104**:1083–95.

Della-Bianca BE, Basso TO, Stambuk BU *et al.* What do we know about the yeast strains from the Brazilian fuel ethanol industry? *Appl Microbiol Biotechnol* 2013;**97**:979–91.

Della-Bianca BE, de Hulster E, Pronk JT *et al.* Physiology of the fuel ethanol strain *Saccharomyces cerevisiae* PE-2 at low pH indicates a context-dependent performance relevant for industrial applications. *FEMS Yeast Res* 2014;**14**:1196–205.

de Vries RP, Visser J. *Aspergillus* enzymes involved in degradation of plant cell wall polysaccharides. *Microbiol Mol Biol Rev* 2001;**65**:497–522.

Dias MO de S, Cavalett O, Maciel Filho R *et al.* Integrated first- and second-generation processes for bioethanol production from sugarcane. In: O'Hara IM, Mundree SG (eds.). *Sugarcane-Based Biofuels and Bioproducts*. John Wiley & Sons, 2016, 313–32.

Dias MOS, Cunha MP, Jesus CDF *et al.* Second generation ethanol in Brazil: can it compete with electricity production? *Bioresour Technol* 2011;**102**:8964–71.

Dias MOS, Junqueira TL, Cavalett O *et al.* Integrated versus stand-alone second generation ethanol production from sugarcane bagasse and trash. *Bioresour Technol* 2012;**103**:152–61.

Dias MOS, Junqueira TL, Cavalett O *et al.* Biorefineries for the production of first and second generation ethanol and electricity from sugarcane. *Appl Energy* 2013;**109**:72–8.

dos Reis TF, de Lima PBA, Parachin NS et al. Identification and characterization of putative

xylose and cellobiose transporters in *Aspergillus nidulans*. *Biotechnol Biofuels* 2016;**9**:204.

dos Santos LV, de Barros Grassi MC, Gallardo JCM *et al.* Second-generation ethanol: the need is becoming a reality. *Ind Biotechnol* 2016;**12**:40–57.

Du J, Yuan Y, Si T *et al.* Customized optimization of metabolic pathways by combinatorial transcriptional engineering. *Nucleic Acids Res* 2012;**40**:e142.

Dunham MJ. Experimental evolution in yeast: a practical guide. *Methods in Enzymology*. Vol 470. 2nd ed. Elsevier Inc, 2010, 487–507.

Duskova M, Borovikova D, Herynkova P *et al.* The role of glycerol transporters in yeast cells in various physiological and stress conditions. *FEMS Microbiol Lett* 2015;**362**:1–8.

Edgley M, Brown AD. Yeast water relations: physiological changes induced by solute stress in *Saccharomyces cerevisiae* and *Saccharomyces rouxii*. *J Gen Microbiol* 1983;**129**:3453–63.

Eliodório KP, de Gois e Cunha GC, White BA *et al.* Blocking mitophagy does not significantly improve fuel ethanol production in bioethanol yeast *Saccharomyces cerevisiae*. *Appl Environ Microbiol* 2022:aem0206821.

Entian KD, Kötter P. 25 Yeast genetic strain and plasmid collections. *Methods Microbiol* 2007;**36**:629–66.

Erdei B, Hancz D, Galbe M *et al.* SSF of steam-pretreated wheat straw with the addition of saccharified or fermented wheat meal in integrated bioethanol production. *Biotechnol Biofuels* 2013;**6**:169.

Eriksen DT, Hsieh PCH, Lynn P *et al.* Directed evolution of a cellobiose utilization pathway in *Saccharomyces cerevisiae* by simultaneously engineering multiple proteins. *Microb Cell Fact* 2013;**12**:61.

Fan L-H, Zhang Z-J, Mei S *et al.* Engineering yeast with bifunctional minicellulosome and cellodextrin pathway for co-utilization of cellulose-mixed sugars. *Biotechnol Biofuels* 2016;**9**:137.

Farwick A, Bruder S, Schadeweg V *et al.* Engineering of yeast hexose transporters to transport D-xylose without inhibition by D-glucose. *Proc Natl Acad Sci U S A*

2014;**111**:5159–5164.

Ferreira R da G, Azzoni AR, Freitas S. Techno-economic analysis of the industrial production of a low-cost enzyme using *E. coli*: the case of recombinant β-glucosidase. *Biotechnol Biofuels* 2018;**11**:81.

Ferreira Silva L, Taciro MK, Raicher G *et al.* Perspectives on the production of polyhydroxyalkanoates in biorefineries associated with the production of sugar and ethanol. *Int J Biol Macromol* 2014;**71**:2–7.

François J, Parrou JL. Reserve carbohydrates metabolism in the yeast *Saccharomyces cerevisiae*. *FEMS Microbiol Rev* 2001;**25**:125–45.

Franken J, Brandt BA, Tai SL *et al.* Biosynthesis of levan, a bacterial extracellular polysaccharide, in the yeast *Saccharomyces cerevisiae*. *PLoS One* 2013;**8**:e77499.

Freer SN. Fermentation and aerobic metabolism of cellodextrins by yeasts. *Appl Environ Microbiol* 1991;**57**:655–9.

Froissard M, Belgareh-Touzé N, Buisson N *et al.* Heterologous expression of a plant uracil transporter in yeast: improvement of plasma membrane targeting in mutants of the Rsp5p ubiquitin protein ligase. *Biotechnol J* 2006;**1**:308–20.

Fukuhara H. The Kluyver effect revisited. *FEMS Yeast Res* 2003;**3**:327–31.

Furlan FF, Filho RT, Pinto FHPB *et al.* Bioelectricity versus bioethanol from sugarcane bagasse: is it worth being flexible? *Biotechnol Biofuels* 2013;**6**.

Galao RP, Scheller N, Alves-Rodrigues I *et al. Saccharomyces cerevisiae*: a versatile eukaryotic system in virology. *Microb Cell Fact* 2007;**6**:32.

Galazka JM, Tian C, Beeson WT *et al.* Cellodextrin transport in yeast for improved biofuel production. *Science (80-)* 2010;**330**:84–6.

Gancedo JM. Yeast carbon catabolite repression. *Microbiol Mol Biol Rev* 1998;**62**:334–61.

Gaspar JM. NGmerge: merging paired-end reads via novel empirically-derived models of sequencing errors. *BMC Bioinformatics* 2018;**19**:536.

Geijer C, Faria-Oliveira F, Moreno AD *et al.* Genomic and transcriptomic analysis of *Candida intermedia* reveals the genetic determinants for its xylose-converting capacity. *Biotechnol Biofuels* 2020;**13**:1–15.

Geijer C, Ledesma-Amaro R, Tomás-Pejó E. Unraveling the potential of non-conventional yeasts in biotechnology. *FEMS Yeast Res* 2022;**22**:foab071.

Gibson DG, Young L, Chuang R-Y *et al.* Enzymatic assembly of DNA molecules up to several hundred kilobases. *Nat Methods* 2009;**6**:343–5.

Gietz RD, Woods RA. Transformation of yeast by lithium acetate/single-stranded carrier DNA/polyethylene glycol method. *Methods Enzymol* 2002;**350**:87–96.

Giuliani F, Grieve A, Rabouille C. Unconventional secretion: a stress on GRASP. *Curr Opin Cell Biol* 2011;**23**:498–504.

Gombert AK, Basso TO. Introdução à engenharia metabólica. *Biotecnologia Industrial - Volume 1*. Blücher. 2020, 281–300.

Gombert AK, van Maris AJA. Improving conversion yield of fermentable sugars into fuel ethanol in 1st generation yeast-based production processes. *Curr Opin Biotechnol* 2015;**33**:81–6.

Gonçalves C, Coelho MA, Salema-Oom M *et al.* Stepwise functional evolution in a fungal sugar transporter family. *Mol Biol Evol* 2016;**33**:352–66.

Gonçalves PM, Griffioen G, Bebelman JP *et al.* Signalling pathways leading to transcriptional regulation of genes involved in the activation of glycolysis in yeast. *Mol Microbiol* 1997;**25**:483–93.

González-Ramos D, Gorter de Vries AR, Grijseels SS *et al.* A new laboratory evolution approach to select for constitutive acetic acid tolerance in *Saccharomyces cerevisiae* and identification of causal mutations. *Biotechnol Biofuels* 2016;**9**:173.

Gramling C. How electric vehicles offered hope as climate challenges grew. *Science News* 2021. https://www.sciencenews.org/article/electric-vehicles-cars-climate-change-challenges-2021 (06 March 2022, date last accessed).

Green MR, Sambrook J. *Molecular Cloning: A Laboratory Manual*. 4th editio. Cold Spring Harbor, New York: Cold Spring Harbor Laboratory Press, 2012.

Groeneveld P, Stouthamer AH, Westerhoff H V. Super life - how and why "cell selection" leads to the fastest-growing eukaryote. *FEBS J* 2009;**276**:254–70.

Guadalupe-Medina V, Metz B, Oud B *et al.* Evolutionary engineering of a glycerol-3-

phosphate *Saccharomyces cerevisiae* strain enables anaerobic growth at high glucose concentrations. *Microb Biotechnol* 2014;**7**:44–53.

Guimarães PMR, Le Berre V, Sokol S *et al.* Comparative transcriptome analysis between original and evolved recombinant lactose-consuming *Saccharomyces cerevisiae* strains. *Biotechnol J* 2008a;**3**:1591–7.

Guimarães PMR, François J, Parrou JL *et al.* Adaptive evolution of a lactose-consuming *Saccharomyces cerevisiae* recombinant. *Appl Environ Microbiol* 2008b;**74**:1748–56.

Guo B, Amano Y, Nozaki K. Improvements in glucose sensitivity and stability of *Trichoderma reesei* β-glucosidase using site-directed mutagenesis. *PLoS One* 2016;**11**:1–12.

Guo B, Sato N, Biely P *et al.* Comparison of catalytic properties of multiple β-glucosidases of *Trichoderma reesei*. *Appl Microbiol Biotechnol* 2016;**100**:4959–68.

Guo Z, Zhang L, Ding Z *et al.* Development of an industrial ethanol-producing yeast strain for efficient utilization of cellobiose. *Enzyme Microb Technol* 2011;**49**:105–12.

Ha S-J, Galazka JM, Joong Oh E *et al.* Energetic benefits and rapid cellobiose fermentation by *Saccharomyces cerevisiae* expressing cellobiose phosphorylase and mutant cellodextrin transporters. *Metab Eng* 2013a;**15**:134–43.

Ha S-J, Galazka JM, Kim SR *et al.* Engineered *Saccharomyces cerevisiae* capable of simultaneous cellobiose and xylose fermentation. *Proc Natl Acad Sci* 2011a;**108**:504–9.

Ha S-J, Kim H, Lin Y *et al.* Single amino acid substitutions in HXT2.4 from *Scheffersomyces stipitis* lead to improved cellobiose fermentation by engineered *Saccharomyces cerevisiae*. *Appl Environ Microbiol* 2013b;**79**:1500–7.

Ha S-J, Kim SR, Kim H *et al.* Continuous co-fermentation of cellobiose and xylose by engineered *Saccharomyces cerevisiae*. *Bioresour Technol* 2013c;**149**:525–31.

Ha S-J, Wei Q, Kim SR *et al.* Cofermentation of cellobiose and galactose by an engineered *Saccharomyces cerevisiae* strain. *Appl Environ Microbiol* 2011b;**77**:5822–5.

Hagman A, Säll T, Compagno C *et al.* Yeast "make-accumulate-consume" life strategy evolved as a multi-step process that predates the whole genome duplication. *PLoS One* 2013;**8**:e68734.

Hara KY, Kobayashi J, Yamada R *et al.* Transporter engineering in biomass utilization by yeast. *FEMS Yeast Res* 2017;**17**:1–14.

Harvey CJB, Tang M, Schlecht U *et al.* HEx: a heterologous expression platform for the discovery of fungal natural products. *Sci Adv* 2018;**4**:eaar5459.

Henrique A. Nissan e IPEN renovam acordo para desenvolver no Brasil elétrico movido a hidrogênio e etanol. *Olhar Digital* 2021. https://olhardigital.com.br/2021/06/16/carros-e-tecnologia/nissan-carro-eletrico-etanol-ipen/ (06 March 2022, date last accesed).

Ho PW, Swinnen S, Duitama J *et al.* The sole introduction of two single-point mutations establishes glycerol utilization in *Saccharomyces cerevisiae* CEN.PK derivatives. *Biotechnol Biofuels* 2017;**10**:1–15.

Hope EA, Amorosi CJ, Miller AW *et al.* Experimental evolution reveals favored adaptive routes to cell aggregation in yeast. *Genetics* 2017;**206**:1153–67.

Hu J, Arantes V, Saddler JN. The enhancement of enzymatic hydrolysis of lignocellulosic substrates by the addition of accessory enzymes such as xylanase: is it an additive or synergistic effect? *Biotechnol Biofuels* 2011;**4**:36.

Hu M-L, Zha J, He L-W *et al.* Enhanced bioconversion of cellobiose by industrial *Saccharomyces cerevisiae* used for cellulose utilization. *Front Microbiol* 2016;**7**:241.

Huang C-J, Lu M-Y, Chang Y-W *et al.* Experimental evolution of yeast for high-temperature tolerance. *Mol Biol Evol* 2018;**35**:1823–39.

IEA, International Energy Agency. *World energy balances: overview*, 2019. https://www.iea.org/reports/world-energy-balances-overview/world (02 March 2022, date last accessed).

Jacobus AP, Gross J, Evans JH *et al. Saccharomyces cerevisiae* strains used industrially for bioethanol production. *Essays Biochem* 2021;**65**:147–61.

Jaiswal D, De Souza AP, Larsen S *et al.* Brazilian sugarcane ethanol as an expandable green alternative to crude oil use. *Nat Clim Chang* 2017;**7**:788–92.

Jansen MLA, Bracher JM, Papapetridis I *et al. Saccharomyces cerevisiae* strains for second-generation ethanol production: from academic exploration to industrial implementation. *FEMS Yeast Res* 2017;**17**:1–20.

Jansen MLA, Diderich JA, Mashego M *et al.* Prolonged selection in aerobic, glucose-limited chemostat cultures of *Saccharomyces cerevisiae* causes a partial loss of glycolytic capacity. *Microbiology* 2005;**151**:1657–69.

Jayakody LN, Liu J-J, Yun EJ *et al.* Direct conversion of cellulose into ethanol and ethyl-β-D-glucoside via engineered *Saccharomyces cerevisiae*. *Biotechnol Bioeng* 2018;**115**:2859–68.

Jessop-Fabre MM, Jakočiūnas T, Stovicek V *et al.* EasyClone-MarkerFree: a vector toolkit for marker-less integration of genes into *Saccharomyces cerevisiae* via CRISPR-Cas9. *Biotechnol J* 2016;**11**:1110–7.

Jin Y-S, Cate JH. Metabolic engineering of yeast for lignocellulosic biofuel production. *Curr Opin Chem Biol* 2017;**41**:99–106.

Jönsson LJ, Alriksson B, Nilvebrant N-O. Bioconversion of lignocellulose: inhibitors and detoxification. *Biotechnol Biofuels* 2013;**6**:16.

Jönsson LJ, Martín C. Pretreatment of lignocellulose: formation of inhibitory by-products and strategies for minimizing their effects. *Bioresour Technol* 2016;**199**:103–12.

Kamble A, Srinivasan S, Singh H. In-silico bioprospecting: finding better enzymes. *Mol Biotechnol* 2019;**61**:53–9.

Kameshwar AKS, Qin W. Metadata analysis of *Phanerochaete chrysosporium* gene expression data identified common CAZymes encoding gene expression profiles involved in cellulose and hemicellulose degradation. *Int J Biol Sci* 2017;**13**:85–99.

Karim AS, Curran KA, Alper HS. Characterization of plasmid burden and copy number in *Saccharomyces cerevisiae* for optimization of metabolic engineering applications. *FEMS Yeast Res* 2013;**13**:107–16.

Kayikci Ö, Nielsen J. Glucose repression in *Saccharomyces cerevisiae*. *FEMS Yeast Res* 2015;**15**:1–8.

Khan NA, Zimmermann FK, Eaton NR. Genetic and biochemical evidence of sucrose fermentation by maltase in yeast. *Mol Gen Genet* 1973;**123**:43–50.

Khattab SMR, Kodaki T. A novel production method for high-fructose glucose syrup from sucrose-containing biomass by a newly isolated strain of osmotolerant *Meyerozyma*

guilliermondii. *J Microbiol Biotechnol* 2016;**26**:675–83.

Kildegaard KR, Hallström BM, Blicher TH *et al.* Evolution reveals a glutathione-dependent mechanism of 3-hydroxypropionic acid tolerance. *Metab Eng* 2014;**26**:57–66.

Kim H, Lee WH, Galazka JM *et al.* Analysis of cellodextrin transporters from *Neurospora crassa* in *Saccharomyces cerevisiae* for cellobiose fermentation. *Appl Microbiol Biotechnol* 2014a;**98**:1087–94.

Kim H, Oh EJ, Lane ST *et al.* Enhanced cellobiose fermentation by engineered *Saccharomyces cerevisiae* expressing a mutant cellodextrin facilitator and cellobiose phosphorylase. *J Biotechnol* 2018;**275**:53–9.

Kim HJ, Lee W-H, Turner TL *et al.* An extra copy of the β-glucosidase gene improved the cellobiose fermentation capability of an engineered *Saccharomyces cerevisiae* strain. *3 Biotech* 2019;**9**:367.

Kim SR, Ha S-J, Wei N *et al.* Simultaneous co-fermentation of mixed sugars: a promising strategy for producing cellulosic ethanol. *Trends Biotechnol* 2012;**30**:274–82.

Kim T-Y, Oh EJ, Jin Y-S *et al.* Improved resistance against oxidative stress of engineered cellobiose-fermenting *Saccharomyces cerevisiae* revealed by metabolite profiling. *Biotechnol Bioprocess Eng* 2014b;**19**:951–7.

Klein-Marcuschamer D, Oleskowicz-Popiel P, Simmons BA *et al.* The challenge of enzyme cost in the production of lignocellulosic biofuels. *Biotechnol Bioeng* 2012;**109**:1083–7.

Klein M, Carrillo M, Xiberras J *et al.* Towards the exploitation of glycerol's high reducing power in *Saccharomyces cerevisiae*-based bioprocesses. *Metab Eng* 2016;**38**:464–72.

Kotyk A, Lapathitis G, Křenková Š. Glucose- and K+ -induced acidification in different yeast species. *Folia Microbiol (Praha)* 1999;**44**:295–8.

Krantz M, Nordlander B, Valadi H *et al.* Anaerobicity prepares *Saccharomyces cerevisiae* cells for faster adaptation to osmotic shock. *Eukaryot Cell* 2004;**3**:1381–90.

Kruckeberg AL. The hexose transporter family of *Saccharomyces cerevisiae*. *Arch Microbiol* 1996;**166**:283–92.

Kupfer DM, Drabenstot SD, Buchanan KL *et al.* Introns and splicing elements of five diverse fungi. *Eukaryot Cell* 2004;**3**:1088–100.

Kurtzman CP. Meyerozyma. *The Yeasts, a Taxonomic Study*. 2011, 621–4.

Kurtzman CP, Fell JW, Boekhout T. Summary of species characteristics. In: Kurtzman CP, Fell JW, Boekhout T (eds.). *The Yeasts, a Taxonomic Study*. Fifth edit. Elsevier, 2011, 223–77.

Kurtzman CP, Robnett CJ. Identification and phylogeny of ascomycetous yeasts from analysis of nuclear large subunit (26S) ribosomal DNA partial sequences. *Antonie van Leeuwenhoek* 1998;**73**:331–71.

Kuyper M, Toirkens MJ, Diderich JA *et al.* Evolutionary engineering of mixed-sugar utilization by a xylose-fermenting *Saccharomyces cerevisiae* strain. *FEMS Yeast Res* 2005;**5**:925–34.

Kuyper M, Winkler AA, van Dijken JP *et al.* Minimal metabolic engineering of Saccharomyces cerevisiae for efficient anaerobic xylose fermentation: a proof of principle. *FEMS Yeast Res* 2004;**4**:655–64.

LaCroix RA, Sandberg TE, O'Brien EJ *et al.* Use of adaptive laboratory evolution to discover key mutations enabling rapid growth of *Escherichia coli* K-12 MG1655 on glucose minimal medium. *Appl Environ Microbiol* 2015;**81**:17–30.

Lagunas R. Sugar transport in *Saccharomyces cerevisiae*. *FEMS Microbiol Rev* 1993;**10**:229–42.

Lapathitis G, Kotyk A. Different sources of acidity in glucose-elicited extracellular acidification in the yeast *Saccharomyces cerevisiae*. *Biochem Mol Biol Int* 1998;**46**:973–8.

Leal MRLV, Galdos M V., Scarpare F V. *et al.* Sugarcane straw availability, quality, recovery and energy use: a literature review. *Biomass and Bioenergy* 2013;**53**:11–9.

Lee SM, Jellison T, Alper HS. Systematic and evolutionary engineering of a xylose isomerase-based pathway in *Saccharomyces cerevisiae* for efficient conversion yields. *Biotechnol Biofuels* 2014;**7**:1–8.

Lennartsson PR, Erlandsson P, Taherzadeh MJ. Integration of the first and second generation bioethanol processes and the importance of by-products. *Bioresour Technol* 2014;**165**:3–8.

Li J, Liu G, Chen M *et al.* Cellodextrin transporters play important roles in cellulase induction in the cellulolytic fungus *Penicillium oxalicum*. *Appl Microbiol Biotechnol* 2013;**97**:10479–88.

Li S, Du J, Sun J *et al.* Overcoming glucose repression in mixed sugar fermentation by co-expressing a cellobiose transporter and a β-glucosidase in *Saccharomyces cerevisiae*. *Mol Biosyst* 2010;**6**:2129–32.

Lian J, Bao Z, Hu S *et al.* Engineered CRISPR/Cas9 system for multiplex genome engineering of polyploid industrial yeast strains. *Biotechnol Bioeng* 2018;**115**:1630–5.

Lian J, HamediRad M, Zhao H. Advancing metabolic engineering of *Saccharomyces cerevisiae* using the CRISPR/Cas system. *Biotechnol J* 2018;**13**:1–11.

Liao Y, Koelewijn S-F, Van den Bossche G *et al.* A sustainable wood biorefinery for low-carbon footprint chemicals production. *Science (80-)* 2020;**367**:1385–90.

Lin Y, Chomvong K, Acosta-Sampson L *et al.* Leveraging transcription factors to speed cellobiose fermentation by *Saccharomyces cerevisiae*. *Biotechnol Biofuels* 2014;**7**:126.

Lino FS de O, Basso TO, Sommer MOA. A synthetic medium to simulate sugarcane molasses. *Biotechnol Biofuels* 2018;**11**:221.

Liu E, Hu Y. Construction of a xylose-fermenting *Saccharomyces cerevisiae* strain by combined approaches of genetic engineering, chemical mutagenesis and evolutionary adaptation. *Biochem Eng J* 2010;**48**:204–10.

Liu G, Zhang J, Bao J. Cost evaluation of cellulase enzyme for industrial-scale cellulosic ethanol production based on rigorous Aspen Plus modeling. *Bioprocess Biosyst Eng* 2016;**39**:133–40.

Liu J-J, Zhang G-C, Oh EJ *et al.* Lactose fermentation by engineered *Saccharomyces cerevisiae* capable of fermenting cellobiose. *J Biotechnol* 2016;**234**:99–104.

Liu W, Tang D, Shi R *et al.* Efficient production of S-adenosyl-L-methionine from DL-methionine in metabolic engineered *Saccharomyces cerevisiae*. *Biotechnol Bioeng* 2019;**116**:3312–23.

Locher G, Hahnemann U, Sonnleitner B *et al.* Automatic bioprocess control. 4. A prototype batch of *Saccharomyces cerevisiae*. *J Biotechnol* 1993;**29**:57–74.

Lõoke M, Kristjuhan K, Kristjuhan A. Extraction of genomic DNA from yeasts for PCR-based applications. *Biotechniques* 2011;**50**:325–8.

Lopes ML, Paulillo SC de L, Godoy A *et al.* Ethanol production in Brazil: a bridge between science and industry. *Brazilian J Microbiol* 2016;**47**:64–76.

Lopes MR, Lara CA, Moura MEF *et al.* Characterisation of the diversity and physiology of cellobiose-fermenting yeasts isolated from rotting wood in Brazilian ecosystems. *Fungal Biol* 2018;**122**:668–76.

López MF, Dietz S, Grunze N *et al.* The sugar porter gene family of *Laccaria bicolor*: function in ectomycorrhizal symbiosis and soil-growing hyphae. *New Phytol* 2008;**180**:365–78.

Losordo Z, McBride J, Van Rooyen J *et al.* Cost competitive second generation ethanol production from hemicellulose in a Brazilian sugarcane biorefinery. *Biofuels, Bioprod Biorefining* 2016;**10**:589–602.

Lowry OH, Rosebrough NJ, Farr AL *et al.* Protein measurement with the Folin phenol reagent. *J Biol Chem* 1951;**193**:265–75.

Luttik MAH, Kötter P, Salomons FA *et al.* The *Saccharomyces cerevisiae* ICL2 gene encodes a mitochondrial 2-methylisocitrate lyase involved in propionyl-coenzyme a metabolism. *J Bacteriol* 2000;**182**:7007–13.

Lynd LR, Liang X, Biddy MJ *et al.* Cellulosic ethanol: status and innovation. *Curr Opin Biotechnol* 2017;**45**:202–11.

Lynd LR, Weimer PJ, van Zyl WH *et al.* Microbial cellulose utilization: fundamentals and biotechnology microbial cellulose utilization: fundamentals and biotechnology. *Microbiol Mol Biol Rev* 2002;**66**:506–77.

Machida M, Ohtsuki I, Fukui S *et al.* Nucleotide sequences of *Saccharomycopsis fibuligera* genes for extracellular β-glucosidases as expressed in *Saccharomyces cerevisiae*. *Appl Environ Microbiol* 1988;**54**:3147–55.

MacRelli S, Mogensen J, Zacchi G. Techno-economic evaluation of 2nd generation bioethanol production from sugar cane bagasse and leaves integrated with the sugar-based ethanol process. *Biotechnol Biofuels* 2012;**5**:22.

Madeira-Jr JV, Gombert AK. Towards high-temperature fuel ethanol production using *Kluyveromyces marxianus*: on the search for plug-in strains for the Brazilian sugarcane-based biorefinery. *Biomass and Bioenergy* 2018;**119**:217–28.

Maiorella BL, Blanch HW, Wilke CR *et al.* Economic evaluation of alternative ethanol fermentation processes. Introduction. *Biotechnol Bioeng* 2009;**104**:419–43.

Mans R, Daran J-MG, Pronk JT. Under pressure: evolutionary engineering of yeast strains for improved performance in fuels and chemicals production. *Curr Opin Biotechnol* 2018;**50**:47–56.

Mariano AP, Dias MOS, Junqueira TL *et al.* Utilization of pentoses from sugarcane biomass: techno-economics of biogas vs. butanol production. *Bioresour Technol* 2013;**142**:390–9.

Marques WL, Mans R, Henderson RK *et al.* Combined engineering of disaccharide transport and phosphorolysis for enhanced ATP yield from sucrose fermentation in *Saccharomyces cerevisiae*. *Metab Eng* 2018a;**45**:121–33.

Marques WL, Mans R, Marella ER *et al.* Elimination of sucrose transport and hydrolysis in *Saccharomyces cerevisiae*: a platform strain for engineering sucrose metabolism. *FEMS Yeast Res* 2017;**17**:1–11.

Marques WL, Raghavendran V, Stambuk BU *et al.* Sucrose and *Saccharomyces cerevisiae*: a relationship most sweet. *FEMS Yeast Res* 2016;**16**:1–16.

Marques WL, van der Woude LN, Luttik MAH *et al.* Laboratory evolution and physiological analysis of Saccharomyces cerevisiae strains dependent on sucrose uptake via the *Phaseolus vulgaris* Suf1 transporter. *Yeast* 2018b;**35**:639–52.

Matsakas L, Raghavendran V, Yakimenko O *et al.* Lignin- first biomass fractionation using a hybrid organosolv – steam explosion pretreatment technology improves the saccharification and fermentability of spruce biomass. *Bioresour Technol* 2019;**273**:521–8.

McBride JE, Zietsman JJ, van Zyl WH *et al.* Utilization of cellobiose by recombinant β-glucosidase-expressing strains of *Saccharomyces cerevisiae*: characterization and evaluation of the sufficiency of expression. *Enzyme Microb Technol* 2005;**37**:93–101.

Meyrial V, Delgenes JP, Moletta R *et al.* Xylitol production from D-xylose by *Candida guillermondii*: fermentation behaviour. *Biotechnol Lett* 1991;**13**:281–6.

Miedes E, Vanholme R, Boerjan W *et al.* The role of the secondary cell wall in plant resistance to pathogens. *Front Plant Sci* 2014;**5**:358.

Milanez AY, Nyko D, Valente MS *et al.* De promessa a realidade: como o etanol celulósico pode revolucionar a indústria da cana-de-açúcar - uma avaliação do potencial competitivo e sugestões de política pública. *Biocombustíveis BNDES Setorial* 2015;**41**:237–94.

Mo X, Cai X, Hui Q *et al.* Whole genome sequencing and metabolomics analyses reveal the biosynthesis of nerol in a multi-stress-tolerant *Meyerozyma guilliermondii* GXDK6. *Microb Cell Fact* 2021;**20**:4.

Modig T, Granath K, Adler L *et al.* Anaerobic glycerol production by *Saccharomyces cerevisiae* strains under hyperosmotic stress. *Appl Microbiol Biotechnol* 2007;**75**:289–96.

Moreno AD, Carbone A, Pavone R *et al.* Evolutionary engineered *Candida intermedia* exhibits improved xylose utilization and robustness to lignocellulose-derived inhibitors and ethanol. *Appl Microbiol Biotechnol* 2019;**103**:1405–16.

Moreno AD, Tellgreen-Roth C, Soler L *et al.* Complete genome sequences of the xylose-fermenting Candida intermedia strains CBS 141442 and PYCC 4715. *Genome Announc* 2017;**5**:e00138-17.

Moreno AD, Tomás-Pejó E, Olsson L *et al.* Candida intermedia CBS 141442: a novel glucose/xylose co-fermenting isolate for lignocellulosic bioethanol production. *Energies* 2020;**13**:5363.

Nan H, Seo S-O, Oh EJ *et al.* 2,3-Butanediol production from cellobiose by engineered *Saccharomyces cerevisiae*. *Appl Microbiol Biotechnol* 2014;**98**:5757–64.

Nandy SK, Srivastava RK. A review on sustainable yeast biotechnological processes and applications. *Microbiol Res* 2018;**207**:83–90.

Nevoigt E, Stahl U. Osmoregulation and glycerol metabolism in the yeast *Saccharomyces cerevisiae*. *FEMS Microbiol Rev* 1997;**21**:231–41.

Nijland JG, Li X, Shin HY *et al.* Efficient, D-glucose insensitive, growth on D-xylose by an evolutionary engineered *Saccharomyces cerevisiae strain*. *FEMS Yeast Res* 2019;**19**.

Nissen TL, Hamann CW, Kielland-Brandt MC *et al.* Anaerobic and aerobic batch cultivations of *Saccharomyces cerevisiae* mutants impaired in glycerol synthesis. *Yeast* 2000;**16**:463–74.

Njokweni AP, Rose SH, van Zyl WH. Fungal β-glucosidase expression in *Saccharomyces cerevisiae*. *J Ind Microbiol Biotechnol* 2012;**39**:1445–52.

Nogueira KMV, de Paula RG, Antoniêto ACC *et al.* Characterization of a novel sugar transporter involved in sugarcane bagasse degradation in *Trichoderma reesei*. *Biotechnol Biofuels* 2018;**11**:84.

Nombela C, Gil C, Chaffin WLJ. Non-conventional protein secretionin yeast. *Trends Microbiol* 2006;**14**:15–21.

Oh EJ, Jin Y-S. Engineering of *Saccharomyces cerevisiae* for efficient fermentation of cellulose. *FEMS Yeast Res* 2020;**20**, doi: 10.1093/femsyr/foz089.

Oh EJ, Skerker JM, Kim SR *et al.* Gene amplification on demand accelerates cellobiose utilization in engineered *Saccharomyces cerevisiae*. *Appl Environ Microbiol* 2016;**82**:3631–9.

Olsson L, Nielsen J. On-line and in situ monitoring of biomass in submerged cultivations. *Trends Biotechnol* 1997;**15**:517–22.

Olz R, Larsson K, Adler L *et al.* Energy flux and osmoregulation of *Saccharomyces cerevisiae* grown in chemostats under NaCl stress. *J Bacteriol* 1993;**175**:2205–13.

Ostergaard S, Olsson L, Nielsen J. Metabolic engineering of *Saccharomyces cerevisiae*. *Microbiol Mol Biol Rev* 2000;**64**:34–50.

Oud B, Guadalupe-Medina V, Nijkamp JF *et al.* Genome duplication and mutations in ACE2 cause multicellular, fast-sedimenting phenotypes in evolved *Saccharomyces cerevisiae*. *Proc Natl Acad Sci U S A* 2013;**110**:e4223–e4231 pnas.

Özcan S, Johnston M. Function and regulation of yeast hexose transporters. *Microbiol Mol Biol Rev* 1999;**63**:554–69.

Papon N, Boretsky YR, Courdavault V *et al.* Genetic manipulation of *Meyerozyma guilliermondii*. In: van den Berg MA, Maruthachalam K (eds.). *Genetic Transformation Systems in Fungi, Volume 2*. Springer, Cham, 2015, 245–62.

Papon N, Savini V, Lanoue A *et al. Candida guilliermondii*: biotechnological applications, perspectives for biological control, emerging clinical importance and recent advances in genetics. *Curr Genet* 2013;**59**:73–90.

Parisutham V, Chandran SP, Mukhopadhyay A *et al.* Intracellular cellobiose metabolism and its applications in lignocellulose-based biorefineries. *Bioresour Technol* 2017;**239**:496–506.

Patyshakuliyeva A, de Vries RP. Biodegradation of carbohydrates during the formation of *Agaricus bisporus* compost. In: Savoie JM, Foulonge-Oriol M, Largeteau M, et al. (eds.). *Proceedings of the 7th International Conference on Mushroom Biology and Mushroom Products (ICMBMP7)*. 2011, 197–202.

Paulino de Souza J, Dias do Pradro C, Eleutherio ECA *et al.* Improvement of Brazilian bioethanol production - Challenges and perspectives on the identification and genetic modification of new strains of *Saccharomyces cerevisiae* yeasts isolated during ethanol process. *Fungal Biol* 2018;**122**:583–91.

Pereira FB, Romaní A, Ruiz HA *et al.* Industrial robust yeast isolates with great potential for fermentation of lignocellulosic biomass. *Bioresour Technol* 2014;**161**:192–9.

Pereira SC, Maehara L, Machado CMM *et al.* 2G ethanol from the whole sugarcane lignocellulosic biomass. *Biotechnol Biofuels* 2015;**8**:44.

Perli T, Moonen DPI, van den Broek M *et al.* Adaptive laboratory evolution and reverse engineering of single-vitamin prototrophies in *Saccharomyces cerevisiae*. Druzhinina IS (ed.). *Appl Environ Microbiol* 2020;**86**:1–23.

Petti CA. Detection and identification of microorganisms by gene amplification and sequencing. *Clin Infect Dis* 2007;**44**:1108–14.

Podolsky IA, Seppälä S, Xu H *et al.* A SWEET surprise: anaerobic fungal sugar transporters and chimeras enhance sugar uptake in yeast. *Metab Eng* 2021;**66**:137–47.

Polizeli M de LTM, Somera AF, de Lucas RC *et al.* Enzymes involved in the biodegradation of sugarcane biomass: challenges and perspectives. In: Buckeridge MS, De Souza AP (eds.). *Advances of Basic Science for Second Generation Bioethanol from Sugarcane*. Springer, Cham, 2017, 55–79.

Pryor SW, Nahar N. Deficiency of cellulase activity measurements for enzyme evaluation.

Appl Biochem Biotechnol 2010;**162**:1737–50.

Qing Q, Wyman CE. Supplementation with xylanase and β-xylosidase to reduce xylo-oligomer and xylan inhibition of enzymatic hydrolysis of cellulose and pretreated corn stover. *Biotechnol Biofuels* 2011;**4**:18.

Rabelo SC, Carrere H, Maciel Filho R *et al.* Production of bioethanol, methane and heat from sugarcane bagasse in a biorefinery concept. *Bioresour Technol* 2011;**102**:7887–95.

Ragauskas AJ, Beckham GT, Biddy MJ *et al.* Improving lignin processing in the biorefinery lignin valorization: improving lignin processing in the biorefinery. *Science (80-)* 2014;**344**, DOI: 10.1126/science.1246843.

Raghavendran V, Basso TP, da Silva JB *et al.* A simple scaled down system to mimic the industrial production of first generation fuel ethanol in Brazil. *Antonie van Leeuwenhoek* 2017;**110**:971–83.

Rajasree KP, Mathew GM, Pandey A *et al.* Highly glucose tolerant β-glucosidase from *Aspergillus unguis*: NII 08123 for enhanced hydrolysis of biomass. *J Ind Microbiol Biotechnol* 2013;**40**:967–75.

Rebnegger C, Vos T, Graf AB *et al. Pichia Pastoris* exhibits high viability and a low maintenance energy requirement at near-zero specific growth rates. *Appl Environ Microbiol* 2016;**82**:4570–83.

Reis VR, Bassi APG, da Silva JCG *et al.* Characteristics of *Saccharomyces cerevisiae* yeasts exhibiting rough colonies and pseudohyphal morphology with respect to alcoholic fermentation. *Brazilian J Microbiol* 2013;**44**:1121–31.

RFA, Renewable Fuels Association. *Annual world fuel ethanol production*, 2021. https://ethanolrfa.org/markets-and-statistics/annual-ethanol-production (06 March 2022, date last accessed).

Riou C, Salmon JM, Vallier MJ *et al.* Purification, characterization, and substrate specificity of a novel highly glucose-tolerant β-glucosidase from *Aspergillus oryzae*. *Appl Environ Microbiol* 1998;**64**:3607–14.

Ro DK, Paradise EM, Quellet M *et al.* Production of the antimalarial drug precursor artemisinic acid in engineered yeast. *Nature* 2006;**440**:940–3.

Rodrigues AC, Haven MØ, Lindedam J *et al.* Celluclast and Cellic® CTec2: saccharification/fermentation of wheat straw, solid-liquid partition and potential of enzyme recycling by alkaline washing. *Enzyme Microb Technol* 2015;**79**–**80**:70–7.

Rodrigues CIS, Della-Bianca BE, Gombert AK. μ_{max} of *Saccharomyces cerevisiae*: so often used, so seldom put into perspective. *Res Sq* 2021, doi: 10.21203/rs.3.rs-182823/v1.

Rodríguez C, Flores C-L. Mutations in GAL2 or GAL4 alleviate catabolite repression produced by galactose in *Saccharomyces cerevisiae*. *Enzyme Microb Technol* 2000;**26**:748–55.

Rodríguez ME, Lopes CA, Van Broock M *et al.* Screening and typing of Patagonian wine yeasts for glycosidase activities. *J Appl Microbiol* 2004;**96**:84–95.

Romaní A, Pereira F, Johansson B *et al.* Metabolic engineering of *Saccharomyces cerevisiae* ethanol strains PE-2 and CAT-1 for efficient lignocellulosic fermentation. *Bioresour Technol* 2015;**179**:150–8.

Ryan OW, Skerker JM, Maurer MJ *et al.* Selection of chromosomal DNA libraries using a multiplex CRISPR system. *Elife* 2014;**3**:e03703.

Rytioja J, Hildén K, Mäkinen S *et al.* Saccharification of lignocelluloses by carbohydrate active enzymes of the white rot fungus *Dichomitus squalens*. Berrin J-G (ed.). *PLoS One* 2015;**10**:e0145166.

Sadie CJ, Rose SH, den Haan R *et al.* Co-expression of a cellobiose phosphorylase and lactose permease enables intracellular cellobiose utilisation by *Saccharomyces cerevisiae*. *Appl Microbiol Biotechnol* 2011;**90**:1373–80.

Sanchez RG, Karhumaa K, Fonseca C *et al.* Improved xylose and arabinose utilization by an industrial recombinant *Saccharomyces cerevisiae* strain using evolutionary engineering. *Biotechnol Biofuels* 2010;**3**:13.

Santos E, Rodriguez L, Elorza MV *et al.* Uptake of sucrose by *Saccharomyces cerevisiae*. *Arch Biochem Biophys* 1982;**216**:652–60.

Sen A, Acosta-Sampson L, Alvaro CG *et al.* Internalization of heterologous sugar transporters by endogenous α-arrestins in the yeast *Saccharomyces cerevisiae*. *Appl Environ Microbiol* 2016;**82**:7074–85.

Shaw AJ, Lam FH, Hamilton M *et al.* Metabolic engineering of microbial competitive advantage for industrial fermentation processes. *Science (80-)* 2016;**353**:583–6.

Shiroma S, Jayakody LN, Horie K *et al.* Enhancement of ethanol fermentation in *Saccharomyces cerevisiae* sake yeast by disrupting mitophagy function. *Appl Environ Microbiol* 2014;**80**:1002–12.

Shkil H, Stoica L, Dmytruk K *et al.* Bioelectrochemical detection of L-lactate respiration using genetically modified *Hansenula polymorpha* yeast cells overexpressing flavocytochrome b2. *Bioelectrochemistry* 2009;**76**:175–9.

Sidana A, Kaur S, Yadav SK. Assessment of the ability of *Meyerozyma guilliermondii* P14 to produce second-generation bioethanol from giant reed (*Arundo donax*) biomass. *Biomass Convers Biorefinery* 2022.

Silva C. Carro híbrido a etanol será "jabuticaba for export", diz presidente da Volkswagen. *O Estado de São Paulo* 2021. https://economia.estadao.com.br/noticias/geral,estanol-sera-jabuticaba-for-export-diz-presidente-da-volkswagen,70003918654#:~:text=Chamado%20de%20'dinossauro'%20por%20executivos,processo%20de%20descarboniza%C3%A7%C3%A3o%20para%20pa%C3%ADses (06 March 2022, date last accessed).

Sindhu R, Gnansounou E, Binod P *et al.* Bioconversion of sugarcane crop residue for value added products - an overview. *Renew Energy* 2016;**98**:203–15.

Singhania RR, Patel AK, Sukumaran RK *et al.* Role and significance of beta-glucosidases in the hydrolysis of cellulose for bioethanol production. *Bioresour Technol* 2013;**127**:500–7.

Soccol CR, Vandenberghe LP de S, Medeiros ABP *et al.* Bioethanol from lignocelluloses: status and perspectives in Brazil. *Bioresour Technol* 2010;**101**:4820–5.

Solomon BD. Biofuels and sustainability. *Ann N Y Acad Sci* 2010;**1185**:119–34.

Somerville C, Youngs H, Taylor C *et al.* Feedstocks for lignocellulosic biofuels. *Science (80-)* 2010;**329**:790–2.

Sonderegger M, Sauer U. Evolutionary engineering of *Saccharomyces cerevisiae* for anaerobic growth on xylose. *Appl Environ Microbiol* 2003;**69**:1990–8.

Stambuk BU, Batista AS, de Araujo PS. Kinetics of active sucrose transport in *Saccharomyces cerevisiae*. *J Biosci Bioeng* 2000;**89**:212–4.

Stambuk BU, da Silva MA, Panek AD *et al.* Active α-glucoside transport in *Saccharomyces cerevisiae*. *FEMS Microbiol Lett* 1999;**170**:105–10.

Stephanopoulos G. Challenges in engineering microbes for biofuels production. *Science (80-)* 2007;**315**:801–4.

Stevenson K, McVey AF, Clark IBN *et al.* General calibration of microbial growth in microplate readers. *Sci Rep* 2016;**6**:38828.

Stovicek V, Borodina I, Forster J. CRISPR-Cas system enables fast and simple genome editing of industrial *Saccharomyces cerevisiae* strains. *Metab Eng Commun* 2015;**2**:13–22.

Stovicek V, Holkenbrink C, Borodina I. CRISPR/Cas system for yeast genome engineering: advances and applications. *FEMS Yeast Res* 2017;**17**:1–16.

Sun FF, Hong J, Hu J *et al.* Accessory enzymes influence cellulase hydrolysis of the model substrate and the realistic lignocellulosic biomass. *Enzyme Microb Technol* 2015;**79**:42–8.

Sun FF, Zhao X, Hong J *et al.* Industrially relevant hydrolyzability and fermentability of sugarcane bagasse improved effectively by glycerol organosolv pretreatment. *Biotechnol Biofuels* 2016;**9**:59.

Tabuchi H, Plumer B. How green are electric vehicles? *New York Times* 2021. https://www.nytimes.com/2021/03/02/climate/electric-vehicles-environment.html#:~:text=If%20you%20assume%20electric%20vehicles,much%20greener%20than%20conventional%20cars (06 March 2022, date last accessed).

Taherzadeh MJ, Gustafsson L, Niklasson C *et al.* Physiological effects of 5-hydroxymethylfurfural on *Saccharomyces cerevisiae*. *Appl Microbiol Biotechnol* 2000;**53**:701–8.

Taherzadeh MJ, Niklasson C, Lidén G. Acetic acid - friend or foe in anaerobic batch conversion of glucose to ethanol by *Saccharomyces cerevisiae*? *Chem Eng Sci* 1997;**52**:2653–9.

Tapia Carpio LG, Simone de Souza F. Competition between second-generation ethanol and bioelectricity using the residual biomass of sugarcane: effects of uncertainty on the production mix. *Molecules* 2019;**24**:369.

Teunissen A, Dumortier F, Gorwa MF *et al.* Isolation and characterization of a freeze-tolerant diploid derivative of an industrial baker's yeast strain and its use in frozen doughs. *Appl Environ Microbiol* 2002;**68**:4780–7.

Tomás-Pejó E, Ballesteros M, Oliva JM *et al.* Adaptation of the xylose fermenting yeast *Saccharomyces cerevisiae* F12 for improving ethanol production in different fed-batch SSF processes. *J Ind Microbiol Biotechnol* 2010;**37**:1211–20.

Toussaint M, Bontemps C, Besserer A *et al.* Whole-cell biosensor of cellobiose and application to wood decay detection. *J Biotechnol* 2016;**239**:39–46.

Trichez D, Knychala MM, Figueiredo CM *et al.* Key amino acid residues of the AGT1 permease required for maltotriose consumption and fermentation by *Saccharomyces cerevisiae*. *J Appl Microbiol* 2019;**126**:580–94.

Turner TL, Kim H, Kong II *et al.* Engineering and evolution of *Saccharomyces cerevisiae* to produce biofuels and chemicals. *Adv Biochem Eng Biotechnol* 2018;**162**:175–215.

Turner TL, Zhang G-C, Oh EJ *et al.* Lactic acid production from cellobiose and xylose by engineered *Saccharomyces cerevisiae*. *Biotechnol Bioeng* 2016;**113**:1075–83.

UNCTAD, United Nations Conference on Trade and Development. *Second generation biofuel markets:state of play, trade and developing country perspectives*, 2016. https://www.unctad.org (23 March 2020, date last accessed).

ÚNICA, União da Indústria de Cana de Açúcar. Uso do etanol evita 515 milhões de toneladas de CO_2 2020. https://unica.com.br/noticias/uso-do-etanol-evita-515-milhoes-de-toneladas-de-co2-na-atmosfera/#:~:text=Entre%20mar%C3%A7o%20de%202003%20(data,Natural%20e%20Biocombust%C3%ADveis%20(ANP) (06 March 2022, date last accessed).

Unrean P, Ketsub N. Integrated lignocellulosic bioprocess for co-production of ethanol and xylitol from sugarcane bagasse. *Ind Crops Prod* 2018;**123**:238–46.

USDA, The United States Department of Agriculture. *Biofuels annual*, 2021. https://www.fas.usda.gov/ (06 March 2022, date last accessed).

USGCRP, U.S. Global Change Research Program. *The fourth national climate assessment - Chapter 2: our changing climate*, 2017. https://nca2018.globalchange.gov/chapter/2/ (06 March 2022, date last accessed).

Valdivia M, Galan JL, Laffarga J *et al.* Biofuels 2020: biorefineries based on lignocellulosic materials. *Microb Biotechnol* 2016;**9**:585–94.

van Aalst ACA, de Valk SC, van Gulik WM *et al.* Pathway engineering strategies for improved product yield in yeast-based industrial ethanol production. *Synth Syst Biotechnol* 2022;**7**:554–66.

van den Brink J, van Muiswinkel GCJ, Theelen B *et al.* Efficient plant biomass degradation by thermophilic fungus *Myceliophthora heterothallica*. *Appl Environ Microbiol* 2013;**79**:1316–24.

van Dijken JP, Bauer J, Brambilla L *et al.* An interlaboratory comparison of physiological and genetic properties of four *Saccharomyces cerevisiae* strains. *Enzyme and Microbial Technology*. Vol 26. Elsevier Science Inc, 2000, 706–14.

van Dijken JP, Scheffers WA. Redox balances in the metabolism of sugars by yeasts. *FEMS Microbiol Rev* 1986;**32**:199–224.

van Leeuwen M, Buijs NAA, Canelas AB *et al.* The Hagen-Poiseuille pump for parallel fed-batch cultivations in microbioreactors. *Chem Eng Sci* 2009;**64**:1877–84.

van Rooyen R, Hahn-Hägerdal B, La Grange DC *et al.* Construction of cellobiose-growing and fermenting *Saccharomyces cerevisiae* strains. *J Biotechnol* 2005;**120**:284–95.

Vardon DR, Franden MA, Johnson CW *et al.* Adipic acid production from lignin. *Energy Environ Sci* 2015;**8**:617–28.

Varela JA, Puricelli M, Ortiz-Merino RA *et al.* Origin of lactose fermentation in *Kluyveromyces lactis* by interspecies transfer of a neo-functionalized gene cluster during domestication. *Curr Biol* 2019;**29**:4284–90.

Vaz S. Sugarcane-biorefinery. In: Wagemann K, Tippkötter N (eds.). *Biorefineries*. Springer, Cham, 2017, 125–36.

Verduyn C, Postma E, Scheffers WA *et al.* Physiology of *Saccharomyces cerevisiae* in anaerobic glucose-limited chemostat cultures. *J Gen Microbiol* 1990;**136**:395–403.

Verduyn C, Postma E, Scheffers WA *et al.* Effect of benzoic acid on metabolic fluxes in yeasts: a continuous-culture study on the regulation of respiration and alcoholic fermentation. *Yeast* 1992;**8**:501–17.

Vishniac W, Santer M. The thiobacilli. *Bacteriol Rev* 1957;**21**:195–213.

Wagner S, Bader ML, Drew D *et al.* Rationalizing membrane protein overexpression. *Trends Biotechnol* 2006;**24**:364–71.

Wahl R, Wippel K, Goos S *et al.* A novel high-affinity sucrose transporter is required for virulence of the plant pathogen *Ustilago maydis*. *PLoS Biol* 2010;**8**:e1000303.

Wei N, Oh EJ, Million G *et al.* Simultaneous utilization of cellobiose, xylose, and acetic acid from lignocellulosic biomass for biofuel production by an engineered yeast platform. *ACS Synth Biol* 2015;**4**:707–13.

Wenger JW, Piotrowski J, Nagarajan S *et al.* Hunger artists: yeast adapted to carbon limitation show trade-offs under carbon sufficiency. *PLOS Genet* 2011;**7**:e1002202.

Weusthuis RA, Adams H, Scheffers WA *et al.* Energetics and kinetics of maltose transport in *Saccharomyces cerevisiae*: a continuous culture study. *Appl Environ Microbiol* 1993;**59**:3102–9.

Wheals AE, Basso LC, Alves DMG *et al.* Fuel ethanol after 25 years. *Trends Biotechnol* 1999;**17**:482–7.

Wisselink HW, Toirkens MJ, Berriel MDRF *et al.* Engineering of *Saccharomyces cerevisiae* for efficient anaerobic alcoholic fermentation of L-arabinose. *Appl Environ Microbiol* 2007;**73**:4881–91.

Wisselink HW, Toirkens MJ, Wu Q *et al.* Novel evolutionary engineering approach for accelerated utilization of glucose, xylose, and arabinose mixtures by engineered *Saccharomyces cerevisiae* strains. *Appl Environ Microbiol* 2009;**75**:907–14.

Yan W, Gao H, Qian X *et al.* Biotechnological applications of the non-conventional yeast *Meyerozyma guilliermondii*. *Biotechnol Adv* 2021;**46**:107674.

Yu J-H, Hamari Z, Han K-H *et al.* Double-joint PCR: a PCR-based molecular tool for gene manipulations in filamentous fungi. *Fungal Genet Biol* 2004;**41**:973–81.

Yuan Y, Zhao H. Directed evolution of a highly efficient cellobiose utilizing pathway in an

industrial *Saccharomyces cerevisiae* strain. *Biotechnol Bioeng* 2013;**110**:2874–81.

Yun EJ, Oh EJ, Liu J-J *et al.* Promiscuous activities of heterologous enzymes lead to unintended metabolic rerouting in *Saccharomyces cerevisiae* engineered to assimilate various sugars from renewable biomass. *Biotechnol Biofuels* 2018;**11**:40.

Zabed H, Sahu JN, Suely A *et al.* Bioethanol production from renewable sources: current perspectives and technological progress. *Renew Sustain Energy Rev* 2017;**71**:475–501.

Zahoor A, Messerschmidt K, Boecker S *et al.* ATPase-based implementation of enforced ATP wasting in *Saccharomyces cerevisiae* for improved ethanol production. *Biotechnol Biofuels* 2020;**13**:185.

Yamada R, Nakatani Y, Ogino C et al. Efficient direct ethanol production from cellulose by cellulase- and cellodextrin transporter-co-expressing *Saccharomyces cerevisiae*. AMB Express 2013;3:34

Zaparolli D. Electric vehicles powered by ethanol. *Pesquisa FAPESP* 2021. https://revistapesquisa.fapesp.br/en/electric-vehicles-powered-by-ethanol/ (06 March 2022, date last accessed).

Zhai R, Hu J, Saddler JN. What are the major components in steam pretreated lignocellulosic biomass that inhibit the efficacy of cellulase enzyme mixtures? *ACS Sustain Chem Eng* 2016;**4**:3429–36.

Zhang C, Acosta-Sampson L, Yu VY *et al.* Screening of transporters to improve xylodextrin utilization in the yeast *Saccharomyces cerevisiae*. *PLoS One* 2017;**12**:e0184730.

Zhang K, Pei Z, Wang D. Organic solvent pretreatment of lignocellulosic biomass for biofuels and biochemicals: a review. *Bioresour Technol* 2016;**199**:21–33.

Zhang W, Kou Y, Xu J *et al.* Two major facilitator superfamily sugar transporters from *Trichoderma reesei* and their roles in induction of cellulase biosynthesis. *J Biol Chem* 2013;**288**:32861–72.

APPENDIX

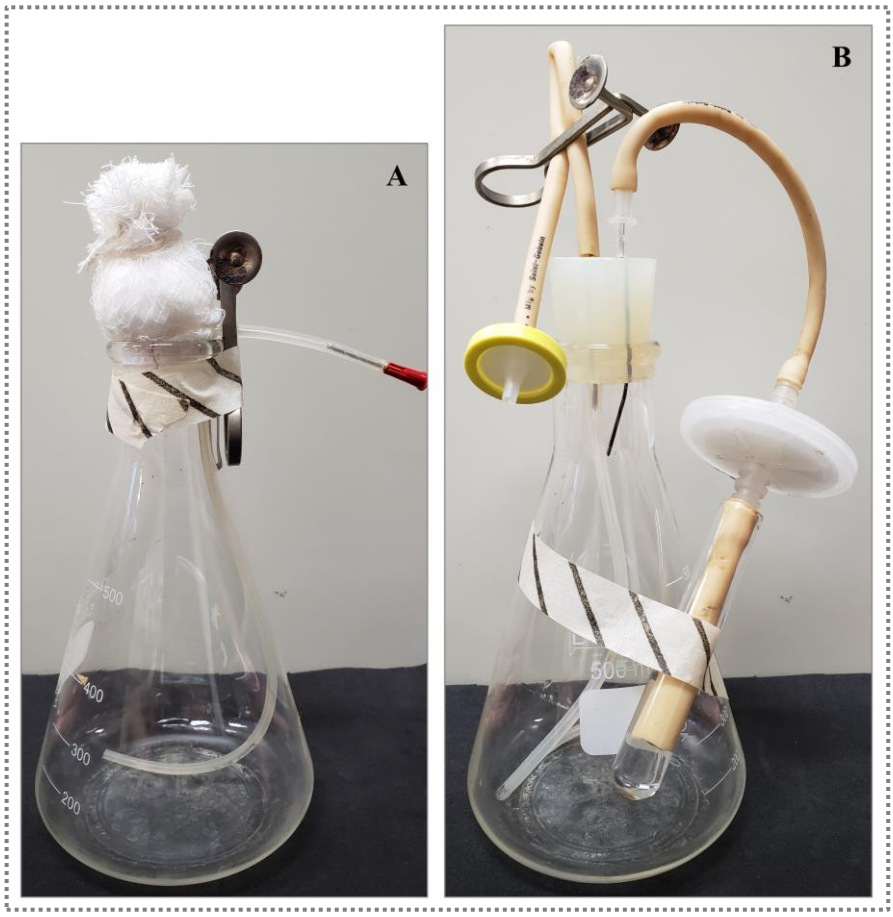

Appendix I. Shake-flask sampling structure for cultivations favouring (A) or minimising (B) oxygen transfer.

(a)

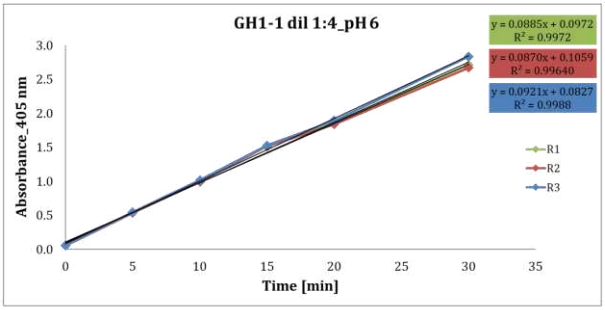

(b)

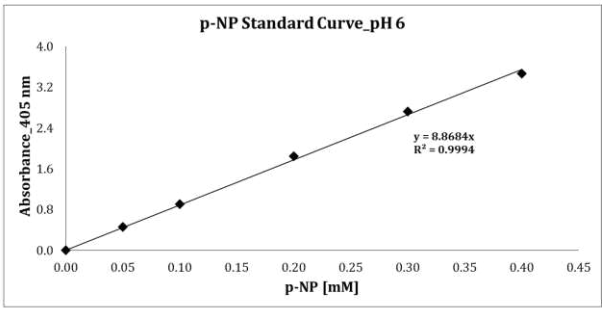

(c)

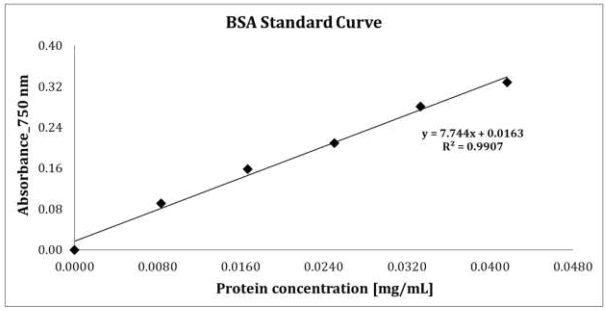

(d)

CALCULATION OF BGL ACTIVITIES

					Slope p-NP	Reaction volume [µL]	Extract volume [µL]
p-NP calibration curves:	pH = 6	y = 8.8684x	r2 = 0,9994	Linear range: Abs = [0 - 3,4644]	8.8684	200	80
	pH = 7	y = 9,0901x	r2 = 0,9999	Linear range: Abs = [0 - 3,6262]	9.0901	200	80

				Slope BSA	Y-intercept BSA
BSA calibration curve:	y = 7.744x + 0.0163	r2 = 0,9907	Linear range: Abs = [0 - 0,328]	7.744	0.0163

			Lowry assay					p-NPG assay						
Strain	Condition	Replicate	Absorbance [750 nm]	Dilution	Protein concentration [mg/mL]	Average protein concentration [mg/mL]	Std deviation	Δabs/min	Dilution	Enzyme activity [U/mL]	Average enzyme activity [U/mL]	Std deviation	Average specific activity [U/mg protein]	Std deviation
PBY_06 (GH1-1)	pH = 6.T = 30 °C	R1	0.056	10	0.052	0.050	0.002	0.0885	4	0.0998	0.1006	0.0030	2.0	0.1062
		R2	0.053		0.048			0.0870		0.0981				
		R3	0.056		0.052			0.0921		0.1039				
PBY_06 (GH1-1)	pH = 7.T = 30 °C	R1	0.056	10	0.052	0.050	0.002	0.0874	4	0.0961	0.0956	0.0013	1.9	0.0880
		R2	0.053		0.048			0.0856		0.0942				
		R3	0.056		0.052			0.0878		0.0966				

$$Protein\ concentration = \frac{Absorbance - yintercept\ BSA}{Slope\ BSA} * Dilution$$

$$Enzyme\ activity = \frac{\Delta abs/min}{Slope\ pNP} * \frac{Reaction\ volume}{Enzyme\ volume} * Dilution$$

$$Specific\ activity = \frac{Enzyme\ activity}{Protein\ concentration}$$

Appendix II. Determination of BGL activities with data from GH1-1 as an example. (a) Progress curves of diluted cell extracts of GH1-1-expressing cells during incubation with 0.5 mM p-NPG in potassium phosphate buffer at pH 6 and 30 °C. Three replicates were performed for each assay. The velocity is obtained from the linear part of the curves. **(b)** p-NP standard curve employed for the quantification of the amount of p-NP released in the reactions performed at pH 6. Each point of the curve (r^2 = 0.9994) corresponds to the average of three replicates. **(c)** Standard curve used for the quantification of the protein content with the Lowry assay. Each point of the curve (r^2 = 0.9907) corresponds to the average of three replicates **(d)**. Calculations performed for the determination of the GH1-1 activities at pH 6 or 7.

Appendix III. Prediction of transmembrane helices in putative CDT sequences using the TMHMM server.

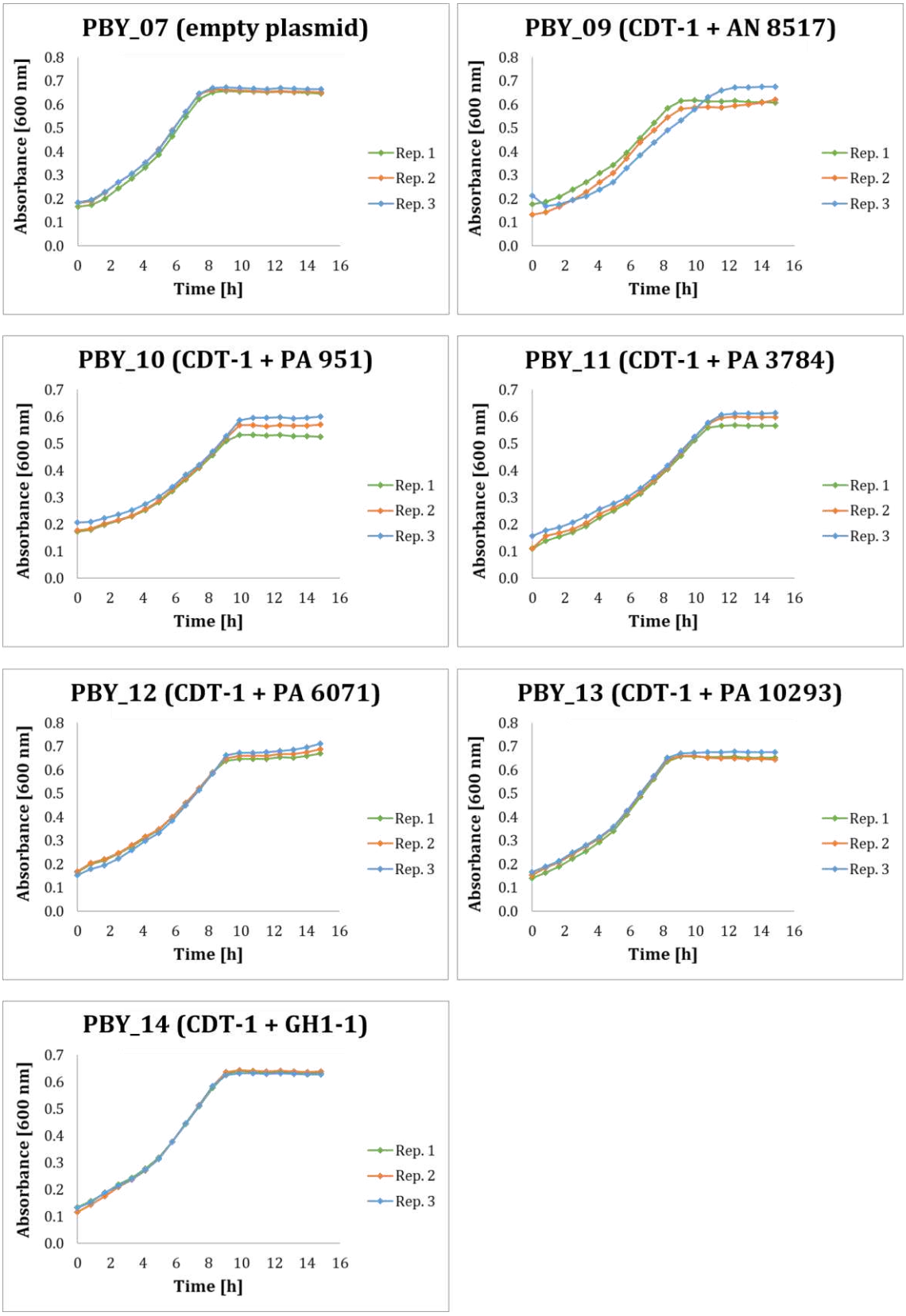

Appendix IV. Growth profiles of strains PBY_07 to PBY_14 during microplate cultivations in synthetic medium with 18 g/L initial glucose. Three replicates for each strain are shown in the figure.

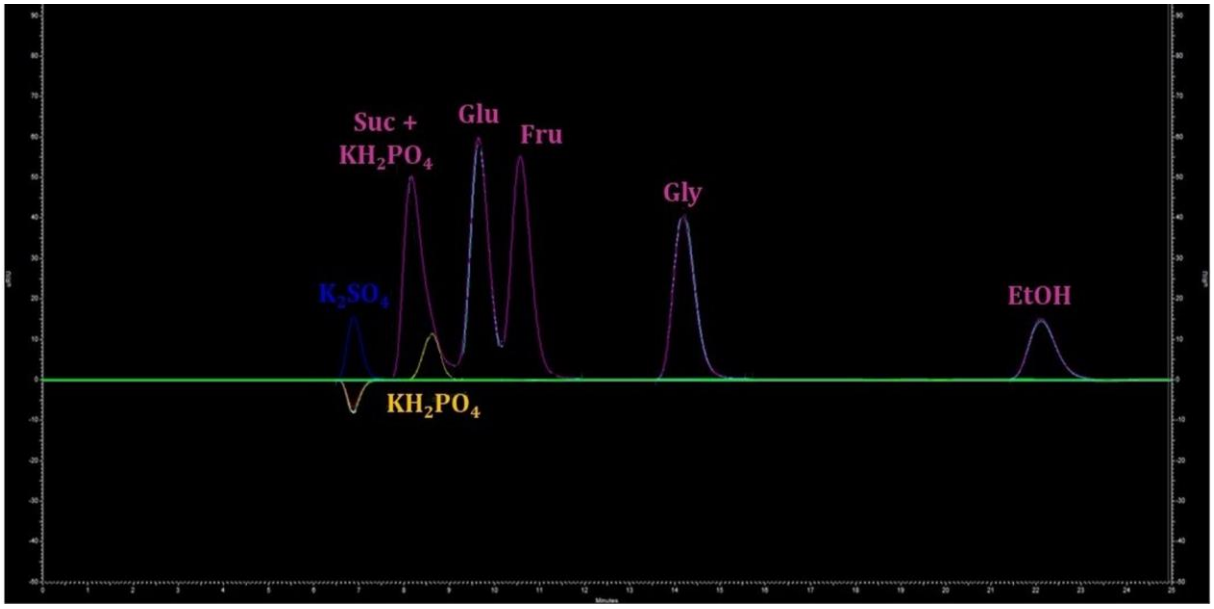

Appendix V. Sucrose and KH_2PO_4 separation via HPLC analysis. Under the conditions of operation performed in this study (section 5.3.5), both components of the synthetic medium leave the column at the same retention time.

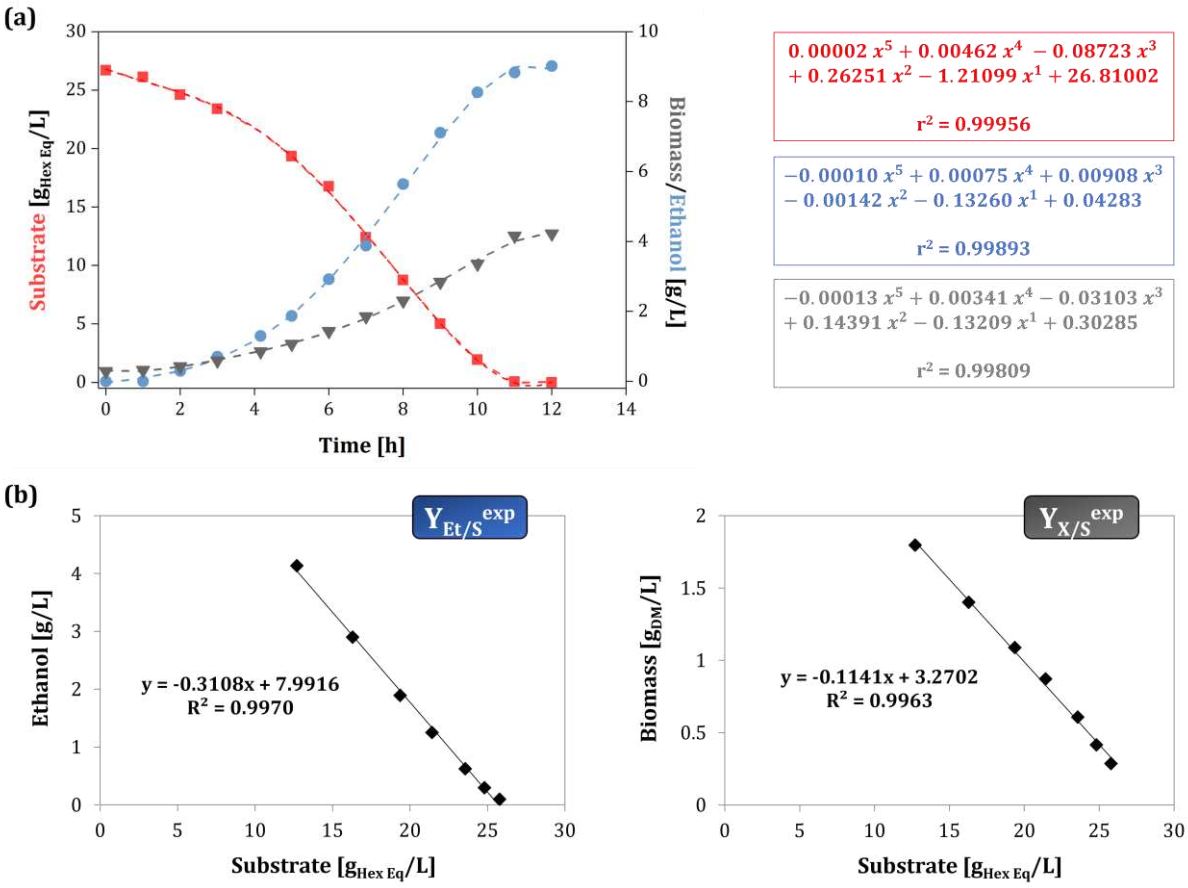

Appendix VI. Determination of physiological yields. Data from *S. cerevisiae* i*SUC2*e cultivation under conditions favouring oxygen transfer is used as an example (one representative of duplicate experiments). **(a)** Substrate, ethanol, and biomass profiles determined experimentally (symbols) or by polynomial fitting (dashed lines with equations at the right). **(b**) Calculation of ethanol and biomass yields on substrate by using fitted concentration values within the exponential growth phase.

Ethanol yield calculations

$$\text{Ethanol yield} = [\text{Ethanol}]_{produced} / [\text{Sugar}]_{consumed} = (\text{g Ethanol})_{produced} / (\text{g Sugar})_{consumed}$$

$$(\text{g Ethanol})_{produced,\ cycle\ n} = (\text{g Ethanol})_{end,\ cycle\ n} - (\text{g Ethanol})_{beginning,\ cycle\ n-1}$$

$$(\text{g Ethanol})_{end,\ cycle\ n} = (\text{g Ethanol})_{wine,\ cycle\ n} + (\text{g Ethanol})_{pellet,\ cycle\ n} =$$

$$= 1\text{L}/1000\text{ mL} * [\text{Ethanol}]_{wine\ n} * \text{Volume}_{wine\ n} + 1\text{L}/1000\text{ mL} * [\text{Ethanol}]_{wine\ n} * 0{,}7\text{ mL}/g_x * x_n) = 1\text{L}/1000\text{ mL} * [\text{Ethanol}]_{wine\ n} * (\text{Volume}_{wine\ n} + 0{,}7\text{ mL}/g_x * x_n)$$

$$(\text{g Ethanol})_{produced,\ cycle\ n} = 1\text{L}/1000\text{ mL} * \{[\text{Ethanol}]_{wine\ n} * (\text{Volume}_{wine\ n} + 0{,}7\text{ mL}/g_x * x_n) - [\text{Ethanol}]_{wine\ n-1} * (2\text{ mL} + 0{,}7\text{ mL}/g_x * x_{n-1})\}$$

$$(\text{g Sugar})_{consumed,\ cycle\ n} = (\text{g Sugar})_{end} - (\text{g Sugar})_{beginning}$$

$$(\text{g Sugar})_{consumed,\ cycle\ n} = \text{Volume}_{sugar\ added} * ([\text{Sugar}]_{end} - [\text{Sugar}]_{beginning})$$

$$(\text{g Sugar})_{consumed,\ cycle\ n} = (9{,}25 * 3)\text{ mL} * 1\text{L}/1000\text{ mL} * ([\text{Sugar}]_{end} - [\text{Sugar}]_{beginning})$$

$$\text{Ethanol yield (as \% theoretical maximum)} = (\text{g Ethanol})_{produced} / (\text{g Sugar})_{consumed} * 100/0{,}511$$

Appendix VII. Ethanol yield calculations made for the mimicked 1G experiment.